# Energy-efficient Communication in Ad Hoc Wireless Local Area Networks

vorgelegt von
Diplom-Informatiker
Jean-Pierre Ebert

von der Fakultät IV – Elektrotechnik und Informatik
der Technischen Universität Berlin
zur Erlangung des akademischen Grades

Doktor der Ingenieurwissenschaften
– Dr.-Ing. –

genehmigte Dissertation

Promotionsausschuss:

Vorsitzender: Prof. Dr.-Ing. Dr. rer. nat. Holger Boche
Berichter: Prof. Dr.-Ing. Adam Wolisz
Berichter: Prof. Dr.-Ing. Rolf Kraemer

Tag der wissenschaftlichen Aussprache: 19. April 2004

Berlin 2004

D 83

# Zusammenfassung

Die Funktechnik wird heutzutage in vielen Bereichen, beispielsweise in der Computer-, Kommunikations- und Steuerungstechnik, verwendet. Eine der populärsten Funktechnologien, die der Klasse der lokalen Netzwerke (LANs) zugerechnet wird, ist IEEE 802.11. Die Mitte der achtziger Jahre konzipierte und 1995 vom IEEE in seiner Urform standardisierte Funktechnologie hat nicht zuletzt wegen den vergleichsweise hohen Übertragungsraten vor allem im Internet-Anschlussbereich von (mobilen) Endgeräten Anwendung gefunden. Trotz der vorhandenen Energiesparfunktion verbraucht eine IEEE 802.11-Funkschnittstelle einen erheblichen Teil des Energiebudgets eines batteriebetriebenen Endgeräts, so dass weitere Maßnahmen zur Senkung des Energieverbrauchs notwendig sind. Diese Dissertation befasst sich mit verschiedenen Aspekten der Energieverbrauchsreduktion von IEEE 802.11-basierten Funknetzen. Das zentrale Element dieser Arbeit ist das Vielfachzugriffsprotokoll. Ausgangspunkt ist die Messung der Leistungsaufnahme einer WLAN-Schnittstelle in verschiedenen Betriebsarten. Unter Zuhilfenahme dieser Messdaten wird der Energieverbrauch der WLAN-Schnittstelle in verschiedenen Betriebsarten und bei verschiedenen Kanalqualitäten bestimmt. Um den Energieverbauch aussagekräftig zu beschreiben, wird eine neue Metrik verwendet, welche der verbrauchten Energie pro erfolgreich übertragenem Informationsbit entspricht. In dieser Arbeit wird ersichtlich, dass die im IEEE 802.11-Standard spezifizierte Energiesparfunktion, die im Grunde einem Ein/Aus-Schema entspricht, bei entsprechenden Maßnahmen den positiven, betriebsdauerverlängernden Effekt einer gepulsten Batterieentladung erzielen kann. Im Weiteren wird der Zusammenhang zwischen der Größe eines gesendeten Pakets und dem Energieverbrauch der WLAN-Schnittstelle untersucht. Die Analyse verdeutlicht, dass

die Anpassung der Funksignalleistung an die Paketgröße zu einer Senkung des Energieverbrauchs führt. Abschließend wird die dynamische Anpassung der Funksignalleistung im Zusammenhang mit einer kontrollierten Mehrschrittkommunikation (multi-hop) hinsichtlich des Reduktionspotentials beim Energieverbrauch und der Immissionsleistung untersucht. In beiden Fällen wird ein Reduktionsgewinn ersichtlich. Die Ergebnisse der Dissertation zeigen, dass weiteres Potential zur effizienteren Nutzung des begrenzten Energievorrats einer Batterie vorhanden ist, was letztendlich zu länger arbeitenden, leichteren und damit zu ergonomischeren, funkbasierten Kommunikationsendgeräten führt. Obwohl die Arbeiten auf der IEEE 802.11-Funktechnologie basieren, haben die erzielten Ergebnisse allgemeine Gültigkeit.

# Abstract

Today there is a widespread utilization of wireless in computation, communication and control. A very popular wireless technology, belonging to the class of local area networks, is IEEE 802.11. Developed in the eighties and specified in its raw form by the IEEE in 1995, it offers comparatively high data rates and competitive ease of use. The main application scenario is the provision of Internet access for (mobile) end systems. Despite a power-saving function IEEE 802.11 network interfaces still consume a vast amount of the overall energy budget of a self-sustained end system. Hence, further efforts are necessary to reduce the energy demand of an IEEE 802.11 network interface. In this thesis several aspects of energy consumption and efficient utilization of limited energy resources of IEEE 802.11 communication systems are explored regarding the Media Access Control protocol. The investigation is based on power consumption measurements of an IEEE 802.11 network interface. These measurements provide parameters for several simulations, which are used to determine the energy consumption of the network interface for various operation modes and different radio link qualities. A new metric, the energy consumed to transmit one payload bit successfully, is employed to determine power consumption meaningfully. The results also reveal that the IEEE 802.11 power-saving creates an On/Off discharge pattern resulting in a pulsed battery discharge. Pulsed battery discharge significantly extends battery life compared to continuous discharge. Furthermore, the relation of the size of a transmitted packet to the energy consumption is analyzed. It is shown that a packet size dependent power control scheme leads to considerable energy savings. Power control is also considered from the network perspective. The particular question, whether power control reduces

energy consumption and radio exposure if a controlled multi-hop ad hoc network communication scheme is used, is positively answered. The achieved results reveal that there still is potential for a more efficient use of the limited energy resources of self-sustained, wireless communication systems. The rewards for an efficient use of energy are either increased operating times or smaller, lighter and therefore more ergonomic wireless end systems. Although the achieved results base on IEEE 802.11, most of them are generally valid.

# Preface

This dissertation concludes a ten year working period at Prof. Dr.-Ing. Adam Wolisz' Chair of Telecommunication Networks (TKN) of the Technical University Berlin (TUB). After my graduation as Diplom-Informatiker at the TUB in 1993, Prof. Wolisz appointed me as the second scientific assistant shortly after his call to the TUB. At this time wireless local area communication, the basis of this dissertation, was in its infancy. Driven by the growing popularity of wireless communication in other areas, Prof. Wolisz had identified the future technical and economical importance of Wireless Local Area Networks (WLAN). Consequentially, he suggested that my research, and finally my dissertation should be in the context of wireless local area networking. The vaguely formulated dissertation goal, the amount of start-up activities of the chair, project work, and the work connected with the great popularity of telecommunication network lectures among students kept me busy for a while. Therefore some time passed until I found a research theme for my doctorate. The impetus to focus on energy efficiency in wireless communication came from a work of my friend and colleague Hagen Woesner and one of his diploma students where I was involved in many interesting discussions. They examined the efficiency of the IEEE 802.11 Power Saving function and determined optimal parameter ratios. Indeed, this work was one of the first engagements in the research community that focused on power saving from a protocol perspective. Fascinated by this work and a short, but fruitful and motivating discussion with Prof. Wolisz I decided to further pursue power saving from a protocol perspective.

In the following, I tackled power saving from different directions, but always with the IEEE 802.11 MAC protocol as originating point. My work towards achieving the Ph.D has had a more or less intermittent character over the years. Prof. Wolisz encouraged all

of his group members to take ancillary activities such as project work with scientific and industrial partners, teaching, student and master thesis supervision. Although this has inter alia been the reason for lagging behind the original dissertation completion plan, I enjoyed these fertile and prosperous activities. In fact they have been very beneficial to my technical and personal development. In a sense this dissertation is a selection and arrangement of my research work at the TKN chair. Most parts of the dissertation have led to several publications in international conferences, proceedings, and journals. Hopefully, the dissertation as a whole will contribute significantly to energy-efficient wireless communication.

During the ten-year working period at the TKN chair I became acquainted to many people working hard together with me, congenially accompanying my daily work life, and contributing in different ways to the eventual success of this dissertation. Without the claim of completeness, I would like to thank some people emphatically. First of all I am particularly grateful to my mentor Professor Adam Wolisz. He has generously supported me in many respects and provided valuable inspiration and criticism. Moreover and beyond doubt, his working style and personal manner has positively influenced my development. I can say that he has become a paternal friend over the years. In this spirit I also want to thank my colleagues and friends Berthold Rathke, Morten Schläger and Dr. Andreas Willig for their inspiration, productive discussions and assistance through the years. I also owe particular thanks to my peer Dr. Jeffrey Monks and the students Brian Burns, Gunnar Kofahl, Stefan Aier, Alexander Becker, Marcos Segador-Arebola, Björn Stremmel, Eckhardt Wiederhold, Enno Ewers, Björn Matzen and Marc Löbbers, who I mentored during their respective diploma/student thesis preparation, student projects or temporary stays abroad, for their inspiration, helpful comments and important contributions. Beyond that I am much obliged to all of my colleagues of the TKN group. Not to mention I want to express my deep gratitude to my friends, my mother Brigitte, my son Maximilian, and my companion Lydia for their motivation, patience, support and confidence particularly during the last period of my dissertation.

# Contents

# List of Tables

# List of Figures

# Chapter 1

# Introduction

This thesis mainly has two combined driving forces - wireless local area communication and energy-efficient communication. Wireless communication devices such as notebooks, Personal Digital Assistants (PDA) and cellular phones penetrate our daily life extensively. Among other similarities between them, their self-sustaining nature, their wireless communication abilities and therefore their flexible use have made them very popular.

One important factor for this develepment is the significantly improved ergonomic handling and function diversity. The former is inter alia a matter of size and weight, the latter is mainly a matter of the vastly improved processing power. Both issues are close-knit with two questions. The first question is about the amount of energy necessary to operate such devices. It is well known that the energy demand of electronic parts can be considerably reduced by more integration, algorithmic improvements and the use of low power technology for the display, processor and memory. However, the functionality of mobile electronic devices has become more powerful and manifold over the time. As a result, the energy demand rather increases than decreases. The second question, how much energy can be provided, is very cardinal. The key feature of mobile electronic devices is the self-sustained operation currently accomplished by (rechargeable) batteries. To limit batteries to an acceptable size and weight, however, either the specific energy density must be improved or the functionality and the associated energy demand have to be balanced with the available energy. Although battery capacities have considerably improved during recent years (for instance, by the Lithium Ion battery technology), they are not completely in pace with the increased energy demands due to the escalating functionality and purpose diversity of mobile electronic devices. Another aspect is related to environmental issues. The less energy is consumed, the less toxic waste is produced, e.g., due to longer battery replacement intervals.

Wireless communications is without doubt well established today. It is widely used in various forms and is still entering new application fields. One of the most accepted wireless data communication technology is Wireless Local Area Network (WLAN) on which I focus throughout this thesis. It is a very popular technology because of its similarity to Ethernet, its flexibility, and the comparatively high transmission rates. The particular WLAN investigated in this thesis in the context of energy consumption is IEEE 802.11b. IEEE 802.11 type networks are not only used commercially. Meanwhile we can find them in many ares where local communication plays a role such as households, cafes, campuses and airport communication spots. IEEE 802.11b belongs to a the radio communication technology family which has recently been extended by high speed versions IEEE 802.11*a* and *g* and by Quality of Service (QoS) functions like IEEE 802.11*e* and *f*. Not to mention HIPERLAN/1 and HIPERLAN/2 systems, which are the IEEE 802.11 network counterparts defined by the European Telecommunications Standards Institute (ETSI), offering similar capabilities. IEEE 802.11 networks can easily be deployed and offer data rates ranging from 1 to 11 Mbit/s for type *b* networks and from 6 to 54 Mbit/s networks for type *a* networks. Networks that follow the IEEE 802.11*g* standard, provide transmission rate sets as in *a* and *b* and additionally 22 Mbit/s. Although the energy demand of IEEE 802.11 network interfaces has been reduced by technological advances over the years, it is still considerable regarding the energy capacity offered by the battery of a wireless self-sustained communication device.

The bottom line of this discussion is that this dissertation is focused on both the energy consumption reduction of IEEE 802.11 network interfaces and the efficient utilization of the limited energy budget of a self-sustained wireless communication device. The particular focus is neither on energy-efficient integrated circuit or hardware design, nor on the development of high capacity batteries. In fact I concentrate on the exploration of MAC protocol properties regarding energy consumption. This is the basis for several energy-related MAC protocol optimization and tuning options proposed later in this thesis.

At this point let me add something concerning topicality and relevance of the research work presented hereafter. The importance of energy efficiency was quickly identified by the research community. This thesis is a composition of selected, energy-related Medium Access Control (MAC)-centric research issues, which I explored during the past years at the Telecommunication Network Chair (Prof. Dr. Adam Wolisz) of the Technical University Berlin. Some research issues of this thesis have already been well explored (in pertinent literature) while others that I worked on shortly before completion of this thesis are new. However, with a delayed thesis completion in mind the respective research results have already been published in journals and in conferences proceedings. For a complete list of my publications see Appendix E. The articles directly related to this thesis are marked with an asterisk (*).

## 1.1 Motivation

As communication capabilities become more important, the energy consumption of the Radio Frequency (RF) interface plays a more significant role in the overall power consumption of a mobile device. For instance, todays notebooks averagely consume 5-10 W and an active WLAN interface approximately consumes 1.5 W, which makes up $15\%$ to $30\%$ of the overall power consumption. This trend increases as other components like processors, memory, displays, etc. are power optimized and mobile or wireless communication devices become purpose-oriented. Examples are Transmeta's low-power Crusoe processor (see [90]) and PDAs , e.g., Handspring (see [38]), which were specifically designed for personal information management, mobile use and large intervals of battery recharge/replacement. In turn, the energy-efficient hardware design of the network interface is a major contribution with respect to the overall energy consumption of mobile communication system. A comprehensive overview of energy-efficient radio communication hardware design is given in [73]. But this is not the only point to consider when optimizing the energy consumption. Another facet of energy-efficient RF communication design, equally important, is the adequate control and operation of the network interface and the wireless network. The control is defined by (communication) protocols whose mode of operation significantly impacts the energy consumption of the network interface and the entire network (see e.g., [53, 99]).

To minimize energy-consumption of a WLAN interface, the IEEE 802.11 standardization group has specified power saving algorithms for ad-hoc and infrastructure mode operation. In [81] the performance of the ad hoc power saving procedure is evaluated and it is shown that the network interface can stay in the low-power *DOZE* mode for a considerable amount of time with the penalty of a throughput loss. The WLAN interface power consumption for certain operation modes such as *IDLE, DOZE, Receive, and Send* as well as the dependency on parameters such as RF transmission power levels, packet sizes, and protocol operation modes were not specified at that time. Therefore it was difficult to estimate the real gain of this power saving algorithm. Moreover the detailed knowledge of energy consumption in the various operation modes is necessary to understand the energy consumption of a network interface and to potentiate an energy-efficient design, tuning or adaption of protocols. The aforementioned ad hoc power saving algorithm can be set into relation to the battery capacity of a wireless communication device. It is well known that batteries recover after a relaxation phase, which is also referred to as self-recharge. This characteristic could be exploited by sufficiently alternating the operation modes of a WLAN network interface between doze and any other mode. Even if there is no capability to control the operation mode change, an understanding of the energy consumption characteristics of a WLAN will allow to determine the relevance of self-recharge for a WLAN communication device.

Furthermore, an energy-efficient protocol design is not a self-contained task. The minimization of the energy demand for wireless communication is always a cross-layer optimization with respect to the Operating System Interconnection (OSI) reference model as explicitly outlined in [47]. Although power saving is addressed in the IEEE 802.11 WLAN specification, little attention is payed to the question how the operation of the MAC protocol and higher layer protocols impact hardware and therefore energy consumption. For instance although the RF transmission power has an obvious impact on energy consumption, the IEEE 802.11 standard leaves the question of power control open. Power control can have several motivations. The most obvious ones are minimizing interference and maximizing the wireless network capacity, not necessarily resulting in a lower energy consumption of the network interface. Neither an energy-efficient power control nor its relation to the MAC protocol have been considered previously.

Energy-efficient power control also has a network perspective. Transmission with a fixed power level leads to a capture of the radio channel or at least interference. The results are either blocked wireless nodes, impaired signal quality at the receiving wireless nodes and in turn higher energy demands. The question that arises is how power control influences the network capacity and network energy consumption. Since wireless networks are multifaceted in network topologies, the gain of power-control (if any) is likely to be different. Therefore it is of great interest which ad hoc network topology types require power control and what ad hoc network topology types deliver the highest gain in capacity and energy consumption. An important issue that arises with RF power control and possible energy consumption reductions is exposure. Radio exposure is a potential health risk, the reason why many people demur the further proliferation of radio communication. Therefore an important goal is to further minimize radio exposure. Until now there is only little research on exposure reduction techniques. RF power control has an obvious potential to reduce exposure. However, it is not clear whether an exposure reduction can actually be achieved since it depends on a multitude of parameters and on the network configuration. It is particularly interesting whether exposure can be further reduced in conjunction with ad hoc networks. The power-controlled multi-hop communication technique seems to be a promising option to be explored.

## 1.2 Dissertation contributions

The work presented in this dissertation pursues one goal - the maximization of the wireless node operation time . The basis of all considerations is an IEEE 802.11b network operating in ad hoc mode. As motivated above, I used a MAC-centric view to explore energy-saving options. Starting with a characterization of the energy consumption of a WLAN interface I investigated several MAC-based energy saving options. Additionally, impacts on network energy consumption and radio exposure are examined. The particular contributions of this thesis are briefly described below:

**IEEE 802.11 MAC model** The main investigation approach is simulation. For that purpose a very detailed simulation model of the IEEE 802.11 MAC protocol was developed. This model is not only the basis of this dissertation but also used in several projects and master/student theses.

**Power consumption measurements of an IEEE 802.11b network interface** To get an idea of the power consumption characteristics, an Aironet PC4800B PCMCIA (Personal Computer Memory Card International Association) network interface was analyzed. As the WLAN network interface operation states and modes were varied, different power consumption values could be recorded. In addition, the influence of parameters such as transmission rate, packet size, and RF transmission power were examined. On the one hand, the results are the basis for an understanding of the energy consumption characteristics needed for further optimizations. On the other hand, the results serve as parameters for some of the following investigations instead of using estimates.

**Definition a of meaningful energy consumption metrics** Power or energy consumption are insufficient metrics to describe energy efficiency. For example, energy consumption will be at its minimum if a WLAN network interface operates continuously during the *DOZE* state. It is obvious that a weighting factor is necessary. I chose the goodput because it describes the achieved result of the wireless communication procedures when using a certain amount of energy. The metric is referred to as consumed energy per successfully transmitted payload bit. In this context the energy consumption of a WLAN network interface relative to goodput is determined. Additionally the influence of an impaired channel is investigated.

**IEEE 802.11 power saving driven battery self-recharge potential** It is a well known fact that batteries recover during relaxation phases, which is also described as *self-recharge* effect. Technically speaking, self-recharge is the compensation of concentration gradients of the active materials in a battery. Concentration gradients lead to voltage drops. Whenever the cut-off voltage is reached, the battery is considered empty, although chemical energy might still be available. It is investigated whether this effect can be exploited by the IEEE 802.11 Power Saving function to extend the operation time of a mobile node. It is shown that the Power Saving function has a considerable positive effect on the exploitation of the chemical energy contained in a battery.

**Packet size dependent energy-efficient power control** The packet size has a strong influence on the packet error rate and the network performance. Here the impact on the energy consumption of a WLAN network interface is determined. It is shown that any packet size has an optimum RF transmission power. By adjusting the RF transmission power according to the packet size significant energy savings are achieved.

**Energy-efficient power control in multi-hop ad hoc networks** The topologies of multi-hop ad hoc networks can be very different. Consequently the impact of power regarding network performance and network energy efficiency varies. This thesis attempts to shed light on the dependency between network topology and RF transmission power control. Three different but common network topologies serve as basis. It is shown that both network capacity and energy efficiency can be improved if a controlled multi-hop communication is used. However, this strongly depends on the network topology.

**Power control as a mean to reduce exposure** Power control is normally used to ensure a certain link quality level. Here I dealt with the question whether it can reduce exposure in conjunction with multi-hop ad hoc networks. It is shown that exposure is reduced by introducing a certain amount of intermediate nodes (forwarders). Although intermediate nodes can cause a vast drop in the (end-to-end link) throughput, it is shown that a compensation by the use of higher transmission rates is possible while still yielding an exposure reduction.

### 1.2.1 Dissertation structure

The structure of the dissertation is shown in Figure 1.1 on the facing page. It reveals the basic interrelations of the aforementioned contributions. The particular objective pursued in this dissertation is to improve the operation time of a wireless node using IEEE 802.11b. As shown in the figure, the basis of this dissertation is the *WLAN Energy Usage Model* block. This block contains the investigations and the achieved results that deliver a detailed energy consumption figure of an IEEE 802.11b network interface in various operation modes and under different operation conditions. Two independent investigation are based on this block. The *Battery Utilization* block addresses the potential to extend the operation time of a wireless system using pulsed battery discharge. In the *Power Control* block several energy efficiency related aspects of RF power control are considered. There are two answers to the consequential question why the *Power Control* block does not follow up the Battery Utilization block. First, most of the work on power control was performed before the work on battery utilization. Second, the achievable results will not justify the required effort. The impact of power control on battery utilization is probably small. The detailed dissertation outline is given next.

**Outline**

This dissertation is organized as follows. After this introductory chapter and before going into more details on energy efficiency, Chapter 2 presents the technical base of the dissertation such as a condensed IEEE 802.11 primer, a description of Aironet's PC4800B WLAN network interface, an introduction of the radio channel and the link budget analysis, and some basics on battery discharge are presented. This chapter can be omitted by readers familiar with these topics. Afterwards, I review relevant research in Chapter 3. The main investigation and verification method used throughout the dissertation is simulation. Therefore Chapter 4 describes the used IEEE 802.11 MAC, traffic sources, radio channel

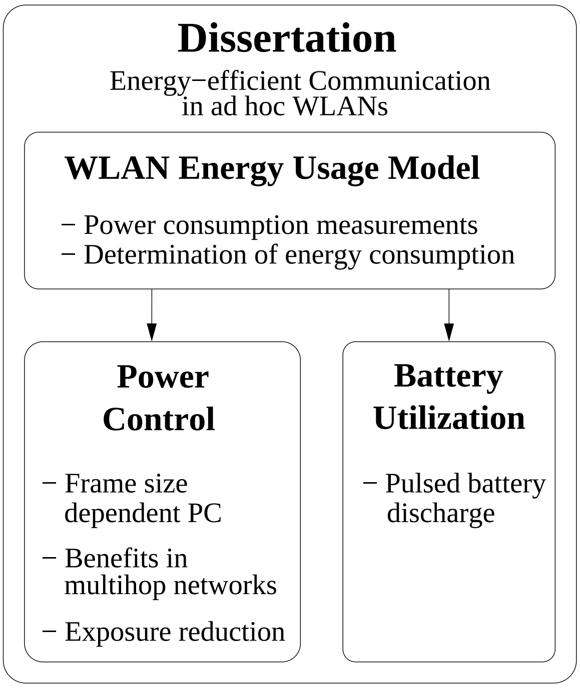


Figure 1.1: Dissertation structure

and battery models as well as their simulation structures in-depth. The models are consistently used throughout the dissertation and referenced as necessary.

The core of the dissertation starts with Chapter 5, which describes how power measurement results of an Aironet PC4800B WLAN network interface were aquired. The purpose of the measurements is twofold. The results clarify which network interface components consume the power. Furthermore the results are necessary for simulation model parameterization. In the following Chapter 6, a sufficient metric to evaluate energy efficiency is introduced. This metric, the *Consumed Energy per successfully transmitted Payload Bit* is used together with the measurement results of the former chapter to determine the energy efficiency of Aironets PC4800B WLAN network interface for different radio link qualities. Afterwards this dissertation focuses on the MAC. In Chapter 7, I follow the question whether the power saving function of an IEEE 802.11 WLAN operating in ad hoc mode opens the opportunity to take advantage of pulsed battery discharge. While pulsed battery discharge is a mean to drive the exploitation of the available energy resources to its limits, packet size based RF transmission power control is a mean to save energy. Chapter 8 motivates and describes this energy-efficient power control technique. In the following two chapters ad hoc network topology related power control issues are discussed. In Chapter 9 I particularly examine whether power control results in an improved energy efficiency by means of three different but general (multi-hop) ad hoc network topologies. In Chapter 10 I evaluate the effect of power control in conjunction with controlled multi-hopping on radio exposure. The dissertation is concluded with a summary of the achieved results and an outlook for further related research. A reference list and some appendices, which provide additional information, complement the dissertation.

# Chapter 2

# Foundations

The first part of this chapter describes the vital elements the research of this thesis is based. Radio communication and power-saving cannot be understood without knowledge of the radio channel and how to dimension the parameters of the radio sender and receiver, respectively. Therefore the basics of the radio channel as well as link budget analysis are given first. Next, the basics of IEEE 802.11 (Institute of Electrical and Electronics Engineers) are described. IEEE 802.11 is selected as the basis for investigations of energy efficiency in wireless communication because it is well known from literature and commonly used for wireless local communication. IEEE 802.11 is still in a state of evolution as the various substandards and committees demonstrate. By now it is proliferating beyond educational and home premises. I also describe an implementation of an IEEE 802.11 WLAN network interface, which is used to determine realistic power consumption parameters. From the hardware configuration I derive a generic network interface model. Later within the dissertation the utilization of the battery capacity of self-sustained communication systems is investigated. Therefore an introduction to batteries, particularly on the discharge process, is given at the end of this chapter to make the work on the maximum utilization of batteries transparent.

## 2.1 Radio channel

Radio systems use electromagnetic waves, which propagate through space to carry information from one entity to another. The transmission media space differs much from cable.

The transmission characteristics can change frequently because of movement of the sender or receiver, and because radio signals can hardly be shielded against impairments. In the following Section 2.1.1 I briefly describe the channel characteristics and in Section 2.1.2 I show, how to compute relevant transmission parameters to achieve a certain transmission quality.

### 2.1.1 Radio channel characteristics

The quality of a radio link is determined by how good the electromagnetic waves can propagate. Among others the signal quality depends on frequency, transmission power and propagation conditions (e.g. reflection materials and obstacles). As a rule of thumb, the lower the frequency the better the propagation. However, a low frequency is not always desirable if radio communication should be locally limited. The RF transmission power setting is crucial since a certain signal energy at the receiver is necessary to decode a signal. When choosing a certain transmission power we also have to account for upper limits, which are either of regulatory or of technical nature to keep both health risks and impairments of other systems low.

Depending on the characteristics, radio channels can be classified. For example the Additive White Gaussian Noise (AWGN) radio channel is a well known channel type that is considered as a worst case channel disregarding channel coding. In an AWGN channel bit errors occur independently, resulting in an even distribution of bit errors over time. Therefore every frame has the same probability to be corrupted by bit errors. This is not the case for a channel where bit errors are correlated. Here, bit errors will occur in bursts assuming, e.g., a Rayleigh fading radio channel. In turn, some frames are corrupted by many bit errors while others are transmitted without any bit error. There are several other radio channel types, e.g., Nakagami or Rice fading radio channel, which are not used in this dissertation.

#### Propagation conditions

The propagation conditions are a major factor with respect to the radio link quality. Radio waves may be reflected, diffracted, refracted, scattered, depolarized and attenuated. The radio signal may also be received several times due to reflections. For example, phase shifts, which are one of the possible effects, can cause frequency selective fading. Propagation conditions can vary considerably due to mobility of the sending or receiving nodes, or changes in the environment of the communication link. All of these factors can significantly decrease the signal quality.

### Multipath

For WLANs, propagation of radio waves over several paths is one of the most prominent phenomenons. WLANs are often used indoor or in urban areas where reflection often occurs (see Figure 2.1). A first order effect of multipath is the arrival of several copies of the same signal at various time instants with different attenuation coefficients, and often with phase shifts at the intended receiver. The signal copies interfere with each other leading to second order effects like amplification or fadign of the signal, delay spread, and Inter-Symbol-Interference (ISI). In the majority of cases the original signal fades due to multipath propagation. This phenomenon is referred to as multipath fading. Direct Sequence Spread Spectrum (DSSS) as used by Institute of Electrical and Electronics Engineers (IEEE) 802.11 Local Area Network (LAN)s (see Section 2.2.2) is one technique to combat multipath fading.

### Path loss

I refer to signal power degradation over distance (propagation loss) as path loss. There are many different models describing the path loss. These models are often derived using a combination of analytical and empirical methods. A very common model is the Log-distance Path Loss Model (Eq. 2.1, see [76]).

$$\overline{PL}(d) \propto \left(\frac{d}{d_0}\right)^n \tag{2.1}$$

$\mathrm{PL}$ is the path loss, $d$ is the transmitter receiver distance and $d_0$ is the close-in reference distance. $n$ is the path loss exponent which defines the rate at which the path loss increases. This parameter depends on the environment. Typical path loss exponents are given in Appendix B.2. I generally assume Line-Of-Sight (LOS) indoor communication and in turn a path loss exponent of $2$.

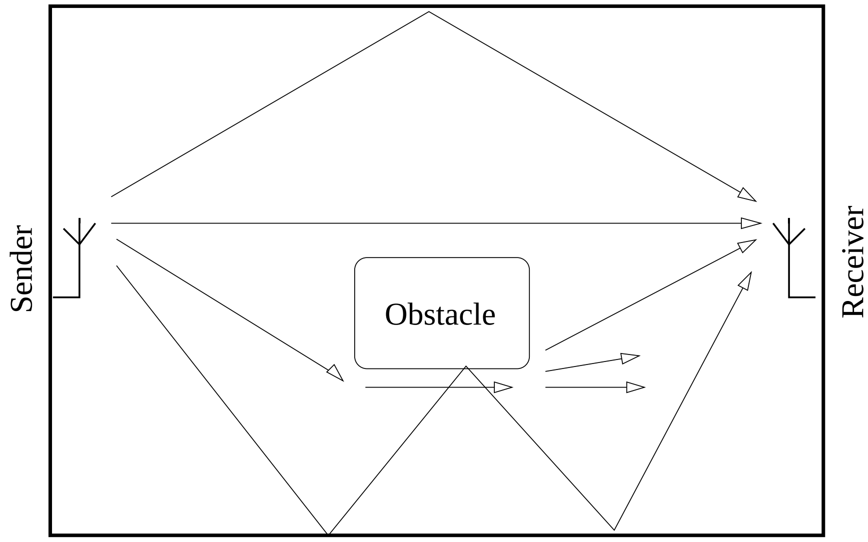


Figure 2.1: Multipath propagation

**Interference**

Interference is not only a result of multipath. There is also white noise and system-generated interference. The latter can be caused by electrical systems leaking energy into the frequency band, causing a certain noise floor which is generally higher in urban areas. Alternatively, interference can be caused by a system sending on the same frequency channel belonging to the same or another network (cell). Both cases can also be referred to as (signal) collision; the latter case is referred to as co-channel interference. Another type of interference is adjacent channel interference, which is a result of signals on adjacent frequencies and imperfect receiver filters. Imperfect filters allow neighbor frequencies to leak into the pass band.

**WLAN frequency bands**

The FCC in the USA and CEPT in Europe assigned the ISM band to be used by WLANs. The ISM band is reserved for several industrial, scientific, and medical applications (see

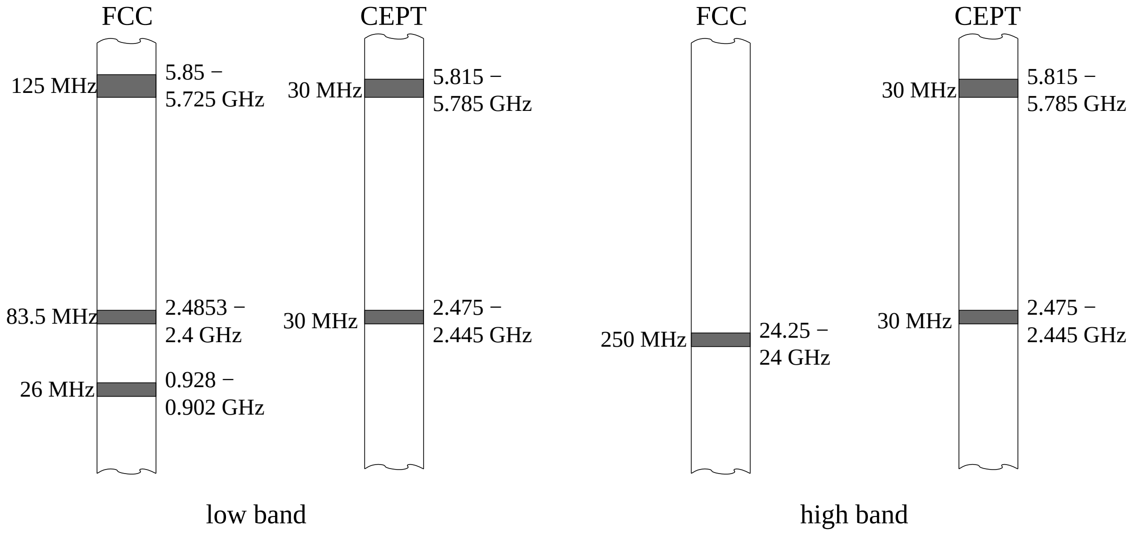


Figure 2.2: ISM bands

Figure 2.2). IEEE 802.11b WLANs use the 2.4Ghz band with a bandwidth of 2 MHz.

### 2.1.2 Link budget analyis

I briefly present the basics of the link budget analysis (LBA, see[87, 101]) by which a radio is dimensioned. As one of the main results, the RF power can be calculated for a given set of parameters and requirements (e.g., level of link reliability or Bit Error Rate (BER)). We need to compute the RF transmission power for the sake of determining the wireless network performance, the interference level, and the power consumed by the RF amplifier. One of the important LBA factors is the thermal (channel) noise $N$ (in Watts). The thermal noise $N$ is defined as

$$N = kTB, \tag{2.2}$$

where $k$ = Boltzmann constant ($1.38 \cdot 10^{-23}$ J/K), $T$ = system temperature (Kelvin) and $B$ = channel bandwidth (Hz). Another important LBA factor is the distance. In free space the power of the radio signal decreases with the square of the distance. The path loss $L$ $(dB)$ for Line-Of-Sight (LOS) wave propagation is given as

$$L = 20 \log_{10}(4\pi D/\lambda), \tag{2.3}$$

where $D$ = distance between transmitter and receiver (meters) and $\lambda$ = free space wave length (meters). $\lambda$ is defined as $c/f$, where $c$ is the speed of light ($3 \cdot 10^8$m/s) and $f$ is the frequency (Hz). The formula has to be modified for indoor use, since the path loss normally is higher and location dependent. As a rule of thumb, LOS path loss is valid for the first seven meters. Beyond seven meters, the degradation is up to 30 dB every 30 meters (see [101]). RF indoor propagation very likely results in multi-path fading causing partial signal cancellation. Fading due to multi-path propagation can result in a signal reduction of more than 30db. The signal is almost never completely canceled. Therefore one can add a priori a certain amount of power to the sender signal, referred to as *fade margin* ($L_{fade}$), to minimize the effects of signal cancellation. A further factor to take into consideration is the Signal-to-Noise-Ratio (SNR), defined by

$$SNR = \frac{E_\mathrm{b}}{N_0} \cdot \frac{R}{B_\mathrm{T}}, \tag{2.4}$$

where $E_b$ = energy required per information bit (Watt), $N_0$ = thermal noise in 1 Hz of bandwidth (Watt), $R$ = system data rate (bit/s) and $B_T$ is the unspreaded bandwidth of the signal (Hz). The SNR is the required difference between the radio signal and noise power to achieve a certain level of link reliability. $E_b/N_0$, which can be obtained by transforming Equation 2.4, is the required energy per bit relative to the noise power to achieve a given BER:

$$\frac{E_\mathrm{b}}{N_0} = \frac{\mathrm{SNR}}{\frac{R}{B_\mathrm{T}}}. \tag{2.5}$$

Given a specific digital modulation scheme, the BER is a function of the Signal-to-Noise-Ratio (SNR). As described in Section 2.2.2, IEEE 802.11b uses 4 different modulation/coding schemes according to the used transmission rate. For 5.5 and 11 Mbit/s Complementary Code Keying (CCK) modulation is used, which is demanding to model. For simplicity I use a 16-QAM for 5.5 Mbit/s and a 256-QAM modulation for 11 Mbit/s instead to allow for an analytical solution. The M-ary QAM modulation is very well documented (see, e.g., [76]) and according to [10] and [41] similar results can be expected for the CCK modulation. Hence, the BER can be computed for an AWGN channel using equation (2.6) for DBPSK and DQPSK modulation[1] and equation (2.7) for 16-QAM and 256-QAM..

$$\mathrm{BER} = \frac{1}{2} e^{-\frac{E_\mathrm{b}}{N_0}} \tag{2.6}$$

$$\mathrm{BER} = \frac{2}{m}\left(1 - \frac{1}{\sqrt{M}}\right) \mathrm{erfc} \frac{E_\mathrm{b}}{N_0} \tag{2.7}$$

By solving Eqs. 2.6 and 2.7, respectively, for $E_b/N_0$ and using equation 2.4, we can now compute the required signal strength at the receiver $P_{rx}$. In addition to the channel noise we assume some noise of the receiver circuits ($N_{rx}$ in dB). The required signal strength at the receiver is given by

$$P_{rx} = N + N_{rx} + SNR. \tag{2.8}$$

Given $P_{rx}$ we can further compute the required RF power $P_{tx}$ (dBm) at the sender given by

$$P_{tx} = P_{rx} - G_{tx} - G_{rx} + L + L_{fade}, \tag{2.9}$$

where $G_{tx}$ and $G_{rx}$ are transmitter and receiver antenna gain, respectively. For simplicity, we assume no antenna gain throughout this thesis.

## 2.2 An IEEE 802.11 primer

In recent years WLANs have become a proliferated network technology. There are several network standards of this type but only IEEE 802.11 has received this popularity. Therefore IEEE 802.11b is used throughout this thesis to conduct research on reduction of energy consumption. A comprehensive overview is given describing the important elements of

[1] The usage of a Gray code for DQPSK is assumed.

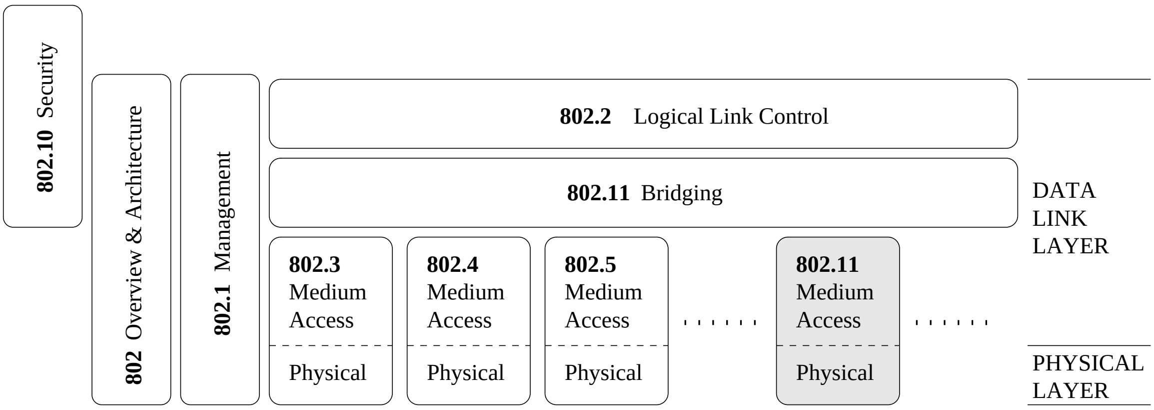


Figure 2.3: Structure of the 802 standard family

IEEE 802.11b: The physical layer, the medium access control protocol, and the power-saving mechanism.

IEEE 802.11 [20] belongs to the family of IEEE 802 standards, see Figure 2.3[2]. It describes a wireless Local Area Network (LAN) with similar characteristics as Ethernet-like LANs [22] offer. The root standard comprises the specification of the network architecture, the MAC layer, three different physical layer, and security issues. The physical layer specification has been amended over the time, now specifying data rates up to 11 [23] and 54 Mbits/s [19], respectively. Additionally functional and QoS support extensions have been developed.

The IEEE 802.11 standard family encompasses various competing technologies. Worth mentioning are HIgh PErformance Radio Local Area Network (HIPERLAN) Type I and II, Bluetooth and HomeRF. HIPERLAN Type I and II [21, 24] are the European counterparts of IEEE 802.11(a/b). HIPERLAN I defines an asynchronous medium access method and a transmission rate of 23,5 Mbits/s using Gaussian Minimum Shift Keying (GMSK). HIPERLAN II defines a synchronous medium access method and a physical layer, which is nearly compatible to the physical layer of IEEE 802.11a. WLANs of these types are supposed to work in the 5 GHz and 17 GHz band. Bluetooth [36] is an industry standard, which has

[2]This and the following figures of Section 2.2 are based on Figures as shown in [20, 23]. They are redrawn and modified to a certain degree to emphasize important elements.

been adopted by the IEEE 802.15 working group to specify a Wireless Personal Area Network (WPAN). Bluetooth addresses a wireless network interface with a very low power consumption to be used to connect peripheral devices to a master device. Therefore the transmission range is limited to a few meters and the raw data rate is 1 Mbits/s. The MAC protocol is based on a synchronous mechanism supporting time critical (up to three 64kbit/s voice connections) as well as non-time critical data (up to 700kbit/s). The physical layer uses Frequency Hopping Spread Spectrum (FHSS) in the 2.4G Hz band. The last major WLAN type network interface is HomeRF. HomeRF [61] has been designed to provide capabilities as needed in a customer premise network. HomeRF networks can work in two modes. One mode is based on an asynchronous medium access scheme for non-time critical data. The second mode is a blend of the synchronous and the asynchronous medium access scheme and therefore needs a base station to control the channel access. Up to eight voice connections, prioritized streaming media connections, and asynchronous data can be supported in a single radio cell. The physical layer is based on the physical layers as specified by the IEEE 802.11 standard. Raw data rates of up to 11 Mbits/s are supported.

The following sections describe the IEEE 802.11b standard to give an overview and to provide the knowledge needed to understand the work presented in later sections.

### 2.2.1 IEEE 802.11 architecture

The IEEE 802.11 architecture is rather complex but enables flexibility, fault tolerance and scalability. Flexibility is an inherent feature of wireless transmission. On the other hand the standard only specifies mechanisms. The policies that define the usage of these mechanisms have been left open in many cases. The distribution system, power-saving strategies, power control and scheduling strategies for time bounded services are left open and can be adapted to a specific application area. Fault tolerance is an inherent feature since there will be no single point of failure if the network is operated as an Independent Basic Service Set (IBSS). Instead, decision making is distributed among the mobile stations, which will permit the continuation of operation even if some nodes or a part of the WLAN network are out of order. Scalability means the opportunity to form a WLAN of arbitrary size. This is achieved by the opportunity to group a certain number of nodes into logical sets and the provision of operations for appropriate addressing, change of affiliation of nodes, and a flexible distribution system. However, some necessary services and protocols remained explicitly unaddressed (e.g., Distribution System (DS)) at the time the standard was written. The IEEE 802.11 architecture is based on the main building blocks Station, Basic Service Set (BSS), Extended Basic Service Set (ESS) and Distribution System (DS).

#### Station

The smallest IEEE 802.11 entity is a station. A station is a component that connects to the wireless medium. It consists of a MAC and a Physical Layer (PHY). A station can be portable, mobile, or embedded and offers fundamental services such as authentication, deauthentication, data delivery and privacy. In the following text a station may also be simply referred to as node.

#### Basic Service Set (BSS)

A BSS is a set of stations communicating with one another. A BSS does not refer to a sharply bounded area because of propagation uncertainties. If all stations within a BSS are mobile and there is no connection to a another (wired) network, the BSS will be referred to as *IBSS*. An IBSS is typically a short-lived network with a relatively small number of stations created for a temporary purpose, e.g., exchange files during a group meeting . All stations communicate directly with one another – there is no relaying capability. Therefore stations which are out of range cannot communicate with each other. An IBSS is also referred to as *ad hoc* network, which does not need any pre-planning to start operation. The investigations in this dissertation are based on an IBSS.

A BSS, which includes an *Access Point (AP)*, is called *infrastructure BSS*. The AP is a dedicated station, which provides additional functionality. Any communication among stations is routed via the access point. While this kind of two-way communication requires twice as much bandwidth, the advantages such as buffering of packets for a stations within the SLEEP mode, explicit assignment of bandwidth to stations, or improved coverage justify the usage of an AP. The AP is also defined as a portal to the wired network or to a DS as explained later.

### Distribution System (DS)

The DS is the architectural component that interconnects multiple BSSs to enable larger WLAN networks. It enables mobility by providing the logical services necessary to handle address destination mapping and seamless integration of multiple BSSs. The AP is a dedicated station that provides access to and from the DS by delivering DS services and acting as a station in parallel. The DS is not specified in the IEEE 802.11 standard family yet.

### Extended Basic Service Set (ESS)

The DS and BSSs allow to form a wireless network of arbitrary size and complexity. This type of network is referred to as Extended Basic Service Set (ESS). All stations within an ESS may communicate with one another and mobile stations may move from one BSS to another. Thereby BSSs can be physically disjoint or colocated, or they can be partially or completely overlapping.

### Services

There are nine services defined by the IEEE 802.11 architecture: four station services and five DS services. These services interact with each other, i.e., some services will only be available if certain other services are used before. This is expressed by a simple bidirectional interconnected three-state machine as shown in Figure 2.4: State1 – Unauthenticated/Unassociated, State2 – Authenticated/unassociated and State3 – Authenticated/Associated.

The station services are delivery, authentication, deauthentication and privacy. The delivery service provides an unreliable delivery from a MAC entity located at one station to the MAC entities located at other stations. The privacy service is designed to provide a protection level in a WLAN that is comparable to that of a wired LAN. Unfortunately it has been shown that the privacy service cannot fulfill this requirement (see e.g., [7, 93]). Therefore, further steps have to be taken to improve the level of privacy. The authentication and deauthentication services are similar to connecting a cable to a wired network. Only authenticated stations may use the data delivery service. The deauthentication service makes it possible to detract usage permissions of the delivery service of a previously authenticated station.

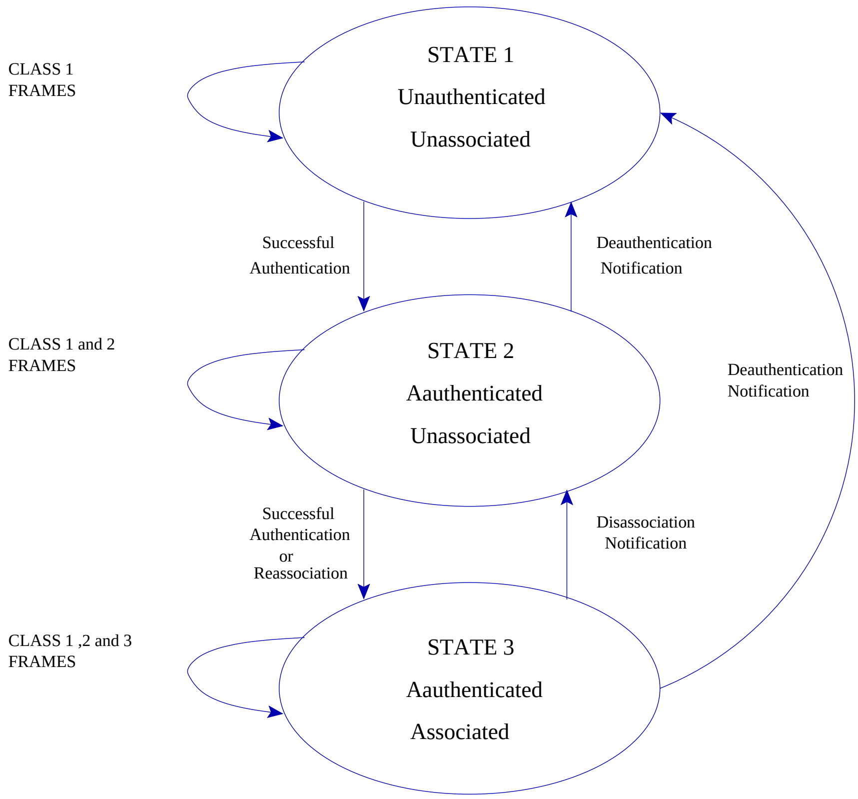


Figure 2.4: IEEE 802.11 service – state diagram

The DS services are association, reassociation, disassociation, distribution and integration. These services allow a station to move freely within an ESS and to connect to a WLAN infrastructure. The association service establishes a logical connection between a station and an AP. Reassociation equals the association service, but it additionally provides information about the former AP (BSS). This service is needed if a station moves to another BSS. Disassociation can be invoked by the AP or the station itself if the access point is unable or does not want to provide service to the station, or if the station wants to inform the access point that the service is no longer needed. The distribution service is used by the AP to decide how to deal with a packet. The access point has to determine whether a frame should be sent back to its own BSS or to the DS to send the frame to a mobile station of another BSS within the ESS. The integration service is used to connect a BSS or ESS to other LANs, e.g., an Ethernet. Therefore it contains portal functionality like conversion of frames and routing.

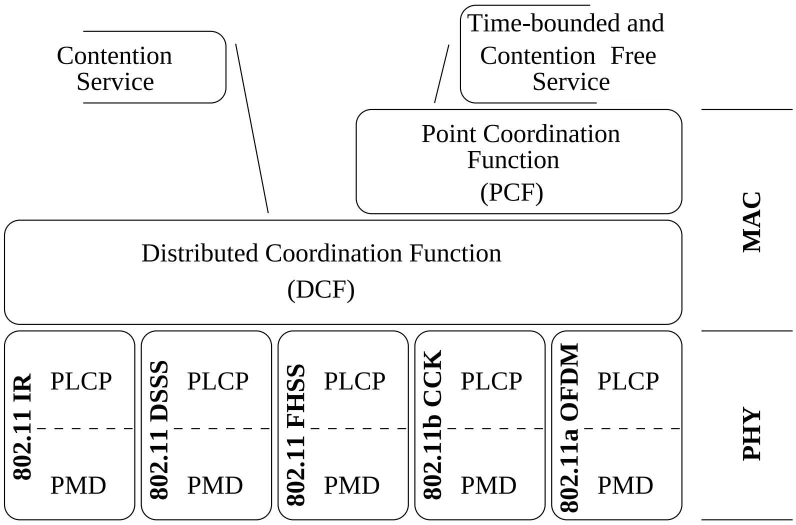


Figure 2.5: IEEE 802.11 protocol architecture

**Protocol architecture**

The IEEE 802.11 protocol architecture is depicted in Figure 2.5. Five different physical layers are available, which are subdivided further into a Physical Medium Dependent (PMD) and a Physical Layer Convergence Protocol (PLCP) layer. The PMD provides the actual interface to send and receive data between two or more nodes. The PLCP allows the IEEE 802.11 MAC to work with a minimum dependence on the PMD sublayer. This layer facilitates the provision of the PHY service interface to the MAC services. It opens the opportunity to use the same MAC protocol on top of several physical layers by offering the same interface. The MAC layer is situated on top of the physical layer and subdivides into a Distributed Coordination Function (DCF) and a Point Coordination Function (PCF). The DCF incorporates all basic MAC functionalities and provides for the fundamental contention service, which is similar to the asynchronous unreliable service offered by the well known IEEE 802.3 networks (see e.g. [22]). The optional PCF resides on top of the DCF and offers time bounded and contention free service. Only the DCF functionality is used later within the thesis. Not shown in the Figure 2.5 is a control plane for layer and inter-layer management.

### 2.2.2 IEEE 802.11 physical layer

The IEEE 802.11 standard family provides five physical layers based on Infrared (IR), FHSS, DSSS, DSSS with the use of CCK modulation, and Orthogonal Frequency Division Multiplexing (OFDM), respectively. DSSS is one of the most commonly used coding schemes in todays available products because of its simple implementation and good transmission characteristics. OFDM, which supports up to 54Mbps in its recent form, will probably play a major role in the near future as products are already available and the bandwidth/QoS requirements increase with the advent of media services such as video conferencing, video broadcasting, and voice services. In the following the DSSS PMD will be outlined in more detail because it is one of the basic elements of this dissertation.

**DSSS**

DSSS spreads the base band signal across a wide frequency band, which makes it more resistant against multi-path fading and frequency selective fading. The operation principle of DSSS at the transmitter's side is depicted in the upper part of Figure 2.6. The spread signal is sent through a correlator at the receiver site, which re-establishes the baseband signal using the same pseudo-random noise sequence (Barker codes) used for spreading. The effect on the frequency spectrum is shown in the lower part of Figure 2.6. The pseudo-random noise sequence spreads the signal across a wider frequency spectrum preserving the same total signal power. Then the signal characteristic is similar to white noise in some frequency band. The correlator reverses this operation and makes the signal post-processable.

The result after spreading is a high speed digital stream, which is modulated onto a carrier frequency using Differential Binary Phase Shift Keying (DBPSK) for the 1 Mbits/s transmission speed, Differential Quadrature Phase Shift Keying (DQPSK) for 2 Mbits/s at a symbol rate of 1 MSps. The transmission speed at 5.5 and 11 Mbits/s differs from the previous ones in that other pseudo-random noise sequences are used. At 5.5 Mbits/s, data bits are divided in groups of four where the first two data bits encode the spread sequence and the second two bits are used to QPSK-modulate (Quadrature Phase Shift Keying) the spread sequence. The used spreading codes are codes with good autocorrelation and cross-correlation properties. For 11 Mbits/s, six data bits are used to choose a spreading sequence from a certain set and two data bits are used to QPSK-modulate the

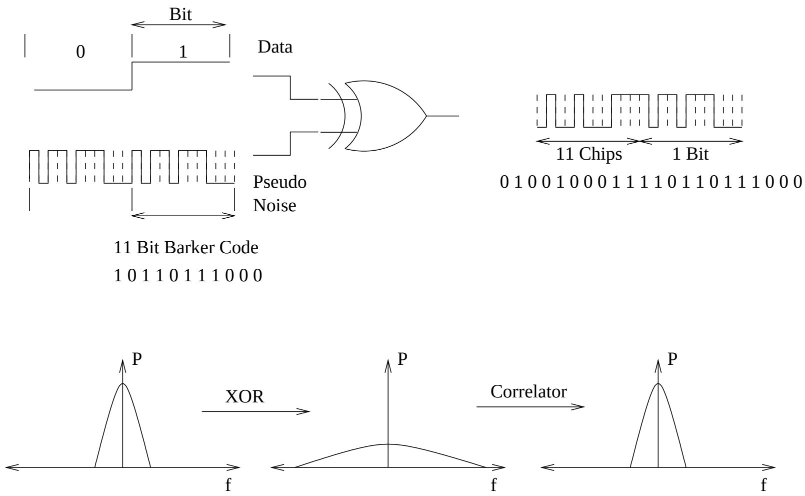


Figure 2.6: DSSS operation principle

spreading code. The spreading code has a length of eight chips (instead of 11 chips) and the symbol rate is 1.375 MSps. This modulation/coding approach is called Complementary Code Keying (CCK). In any case the chipping rate is 11 Mbps. There is also another optional modulation scheme referred to as Packet Binary Convolutional Coding (PBCC) for enhanced performance, which is not considered in the context of this thesis .

The two possible PLCP frame structures are depicted in Figure 2.7. The long preamble type frame is backwards compatible with the 1 and 2 Mbits/s version. It consists of a SYNC field (scrambled 1's) for receiver synchronization purposes, a Start Frame Delimiter (SFD) field marking the start of the frame, a Signal field indicating which data rate must be used to receive the Protocol Service Data Unit (PSDU), a Service field, which primarily indicates which type of modulation (CCK, PBCC) must be used to demodulate the PSDU, a Length field indicating the frame end to the receiver, and a Cyclic Redundancy Check (CRC) field used to check the correctness of the received header. The next field called PSDU contains the payload data. The preamble and the header are sent at 1 Mbits/s using DBPSK modulation. The PSDU is sent at the speed indicated by the Signal field. Since the long frame preamble imposes a considerable overhead at higher data rates, a frame with a short preamble, which is not backwards compatible to the 1 and 2 Mbits/s frame version with the long preamble, was introduced. Therefore all stations in a BSS will have to support a short

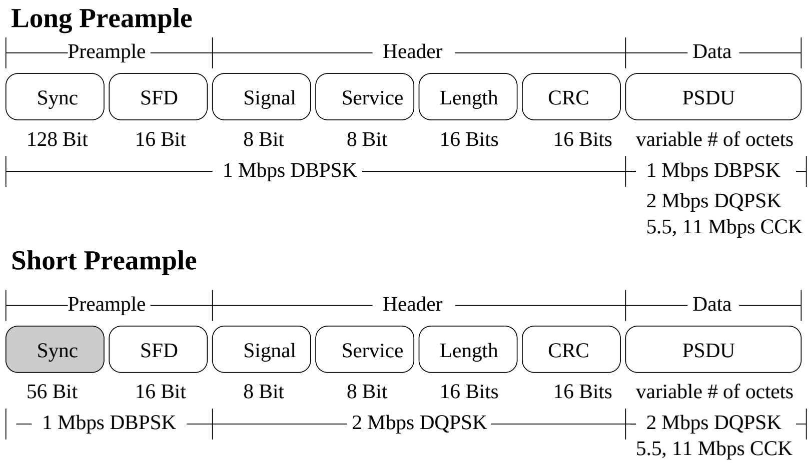


Figure 2.7: DSSS PLCP frame structures

preamble frame type if it is used by one station. A frame with a short preamble primarily differs from its counterpart in the SYNC field, which is considerably shorter and consists of scrambled $0$'s. The preamble part of the frame is sent at 1 Mbits/s while the header part of the frame is sent at 2 Mbits/s. The PSDU is sent at 2, 5.5 or 11 Mbits/s.

### 2.2.3 MAC protocol

The primary task of the IEEE 802.11 MAC protocol is to provide an efficient, fair, secure, and reliable data transfer service. Several problems arise if the communication medium is a radio channel. The MAC protocol has to take the noisy and unreliable channel into account. This includes that the channel conditions may change rapidly. Stations may not be able to communicate directly, which leads to the *Hidden terminal Problem* and *Exposed Terminal Problem*. In the first case, communication is established, although it possibly interferes with a packet reception of neighboring stations. In the Exposed Terminal Scenario no communication is established because of an ongoing communication between a pair of neighbor stations although their communication would not be impaired. The IEEE 802.11 MAC protocol deals with this and other problems and fulfills the requirements appropriately as mentioned above (see Table 2.1).

The basic MAC protocol is similar to the 802.3 MAC. It belongs to the Listen Before

| Problem | Counter Measure |
|---|---|
| Error-prone radio channel | immediate acknowledgements in conjunction with limited # of retransmissions and/or MAC packet fragmentation |
| Hidden Terminals | RTS/CTS mechanism |
| Exposed Terminal | — |
| Mobility, variation of channel quality | adjustable data rates |
| Distance | adjustable data rate / RF power level |
| Eavesdropping | RC4 encryption |
| Fairness | Rotating priorities |
| Reliability | Retransmissions |
| Power consumption | Power save mode |
| Efficiency | PCF mode for higher loads |

Table 2.1: Problems and countermeasures in radio communication

Talk (LBT) protocol class, but use additional features, e.g., immediate acknowledgments or channel reservation. The IEEE 802.11 MAC works in a distributed manner, although it also supports centralized control. This centralized control, which is not covered in this thesis, uses the basic distributed access scheme and requires a dedicated station (AP) as master. Distributed access and the centralized controlled access are interoperable.

#### Frame formats

An IEEE 802.11 frame as shown in Figure 2.8 basically consists of a frame header, a frame body, and a Frame Check Sequence (FCS). The MAC header appears to be very long, but not all fields are used for all MAC packets. The

**Frame Control** field comprises information needed by the receiving MAC to interpret the subsequent fields of the MAC header. Inter alia, it contains information about the type (data, control, management) and subtype (specific type of frame, e.g., Beacon) of the frame, whether the frame is a fragment and further fragments are outstanding, whether the frame is retried and encrypted, and what the power mode of a station is or will be after a successful frame exchange.

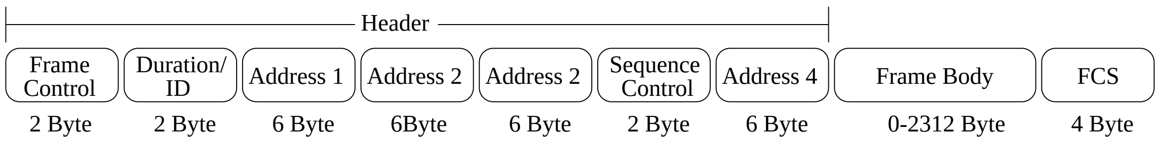


Figure 2.8: General IEEE 802.11 MAC frame format

**Duration/ID** field indicates how long an ongoing frame exchange lasts. The value is used to update the Network Allocation Vector (NAV), which provides a virtual carrier sense capability. If the frame is a Power Saving (PS)-Poll, the field contains the Association Identifier (AID).

**Address fields** describe the originator (source address) and/or the receiver (destination address) of a particular frame. Two additional address fields can be incorporated, depending on the type of the frame. These two fields are used to facilitate the level of indirection as necessary for transparent mobility and may be used for the BSS identifier (only probe request frames), for the transmitter address, and for the receiver address (which can be different from source and destination address because the frame is sent via an AP into another BSS).

**Sequence Control** field identifies the frame by a particular number and enables the receiver to detect duplicate frames. Four Bits of this field are used to number fragments if the packet is fragmented.

**Frame Body** contains the information specific to each data or management frame. It may be as long as 2312 Bytes to carry up to 2048 Bytes of data sent by applications. The remainder is used for higher layer protocol headers and trailers.

**FCS** field contains the result of the CCITT CRC-32 polynomial applied to the MAC header and the frame body. It is used to check the correctness of the entire MAC frame.

The actual frame composition using the aforementioned fields and its exact meaning depends on the type and subtype of the frame.

### DCF operation

DCF is the abbreviation for Distributed Coordination Function, the basic operation mode. The medium access rules of this mode are composed of several elements as described below. Some of them are optionally usable.

**Basic access mechanism** Carrier Sense Multiple Access / Collision Avoidance (CSMA/CA) is used for the basic access mechanism. It basically is a Multiple Access (MA) scheme with a Carrier Sense (CS) and a Collision Avoidance (CA) component. If the MAC receives a request to transmit a frame, it virtually (by means of the NAV) and physically checks the availability of the radio channel. If both indicators are positive for a Distributed Inter-Frame Space (DIFS) time interval[3], the frame transfer starts immediately. There may be an additional random delay introduced by the CA mechanism if there was an ongoing transmission while the transmit request was received. The CA mechanism is explained later in more detail. If no other station starts a frame transmission before the CA phase is over, the MAC will start the transmission of the frame. Afterwards the MAC awaits an Acknowledgment (ACK) from the receiver of the frame within a Short Inter-Frame Space (SIFS) time interval. Upon reception of the ACK the whole procedure starts over for a new request to transmit a frame, if any. Otherwise the frame is retransmitted until it is successfully received or the maximum retry counter expires. Retransmissions influence the CA mechanism as explained later. The basic access mechanism is depicted in Figure 2.9.

**Collision Avoidance (CA) Mechanism** A frame is usually transmitted without any delay after a silent DIFS listen interval during which the radio channel was idle. If there just was a transmission, contention for the radio channel is assumed, which can lead to a higher collision probability. The MAC counteracts contention with the CA mechanism, which basically introduces an additional delay before the actual frame transmission to spread the channel access of different stations in time. If the radio channel remains idle within in this random interval, the frame transmission is started. The interval is computed as shown in equation (2.10).

[3]The DIFS interval is replaced by a longer Extended Inter-Frame Space (EIFS) in case of a previous erroneous transmission attempt.

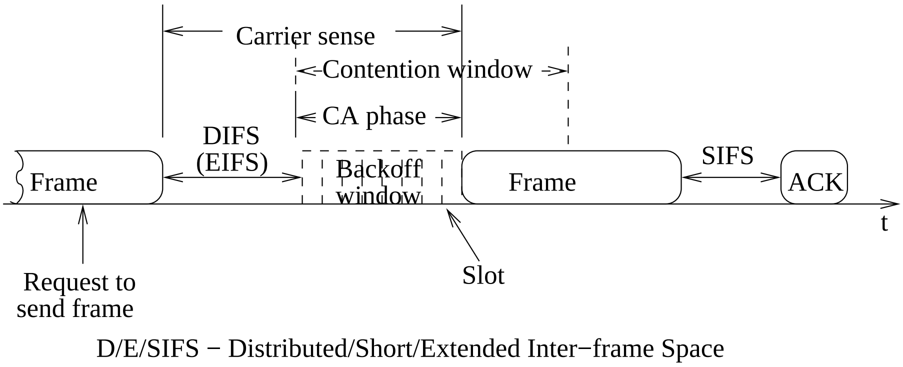


Figure 2.9: Basic access mechanism

$$\mathrm{BW} \sim \mathrm{uniform}(0, \mathrm{CW}) \times \mathrm{ST}, \tag{2.10}$$

where the Backoff Window (BW) constitutes the random delay, Contention Window (CW) is the upper limit of an interval to choose from, and Slot Time (ST) is a physical layer specific time. The CW is initially set to a minimum value and is increased with every retransmission of a certain frame according to Equation 2.11 up to a maximum value. After a successful frame transmission the CW is set back to its initial value.

$$\mathrm{CW(x)} = \begin{cases} 2^{\mathrm{m}} & \mathrm{x} = 1 \\ 2^{\mathrm{m+x-1}} - 1 & \mathrm{x} > 1 \text{ and } \mathrm{CW} \leq \mathrm{CW_{max}} \\ \mathrm{CW_{max}} & \text{else} \end{cases} \tag{2.11}$$

$m$ is a physical layer dependent parameter and $x$ is the number of the frame transmission attempt.

**Fairness** A station, which receives a signal from another station while listening to the radio channel during the BW interval, defers until the channel was idle for a DIFS interval again. Instead of computing a new BW value it uses the old value minus the time already spent during the BW interval of the previous channel access attempt. Therefore a station that lost the competition for channel access has a higher priority for the next channel access attempt.

**Virtual carrier sense (NAV)** To facilitate the assessment of the channel availability, the Network Allocation Vector (NAV) is used. It indicates usage of the channel, independent of the outcome of the physical layer channel assessment function. The NAV is set according to the duration field of a received frame. The duration field contains the time in microseconds (still) needed for a successful completion of the frame exchange sequence (e.g., DATA-ACK). Even if a station cannot detect the entire frame exchange, e.g. due to range limitations, it will not disturb an ongoing transmission by accessing the channel itself, since the set NAV indicates an unavailable channel. An example is given in Figure 2.10.

**Ready-to-Send (RTS)/Clear-to-Send (CTS) mechanism** The primary reason for using the RTS/CTS mechanism is the hidden terminal problem, where not all stations within a BSS or IBSS are aware of an ongoing transmission because of range limitations. As a result collisions can occur at the receiver. Therefore a four-way handshake transmission mode referred to as RTS/CTS mechanism can be used optionally. The RTS mechanism informs all stations in the vicinity of the sender about the start of a transmission. Although we could assume collisions only to occur at the receiver, the sender has to inform its vicinity as well, since it has to receive the ACK frame to complete a frame transfer successfully. Accordingly the intended receiver of a frame sends a CTS to inform its vicinity. The surrounding stations update their NAV and will not transmit as long as the NAV is set. The RTS frame may collide with other frames as well since the basic channel access rules apply. But the collision time, i.e., the total time between the start of the transmission of at least two frames and the end of the transmission of the frames, is significantly reduced as a secondary effect. Only short RTSs instead of the longer MAC Protocol Data Unit (MPDU)s collide. The RTS/CTS operation is shown exemplarily in Figure 2.10.

**Fragmentation** Fragmentation is an IEEE MAC feature to combat packet errors. Generally, long packets are more likely to be hit by an error than shorter packets. Therefore a frame can be split into several fragments if the frame size exceeds a certain adjustable threshold value. Fragmentation may be combined with the RTS/CTS mechanism. Fragmentation is transparent to the upper protocol layers. In order to transmit a fragmented frame efficiently, the frame is sent as a fragment burst as shown in Figure 2.10. Normal access

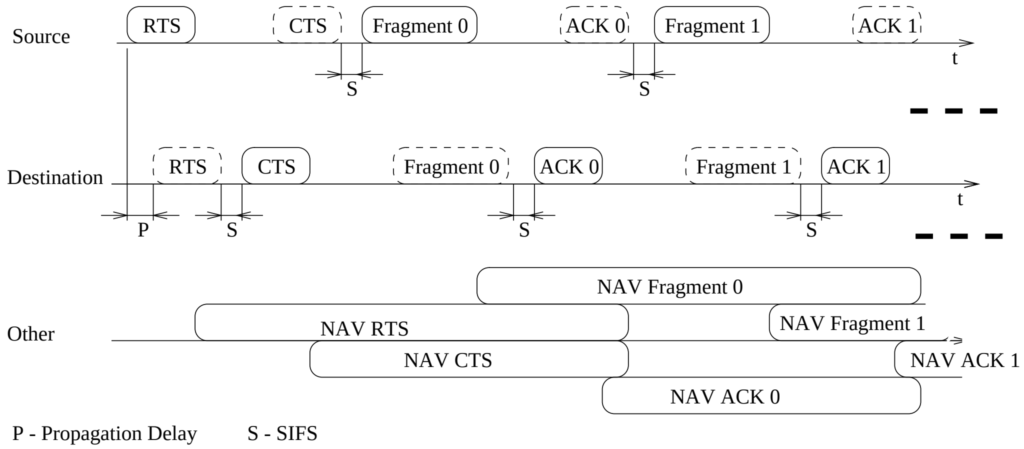


Figure 2.10: Frame fragment burst transmission and NAV setting
The figure shows the transmission of a fragmented MPDU. If there is no error, the transmission will take place continuously with small interruptions to receive the ACKs. Additionally, the setting of the NAV is shown for a station, which receives sender frames or receiver frames or both. The NAV may be overridden/extended by following frames.

rules apply for the first fragment. The remaining fragments are sent immediately after a SIFS, if the previous frame was acknowledged. If one fragment remains unacknowledged, the transmission of the frame is resumed with unacknowledged fragments following the basic access rules. In other words, instead of transmitting the entire frame again, which can incur a considerable overhead, only the missing part of the frame is sent.

The packet size plays a major role regarding the performance. The largest payload of a MAC packet is 2312 Bytes and the smallest is 0 Byte. Assuming an ideal radio channel, large packets would result in a high throughput performance because of the small overhead-payload ratio. However, the collision window and the channel access delay may be increased, in turn reducing the throughput. Small packets a priori lead to a lower throughput because of the higher overhead-payload ratio, but the packet error probability is reduced. Therefore the likelihood of a successful transmission over an impaired radio channel can be increased to a certain extent if shorter packets are used.

### PCF Operation – Centrally Controlled Access Mechanism

There is a second operation mode besides the DCF. The PCF mode, also referred to as centrally controlled access mechanism, is an option based on the DCF. The PCF enables the transmission of time critical data. The Point Coordination Function (PCF) provides a contention free frame transfer. A dedicated station referred to as AP takes on the functionality of a necessary Point Coordinator (PC). The PCF is based on the basic access mechanism and therefore enables both stations to use the contention free service, and stations lacking this functionality to work in a centrally controlled network. Details are not given because this function is neither used nor considered in this thesis.

**PHY layer dependencies**

The actual setting of MAC parameters like CW size and turnaround times heavily depend on the PHY layer and also determine the efficiency of the MAC mechanism. Selected values are shown in Appendix B, Section B.1.

### 2.2.4 Power Saving

Power consumption is crucial in mobile communications. Therefore a wireless Network Interface Card (NIC) should consume as little power as possible. Power Saving (PS) is an optional and complex function, which can be used in IBSSs or infrastructure BSSs. The latter is not considered, since this thesis focuses on ad hoc networks. The principle of power-saving in IEEE 802.11 is to turn off the transmission and reception hardware (NIC). Although IEEE 802.11 does not define under which circumstances a station can enter the PS mode, it is obvious to turn off the transmission/reception circuitry if no traffic has to be served. Unfortunately, several problems arise that can result in the opposite effect of power-saving if not appropriately addressed. The "turn off" mechanism creates two problems to be solved:

- How does a station send packets to another station in power saving mode?
- How does a station in power save mode receive packets?

IEEE 802.11 power saving is based on buffering and synchronization. Packets destined to a station in PS mode have to be buffered until the station is "awake" to receive buffered packets. Stations have to be synchronized in a such manner that packets are only transmitted if the intended receiver is ready (awake) for reception. In infrastructure mode, buffering and synchronization is performed centrally by the AP. It is more complicated in an IBSS network, since buffering and synchronization have to be performed in a distributed manner. Eventually PS in IEEE 802.11 networks is implemented by means of a timing synchronization function and the actual PS function, which are described in the following subsections. Current WLANs implement power saving for the ad hoc (DCF) mode.

### Timing Synchronization Function

The purpose of the PS Timing Synchronization Function (TSF) is to provide globally known instants in an IBSS (or BSS) where stations in PS mode can be informed about pending traffic of other stations. Therefore all stations within one IBSS have to be synchronized to a common clock.

In an IBSS, timing synchronization is achieved in a distributed manner. All station are capable to generate and send a beacon packet containing a copy of its own timer. Stations that receive a beacon adopt the time value if it is later than its own timing value. In a long run all station tend to have the "earliest" time of all nodes[4].

Beacons have to be sent at a rate determined by the *BeaconPeriod*, which is contained in beacons and Probe response messages. Stations joining an IBSS must adopt this value. The beacon interval is established by the station, which started the IBSS. At the beginning of a Beacon interval all stations have to suspend ongoing backoff procedures of non-beacon traffic. All stations choose a random backoff delay from the interval $[0 \ldots (2 \times \mathrm{CW}_{\mathrm{min}})] \times \mathrm{ST}$ and backoff for this time after the wireless medium becomes idle. If another beacon arrives before the backoff timer expires, the beacon transmission is canceled. If the backoff timer expires and no other beacon has arrived, the beacon is transmitted. Hence, convergence of the the synchronization algorithm is only probabilistic. Figure 2.11 depicts the beacon generation process.

### Power Saving function

The PS function describes the necessary steps for a station in PS mode to turn off the transmitter/receiver circuitry, to inform other stations or to retrieve information about pending

[4]Every NIC harbors a local clock. Time synchronization does not effect the operating system clock .

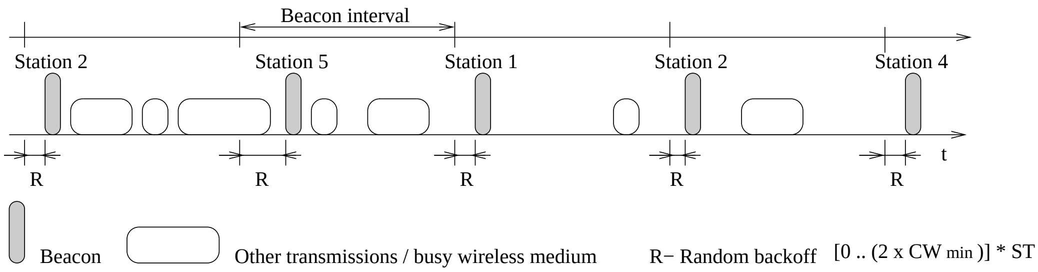


Figure 2.11: Beacon generation in an IBSS

packets, and to transmit or receive traffic. The PS function is different for ad hoc and infrastructure networks.

The Power Saving function for an IBSS (ad hoc network) operates in a distributed manner. That is, frames destined to nodes in PS mode have to be buffered locally instead at a centralized facility. A station, which wants to enter the PS mode, has to successfully complete a frame exchange with another station with the power bit set in the frame header. Note that neither a specific nor all stations need to be informed. Once the frame exchange has been successfully completed, the station may enter the PS state. In the PS state the station has to wake up periodically at the estimated time of a beacon transmission. The station is further required to stay "awake" for a period referred to as Asynchronous Traffic Indication Map (ATIM) window to receive announcements from other stations with buffered traffic. The ATIM window can be used by the station itself to announce buffered traffic. If there is no traffic announcement for the station, the PS state is reentered. If an announcement in the form of an ATIM arrives, the station has to acknowledge the ATIM and has to stay "awake" beyond the ATIM window until all of the announced buffered frames were received. During the data frame transmission period which follows the ATIM window, announced traffic can be sent following the basic channel access rules. Both form the Beacon interval.

The PS specification requires a station desiring to transmit a frame to another station to estimates the power save status of the other station. The estimate can be based on local informations and/or the last data frame exchange with that station. The IEEE standard leaves the solution of the problem how the estimate is created and on which information the estimate is based open. If the sending station determines that the receiving station is in

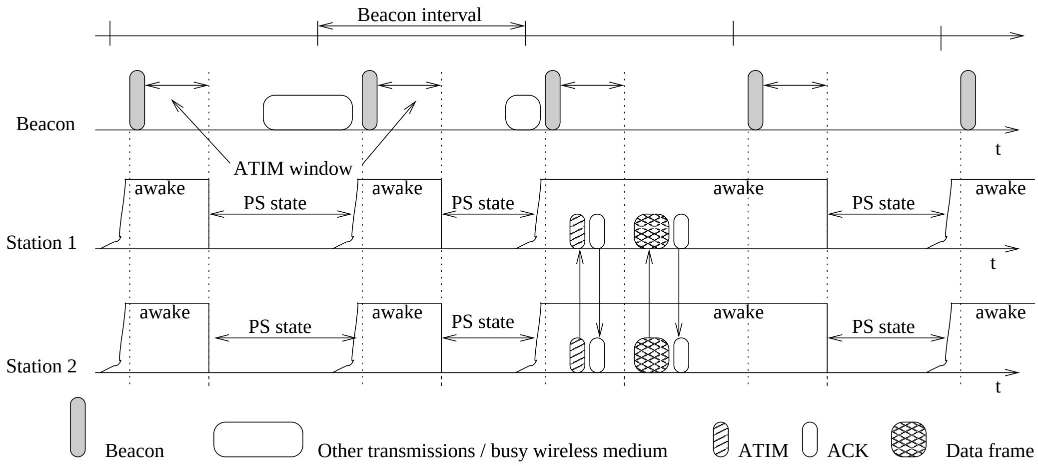


Figure 2.12: PS operation in a IBSS

The figure shows two stations operating in PS mode. Both stations are required to wake up upon every Beacon and to listen throughout the ATIM window. Station 2 wishes to send a frame to station 1 and therefore announces that frame by an ATIM. Station 1 responds with an ACK whereupon station 2 starts data frame transmission after completion of the ATIM window.

the PS state, the sending station creates an ATIM, which is sent during the ATIM window. Once the ACK of the intended station is received, the station send the data frame after completion of the ATIM window. For this thesis it is assumed that a station always is in PS mode if it has not explicitly indicated that it will stay awake by an ACK in response to an ATIM (even in the case that it is awake because it has pending traffic). Multicast frames must also be announced by the sending station during the ATIM window before transmitting the data frame. Both multicast ATIM and multicast data frame do not need to be acknowledged. The transmission of ATIMs during the ATIM window is randomized by means of the backoff procedure as described before. The backoff procedure uses a CW window size of exactly $\mathrm{CW}_{\mathrm{min}}$ independent of whether it is an initial transmission of an ATIM or a retry. The transmission of data frames follows the normal DCF access procedure. An example of the PS operation in an IBSS given in Figure 2.12.

### Power Saving potential

There are significant differences in the PS function for infrastructure BSSs and IBSSs, which lead to differences in their PS potential. PS in the IBSS places a larger burden on the mobile station than in the BSS with AP case, since (mobile) stations are responsible for beacon management and transmission. In addition, announcements (ATIMs) have to be generated and transmitted, and corresponding ACKs have to be received in order to transmit data frames. The buffering of frames also has to be performed by every station in PS mode. In a BSS these functions are performed centrally by the APs, which normally do not suffer from energy limitation because of a wired power supply.

Another significant difference is the ratio of PS state and "awake" state holding times, which tends to be more advantageous for BSS with AP. A station operating in a BSS with AP does not need to wake up every beacon time. Furthermore, stations can return to the PS state immediately after the beacon instead of staying awake for an ATIM window to listen for announcements, because the AP sends the announcements for buffered packets within the beacon without requiring acknowledgments.

The protocol overhead incurred by the backoff procedure prior to sending the announcements as well as possible collisions limit the PS potential. This overhead does not exist in a BSS with AP since generation of beacon and announcements are centrally managed by the AP. Another reason is the vulnerability of wireless transmission regarding the transmission range. It can be assumed that the AP has an exposed placement within an infrastructure BSS, while IBSS stations may suffer from range problems. This leads to necessary repetitions of ATIMs and data frames and less time to be in the PS state. Note that PS in an IBSS does not cover the case of hidden terminals. In this case PS can not be applied because of synchronization inconsistencies within the network.

## 2.3 Aironet PC4800B network interface

An early representative of WLAN network interfaces is Aironet's PC4800B Personal Computer Memory Card International Association (PCMCIA) interface that will be used later in this dissertation for power consumption measurements. I decided to use this WLAN network interface since it was one of the products that claimed to comply with the IEEE 802.11b specification and it was the only one with a freely available Linux source driver (at the time I planned the measurements). The circuitry of this card is based on the formerly popular PRISM I 11 Mbit/s chipset from the Intersil Corporation (formerly Harris), USA. A schematic of the chipset is shown in Figure 2.13.

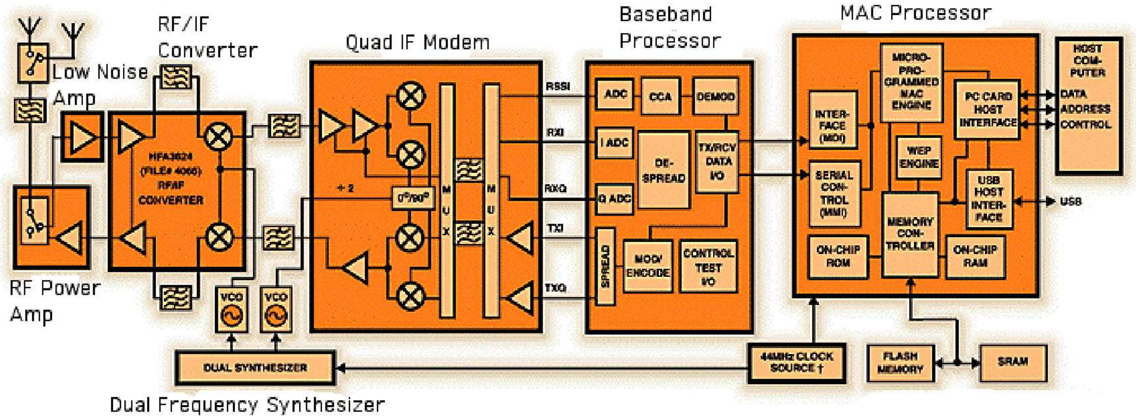


Figure 2.13: Schematic of Intersil's PRISM1 chipset [32]

The PC4800B network interface can work in infrastructure as well as ad hoc mode. The latter is used for measurements. It only implements the DCF with additional options such as power-saving, fragmentation, RTS/CTS, etc. The supported packet sizes range from 0 Byte up to 2312 Bytes. The PRISM I 11 Mbit/s circuitry supports transmission rates of 1, 2, 5.5, and 11 Mbit/s where RF transmission power levels of 1, 5, 20, and 50 mW can be chosen.

### 2.3.1 Generic hardware model

Abstracting the Aironet PC4800B NIC, a WLAN network interface consists of seven major logical blocks. These are realized by the PRISM I 11 Mbit/s chipset plus one IC for the MAC processor. These elements are sketched below in Figure 2.14. The antenna sends or receives the radio wave. Depending on the design, the antenna normally has a gain of 2 to 6 dB to ensure omni-directionality. The RF power amplifier amplifies the transmission signal. The signal strength determines coverage and signal quality at the receiver. The RF/IF block converts the intermediate frequency signal to the actual 2.4 GHz radio signal and vice versa. The IF modem modulates and demodulates the baseband signal and the intermediate frequency signal respectively. The baseband processor does the baseband work such as spreading/despreading and modulation/demodulation according to the modulation type, e.g., Binary Phase Shift Keying (BPSK), Quadrature Phase Shift Keying (QPSK), or CCK. The MAC processor and some additional Integrated Circuits (IC)s are responsible

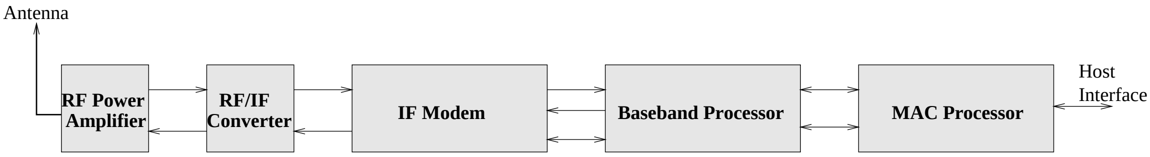


Figure 2.14: Generic WLAN network interface

for performing the MAC protocol and associated tasks such as packaging of information or computation of checksums. The host interface depends on the form factor; in our case a PCMCIA interface. All of these building blocks consume a certain amount of power depending on the operation mode and parameterization that sum up to the power consumption of the WLAN network interface.

### 2.3.2 Operation modes and power consumption estimates

Aironet's network interface consumes power depending on the actual task in five different modes: Transmit (TX), Receive (RX), IDLE, SLEEP and OFF. Each logical block of the generic WLAN network interface (see Figure 2.14) consumes a certain amount of power in these modes. Table 2.2 shows the power consumption estimates of the WLAN network interface building blocks, which were extracted from the data sheets of the PRISM I IC. The bottom line of the table represents the total power consumption. This is the power consumption estimate of the network interface in a certain operation mode. Note that the actual power consumption can vastly deviate from the estimates, as it is difficult to incorporate all parameter settings, e.g., the RF power level or the modulation type. This motivates measurements that further clarify the power consumption. However, the estimates show that the TX mode followed by the RX mode results in the highest power consumption. Thus it is most promising to investigate these power modes in more detail to reduce energy consumption of a WLAN network interface.

The data sheet of the PC4800B card provided on the manufacturer web site states an overall power consumption of 2.2 W in TX mode for an 100 mW RF transmission power level setting, 1.35 W in RX mode, and .075 W in SLEEP mode. IDLE mode is assumed to be similar to the RX mode since the card has to scan for a valid signal, which is similar

Table 2.2: Estimated power consumption of PC4800B in mW ($V_{dd}$=3V/5V, $I_{dd}$=max)

| IC/Mode | SLEEP | Idle | TX | RX |
|---|---|---|---|---|
| MAC | 5 | 40 | 125 | 125 |
| Baseband | 2 | 23 | 33 | 100 |
| IF Modem | 10 | 10 | 400 | 500 |
| Dual Freq. Synth. | .075 | .075 | 40 | 40 |
| RF/IF converter | .05 | .05 | 300 | 100 |
| Low noise amp. | off | 35 | of | 35 |
| RF power amp. | off | off | 1600 | off |
| max. total power | $\approx 20$ | $\approx 110$ | $\approx 2500$ | $\approx 900$ |

to being in RX mode. The trend of these power consumption values matches the computed total power values shown in table 2.2 quite well.

## 2.4 Battery characteristics

It is known that batteries do not exhaust linearily and that batteries have the ability to recharge themselves to a certain degree after a rest period. The understanding of these characteristics is important for achieving a better battery utilization. Therefore I give a brief overview of battery technology and discharge characteristics.

The demand for electric power in portable consumer devices is increasing rapidly instead of falling. This is a result of the integration of many different functions, powerful processors and communication interfaces into portable communications devices to support customer demands. Currently, primary and rechargeable batteries are the state of the art power sources for portable and mobile devices, although alternative concepts are being developed [82].

Lithium-ion batteries are the preferred type of high performance batteries besides Nickel-Cadmium (NiCd) and Nickel-Metal-Hydride (NiMH) batteries (see Figure 2.15 and Table 2.3). They offer a very high energy density. All battery types have a self-recharge effect after relaxation time. The use of this effect would increase battery durability, but it is not clear whether the power-saving function of WLANs can exploit this phenomenon.

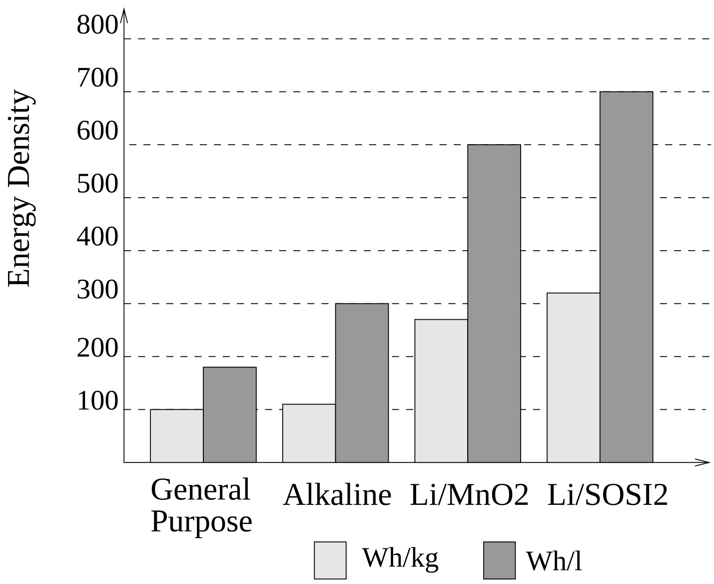


Figure 2.15: Energy densities of selected primary battery types

### 2.4.1 Continuous discharge

The energy of the battery is delivered by an electro-chemical conversion process. Batteries consist of one or more cells, which store chemical energy. Each cell consists of an anode, a cathode and the electrolyte between the two electrodes. The electrolyte is the media through which ions travel from the cathode to the anode.

The quantity of the active material in a cell (e.g., Lithium) limits the electrical energy that can be delivered. Additionally the delivered energy depends on the characteristics and the intensity of the discharge process. In other words, the delivered energy depends on the current and the continuity of the discharge process.

The theoretical capacity of the battery (in Ah) equals the chemical energy. In practice it is impossible to completely exhaust a battery. A battery is therefore usually labeled with a nominal capacity which is smaller than the theoretical capacity. During the discharge process the battery voltage decreases. The voltage, at which a battery is considered empty, is referred to as cut-off voltage. Henceforward, the nominal capacity (in Ah) is defined by the discharge of the battery with a constant current at a discharge rate $C$ to a defined cut-off voltage. The discharge rate C defines the current needed to discharge the battery in one

Table 2.3: Energy densities of selected rechargeable battery types

| Characteristic / Type | LiPB | LiB | NICd | NiMH |
|---|---|---|---|---|
| Voltage (V) | 3.7 to 3.8 | 3.7 | 1.2 | 1.2 |
| Gravimetric energy densitiy | 120 to 160 | 120 to 160 | 40 to 80 | 60 to 80 |
| Volumetric energy density | 230 to 270 | 230 to 270 | 120 | 150 |
| Cycle life | 500 | 500 | 2000 | 1000 |
| Memory effect | No | No | Yes | Yes |

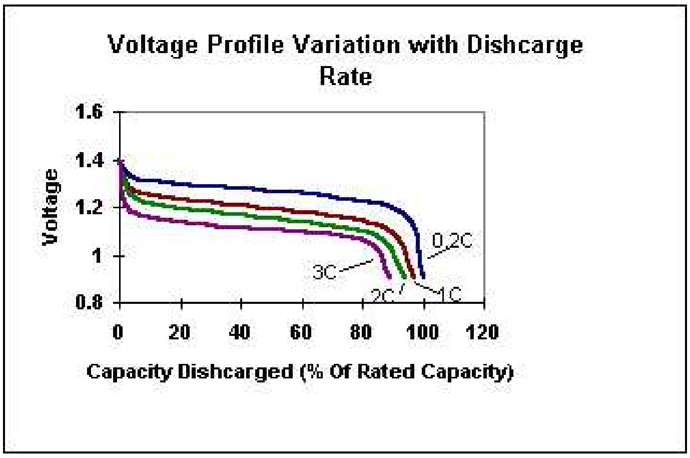


Figure 2.16: Continuous discharge with different C's [17]

hour[5]. The discharge rate also defines the durability of the battery as shown in Figure 2.16. A rule of thumb is that the available capacity with a C/5 discharge rate is 10% higher than that with a C discharge rate (see [92]).

## 2.4.2 Pulsed discharge

We mentioned above that even under ideal conditions it is impossible to exhaust the battery to its theoretical capacity limit. But it is possible to move the nominal capacity closer to the theoretical capacity using the so called self-recharge process. During the discharge process

[5]Some battery manufacturers measure the capacity at a discharge rate of C/5, which means a complete discharge of the battery within 5 hours. For example, the discharge current for an ideal battery of 600 mAh at C is 600 mA, and at C/5 120 mA respectively.

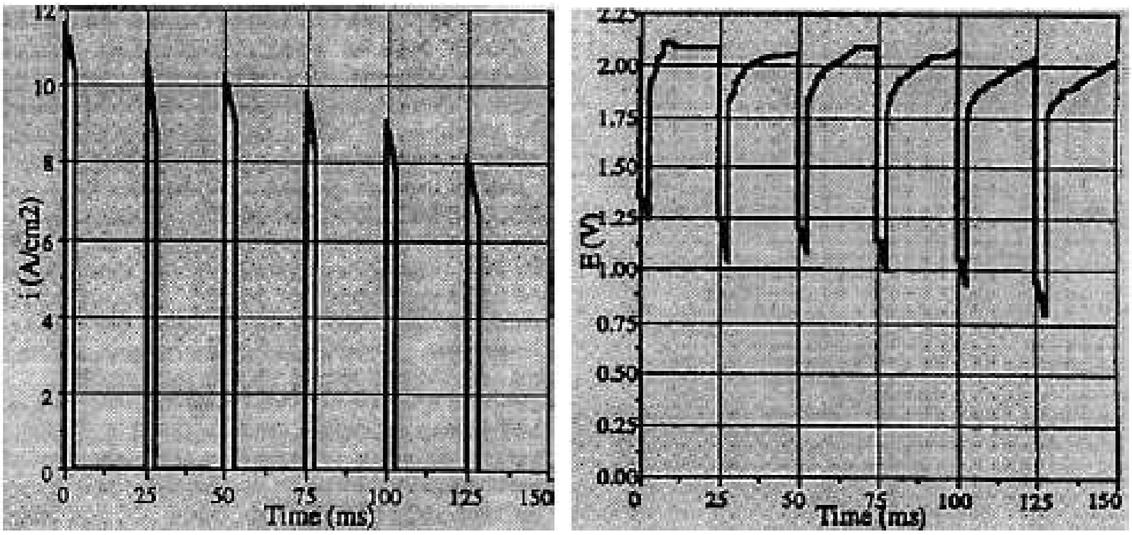


(a) Discharge (b) Self-Recovery

Figure 2.17: Pulsed discharge characteristics of a lead acid battery [51].
The pulse length is 3ms and the rest period is 22ms.

active material, which is initially uniformly distributed in the electrolyte of the battery, is consumed. Therefore, the concentration of active material decreases continuously. By the same token another phenomenon, a concentration gradient of active material, can appear. This is also referred to as polarization effect: The electrodes consume the active material. Depending on the discharge rate $C$, the diffusion process is too slow to reconcile active material concentration. As a result the electro-chemical conversion process slows down and consequently the voltage drops. From this it follows that self-recharge compensates active material concentration differences in the electrolyte by diffusion during discharge pauses. Another lesson to be learned is that a battery can even be discharged at high rates without depleting it faster if there is enough regeneration time every once in a while.

This is backed by the experiments presented in [51]. Here a lead acid battery pulse-discharged as shown in Figure 2.17. Obviously, the battery is able to recover the initial voltage value during the first rest periods. After four discharge pulses the battery voltage slightly decreases. This is an indication that the recharge process depends on the charge state of the battery. Furthermore the length of the rest period also plays a significant role. To take advantage of the self-recharge phenomenon it is necessary for a battery powered device to either work intermittently or that the current is reduced to a very low level from time to time. For example, the formerly mentioned condition might be the case for sensor nodes, which acquire data and communicate it from time to time, but sleep or power off in between. The latter strategy is also followed by cell phones, which only consume power for keep alive functions if not in use. Summarized, exploiting pulsed discharge yields longer intervals for replacement or recharge of batteries, less (toxic) waste and finally more convenience.

# Chapter 3

# Related work

This section briefly reviews the major protocol concepts of power saving suitable for WLANs. A comprehensive overview of power saving techniques for personal communications systems and mobile computing starting from the physical layer up to the application software level is given in [69], while this section reviews work on energy saving from the communication protocol perspective.

## 3.1 Measurement of WLAN power consumption

While the power consumption of mobile computers and their components such as Central Processing Unit (CPU), Display, hard disk, etc. is often targeted (see [55]), power measurements of WLAN interfaces are seldom covered in literature. Although data sheets for WLAN ICs including power consumption data are available, it is difficult to deduce the power consumption of the rather complex WLAN interface hardware. Even worse, the resulting energy consumption additionally depends on used protocols, processing elements and parameter sets, which make it hard to calculate from the data sheets. Therefore, measurements are necessary to identify energy saving options.

### 3.1.1 System measurements

The very first results on power consumption of WLANs are reported in [88] by Stemm and Katz. They measured the power consumption of a Metricom Ricochet and a WaveLAN

AT&T network interface in conjunction with different host devices. The results are used to investigate the energy efficiency of various transport protocols and applications such as mail and the World Wide WEB (WWW). They are further used to formulate a power saving strategy in the form of an explicitly controlled On/Off switching of the NIC. Although the measurement results are outdated, the developed power saving approach is still current and may be adapted to newer wireless network interfaces. Furthermore the proposed power measurement methodology is used in many later publications on power measurements of WLANs and wireless devices (see e.g., [15]).

Kravets et al. [48, 49] concentrate on measurements of the accumulated energy consumption of a wireless node as a complete system. The measurements are based on sampling the current consumption of a notebook in IDLE mode and during sending and receiving network traffic across its WLAN interface. The authors argue that the battery life depends on the system as a whole and emphasize the need to optimize the overall transmission process. Their results indicate that the WLAN interface plays a minor role in the energy consumption of the entire system. A method like this is a good approach to minimize a specific system, but is not easily applicable to other devices. This is particularly true for systems equipped with customized low power components, e.g., PDAs and subnotebooks, where a wireless network interface plays an important role in power consumption. Furthermore the measurement approach does not reveal details of the power consumption of the WLAN interface in order to develop optimizations concerning only the wireless interface.

Flinn and Satyanarayanan [30] follow an energy profiling approach in combination with an adaptable application fidelity to save energy. By means of the PowerScope profiling tool and an external digital multimeter, the energy consumption is mapped to specific software components, including the energy consumption of a WaveLAN interface while performing a network interrupt. They have shown that by adapting the application fidelity, e.g,. reducing the quality of the speech synthesizer or video, a considerable amount of energy can be saved. They additionally proposed a target-directed energy adaption scheme where the user specifies the operation time of the mobile device. The adaption mechanism then controls the fidelity based on energy consumption data collected for certain processes, which have to be performed if certain applications run, to meet the requested operation time.

### 3.1.2 WLAN NIC measurements

The measurements reported in [27] by Feeney and Nilson provide detailed energy consumption data. The hardware under scrutiny were Lucent WaveLAN 802.11 PCMCIA "Silver" and "Bronze" NICs running in ad hoc mode configuration. The instantaneous power consumption was measured in different working modes (TX, RX, IDLE and SLEEP) for 2 and 11 Mbit/s. The detailed power consumption during TX, RX, and IDLE processes as a whole were measured and the energy consumption was derived in the form of linear equations. The measurements indicate how modulation influences the energy consumption although no values for 1 and 5.5 Mbit/s are given. In addition the measurements do not state at which RF power level the NIC works and how the RF power level impacts power consumption. This is important because the power amplifier has a strong impact on the power consumption of a WLAN interface.

Further power consumption measurements are contained in the WLAN product specifications, which are normally published on the manufacturer WWW pages. The power consumption normally is given as an average for every working mode and there is no differentiation between modulation scheme and RF transmission power level. Nevertheless, these values might be used for a rough verification of measurement results.

## 3.2 Protocol techniques for power saving

While the underlying hardware determines the general power consumption characteristics of a wireless communication device, communication protocols can exploit these characteristics to save energy. This section gives an overview which parameters and mechanisms of communication protocols can have a large impact on the overall power consumption and energy efficiency of wireless communication devices. It also highlights major approaches to improve communication protocols regarding these metrics.

### 3.2.1 Transmission power control

**Choosing transmission power to communicate with a given partner** In the majority of cases transmission power control is used to optimally communicate with a given receiver, for example achieving a certain SNR under the constraint of a low interference to other communicating nodes. The signal amplification process is a power-intensive process. A very simple method for saving energy is the optimization of the amplifier to efficiently operate at the most commonly encountered transmission power. But a good amplifier efficiency on its own does not necessarily result in a low power consumption and the RF power has to be adjusted to cope with changing radio channel characteristics. Depending on the RF hardware, dynamically choosing transmission power can also save energy. In traditional cellular environments transmission power is adapted to account for signal degradation and interference (e.g., in CDMA systems). However, energy efficiency is usually not regarded as the primary optimization goal. In ad-hoc networks the situation is usually somewhat different: Ad-hoc networking is often identified with multi-hop communication and therefore power assignments are not necessarily controlled by a single (central) entity. If centralized knowledge is available, the necessary power setting is determined as described in [75], simultaneously controlling the network topology. Other approaches attempt to only use local information, either exploiting them heuristically [75, 26] or by integrating some additional data such as location [50, 80] or direction to neighboring nodes [96] to find optimum transmission power values by using distributed algorithms. Of high interest from a reliable and scalable point of view are the distributed algorithms of Rodoplu and Meng [80], who try to find the most energy-efficient neighbors to be used as relays[1] in the vicinity of a node, and Wattenhofer [96], who also tries to find the most energy-efficient neighbors using the angle of the received signal to estimate direction. These algorithms face a number of open problems: How are the time-varying characteristics of the radio channel taken into account by these algorithms? What about mobility? How does additional information like location correlate with the radio channel? What is the performance penalty if estimations are incorrect?

[1]A relay node constitutes a necessary and/or volitional indirection in the communication relation of two wireless nodes. A relay is comparable to a line driver or a bridge in the wired world.

**Adapting transmission power to the channel state** Depending on the channel state, transmission power can also be adapted on short time scales. Thereby if the channel quality is estimated as better, a lower transmission power is assigned resulting in less interference and power consumption by the amplifier. On the other hand if the channel quality is estimated as worse, a higher transmission power is assigned or the transmission process might be stopped temporarily until the communication channel is good again. Such an approach is followed in [99].

### 3.2.2 MAC techniques

Apart from deciding how much transmission power to use, the decision whether power should be invested at all is crucial, e.g., after a transmission fails due to collisions or bad channel conditions. The MAC layer decides about the point in time when a transmission starts.

**On/Off switching of network interface and processor** An promising method to save energy is to shut down nodes or network interfaces within a wireless network. The decision when to shut down can depend on the network as a cooperative system, or local information where each node optimizes the energy consumption for itself. The main problem is uncertainty of when the network interface has to be turned on again in combination with the fact that powering up an interface incurs both time and energy overhead. Power saving protocols as applied in common IEEE 802.11 WLAN cards [19] decide to turn off the network interface based on the traffic need. If a node has to transmit or receive data, it will stay awake; otherwise it can go asleep for a while to save energy. A node periodically has to check whether packets have to be sent or received, which requires a centralized or more complex distributed synchronization algorithm. In a centrally scheduled communication system, e.g., HiperLAN/2, some of these decisions are simplified. Because of the additional overhead in both time and energy to turn a transmitter on again, the scheduling periods (e.g., two milliseconds for HiperLAN/2) can be too short to justify an aggressive turning off. Turning off network interfaces can also be applied to multi-hop networks. For instance the ASCENT protocol [11] is a distributed protocol where each node assesses its connectivity and adapts its participation in the multi-hop network according to the measured operating region with the objective to minimize the network energy consumption. Similar concepts can be applied to the processor or other components of a mobile device or network interface. The processor is a particularly promising component, which can additionally enable a gradual adaptation of energy consumption and delivered performance by techniques like dynamic voltage scaling [70]. Such gradual strategy can be more effective than completely turning off a processor. However, a certain amount of previous knowledge about processing requirements is necessary. This information is available for many types of interactive applications. As many processor cores for embedded devices support this concept (e.g., Intel StrongArm), dynamic voltage scaling is promising for practical applications and could also be used for MAC and base band processors.

**Avoiding collision** Collisions may have several reasons. One reason might be the protocol itself which is explicitly designed to deal with (rare) collisions. Another reason is the network topology which may lead to hidden terminals. Collisions in turn cause retransmissions and waste of energy. Hidden terminals can be avoided by using a derivate of the PAMAS protocol [84], which is a more complex derivate of the MACA protocol [46]. It belongs to the class of single-channel-based busy tone protocols like the one published in [31]. MAC protocols, which are explicitly designed to work energy-efficiently,will avoid or minimize the likelihood of collisions during data transfer. An example is the EC-MAC protocol [29]. Centralized MAC protocols like HIPERLAN/2 also belong to this category as do other TDMA-based systems. The downside of these protocols is the additional synchronization overhead, which requires some energy as well. The tradeoff between these two aspects is crucial in evaluating the energy efficiency.

**Rate adaption** Another MAC option to conserve energy is to adapt the transmission rate according to varying channel conditions for the sake of an optimized throughput and a higher energy efficiency [41, 45]. If the channel quality decreases, a more robust modulation scheme is used which usually results in lower transmission rates. Rate adaptation may also be used to avoid energy-demanding radio processing. For instance, in HIPERLAN 1 [25] packet headers are sent at 1 Mbit/s while the payload information is sent at a rate of

23 Mbit/s; IEEE 802.11 follows a similar paradigm. Processing received data with a high data rate consumes considerably more energy than with low data rates. Therefore, based on the control information of the packet header sent at 1 Mbit/s (or 2 Mbit/s), a node can decide whether the payload should actually be received.

**Miscellaneous** In addition to the options mentioned above, energy-efficient scheduling, e.g., [71] and Section 3.2.3), and the problem of unnecessary TX/RX and RX/TX turnarounds should also be considered. The latter can be achieved by buffering data and sending it out in consecutive transmission slots [86]. This technique might not be applicable in interactive time-bounded applications.

### 3.2.3 Logical Link Control

While the MAC layer decides when to attempt to send a packet, the link layer control (LLC) determines the exact form of the packet, e.g., its size and how deal with errors. Most of the link layer procedures have a direct impact on the energy efficiency of a communication system.

**Packet size adaptation** On the link layer protocol level the packet size may be adapted according to the channel characteristics as proposed by Modiano in [58]. Modiano developed an ARQ protocol that automatically adapts the packet size to changing channel conditions (bit error rates) with the objective to improve the performance. As a side effect energy consumption is decreased while performance is increased. The challenge for this protocol is to obtain a sufficiently good estimate of the channel condition and the predictive power of such estimations.

**Combined FEC/ARQ schemes** While Automatic Repeat Request (ARQ) schemes simply repeat packets in the case of transmission errors, Forward Error Correction (FEC) contributes to a more robust transmission of data with an overhead penalty. There is inter alia a tradeoff between these two techniques in terms of energy conservation, which varies with changing the channel conditions. Therefore Lettieri and Srivastava [53] proposed a combined FEC/ARQ scheme. The tradeoff between the number of retransmissions and longer packets with FEC is evaluated and an algorithm is proposed, which adapts both values for energy efficiency.

**Packet pacing** An adaptive energy-efficient ARQ protocol which slows down the transmission rate (pace of packet transmission) when the channel is impaired and vice versa is proposed by Zorzi [99]. Additionally he proposes a kind of channel probing where the channel is tested with short low power packets at a certain pace as long as the channel is impaired and data transmission is resumed at high power when the channel is assumed to be good again. This is exemplary of a basic approach: Do not waste energy on a bad channel as attempting to overcome the bad channel is prohibitively expensive.

**Asymmetric protocols** Another approach towards energy-efficiency and lifetime extension of mobile nodes is the asymmetric protocol design. An example for this approach is the AIRMAIL protocol [1]. Protocol processing and scheduling in conjunction with a combination of FEC and ARQ is mainly performed at a central facility (base station) having extended power sources or access to a fixed power supply. This concept is commonly used by most cellular systems and in a sense it is extended to multi-hop communication systems where responsibilities are exchanged or carried forward among nodes, e.g., depending on the currently available resources. Responsibilities are often assigned to so-called "clusterheads" which temporarily take over certain tasks in the context of relaying and routing [40].

**Exploiting channel predictions** If the future channel state can be predicted with some minimal accuracy even for a rather short period of time, this knowledge will evidently be exploited to improve the protocol's energy efficiency by postponing transmissions, modifying transmission power, selecting appropriate modulation schemes, etc. The main questions to answer here are:

- Does the prediction process result in any additional power consumption on its own? For example, does prediction involve active probing?
- What is the accuracy of the prediction process, what is the consequence of incorrect predictions of the energy efficiency?

This is currently a field of active research and only few actual results are known in this field.

**Pulsed battery discharge** From the battery point of view a pulsed discharge of the battery can considerably extend the operation time of a wireless node [12]. Battery relaxation phases may be achieved by On/Off switching of the interface hardware (see above) and can be sufficiently triggered by packet pacing or packet scheduling. The premise is a separate battery for the network interface or an intelligent battery control which appropriately controls the discharge of single battery cells which in turn are fixed or dynamically assigned to certain hardware parts of a mobile node.

### Routing

In traditional cellular systems the routing problem changes to the handover problem: Which access point should be selected to serve a mobile device? As a handover decision is usually based on the channel quality between mobile device and access points, energy efficiency is at least implicitly considered in this process. From a system perspective it could be conceivable that a handover decision that is energy-conserving for a particular mobile device could be suboptimal when considering all mobiles together; this suboptimality could, e.g., be due to a different interference situation in neighboring cells.

The routing problem becomes much more difficult if multi-hop radio communication is considered. In such a multi-hop system it is no longer clear which sequence of nodes should be traversed to reach a given destination. Several optimization metrics can be introduced to support this choice. A number of routing protocols have been developed to meet the specific needs of such multi-hop networks, e.g. pro-active protocols like DSDV [66], which periodically sends route updates to learn all routes to a destination in the network, reactive protocols like DSR [44] and PARO [34], which start searching for the destination only if there is a packet to transmit, and hybrid schemes like AODV [67], FSR [65] and TORA [64], but energy-efficiency is not the prime target of these protocols. More recently energy efficiency has moved into focus, particularly motivated by the vision of wireless sensor networks. A frequently used concept is to assign routing and forwarding responsibilities to a node acting on behalf of a group of nodes (a "cluster"); routing and forwarding then only takes place among these "clusterheads". The choice of clusterheads can be based on the availability of resources (battery capacity) and is rotated among several nodes in many approaches. Examples for such clustered protocols are ZRP [85] and LEACH [40]. Additionally some routing protocols take the physical location of nodes into account (e.g., GAF [98]). The challenge for all of these multi-hop routing protocols is the evaluation of the trade-off between energy savings by clever routing and the overhead required to obtain the routing information, particularly in the face of uncertainties induced by mobility, time-varying channels, etc.

### 3.2.4 Transport protocol variants

TCP protocols are studied with respect to energy efficiency in [100, 91] although no single TCP version can be considered appropriate for wireless or heterogeneous environments. Current transport protocols are designed to work optimally with reliable links. They get confused in the sense of energy efficiency (unnecessary retransmission, long awake times of the NIC) if one or more intermediate links are error prone (e.g. wireless links). To remedy this problem, several approaches can be used:

**Splitting Connection** A specialized protocol is used on the wireless sub-link (e.g., I-TCP [2], M-TCP [8, 37], and ReSoA [83]).

**Supporting link protocols** A specialized link protocol for the wireless part is used which actively influences the control and data message exchange of TCP by means of a daemon at the edge of the wireless part (SNOOP protocol [4, 3]).

**TCP-Probing** In [], TCP-Probing is proposed. Here data transmission is suspended if a data segment is lost rather than immediately invoking congestion control. Instead a probe cycle is invoked, which tests the link characteristics. Transmission is resumed with the available bandwidth if the error conditions are random and transient. If the error conditions persists, normal congestion control is invoked.

**Interaction of the MAC power saving protocol with TCP** Here the awake time of a mobile is adapted to the pace/rate of packet transmission. Adaptation of the beacon window according to TCP throughput characteristics: Having the IEEE 802.11 power saving protocol in mind, the beacon window size is adapted according to the measured TCP throughput.

### 3.2.5 System concepts

Along with optimizations on a single protocol layer or between two protocol layers towards energy efficiency, the entire system [30] or a vertical approach including all protocol layers [47] can be taken into consideration. Furthermore software radio technology [68] opens up new perspectives towards energy efficient communication. Although both problems of how to determine and choose the energy-conserving radio technology in a certain environment are not yet solved, software radios allow for dynamic switching. In addition, relocation of power demanding network complexity , as done in the UC Berkeley's InfoPad project, is a basic system approach towards energy efficiency. From the system point of view, wireless nodes and particularly the communication part can be designed to conserve power by optimizing data flow and protocol processing order. This is demonstrated by Lettieri in [54]. Furthermore applications should be designed to appropriately match user requirements while saving energy. Imielinsky [42] describes a method for disseminating data in an energy-efficient way, which is applicable to different wireless technologies.

# Chapter 4

# Models

The investigations presented in this dissertation and the achieved results are based on experiments with Aironet's PC4800B WLAN network interface and simulations with corresponding models. The technical basis for this purpose is given in the Chapter 2. What follows is the description of the assumptions, the models as well as the used simulation tool CSIM18.

## 4.1 Basic assumptions and simulation model overview

I assumed an IEEE 802.11b network for the intended energy consumption investigation, which operates in ad hoc mode using the DCF with all of its optional features. Such a network basically consists of a certain number of wireless nodes each offering the same functionality, a wireless channel, and traffic sources. The general model structure shown in Fig. 4.1 accommodates these three parts. Each of the wireless nodes is connected to a source/sink. The source generates frames according to a model described later and the sink deletes these frames after transmission and possible reception. The MAC entity controls the channel access according to the IEEE 802.11 specification. The radio channel connects all of the MAC entities with each other. It contains an error generator, which corrupts transmitted frames according to channel characteristics described later. These characteristics depend on, e.g., channel type, RF transmission power and interferences.

The questions concerning the abstraction level and the parameterization of a wireless node are particularly interesting. With the purpose of the dissertation in mind I decided to

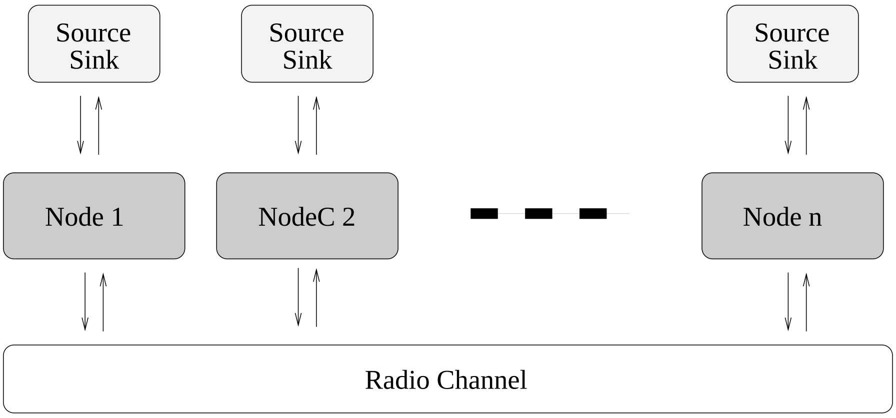


Figure 4.1: IEEE 802.11 basic model architecture

model a wireless node only by its functions, that is to say the MAC protocol as well as transmission/reception functions. I completely abstract from the hardware of an IEEE 802.11b network interface, but not from the parameters, which significantly simplifies the modeling process. The basis for parameterization is the Aironet PC4800B WLAN network interface (see 2.3). According to the actual operation state of the MAC protocol, the wireless node is in a certain operation state (TX, RX, IDLE, SLEEP, OFF) with corresponding power consumption values. This in turn allows to infer the used node hardware such as processors and amplifiers, i.e., every specific wireless node product has its specific power consumption profile, and makes the complex hardware modeling dispensable. Most of the necessary model parameters can either be taken from the specification of the PC4800B network interface or from the IEEE standard descriptions. But some of them, especially power consumption values, are implementation dependent and need to be explored by measurements. A wireless node is also equipped with a battery. In this case the battery is rather modeled by its characteristic than by its physical composition.

The radio channel model keeps track of interferences, distances and the used modulation between nodes. Furthermore it corrupts transmitted frames accordingly, delivers these packets to the intended wireless node and provides individual current noise levels for the wireless node.

## 4.2 IEEE 802.11 node model

In the following investigations I consider the so-called ad hoc mode. Therefore only the DCF functionality is implemented. According to the specification, all necessary packet types and functions are implemented. The MAC functions are listed below; for a detailed explanation see Section 2.2.3.

- Basic channel access
- RTS-CTS frame exchange
- IBSS Power saving
- Frame fragmentation
- Setting of the NAV
- Retransmission of frames

In Figure 4.2 shows the structure of a wireless node (MAC entity). A wireless node consists of several MAC sub-processes and interfaces. It is highly configurable; MAC functions, parameters as well as queueing disciplines (blocking/non-blocking) can be changed. The sub-process *multiplexer* stores source generated frames in a First-In-First-Out (FIFO) queue. The capacity as well as the blocking characteristics of the queue are configurable. Source frames will be forwarded to the MAC process if there is no pending frame generated by the *MIB* entity. Likewise, management and data frames received from the MAC process are forwarded to the *MIB* process and the sink process, respectively.

The *MIB* sub-process contains the TSF functionality and can be configured to perform the optional PCF functionality. It is responsible for periodically generating beacon frames and controlling the power saving synchronization as well as ATIM/data intervals (see Section 2.2.4).

The *transceiver* sub-process harbors the DCF. It is subdivided into two further nearly independent sub-processes, the *send* and *receive* process. The send process takes frames from the multiplexer in a send-and-wait manner. It additionally performs packetization, RTS/CTS, fragmentation, retransmission, basic channel access, etc., if configured, and transfers the frame(s) (e.g. DATA, ATIM, RTS, Beacon) to the channel entity via the transmit (TX) function. The TX functions emulates modulation.

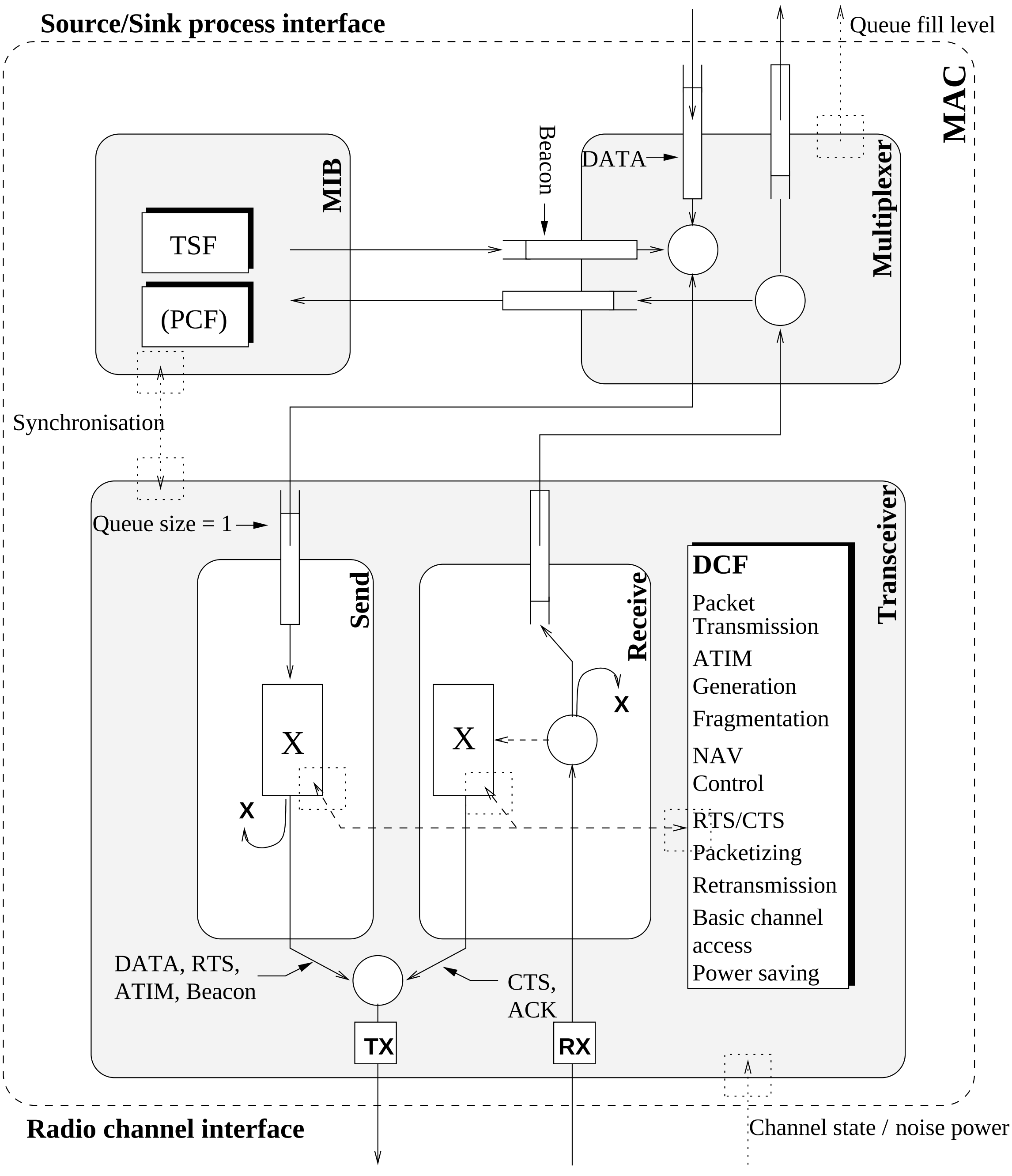


Figure 4.2: Model structure of the MAC entity

The receive process receives frames from the channel process via the receive (RX) function, which emulates demodulation. Additionally, the receive function checks the received frame for errors and it checks the destination address. If the frame is free of errors and the destination address of the frame equals its ID, it further processes the frame; otherwise the frame is deleted. A successfully received frame is forwarded to the multiplexer if it is a management frame or a data frame; otherwise it is deleted. If it is a data frame, an acknowledgement frame is generated; if it is an RTS frame, the receive process responds with a CTS. If an acknowledgement or a CTS frame is received, the send process is informed about the successful transmission of RTS and data frame respectively to stop (upper-bounded) retransmissions. Further details on MAC processing are contained in Section 2.2.3.

## 4.3 User source models

The source model is a concisely structured process, which generates frames in substitution of real applications. The frame generation process is continuous, but stops if the multiplexer process frame queue of the MAC entity is full and in blocking mode. Additionally, addressing and a rudimentary routing functionality are integrated. For the following investigations I used two types of source models which are described in more detailed below.

### 4.3.1 Synthesized traffic

For various simulations I used synthesized traffic, which is varied regarding frame size and inter-arrival time. A general description is given below, which particular combination of frame size generation process and inter-arrival time process is actually used is described in the assumption subsections of the investigations presented later.

#### Frame size

The frame size may be fixed or variable according to the simulation requirements. In the latter case the frame sizes are derived from the distribution shown in Figure 4.3. For that purpose I analyzed traffic trace file of a 10 Mbit/s Ethernet segment connecting the main

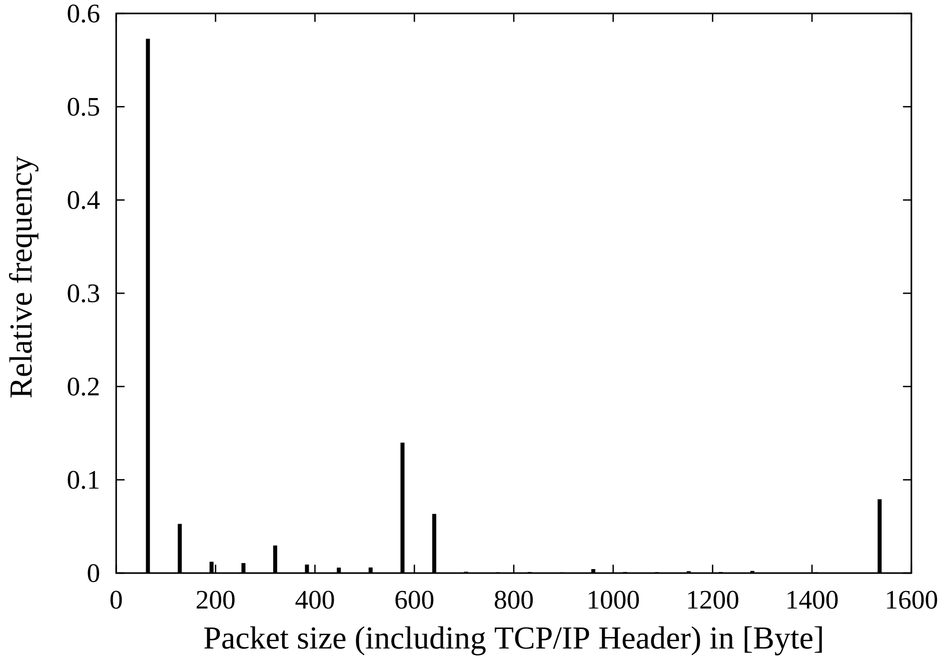


Figure 4.3: Frame size distribution of the Harvard trace

campus of Harvard University (USA) with the Internet in the year 1997 (see [95]). I condensed the packet size distribution of the Transmission Control Protocol (TCP) traffic[1] by quantization of possible frame sizes to a multiple of 64 Bytes and recorded the respective occurrence of frames of a certain length.

### Interarrival times

The interarrival times can be set to a fixed value as needed for Constant Bit Rate (CBR) traffic. Alternatively, it can follow a Pareto distribution. I did not sample the inter-arrival times of the packets from the Harvard trace file, since it is not an easy task to scale from 10 Mbit/s to 1, 2, 5.5 or 11 Mbit/s. Instead, the load level can be easily changed with the Pareto distribution. The Pareto distribution offers a heavy-tailed characteristic, which sufficiently models the (commonly assumed) bursty nature of Internet traffic [89, 52] . The samples drawn form the following formula, which was used in the source model, show a

[1]It is neither claimed that the statistical behavior of the Harvard trace is representative nor that the trace is selected because of certain characteristics.

heavy-tailed distribution:

$$\mathrm{IAT} = \left(\frac{k}{z^{\frac{1}{\alpha}}}\right). \tag{4.1}$$

IAT is the interarrival time and $z$ is a uniform random number of the interval [0 .. 1]. With $\alpha$, the distribution characteristics (variance) can be determined. Throughout all simulations I used an $\alpha$ value of 1.5. The $k$ value was used to control traffic intensity. In this case it defines an upper bound for the interarrival time.

### 4.3.2 Multimedia traffic

Other traffic types used in this dissertation are voice and video, which are described in more detail below.

#### Voice traffic

Voice transmission is the major task of cellular telephone networks. Other existing wireless technologies such as WLANs are also used to transmit voice over shorter distances to a backbone network. Therefore I incorporated a voice traffic source in my investigations.

Voice is perceived as a sequence of silence and talk periods, which serves as the basis for the traffic model. Various investigations show that it is sufficient to assume $1.35$ seconds for the silence period and one second for the talk period. I assumes Pulse Code Modulation (PCM) for voice transmission with and without silence detection. That is to say, during talk periods the voice stream results in a $64$kbps stream.

The simple voice model uses a packetization interval of $20$ ms, which results in a continuous generation of a 160 Bytes packets. The more sophisticated voice traffic model accounts for the silence periods, which have a mean length of one second. During this time no voice packet is generated. As mentioned above, 160 Bytes packets are generated during the talk periods.

Table 4.1: Encoded video sequences

| **Trace** | **Coding standard** | **Mean frame size** [byte] | **Bit rate** [kbit/s] |
|---|---|---|---|
| From Dusk Till Dawn | High Quality MPEG-4 | 3400 | 680 (mean) |
| From Dusk Till Dawn | H.263 with 256 kbit/s | 1278.79 | 256 |
| From Dusk Till Dawn | H.263 with VBR | 1969.69 | 390 (mean) |
| ARD news | High Quality MPEG-4 | 3600 | 720 (mean) |
| ARD news | H.263 with 256 kbit/s | 1279.99 | 256 |
| ARD news | H.263 with VBR | 1884.48 | 380 (mean) |
| Office-Cam | High Quality MPEG-4 | 2000 | 400 (mean) |
| Office-Cam | H.263 with 256 kbit/s | 1278.88 | 256 |
| Office-Cam | H.263 with VBR | 452.52 | 91 (mean) |

**Video traffic**

For video traffic I used the work presented in [29]. Here several different sequences ranging from movie, TV news to office cams are MPEG-4 or H.263 encoded and statistically evaluated. As shown in Table 4.1, I selected three different types of video sequences: High quality MPEG-4 , H.263 with a target bit rate of 256 kbit/s[2] and H.263 with a Variable Bit Rate (VBR). Figure 4.4 shows their respective frame size distribution. The frame size distribution depends on the type of video sequence and the employed encoding approach.

In some of the simulations we used the encoded video streams. That is to say, the extracted frame inter-arrival times and frame sizes of every trace were used for the video source model construction. Every trace has a length of 60 minutes. If all samples are consumed during the frame generation process, the whole process starts over from the beginning.

## 4.4 Radio channel model

I assume an indoor environment for radio wave propagation for most of the following investigation; otherwise it is explicitly stated. That is distances are relatively small, there is not necessarily a predominant communication path and multi-path and movements are a

[2] I refer to H.263 with a target bit rate of 256 kbit/s as H.263 with 256 kbit/s in the following.

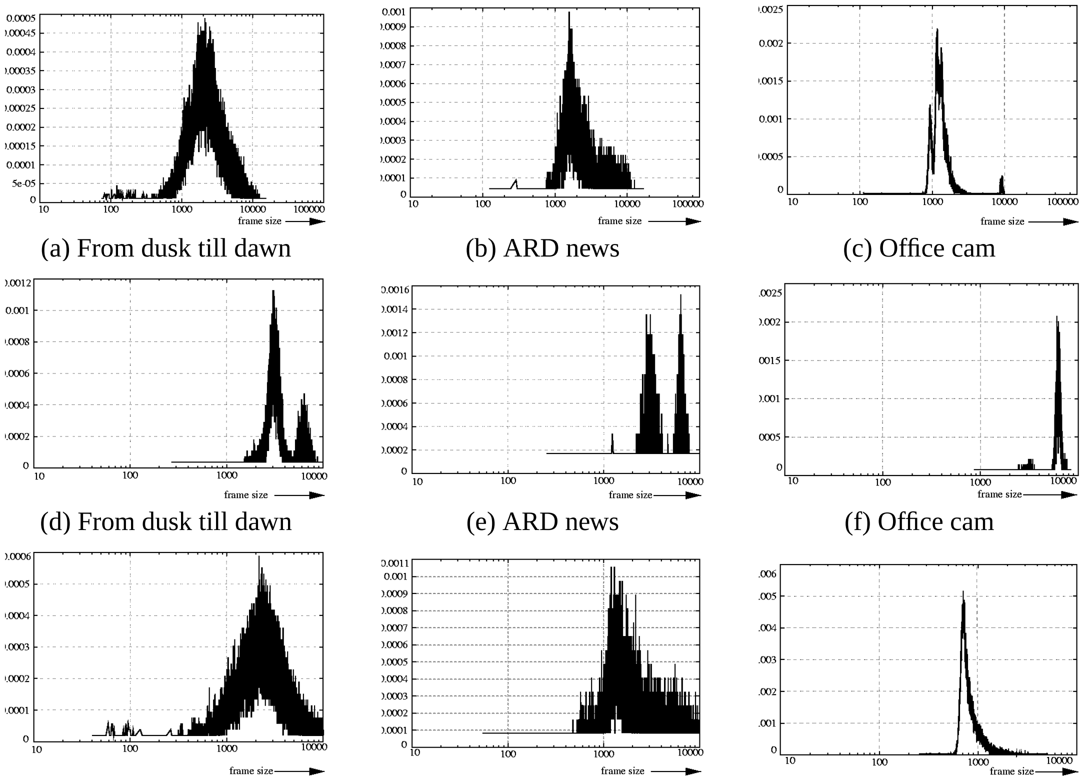

(a) From dusk till dawn (b) ARD news (c) Office cam

(d) From dusk till dawn (e) ARD news (f) Office cam

(g) From dusk till dawn (h) ARD news (i) Office cam

Figure 4.4: Frame size distribution for High Quality MPEG-4 (a,b,c), H.263 with 256 kbit/s (d,e,f) and H.263 VBR encoding (g,h,i) [28]

severe source of impairments. The radio channel (see Section 2.1) is modeled as separate process with an interface to the MAC entity. The tasks performed by the radio channel are transport of frames from one node to all other nodes (duplication of frames) and injection of errors according to the desired error model. In Figure 4.5 the general structure of the radio channel model is shown. Within the dissertation two different channel error models are used.

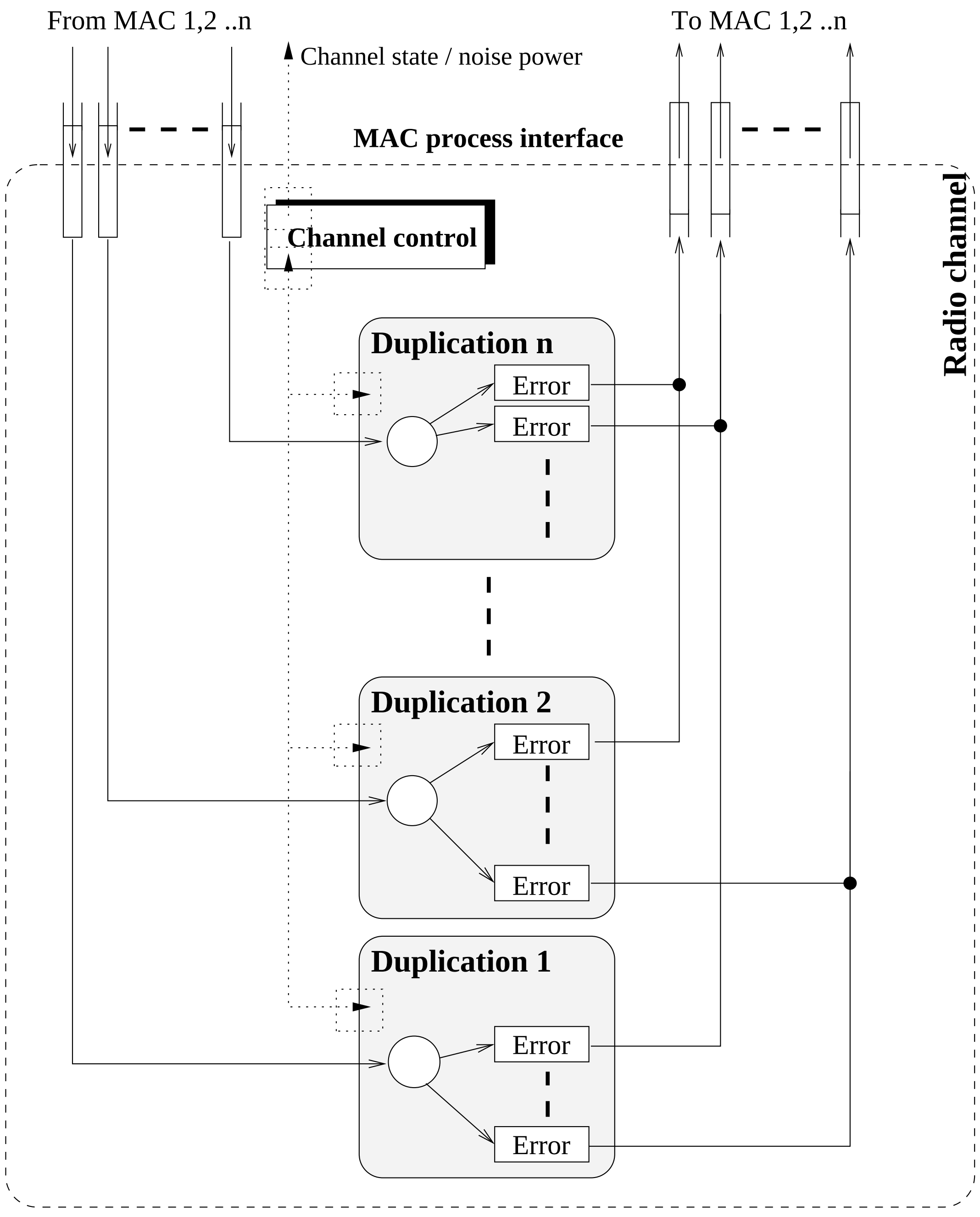


Figure 4.5: Structure of the radio channel model

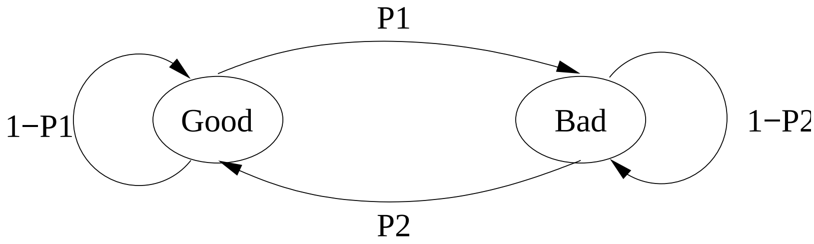


Figure 4.6: Gilbert-Elliot channel model

### 4.4.1 Gilbert-Elliot error model

To consider dynamic changes in the bit error rate, I used the widely accepted Gilbert-Elliot channel model (see [33]). It is based on the fact that the channel quality varies in time because of movements. For instance, in [79] it is shown that the throughput of a WLAN with similarly chosen parameters heavily depends on the position of the mobiles and time. The varying throughput is caused by varying bit error rates during the measurements.

The Gilbert-Elliot channel model basically is a two state discrete time Markov chain (see Figure 4.6). One state of the chain represents the Good-State, the other one represents the Bad-State. In every state the bit errors occur with a certain probability. In [94] an analytical solution is proposed, which parameterizes the Markov chain for BPSK and DQPSK modulation respectively, assuming a Rayleigh-fading channel, that is to say no predominant paths and movements of mobile terminals. The main application area of WLANs, namely the indoor scenario, is met quite well by these elements. I followed this approach in computing the channel model . A detailed description of channel parameter computation is given in Appendix C.

The logical channel structure used in conjunction with the Gilbert-Elliot error model is shown in Figure 4.7. I assumed full connectivity between all nodes. In other words, every node has an independent Gilbert-Elliot bit error generation process for every (logical) link to the other nodes. I also assumed that the distance between all the nodes is relatively small with respect to the radiation power. As a result, if a node transmits a packet, all other nodes within the network definitely know that the channel is in use. I modeled this feature by a signal, which is provided by the radio channel process to all wireless nodes. Further on if two or more nodes transmit frames simultaneously, a collision occurs. That is to say,

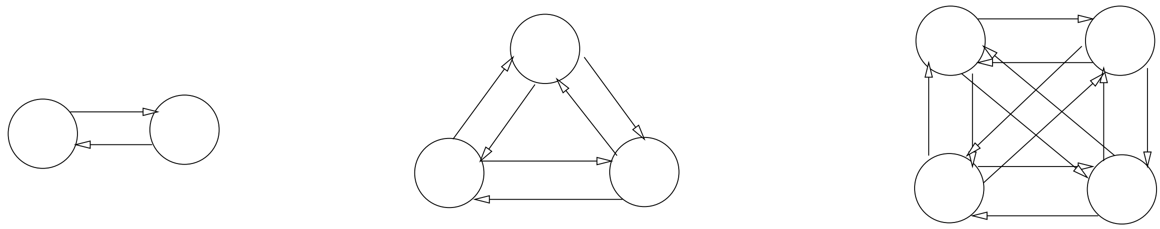


Figure 4.7: Logical channel structure chosen for the Gilbert-Elliot error model

frames involved in a collision are marked as corrupted. Consequently, a received frame can be erroneous because of bit errors generated by the Gilbert-Elliot bit error process and/or collisions.

### 4.4.2 Interference-based error model

For the sake of multi-hop investigations where interference by other nodes plays an important role, another interference-based channel error model was used. The assumption is that every node generates noise for other nodes while transmitting a frame. If it exceeds a certain threshold, the noise causes a deference of frame transmission, since the channel has to be free before transmission. The threshold is referred to as Clear Channel Assessment (CCA) and is set to 70 dB[3] throughout all simulations. On the other hand, the frame transmission can interfere with an ongoing reception process, which in turn increases the probability of bit errors. Note that a collision of frames is nothing else than interference.

The channel process continuously signals the interference level to the wireless node. Errors are also generated according to the RF transmission power, distance and the simultaneously transmitted frames assuming AWGN channel error characteristics. To determine the BER and eventually the correctness of the transmitted frame, I computed the Signal-to-Interference-Noise-Ratio (SINR) according to the following equation:

[3]In the IEEE 802.11b specification the CCA is specific for any transmission speed but close to 70dB. For the sake of simplicity I applied a single threshold value for all transmission rates (modulation types). This influences the results quantitatively but not qualitatively.

$$\text{SINR} = \frac{P_i}{N_0 + \sum_{j=1}^{N} Pj}, \; \forall \, i \neq j. \tag{4.2}$$

where $P_i$ is the received signal strength of the frame to be decoded, $P_j$ is the received signal strength of simultaneously transmitted frames, if any, and $N_0$ is the white noise power. With the help of Equation 2.5 we are able to derive $\frac{E_b}{N_0}$ which in turn is needed to compute the BER according to the used modulation scheme (see Equations 2.6 and 2.7).

Packet error can be easily determined by means of the BER with the following equation:

$$\text{PER} = 1 - (1 - \text{BER})^i, \tag{4.3}$$

where PER is the Packet Error Rate and $i$ is the number of the considered frame bits. The correctness of the frame is determined by a Monte Carlo experiment using the computed Packet Error Rate (PER). The actual SINR and in turn the BER can change during an ongoing frame reception since other nodes could start or stop frame transmission respectively. This scenario is also taken into account by computing a partial packet error whenever a SINR change occurs. A frame is considered error-free if the Monte Carlo experiments indicates no error for any frame part. Note, that this radio channel model inherently assumes independent bit errors.

### 4.4.3 Simple path-loss error model

In certain cases where only a communication between two mobiles is considered, I used a simple path-loss based error model. Based on the transmission speed (modulation scheme), transmission power, and distance, the BER and in turn the PER can be computed. I assumed an AWGN channel that is equivalent for independent bit errors. To compute the PER, Equation 2.9 (in Section 2.1.2) has to be solved for $\frac{E_b}{N_0}$ and Equation 2.6 or 2.7 has to be applied afterwards according to the transmission speed of the considered WLAN. The PER is used in a Monte Carlo experiment to determine whether a transmitted packet is corrupted.

## 4.5 Battery model

The capacity of a battery cannot be exactly determined. It depends on its usage pattern as explained in Section 2.4. I wanted to investigate the impact of a WLAN network interface on the battery utilization. For this purpose I developed a battery model, which is based on the experiments presented in [51].

### 4.5.1 Battery capacity

The battery is modeled as a resource entity with a certain theoretical capacity $N$ with the unit Ah. Because the theoretical capacity cannot be completely exploited under continuous discharge conditions, a nominal capacity $T$ is defined. The nominal capacity of a battery is not fixed but depends on the discharge process. In either case it yields $T \leq N$. Initially I assume

$$T_{\mathrm{init}} = 0.2N, \tag{4.4}$$

which is an optimistic presumption for the case of optimal continuous discharge conditions [12]. Hence, the exploitation of the battery self-recharge phenomenon by using a better usage pattern is simply an attempt to exhaust the battery completely so that $T \approx N$.

### 4.5.2 Battery exhaustion

The cut-off voltage describes the battery state where the battery is considered to be depleted. To simplify matters, I did not directly model the battery voltage. Instead, I assumed that the cut-off voltage is reached if the current battery capacity $T_{\mathrm{cur}}$ reaches $10\%$ of $T_{\mathrm{init}}$.

The current battery capacity $T_{\mathrm{cur}}$ decreases over time because of WLAN network interface energy consumption. On the other hand $T_{\mathrm{cur}}$ increases due to the self-recharge phenomenon during the relaxation phases. Under certain circumstances the cut-off voltage respectively $T_{\mathrm{cur}} = 0.1T_{\mathrm{init}}$ is never reached. To avoid this artificial behavior, I also consider the battery as depleted if all of its theoretical capacity is consumed. For that purpose a variable $T_{\mathrm{cons}}$ is defined, which keeps track of the already consumed capacity. The battery depletion exhaustion criteria are summed below:

$$\text{Battery exhausted, if } T_{cur} = .1T_{\text{init}} \text{ or } N - T_{\text{cons}} = 0. \tag{4.5}$$

### 4.5.3 Battery discharge and recharge

The battery discharge is defined as a linear function $f(t) = a \cdot t + b$ and depends on the actual load. $t$ describes the duration of discharge and $a$ and $b$ are activity dependent coefficients. For instance, a network node consumes more energy in the TX mode than in the IDLE mode. I do not give actual discharge parameters since they depend on the considered system.

The basis for the recharge function are the results of LaFollete [51] shown in Figure 2.17 of Section 2.4. I tried to approximate the recharge behavior accordingly: A fast recovery at the beginning of the battery relaxation fading over time. An exploratory search showed that the following function models this behavior adequately:

$$f(m,t) = \sqrt[4]{t} \cdot m, \tag{4.6}$$

where $t$ is the time to recharge and m is a recharge intensity parameter controlling the slope of the function which depends on the current overall charge state of the battery and the intensity of the previous power drain.

To compute $m$ I assumed a discharge pulse of length $t_{\text{d}}$ and a relaxation time $t_{\text{r}}$ which is about seven times as long ($t_{\text{r}} = 7 \cdot t_{\text{d}}$) to recover to the capacity level prior to the discharge (see Fig 2.17 of Section 2.4):

$$\begin{aligned} I \cdot t_{\text{d}} &\approx \sqrt[4]{t_{\text{r}}} \cdot m = \sqrt[4]{7 \cdot t_{\text{d}}} \cdot m \\ m(I, t_{\text{d}}) &\approx \frac{I \cdot t_{\text{d}}}{\sqrt[4]{7 \cdot t_{\text{d}}}}, \end{aligned} \tag{4.7}$$

where $I$ is the pulse current.

As mentioned above the recharge capability depends on the overall state of the battery. That is the quantity of the active material still available in the battery. A nearly depleted battery recharges less than a full battery. To cope with this behavior, I modeled $m$ as a

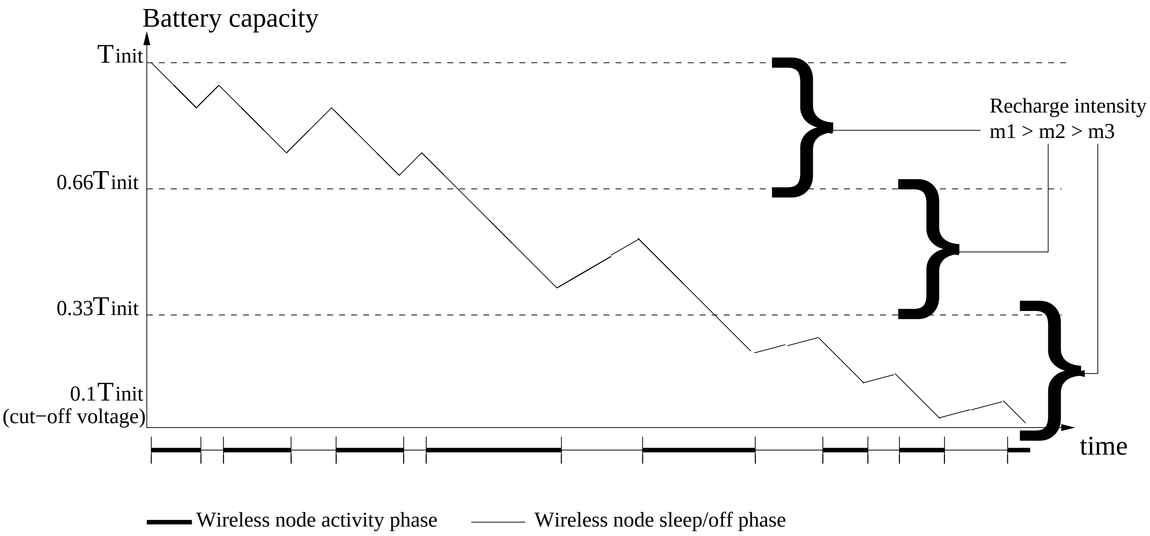


Figure 4.8: Battery discharge/self-recharge example

discrete process, which depends on the charge state of the battery. I specified three recharge capability regions so that

$$m = \begin{cases} m(I, t_\mathrm{d}), & \text{if } \frac{2}{3}T_\mathrm{init} < T_\mathrm{cur} \leq T_\mathrm{init} \\ \frac{3}{4}m(I, t_\mathrm{d}), & \text{if } \frac{1}{3}T_\mathrm{init} < T_\mathrm{cur} \leq \frac{2}{3}T_\mathrm{init} \\ \frac{1}{2}m(I, t_\mathrm{d}), & \text{if } 0 \leq T_\mathrm{cur} \leq \frac{1}{3}T_\mathrm{init} \end{cases} . \tag{4.8}$$

Furtheron there never is a recharge across the upper recharge region boundary ones $T_\mathrm{cur}$ crossed into the lower region. Figure 4.8 sketches a possible discharge/self-recharge process.

## 4.6 CSIM18

Because of the functional complexity of the models and the desired abstraction level I used simulation as investigation approach. In general simulation allows a higher degree of detail and a faster description (implementation) with respect to the quite complex models.

For the implementation of the models I used the CSIM18 [57] toolkit under the Linux Operating System (OS). CSIM18 is a general purpose simulation toolkit, which suits my expectations well. The rational reasons why I chose this tool are:

**Process orientation** Modeling and execution of models is process oriented. By this, a good abstraction and separation of entities and functions could be achieved. This fits the main purpose of modeling the IEEE 802.11 MAC protocol very good.

**Slimness** Basically, CSIM is a slim effective C/C++ library of a few hundred kilobytes providing a fast simulation engine, basic modeling constructs and statistical evaluation functions. This makes it easy to work with.

**Execution speed** Because of the fast simulation engine and the slim design, execution speed of models is outstanding. Simulations of a simple M/M/1 queue showed it uses 3 to 20 times less than other tools like NS2, BoNES, etc.

**Statistical evaluation of results** Besides basic modeling constructs CSIM18 implements several statistical evaluation functions which are often ignored in other simulation tools. Moreover it provides an automatic run-length control which is based on a sequential stopping rule.

On the other hand, CSIM18 does not have a Graphical User Interface (GUI) and is based on C/C++, which requires a certain level of self-discipline in code design to keep the model understandable, extendable and debugable. Also no public CSIM18 model libraries are available from which approved simulation elements could be taken. In my case this was no problem, since at the time when I coded the IEEE 802.11 model, no model with an appropriate level of detail was available. Another problem that arose from the CSIM18 license policy had been the unavailability of the CSIM18 library source code. Without the library source code debugging of model implementations is always difficult.

The available CSIM18 objects are shown below. Attached to any object but not listed here are functions to initialize or control the objects, to query states or statistical data, and to provide inter-process communication.

CSIM18 objects are:

- processes
- facilities
- storages
- events
- mailboxes
- data collection structures
- process classes
- streams

# Chapter 5

# Power consumption measurements of a WLAN interface

Power consumption measurements of WLAN hardware were not available in literature when I started to investigate the energy consumption. Therefore the power consumption measurements of a WLAN network interface for various operational modes and ideal measurement conditions, that is a non-impaired RF channel, were performed. These power consumption measurements have a multitude of goals. First, they help to understand which operations are power demanding and which are not. Secondly, they clearly show which parameters impact the power consumption of the WLAN network interface. And last but not least these results are used later in this dissertation to parameterize simulation models. Power consumption should not be confused with energy consumption although both depend on each other. However, network interface management and the implemented protocols decouple both metrics to a certain degree. Note that both metrics do not sufficiently describe the degree of energy efficiency in wireless communication. A suitable metric is given in Chapter 6, describing the energy efficiency of a WLAN network interface by means of the power consumption results given below.

Mobile nodes are required to minimize power consumption to prolong recharge intervals, to decrease the weight of the battery and to decrease the size of the wireless nodes (e.g., palmtops). As other components of wireless nodes, such as main processors, hard disks, main memory and sound system to name a few, become more and more energy efficient (see e.g., [55]), the power consumption of wireless network interfaces has to be addressed.

The average power consumption of a WLAN network interface ranges from 1 to 2 Watts in current products. This is up to 12 times higher than for a typical Ethernet card [63]. In comparison to a Palm-like handheld, a WLAN interface can consume up to 10 times more power, which amounts to more than 80% of the overall power budget (see e.g., [15]). It is evident that the operation of a WLAN should be as energy efficient as possible. While the WLAN standard IEEE 802.11 supports power saving by a traffic load dependent On/Off switching of the interface hardware, it is not exactly clear how the different operation modes contribute to the overall power consumption of the WLAN interface card. To the best of our knowledge, no information exists on how the combination of parameters like RF transmission power, modulation schemes (transmission rate), and packet size influence the power consumption of a WLAN interface. Particularly the influence of the RF power level has not been shown.

This work presents power measurement results of Aironet's PC4800B PCMCIA WLAN network interface that was already introduced in Section 2.3. Of particular interest are the power consumption values for the operations modes TX, RX, IDLE and SLEEP and the dependency on packet size and on RF transmission power level while sending or receiving packets. All measurements were performed using a distance of 5 meters between the sending and receiving node to ensure an error-free communication for all possible RF transmission power settings (1, 5, 20, 50 mW). Additionally, I ensured that there were no colocated or overlapping WLANs. The following section describes the power measurement setup. Section 5.2 presents and discusses the measurements of the instantaneous and the average power consumption for different modes of operation.

## 5.1 Power measurement setup

The measurement setup is designed to measure and record the instantaneous and average power consumption and additional parameters described in [9]. The measurement setup as depicted in Figure 5.1 contained two Sony Vaio laptops equipped with Intel Pentium II 360 MHz processors, 64 MBytes main memory and a 1 GByte hard disk. Both laptops are also furnished with PC4800B WLAN interfaces with one laptop acting as the receiver and the other laptop as the sender. Furthermore there is a control PC equipped with a

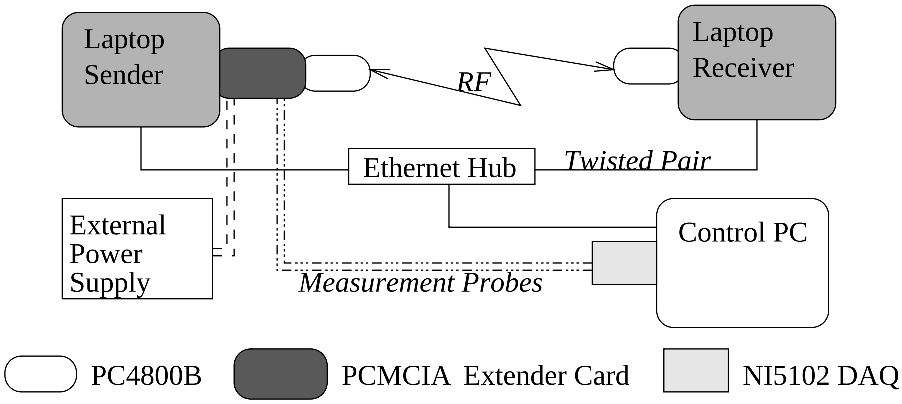


Figure 5.1: General measurement setup

750 MHz Intel Pentium III, 1 GByte of main memory and a 30 GByte harddisk. The control PC is connected to the laptops via an Ethernet hub in order to initiate, stop and control measurements, and record data (e.g., power, throughput) gathered at each laptop. One of the laptops is also equipped with a PCMCIA extender card to extend the PCMCIA bus to the PC4800B NIC so that $V_{cc}$ can be isolated facilitating measurements of both $V_{cc}$ and the current consumed.

The power dissipated by the PC4800B NIC is the product of the voltage and the current of the NIC. As shown in Figure 5.2 the voltage is measured as $V_{cc}$ to ground. The current was measured by placing a resistor in line with the PC4800B NIC. The voltage drop across the resistor was then measured and divided by the value of the resistor (1.07 $\Omega$) to determine the value of the current. The voltages were sampled by a National Instrument digital oscilloscope (NI5201) at a rate of 20 MS/s using X1 probes. The digital oscilloscope was attached to the control PC. To ensure an operating voltage of 5 Volts for the PC4800B NIC and to ensure power supply stability, the power supply was detached from the PCMCIA bus of the laptop and connected to an external Wandel & Goltermann high quality power source.

The laptops ran Linux OS using a 2.2.13 kernel. The PC4800B NIC was controlled by an open source device driver from Ben Reed [43], which facilitates the control of the card as it was needed for the measurements. It was necessary to change the driver in order to support a Maximum Transfer Unit (MTU) of up to 2312 Bytes since only a maximum

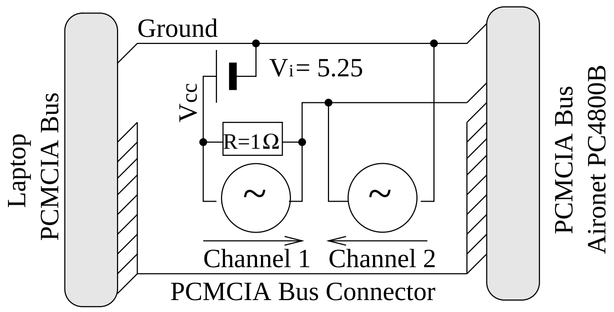


Figure 5.2: Power measurement setup

of 1500 Bytes was supported by the driver in its early stage. Additionally, kernel hooks had to be installed in the interrupt service routines to accurately record the goodput as direct output of the card. The SNUFFLE trace tool (see [78]) facilitates the kernel data collection process by providing kernel data structures and routines to transfer the data into the user space of the OS. Traffic generation is accomplished by the Netperf tool (see [62]). Netperf was configured to use UDP as the transport protocol and to generate packets of a given size as fast as possible in order to keep the transmission queues filled. For all parameters set Netperf was started three times with a runtime of 20 seconds each, which in all cases amounted to more than 7000 transmitted packets. I did not use Netperf's built in performance reports because here measurements are performed at the transport layer, which can account for some inaccuracies due to packet drops. The control PC accommodates the NI5102 oscilloscope, runs a measurement control program that performs the configuration of the laptops, starts and stops the measurement routines, and stores the traced laptop and oscilloscope data on its hard disk.

## 5.2 Power measurement results

Two kinds of power dissipation results are presented in this chapter. The first is referred to as instantaneous power consumption. It describes the actual power consumption of the NIC for a particular working mode and for a particular set of parameters. As mentioned above, there are four different working modes (TX, RX, IDLE, SLEEP) and three parameters for variation (packet size, transmission rate, and RF power level). The second kind of power dissipation results are referred to as average power consumption. It describes the power consumption for the TX and RX processes as a whole, including the transmission and the reception of data and acknowledgments respectively as well as idle times. SLEEP times are not incorporated here because the measurements are performed with the maximum load and PS is not supported in the ad hoc operation mode of the PC4800.

The measurements are performed in ad hoc mode. No results for the infrastructure mode are obtained. The RTS/CTS frame exchange, as well as fragmentation are not used for the measurements. Additionally, to provide an exact figure of the PER, no MAC level retransmissions are allowed. Otherwise a frame could be recorded as correctly transmitted although several MAC level retransmissions were necessary to correctly transmit the frame. The RF channel was chosen so that no impairment from other WLAN NICs can occur during the measurements as indicated by several tests of the setup. The distance between the mobiles is set to five meters, which offered excellent wireless communication conditions. The PER is in the range of $2 \times 10^{-4}$. I do not investigate longer distances. Longer distances would require significantly longer measurement runs to reach statistical relevance because of the unstable wireless channel at longer distances. Instead, results of simulations using the obtained power consumption results are given in the next chapter. A selection of the most important parameter settings can be found in Table 5.1.

### 5.2.1 Instantaneous power consumption results

For all sets of parameters the instantaneous power consumption in different operating modes are recorded. From the obtained trace files the time phases of interest (TX, RX, IDLE, SLEEP) are cut out using a threshold method. Because of occasional unwanted power spikes, which are probably caused by measurement inaccuracies (e.g., sampling error, measurement resolution), the traces first had to be low pass filtered. That means the high frequency part of the trace file is cut off. This is performed with a sliding window averaging approach using a window size of 40 samples to determine a continuous average. According to [39], the low pass filtering results in an increased (power) amplitude accuracy but a decreased time accuracy; the degree of accuracy can be adjusted by the window size. The latter is negligible for a window size of 40 samples as a comparison of the original

Table 5.1: Measurement parameter settings of PC4800

| Parameter | Value |
|---|---|
| MTU | 2400 Bytes |
| Working mode | ad hoc |
| Channel # | 6 |
| TX/RX Diversity | both |
| Long/short retry limit | 1 |
| RTS threshold | 2312 Bytes |
| Fragmentation threshold | 2312 Bytes |
| Modulation | BPSK, QPSK, CCK |
| Power mode | Constant Awake Mode (CAM) |
| Transmission rate | 1, 2, 5.5, 11 Mbit/s |
| Packet size | 64, 128 . . . 2048, 2312 Bytes |
| RF power level | 1, 5, 20, 50 mW |
| Sender/receiver distance | 5 meters |

trace with the pass filtered trace indicates. The measurement results are given in Figure 5.3.

The results show that there is a strong dependence between the power consumption of the PC4800 NIC and the RF power level used in the TX mode as shown in Figure 5.3(a): The higher the power level, the higher the power consumption. In fact, the increase in power consumption is over-proportional. If the RF power level is changed from 1 to 50 mW, the increase in power consumption is about 500 mW. The results confirm that the power amplifier uses major share of the overall power budget. The change in transmission rate leads to a smaller change in power consumption. Higher transmission rates cause a slight increase in power consumption, which is probably caused by a slightly higher power consumption of the baseband processor. The RF power level does not have any influence on the reception mode as shown in Figure 5.3(b). Only the transmission rate slightly influences the power consumption in RX mode. The packet size does influence the power consumption neither in TX nor in RX mode. It can be seen that the TX mode can consume considerably more power than the RX, IDLE, or SLEEP mode. There is only a small difference in power

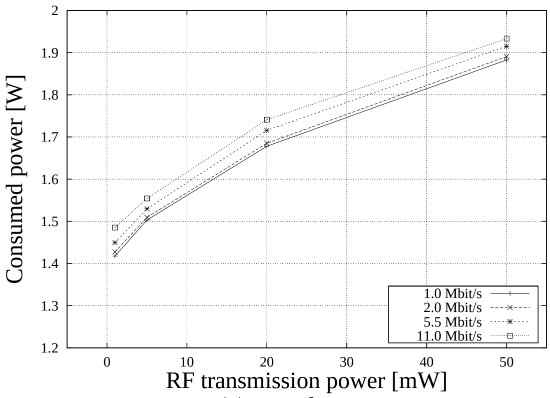


(a) TX phase

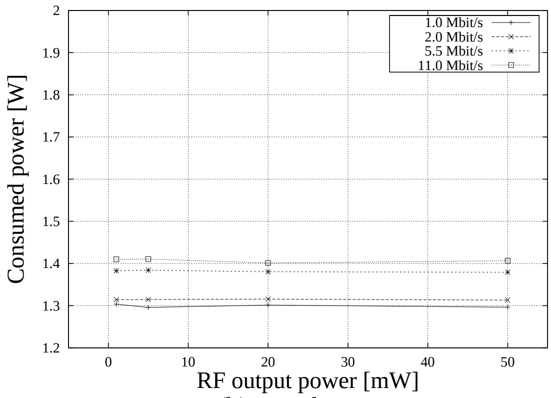


(b) RX phase

| Mode | Power consumption |
|---|---|
| Ctrl. response messages | 1.76 W |
| IDLE | 1.34 W |
| SLEEP | .075 W† |

† The value were taken from the PC4800 specification since PS is not supported in the "ad hoc" mode configuration of PC4800

(c) Others

Figure 5.3: Instantaneous power consumption vs. RF power level for various transmission rates

consumption between the RX and the IDLE modes. The reason is that all of the reception hardware is turned on in the IDLE mode to scan for valid RF signals. The difference is probably caused by the MAC processor, which is assumed to be idle during the IDLE mode of the NIC, dissipating less power. In SLEEP mode the NIC has the lowest power consumption level[1]. It is more than 17 times smaller than the power consumption in IDLE mode. This indicates that the SLEEP mode saves a considerable amount of power if applicable. Unfortunately SLEEP mode is not applicable in all no-work-load situations since it might take too long to switch to any other working mode from SLEEP mode. This may not be acceptable for the timing requirements of the MAC protocol. Further on the power consumption during transmission of immediate acknowledgments remains on the same high power level regardless of the RF power level settings. This leads us to the assumption that all control response messages are always sent at the highest power level to ensure a safe

[1]The sleep mode is not supported by the PC4800 in ad hoc mode operation. Therefore I reported the value given in the specification of the card, which may differ from the actual achievable value.

transmission. The obvious reason is their importance for the overall network operation. Our measurement results are in the range of the results as they are provided by the manufacturer and later shown in [27].

### 5.2.2 Average power consumption results

For determination of the average power consumption results all power samples contained in a measurement trace file are averaged for every single packet size, RF power level and working mode. Since a trace file contains power samples for TX, RX and IDLE phases, the average reflects all samples . Thus the results provide a complete power consumption figure of the send and the receive process as a whole (for more details see technical report [9]). The average power consumption results for the TX case are given in Figure 5.4. The curves reveal that a higher RF power level generally leads to a considerably higher power consumption. The reason for this is the power amplifier, which consumes more power if it generates a stronger antenna signal. The data rate has a slight influence on the average power consumption since most of the ICs have to run at the same frequency regardless of the data rate. The power consumption generally increases with the transmission rate (see Figure 5.4(a)) since higher transmission rates require slightly more power. If the RF power level increases, the effect will be inverted. This effect can be seen at a 50 mW RF power level (see Figure 5.4(d)). The reason is a noticeably higher power consumption during transmission than for staying in IDLE or RX mode. At a higher data rate the TX time of packets is considerably reduced, which results in power saving. Furthermore it is interesting that the packet size has a notable impact on the average power consumption: The larger the packet, the higher the average power consumption. The percentage of time the NIC spends in TX mode increases and the percentage of time in RX and IDLE modes decreases with larger packets. This leads to a higher average power consumption because the TX mode consumes more power.

Figure 5.5 shows the average power consumption during reception. The RF power level does not impact the power consumption since the transmission branch of the PC4800 NIC circuitry, including the power amplifier, is turned off. Therefore, I only show the 1 mW power level curve as a representative (see Chapter D Figure D.1 for other curves). The

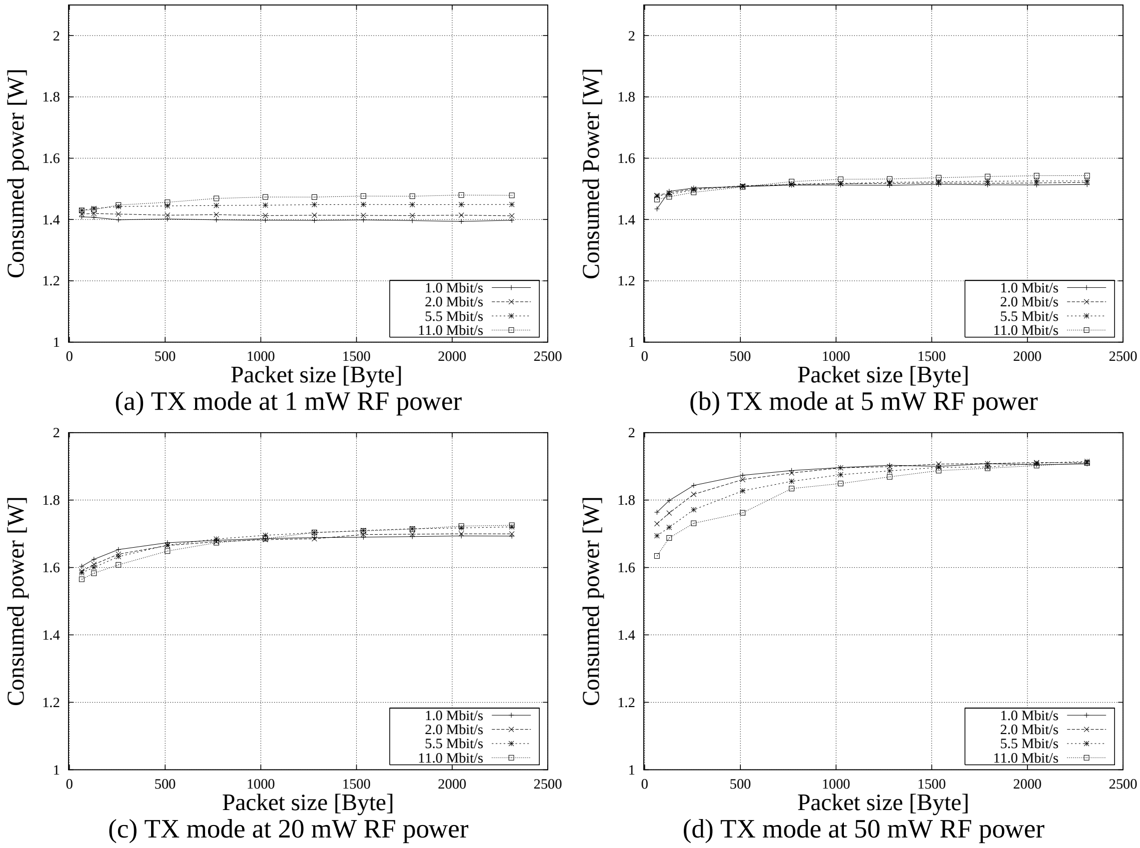


Figure 5.4: Average power consumption for different RF power levels and packet sizes during transmission

average RX mode power consumption is generally lower than the average TX power consumption, although the difference is small compared to the case of the 1 mW RF power level in TX mode. For small packets ($\lessapprox$1000 Bytes) the average RX mode power consumption is actually higher than the average TX power consumption for the 1 mW and 5 mW RF power level. This is because acknowledgments are always sent at the highest power level (compare Table 5.3(c)) and they have to be transmitted more frequently for short packets within a certain time frame. The transmission rate again slightly effects the power consumption. At a rate of 11 Mbit/s the power consumption is higher than for 5.5 Mbit/s and so on because the packet length decrease in terms of receive time, and the percentage of time in TX mode increases due to the necessary transmission of acknowledgments. The

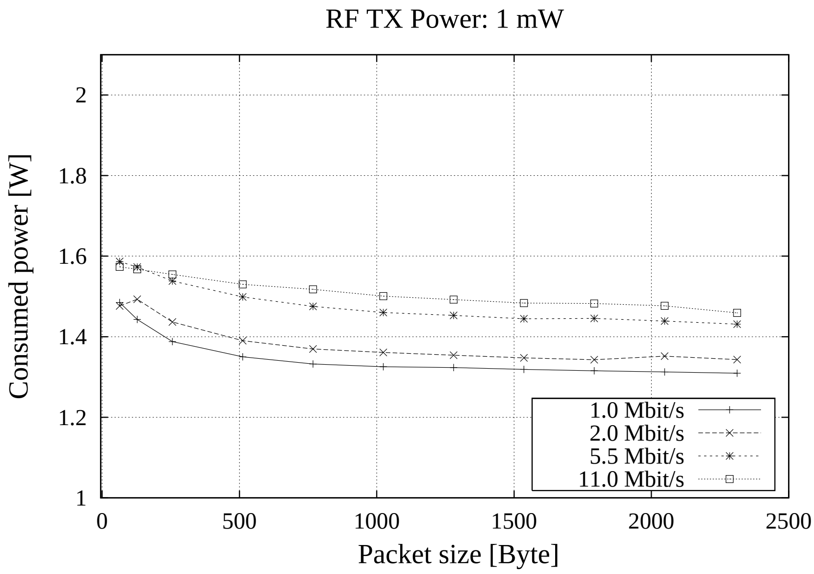


Figure 5.5: Average power consumption for different packet sizes during reception

length of the acknowledgments remains constant in time regardless of the transmission rate since they have to be sent at the configured basic rate, which is 1 Mbit/s throughout the measurements. The packet length itself has no influence on the average power consumption in receive mode for larger packets, since the difference in power consumption during the RX and IDLE phase is small (compare values in Figures 5.3(b) and 5.3(c)).

## 5.3 Summary

This chapter presents the main results of the power consumption measurements; the full set of results can be found in my TKN Technical Report TKN-01-007 ([9]). The measurements confirm the fact that WLAN network interfaces consume a considerable amount of energy with respect to the overall consumption of the mobile node. I found that the TX, RX, and IDLE modes use most energy. I also found a dependency on the transmission rate and a considerable dependency on the RF transmission power. While the built-in IEEE 802.11 power saving functionality can exploit the fact that the IDLE mode consumes fewest energy very well, no attention is paid to the potential of power control.

Furthermore, I investigated the power consumption for the process of sending and receiving packets as a whole. I found a dependency on the packet size, whereas sending larger packets tends to consume more power, which is the opposite for the receiving process. I also found a dependency on the transmission rate, which shows that higher transmission rates can lead to a lower power consumption than lower transmission rates in the case of a higher RF transmission power level. These characteristics can be exploited by an sophisticated power control algorithm to further minimize power consumption. Note that power consumption by itself is an insufficient metric to describe energy efficiency since it cannot provide information on how long the battery of a mobile node will actually last. Therefore in the following chapter I derive the energy, which is used to transmit one bit of goodput data.

The (instantaneous) power consumption investigation results are used in the following chapters to parameterize the power consumption of the wireless node simulation model in the respective operation modes. As in the reality, the model operation constitutes a certain sequence of TX, RX, IDLE or SLEEP mode changes. By recording the length of stays of the different operation modes it is easily possible to determine the average power consumption as well as the energy consumption of the wireless node in different operation modes.

# Chapter 6

# Energy efficiency of a WLAN interface

The energy efficiency of a wireless network interface is a major design issue, since the mobile device operation is often constrained by the battery. The investigation presented here explores the question which parameters of a WLAN interface can be adjusted to improve energy efficiency. By means of the power consumption measurement results obtained in Chapter 5, the energy consumed to transmit one bit of payload, a new metric to describe the energy efficiency sufficiently, is determined. These power consumption results are used to parameterize a simulation model of the WLAN interface, which is in turn used to investigate the influence of parameters like RF power level, packet size, and data rate on the energy efficiency for different bit error probabilities. Additionally an analytical energy consumption model for a point-to-point communication is developed. I observed that the RF power level control and data rate adaption have a considerable impact on the energy efficiency. As I mentioned before, power consumption itself cannot appropriately express how efficiently the consumed power is used. For instance, if the NIC constantly operates in SLEEP mode, the power consumption will be at its lowest level, but not a single bit of information would have been transmitted. Therefore another metric is necessary to impartially value the WLAN NIC power consumption.

Another issue that remained untouched so far is how the channel quality influences the energy consumption. The channel quality may be impaired by, e.g., the environment, mobility and distance. For example a data rate of 1 Mbit/s can have a better energy efficiency than 11 Mbit/s because the channel quality (BER) is not sufficient to transmit at 11 Mbit/s. The energy performance can be influenced by packet fragmentation, rate switching or RF power control approaches to name a few. To which extent such mechanisms improve the energy consumption performance for poor RF channel conditions is also the subject of the following sections.

In this chapter I first explain the metric used throughout this chapter to characterize the energy expenditure by the WLAN NIC. Next, in Section 6.2 the energy consumption results for low BER, which are derived from the measurement results of Chapter 5, are shown and evaluated. Simulation, which uses of the measurement results obtained in chapter 5, are performed to derive the WLAN NIC energy consumption for higher BERs. Section 6.3 describes the modeling assumptions and the setup of the simulation model. The results are presented in Section 6.3.3 and discussed in Section 6.3.4. In section 6.4 an analytical model is given which takes data rate, packet size, BER, and RF transmission power level into account. A summary of the investigation and results are given in Section 6.5.

## 6.1 Energy per goodput bit

Power as well as energy consumption alone cannot appropriately reflect the transmission expenditure of a WLAN network interface. Therefore a new metric is defined, which is referred to as energy per goodput bit:

$$E_{\text{bit\_good}}\,[J/Bit] = \frac{\text{Average\_Consumed\_Power [W]}}{\text{Goodput [Bit/sec]}}. \tag{6.1}$$

The energy per goodput bit tells how much energy the NIC has to spend to successfully transmit one bit of (MAC) payload data. Besides payload the energy expenditure includes all the overhead, e.g., transmission of acknowledgments, IDLE times because of interframe spaces, and packet header/trailer. To determine $E_{\text{bit\_good}}$, the (MAC) goodput (see Figure D.2 on page 194 and Chapter 5) is measured and recorded simultaneously with the power consumed.

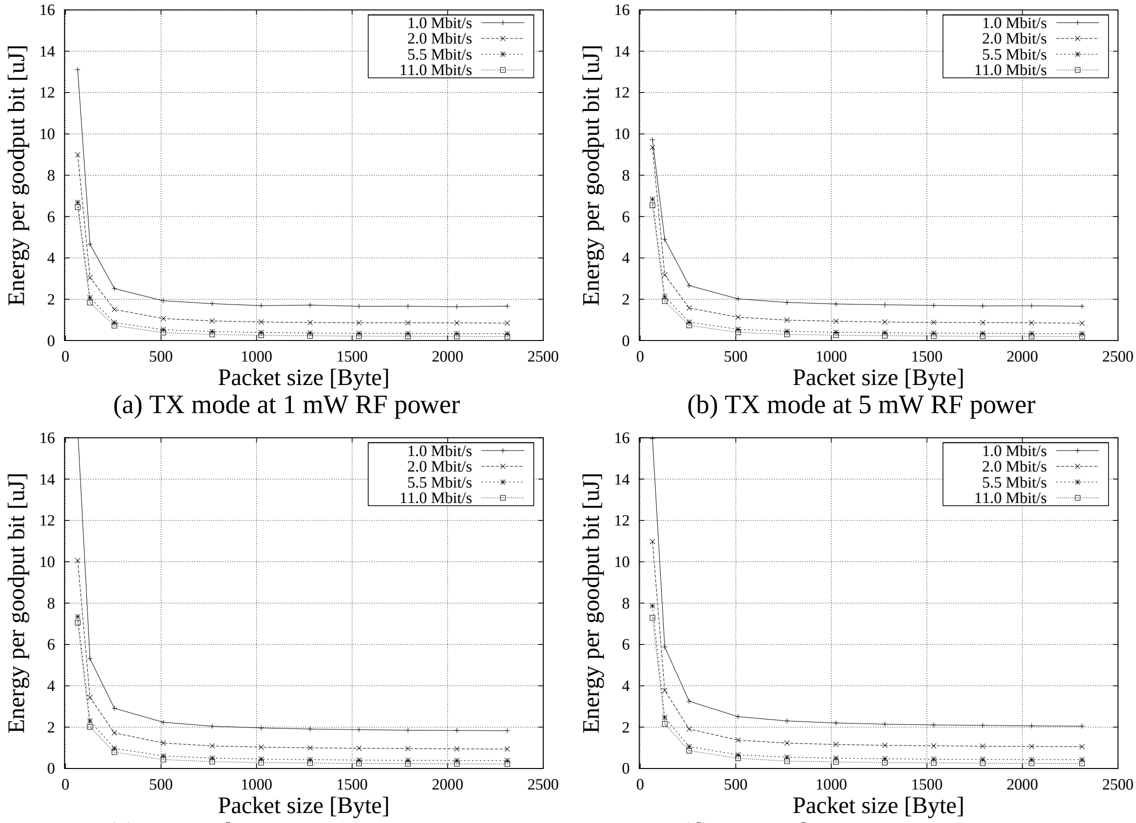


(a) TX mode at 1 mW RF power

(b) TX mode at 5 mW RF power

(c) TX mode at 20 mW RF power

(d) TX mode at 50 mW RF power

Figure 6.1: Measured energy per goodput bit for different power levels and packet sizes during transmission

## 6.2 Energy consumption for low bit error rates

$E_{\text{bit\_good}}$ results were generated from the average power consumption results and the goodput at a distance of five meters for the reception and the transmission case as shown in the Figures 6.1 and 6.2 using equation 6.1, . The graphs reveal that the packet size has a strong impact on energy consumption. Very small payloads ($< 100$ Bytes) like the ones generated e.g., by the TCP protocol for acknowledgments, consume a substantially higher amount of energy than larger packets because of the proportionally larger packet and protocol overhead. This is contrary to the average power consumption results in Section 5.2.2 where small packets consume less power. Therefore, if applicable, packets should be made as large as possible to optimize energy consumption. Of course this certainly depends on the

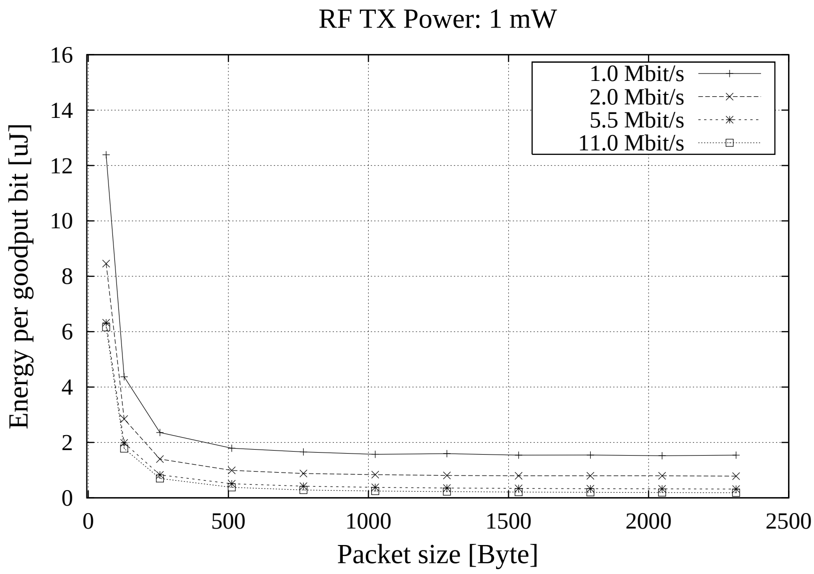


Figure 6.2: Energy per goodput bit for different packet sizes during reception

channel quality (which was excellent throughout our measurements) since larger packets are generally more error prone. With an increased RF power level the energy consumption slightly increases in the TX curves because of the higher amount of power consumed during transmission. This effect is not visible for the reception case (Figure 6.2) because the transmission part of the PC4800B NIC circuitry is turned off during reception. Therefore I only show the 1 mW power level graphs as a representative[1]. In contrast to the power consumption results the energy curves for 11 Mbit/s show a better performance than the 5.5 Mbit/s curve and so on. This is true for TX and RX energy graphs because of the reduced transmission and reception time at higher data rates. It can be considered as an indication that the use of high data rates is desirable as long as the channel quality is good.

## 6.3 Energy consumption for high bit error rates

As measurements are costly regarding setup, measurement time and result processing, a simulation approach to determine the energy consumption for higher BERs was chosen.

[1]The graphs for 5, 20, and 50 mW can be found in Figure D.3 on page 194.

Higher BERs are often the result of an increased distance between two wireless nodes communicating with each other. This is also assumed for my simulation model. The bit error characteristics are chosen according to an AWGN channel.

### 6.3.1 Simulation setup

The simulation configuration basically is similar to the measurement setup. There is a sending node and a receiving node. The sending node transmits packets of a certain size continuously according to the rules specified in IEEE 802.11 over a fixed distance to the receiver. During each simulation the consumed power as well as the obtained goodput are recorded, which allows for determining the energy consumption per payload bit as shown in Equation (6.1). The simulations are performed until a confidence level of $90\%$ for an accuracy of 0.01 for every result of interest is achieved. Either the data rate, the transmission power, the packet size or the distance are changed for the simulation runs.

### 6.3.2 Simulation assumptions

The PC4800 NIC is modeled using the IEEE 802.11 model as described in Section 4.2. As far as the physical parameters are concerned, I used the set shown in Table B.1 with a long Physical Layer Protocol Data Unit (PPDU). The MAC was configured to only conduct its basic access functionality. That is to say, there were no fragmentation, no RTS/CTS, no power saving, and no retransmission. Additionally, the model is extended with a state description, which puts the model into one of the three states: TX, RX and IDLE. Power consumption values as measured in Section 5.2.1 are assigned to every state. This is needed to calculate the average power consumption.

For the source I assumed a UDP stream according to the measurements shown in Chapter 5. The source generates packets of a fixed size and constantly keeps the transmission queue filled up. For the radio channel I assumed an AWGN channel and a path loss exponent of two as described in Section 4.4.3.

In Figure 6.3 the BER versus the distance for 1 and 50 mW transmission power are shown for various modulation schemes. It can be seen that the BER stays very low up to a certain distance threshold value, which depends on the used RF power level. Therefore

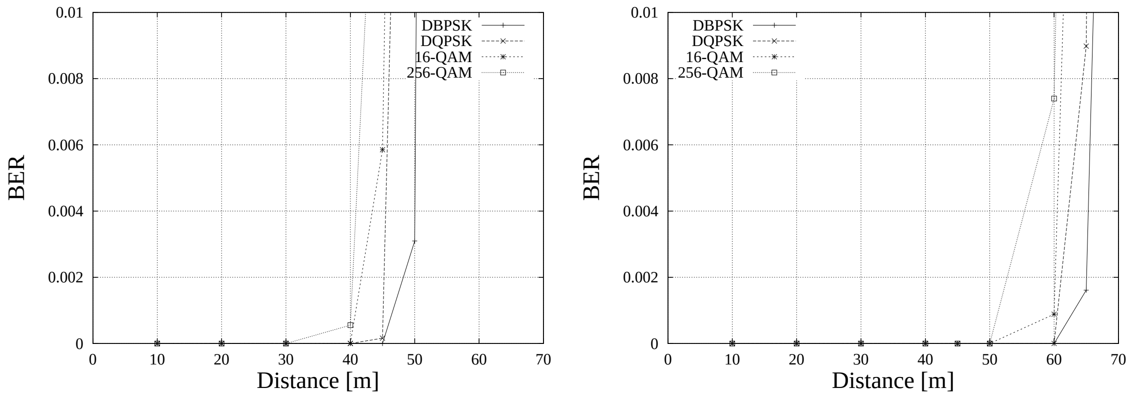


(a) 1 mW RF power (b) 50 mW RF power

Figure 6.3: BER vs. distance for various modulation schemes
The graphs were computed using a channel noise $N$ of -111 dBm, a receiver noise figure $N_{\mathrm{RX}}$ of 7 dB, transmission frequency of 2.4 GHz and a bandwidth (despread) $B_{\mathrm{T}}$ of 2 MHz. No antenna gain is assumed.

an RF power level increase can be seen as an extension of the low BER range. After this value the BER jumps to a high level, which makes it impossible to transmit any MAC frame correctly. From my experience, the highest acceptable mean BER for an AWGN channel ranges from $10^{-2}$ to $10^{-3}$, depending on the packet size. The "good or bad" effect is in line with the behavior of the PC4800 NIC throughout test measurements. Up to a certain distance the card works perfectly, whereas beyond that value no communication is possible at all. The modulation scheme plays a secondary role in terms of distance because the considerable reduction of the BER occurs in a small range depending on the RF power level. Generally, simpler modulation schemes are more robust.

### 6.3.3 Results

I started with the validation of my model. For that purpose I selected a distance of five meters to assure a very low BER. This distance is used throughout the measurements. When comparing Figures 6.1(a) and 6.1(d) with 6.4(a) and 6.4(b), containing measurements and simulation results respectively, it can be seen that the results match very well. A slight difference is only visible for small packets, which may be the result of inaccuracies in the evaluation of the measurement traces. The results prove my model to be sufficient for further investigations.

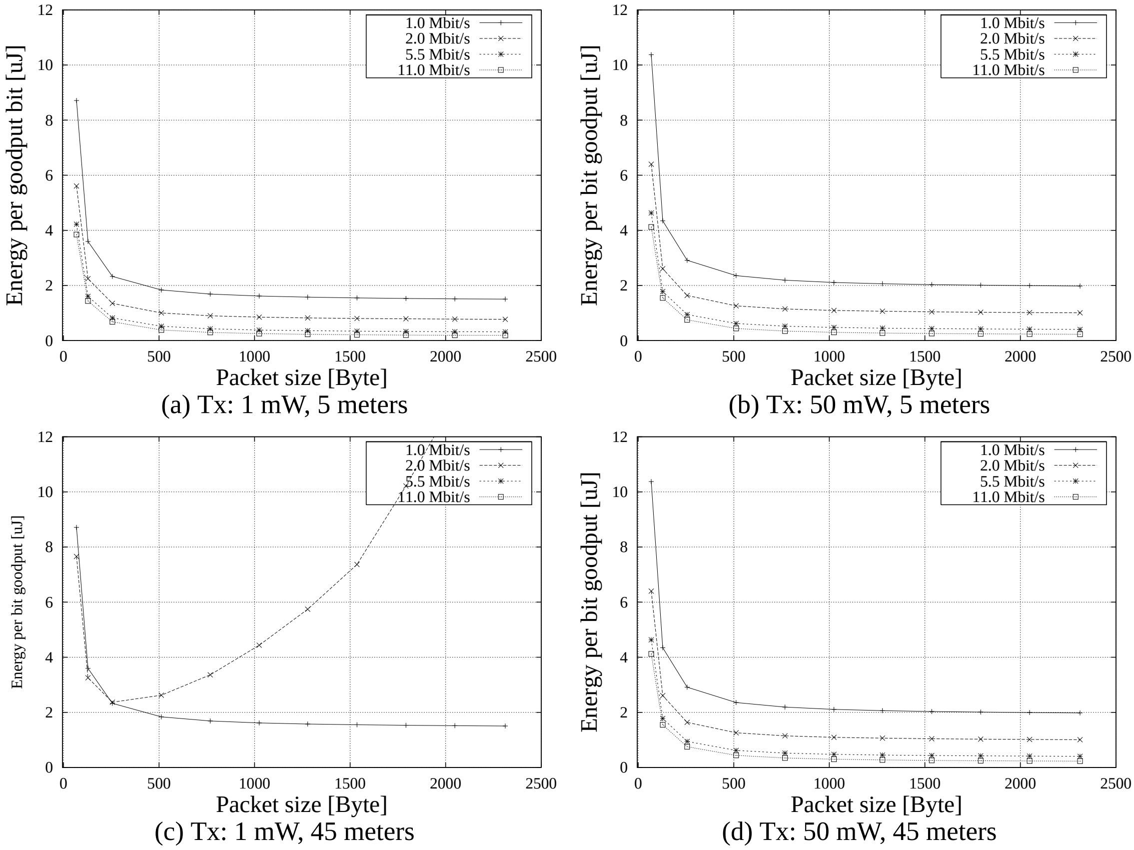


Figure 6.4: Simulated energy per goodput bit at 5 and 45 meters

Next I investigated the energy consumption at various distances[2]. At five meters (see Figure 6.4(a) and 6.4(b)) an increased RF power level leads to an increase in the consumed energy per bit. The data rate and packet size also impact the energy consumption. Higher data rates and large frames consume less energy. This leads us to the conclusion that as long as the BER (distance) stays low, the highest data rate as well as large (non-fragmented) MAC frames should be used. Similar results are achieved up to a distance of 40 meters.

At around 45 meters the dramatically increased BER (see Figure 6.3) for 5.5 and 11 Mbit/s transmission rates comes shows effect at 1 mW RF TX power. Figure 6.4(c) reveals that the energy expenditure becomes higher as the data rate increases because higher data rates are more vulnerable. In fact the energy expenditure is infinite for 5.5

[2]For readability reasons, only some performance graphs are shown. Results for other RF transmission powers and distances are shown in Figure D.4 and D.5 on page 195, D.6 on page 196, D.7 on page 197.

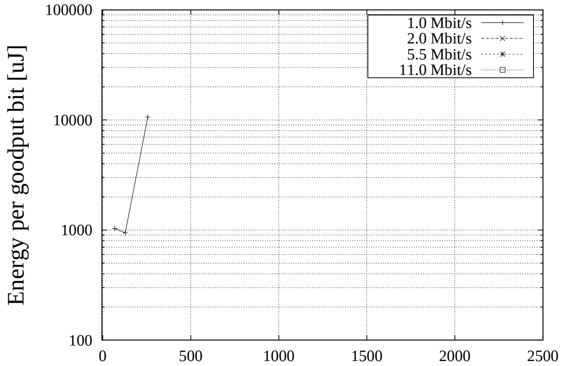


(a) Tx: 1 mW, 50 meters

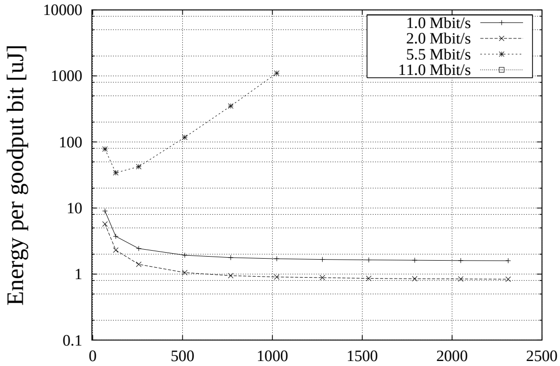


(b) Tx: 5 mW, 50 meters

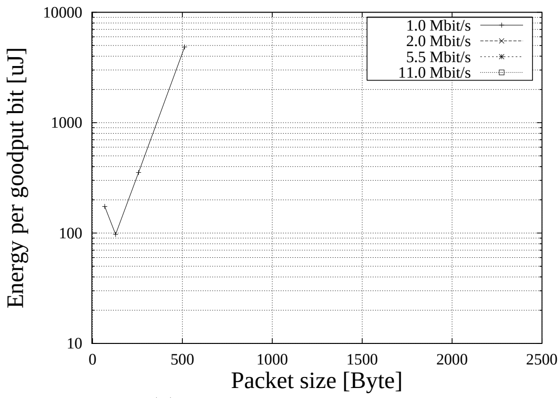


(c) Tx: 50 mW, 65 meters

Figure 6.5: Simulated energy per goodput bit at 50 and 65 meters

and 11 Mbit/s at 1 mW RF power level because no frame can be successfully transmitted. Therefore the results cannot be represented in the graph. At a transmission rate of 2 Mbit/s very small packets lead to a high energy consumption because of the protocol overhead, while large packets consume more energy because of the increased packet error rate, which considerably reduces the amount of successfully transmitted frames. There is an optimum frame size for 2 Mbit/s at around 256 Bytes. While packets cannot be enlarged in IEEE 802.11, a transparent reduction of the frame size is possible using the fragmentation mechanism to improve energy efficiency. For higher RF power levels the energy consumption is similarly high as for smaller distances (Figure 6.4(d)).

When further enlarging the distance to e.g., 50 meters, 1 mW RF TX power is not sufficient anymore, except for a data rate of 1 Mbit/s and small frame sizes ($\leq 256\,\mathrm{Bytes}$, Figure 6.5(a)). In this case the BER is so high that no MAC frame can be successfully transmitted. At an RF power level of 5 mW, a transmission rate of 11 Mbit/s leads to an infinite energy expenditure per goodput bit while an optimum frame size can be found at 128 Bytes for 5.5 Mbit/s (see Figure 6.5(b)). Lower data rates at 50 meters and 5 mW show similar results as before. Furthermore the graphs show that an inappropriate selection of the data rate (modulation scheme) and the RF power level can considerably increase the energy expenditure per goodput bit by more than two orders of magnitude up to where no data can be transmitted at all. I do not show the results for 20 and 50 mW RF power since they are similar to the graphs shown in Figure 6.4(b). At a distance of 65 meters (Figure 6.5(c)) communication between the sending and the receiving node is only possible if an RF power level of 50 mW and a data rate of 1 Mbit/s is used.

### 6.3.4 Discussion of the energy simulation results

The obtained results lead to a few general conclusions about WLAN interface energy consumption despite the fact that the assumed channel model used in the simulations is rather simple.

A rather straightforward result is that as long as the channel is good or the distance is small, the lowest RF power level should be used. Furthermore the highest transmission rate and largest packet size should be used to further reduce the energy expenditure per payload bit. The latter should also be interpreted in the IEEE 802.11 context; packets should not be fragmented into smaller chunks.

For packet transmission as in IEEE 802.11 networks, the distance negatively impacts the RF channel in a bi-state manner assuming a certain fixed RF transmission power level. Either the RF channel offers a good quality (low distance) so that almost all packets can be transmitted without errors or nothing can be transmitted (long distance). There is only a region of a few meters ($\approx 10m$) where a rate fall-back or increase would make sense. In fact an oversimplified control scheme could suggest the use of the highest transmission rate (11 Mbit/s) as long as the BER is low; otherwise the lowest transmission rate (1 Mbit/s) should be chosen, since it provides a frame delivery service even under poor channel conditions at a moderate energy expenditure. Of course this could be suboptimal with respect to other quality of service metrics such as throughput and access delay. In this thesis the

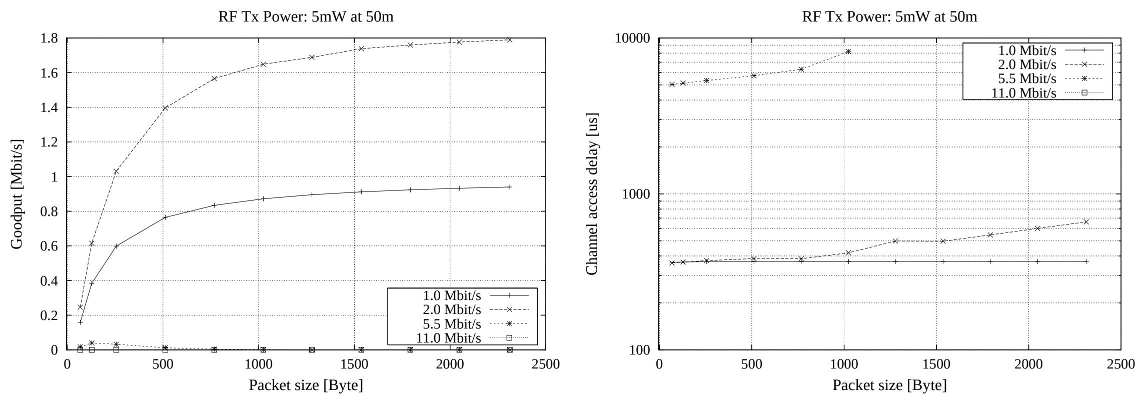


(a) Goodput (b) Delay

Figure 6.6: Simulated goodput and channel access delay for 5 mW RF power level at 50 meters

RF channel is also assumed to be an AWGN channel, but in an indoor environment I expect the channel quality to be time variable due to multi-path propagation and movements, for example. A more granular rate adaptive algorithm as the one proposed by Holland et al. [41] could further optimize the energy expenditure per payload bit for lower distances (BERs).

The results show that MAC level fragmentation is an option to reduce power consumption while keeping the same data rate (see Figures 6.4(c) and 6.5(b)). I think that switching to a lower transmission rate or increasing the RF transmission power are better options since other quality of service metrics like goodput or channel access delay are worse for small (fragmented) packets, higher data rates and an error prone channel. This is exemplarily shown in Figure 6.6 for an RF power level of 5 mW and a distance of 50 meters.

The results also indicate that the RF power level should be controlled corresponding to the SNR level, which results in a certain bit error rate. It can be concluded that the RF power level should generally be adjusted in a way that the error rate of large packets is reduced to a level to allow the highest transmission rate. Note that the higher the transmission rate and the larger the packet size, the lower the consumed energy per goodput bit. Of course there are radiation power limits (30 dBm in the US, 20 dBm in Europe), which must not be exceeded and which can constrain the highest usable data rate to a value below 11 Mbit/s. Although an increased RF power level does not increase the energy consumption by an order of magnitude, the lowest/highest energy-efficient value should also be harmonized with spectrum efficiency issues for overlapping or co-located radio cell situations.

## 6.4 A first order mathematical model of energy consumption

The energy expenditure to transmit one bit of information is a function of the data rate $i$, the RF power level $j$, the BER $k$ and the packet size $l$. The same simplifying assumptions as for the measurements and simulations are made to facilitate an analytical solution. The energy consumed to transmit one bit of payload can be determined by computing the energy expenditure to transmit an entire MAC frame and dividing it by the number of payload bits. Note that several frame transmission attempts might be necessary to transmit one frame successfully. Effects from possible collisions or fragmentation, which would introduce additional transmission costs, are not taken into consideration. Additionally the transmission attempts for a MAC frame are limited to one. That is, a frame is only transmitted once no matter what the transmission result is. According to the IEEE 802.11 MAC protocol and the aforementioned assumptions, the following equation (6.2) describes the energy per goodput bit.

$$\begin{aligned} E_{\mathrm{bit\_good}}(\mathrm{i,k,j,l}) \;=\; ( \;& (T_{\mathrm{BACKOFF}} + T_{\mathrm{SIFS}} + T_{\mathrm{DIFS}}) \times P_{\mathrm{IDLE}} \\ +\;& T_{\mathrm{PACK}}(\mathrm{i,l}) \times P_{\mathrm{TX}}(\mathrm{i,k}) + T_{\mathrm{ACK}} \times P_{\mathrm{RX}}(\mathrm{i}) \quad \mathrm{(a)} \\ +\;& ((T_{\mathrm{BACKOFF}} + T_{\mathrm{EIFS}} + T_{\mathrm{DIFS}}) \times P_{\mathrm{IDLE}} \\ +\;& T_{\mathrm{PACK}}(\mathrm{i,l}) \times P_{\mathrm{TX}}(\mathrm{i,k})) \times N_{\mathrm{attempt}}(\mathrm{j,l})) \quad \mathrm{(b)} \\ /\;& N_{\mathrm{bit\_payload}} \end{aligned} \tag{6.2}$$

Part (a) of the equation describes the energy expenditure for the successful transmission of a frame of a certain length $T_{\mathrm{PACK}}[\mu\mathrm{s}]$ if power $P_{\mathrm{TX}}$ [W] is consumed. The frame length depends on the data rate and the actual packet size, while the consumed power depends on the data rate and the RF power level. Additionally the energy expenditure for idle time is contained, which comprises the SIFS time interval ($T_{\mathrm{SIFS}}$ = 10$\mu$s) between the data frame and the ACK frame, the fixed wait time interval DIFS ($T_{\mathrm{DIFS}}$ = 50$\mu$s) prior to any transmission attempt and a random backoff time[3] ($T_{\mathrm{BACKOFF}}$), which has to pass between DIFS and the actual frame transmission. The average backoff value is 16 resulting in $T_{\mathrm{BACKOFF}} = 16 \times T_{\mathrm{SLOT}}$ ($T_{\mathrm{SLOT}} = 20\mu s$) in a long run. In other words, a node will randomly chose one slot out of the initial backoff window comprising 32 slots if only one transmission attempt is allowed for any frame . $P_{\mathrm{IDLE}}$ is the power consumed in IDLE mode. Furthermore part (a) of equation (6.2) contains the energy consumed for the reception of the acknowledgment. $T_{\mathrm{ACK}}$ [$\mu$s] denotes the rate independent length of the acknowledgment and $P_{\mathrm{RX}}$ [W] denotes the consumed power for reception at 1 Mbit/s. Part (b) represents the amount of power consumed during unsuccessful transmission attempts. It is similar to part (a), but there are no costs for the ACK reception[4] and $T_{\mathrm{SIFS}}$ has to be replaced with a $T_{\mathrm{EIFS}}$. After an unsuccessful transmission attempt (e.g., missing acknowledgment) a node has to wait for at least an EIFS before starting the next transmission attempt. For DSSS WLAN systems EIFS has a considerable length of 1140$\mu$s. The energy expenditure for an unsuccessful transmission has to be multiplied with the number of (unsuccessful) transmission attempts $N_{\mathrm{attempt}}$ before the successful transmission attempt. $N_{\mathrm{attempt}}$ can be derived from the BER according to equation (6.3) and (6.4). Finally $N_{\mathrm{bit\_payload}}$ denotes the number of payload bits in a MAC frame. The ratio of the energy expenditure to transmit one frame successfully after several attempts and $N_{\mathrm{bit\_payload}}$ leads to $E_{\mathrm{bit\_good}}$.

The number of unsuccessful transmission attempts before a successful one is shown below.

$$N_{\mathrm{attempt}} = \frac{q}{1-q}, \tag{6.3}$$

$$q = 1 - (1 - \mathrm{BER})^{l}, \tag{6.4}$$

where $q$ is the packet error rate for independent bit errors as assumed for an AWGN channel, BER is the Bit Error Rate, and $l$ denotes the number of bits in a MAC frame.

[3] Because the sender is continuously transmitting, it is reasonable to assume that a backoff is always performed.

[4] The ACK transmission is very robust because ACKs are always sent at the highest power level and the lowest data rate. Therefore in the case of a transmission failure it is reasonable to assume that the data frame transmission was erroneous and no ACK was sent by the intended receiver.

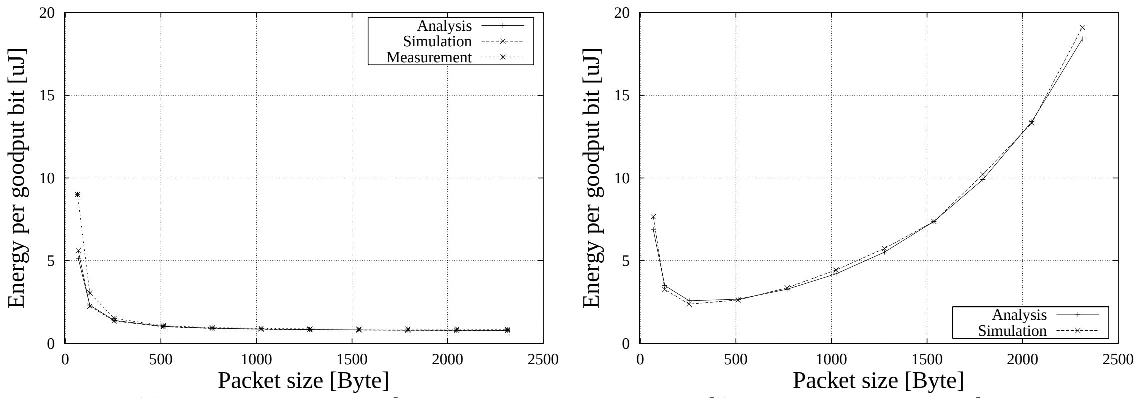


(a) 5 meters, 1 mW, 2 Mbit/s

(b) 45 meters, 1 mW, 2 Mbit/s

Figure 6.7: Comparison of measurement, simulation and analytical results for $E_{\text{bit\_good}}$ vs. packet size in the transmission case

In Figure 6.7 measurement, simulation, and analytical results are shown for a distance of 5 and 45 meters respectively, a transmission rate of 2 Mbit/s, an RF power level of 1 mW and various packet sizes. The computed curves match the simulation results since both simulation and equation (6.2) exactly models the energy expenditure for the assumption described above. The measurement results also match the analytical results. There are only small deviations for small packet sizes. A more sophisticated analytical model is needed to account for collisions or retransmissions. A similar, straightforward approach can be used to model the energy expenditure for the reception case.

## 6.5 Conclusion

In this chapter the energy per goodput bit, which is the energy expenditure required to successfully transmit one bit of payload data, was derived from the measurement results given in Chapter 5 for low BERs. In a next step, the energy per goodput bit for an AWGN channel with increased BERs was investigated by a simulation approach.

The results show the impact of the packet size, the transmission rate, and RF power level. The measurements reveal that packets should be fairly large ($>$100 Bytes payload) to keep the overhead associated with every packet and transmission attempt small. For low BERs, high data rates consume the least energy. Particularly for small distances, the data rate should be set to the highest possible value since it reduces the time where the WLAN NIC is in the TX or RX phase, which consumes the most power. The RF transmission power level should be at its lowest level since it causes the power amplifier of the NIC to consume less power.

If the channel is degraded by high BERs, switching to a higher RF power level is a good way to decrease the BER in order to extend the usage of high data rates which deliver the best energy efficiency. Another method to combat BER is to use smaller data rates, since they are more robust than higher ones. The energy expenditure to transmit packets at higher data rates can be considerably higher for large BERs due to necessary retransmissions. Fragmentation might be used to extend the usage of higher data rates under bad channel conditions, but the results indicate that RF power control in conjunction with packet size control and data rate adaption could yield further improvements.

# Chapter 7

# Power saving driven battery self-recharge

It is a well known phenomenon that batteries self-recharge during a relaxation phase. The self-recharge process requires low or very small discharge currents. In reality, discharge at a large discharge rate $C$ leads to polarization effects. This means that a concentration gradient of active material builds up, which in turn leads to a fast voltage drop although there theoretically is more energy to be delivered by the battery. Two countermeasures are possible: Reduction of the discharge rate $C$ and/or periodic insertion of relaxation times. In both cases the nominal capacity $T$ of a battery converges with the theoretical capacity $N$; the latter is determined by the amount of active (chemical) material in the battery. For further details refer to Section 2.4.

In this section I want to investigate whether the self-recharge effect can be exploited by a WLAN network interface to prolong the operation time of a mobile or wireless device by driving the utilization of the battery capacity to its theoretical limit. The relationship between battery self-recharge and a WLAN network interface is given by the power saving functionality (see Section 2.2.4). Whenever the network interface card is in power saving mode, that is to say virtually all components of the network interface hardware are powered down, almost no energy is consumed leaving time for battery self-recharge.

There are two technical pitfalls. The first one is that a battery normally is not exclusively devoted to the network interface card. There is other hardware in a wireless node, e.g., display, memory or processors, which still consume energy while the wireless network interface is powered down. As a result there is no self-recharge. I will address this issue later in this chapter. For our investigations I assume a battery which is exclusively used for the wireless network interface. Second, the MAC protocol in conjunction with power saving could provide sufficient relaxation time. In IEEE 802.11 networks, the wireless nodes transmit announcements at periodic points in time if there is pending traffic. In order to keep synchronized and to receive these announcements, every node has to be awake at these points in time, which could result in an insufficient relaxation time. Furthermore there could be other inefficiencies of the power saving protocol like the decision when to go asleep or the time synchronization itself preventing self-recharge.

In the following I want to investigate and dicuss the latter question whether and how the power saving mechanism of an IEEE 802.11b network interface can be used to prolong the operation time. For that purpose I explain our modeling assumptions in the next section. In Section 7.2 I show and discuss the simulation results, which reveal that the IEEE 802.11b power saving mechanism not only saves energy by turning off parts or most of the circuitry of a network interface, but also extends battery life by exploiting more of the available chemical energy of the battery. At the end of chapter I discuss the practicability (Section 7.3) and conclude with Section 7.4.

## 7.1 Simulation model and assumptions

I used simulation for analyzing how the IEEE 802.11 Power Saving function improves exploitation of the chemical resources of a battery. The network consists of IEEE 802.11 nodes using the Power Saving function. Further I assume a battery which is exclusively used by the network interface. A description of the network and simulation setup as well as the implications follow below.

### 7.1.1 Network and simulation setup

I used a straightforward simulation setup with a mobile sender (node A) and a mobile receiver (node B) to simplify matters. The setup is sketched in Figure 7.1. Both nodes use the IEEE 802.11 media access control protocol to send and receive data. The radio channel

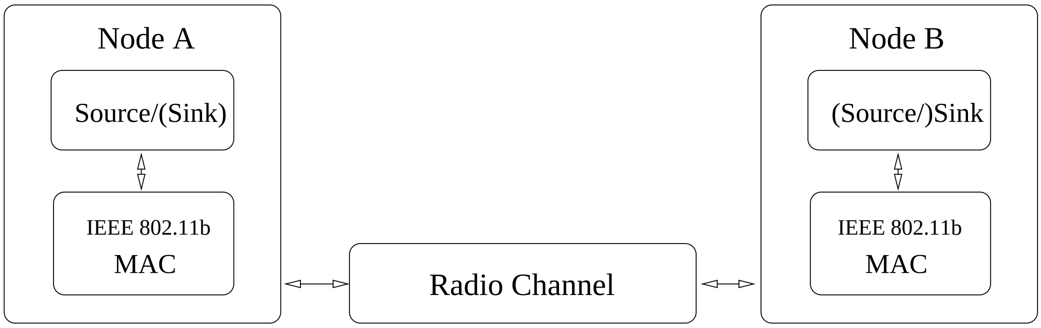


Figure 7.1: Setup for pulsed battery discharge simulations

used is an AWGN channel with a mean, very low bit error rate of $10^{-8}$. The maximum frame size is limited to 1536 Bytes. Larger packets are fragmented before they are passed to the MAC layer. The setup as presented before ensures that the results are only influenced by the MAC protocol in conjunction with power saving but not by the channel or interfering nodes. Therefore the results presented later show the maximum potential of the Power Saving function with respect to the exploitation of the chemical energy of the battery. In nearly all simulations the data rate is fixed at $11$ Mbit/s. A simulation run stops as soon as the battery of node A is discharged. Variations of this setup are possible and mentioned in the text.

### 7.1.2 Battery and self-recharge modeling

The considered battery type is described in detail in Section 2.4. I consider a battery with a nominal capacity $T$ of $50$ mAh. The battery is discharged according to the actual state of the network interface card (TX, RX, IDLE, SLEEP). I assumed a fixed transmission power of $50$ mW and a network interface card voltage of $5$ Volts. The corresponding power consumed in the respective working modes of the network interface card is presented in Figure 5.3 in Section 5.2.1. Using this data I was able to compute the amount of battery discharge during operation of the IEEE 802.11 network interface. I assumed the discharge process to be linear but the coefficient changes according to the operation mode.

Whenever the card is in SLEEP mode, I assumed that the battery relaxes. That is to say, the capacity of the battery increases during this state to a certain extent, but not to more than the initial nominal capacity. The recharge process is modeled by a root function to the power of four, which approximates the real battery relaxation behavior: The relaxation process gradually slows down. Furthermore, the ability to self-recharge decreases as the theoretical (chemical) capacity N decreases. I accounted for it with a coefficient, $m$ which gets smaller the more the battery is exhausted. For that purpose I divided the nominal capacity into equally spaced recharge intensity regions of number $i$ . In the simulations I used $i = 3$ intensity regions with $m_0 > m_1 > m_2$ and $T = 50$ mAh $> T_2 = \frac{2}{3}T > T_1 = \frac{2}{3}T > T_0 = 0$ mAh. The value of $m$ depends on the beacon interval length (see Section 4.5.3).

A battery is considered to be empty, that is to say the cut-off voltage is achieved, if either 10$\%$ of the nominal capacity is reached or the theoretical capacity of the battery is exhausted.

### 7.1.3 Load models

Traffic is modeled using three different video sequence traces (movie: „From Dusk till Dawn", news: „ARD", office cam) and a phone call. In the latter case the communication is bidirectional while for the video sequences communication is unidirectional. As far as the video sequences are concerned, there are two main issues which can impact the results: First the videos have different characters. While the first is a movie sequence with a lot of scenery changes, the second is a news broadcast with a quite stable scenery. In the last video sequence the scenery does not change at all, but some objects move occasionally. The movies have been encoded with different, very common compression algorithms resulting in traces with different characteristics. I used high quality MPEG-4, H.263 with 256 kbit/s transmission rate and H.263 with VBR. The phone call is simulated with and without Silence Detection (SD). A detailed description of the load models and their characteristics can be found in Section 4.3.2. A selection of the most important simulation parameters is shown in Table 7.1.

Table 7.1: Simulation parameters

| Parameter | Value |
|---|---|
| Number of nodes | 2 |
| Traffic model | Audio and compressed video |
| Audio codec | PCM |
| Video codec | {MPEG-4, H.263 with 256 kbit/s, H.263 VBR} |
| Max. frame sizes $[Byte]$ | 1536 |
| TX power $[dBm]$ | 17 |
| BER | $10^{-8}$ |
| Data rate $[Mbit/s]$ | 11 |
| Nominal battery capacity T $[mAh]$ | 50 |
| Recharge intensity regions | 3 |
| Network interface card voltage $[V]$ | 5 |
| Beacon interval $[ms]$ | {50, 90, 130, 170, 210} |
| ATIM window $[ms]$ | {5, 10, 15, 20} |

## 7.2 Results

The simulations and the achieved results serve several purposes. I wanted to clarify whether and how the power saving mechanism of IEEE 802.11 can contribute to a better exploitation of the chemical energy resources of a battery. Furthermore, I try to clarify which is the most energy efficient compression scheme for the respective type of video sequences.

For this purpose different simulations with fixed parameter sets were performed with power saving turned on. For comparison reasons I started each simulation twice: One with self-recharge of the battery, which is equivalent to an exclusively used battery by the wireless network interface, and one without self-recharge where the battery is used by many node components impeding battery relaxation. The duration of a discharge pulse is equivalent to the beacon time (compare Section 2.2.4). Each of the used beacon times (50, 90, 130, 170, 210 ms) were simulated respectively with ATIM windows of 5, 10, 15 and 20 ms.

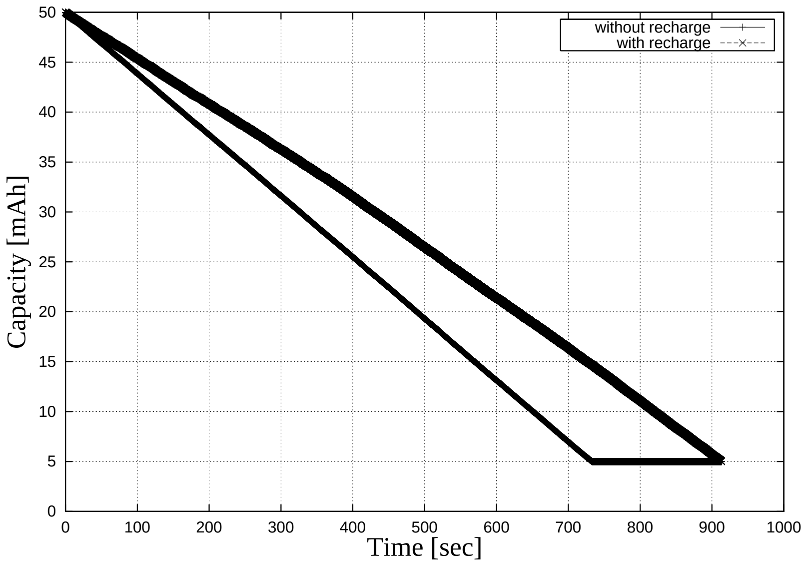


Figure 7.2: Battery life for voice transmission w/o SD: Capacity vs. time

The horizontal run of the lower curve after the cut-off voltage is reached is the result of an ongoing simulation run until the simulation with self-recharge stops.

### 7.2.1 Test of the recharge function

I used a derivation of the simulation model as described in Section 4.2. This model had been proven sufficiently precise several times before by comparison with published results and own measurements. Basically this model is extended by the self-recharge function and the power consumption of the respective operation modes. Therefore it is assumed that the model works correctly as far as the network performance values are concerned. The necessary test of the recharge function was proven correct by visual inspection of the discharge/self-recharge profile.

In Figure 7.2 the battery life vs. the nominal capacity is exemplarily shown for a bidirectional voice transmission (phone call) without silence detection, a beacon interval of 50 ms and an ATIM window of 5 ms. The upper curve in Figure 7.2 represents the capacity with self-recharge of the battery. It ends at 913.3 seconds, the point where the cut-off voltage is reached. Contrary to that both wireless nodes can talk 733.05 seconds without self-recharge (lower curve), which is approximately 24% less.

In Figure 7.3, which contains magnified sectors of the nominal capacity evolution, the correctness of the recharge function and whether there is a recharge at all is proven. In the

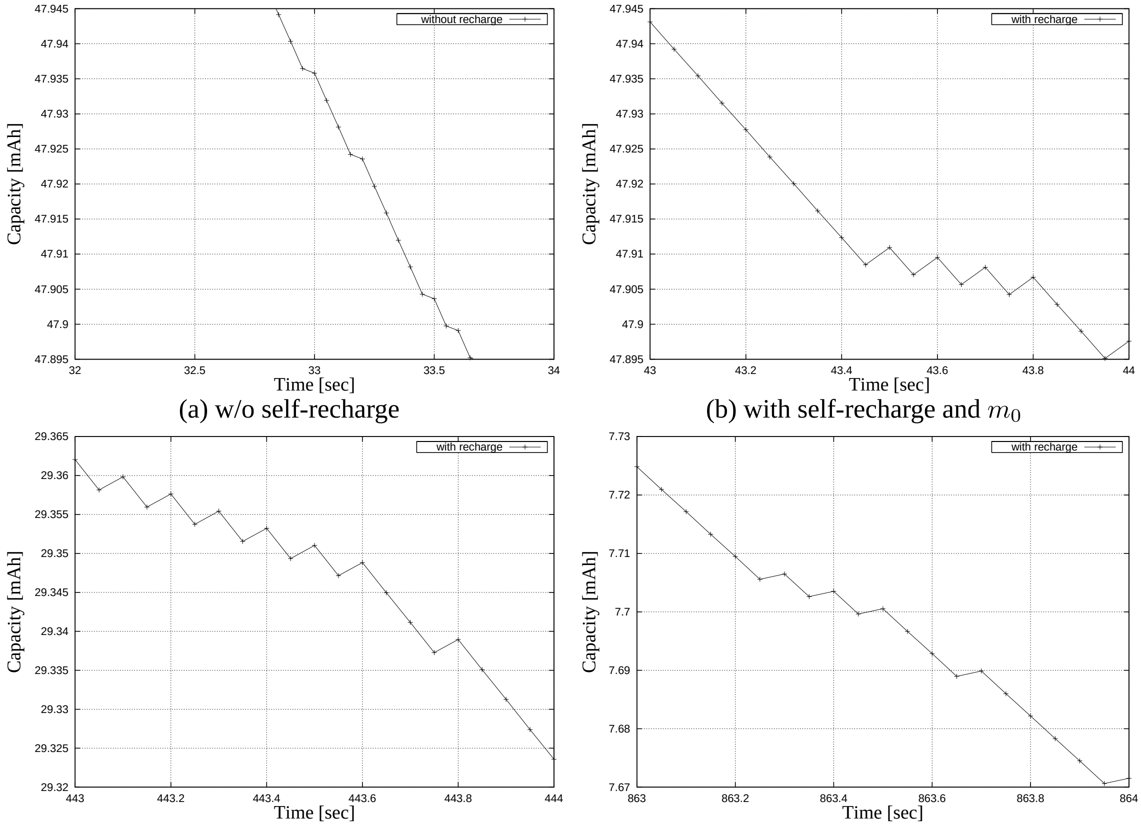


(a) w/o self-recharge

(b) with self-recharge and $m_0$

(c) with self-recharge and $m_1$

(d) with self-recharge and $m_2$

Figure 7.3: Intensity region dependent recharge slope: Capacity vs. time

simulation without recharge in Figure 7.3(a) there is a continuous decrease of the nominal capacity of the battery. The main trend in Figures 7.3(b), 7.3(c), and 7.3(d) is also falling, but not continuously because of relaxation phases where an increase of the nominal capacity is visible. The closer the current available nominal capacity is to the initial nominal capacity, the greater is the increase. The more the battery is exhausted, the smaller is the ability to recharge, which can be recognized by a lower upward slope in the relaxation phases.

If silence detection for voice transmission is applied, battery life is further increased as shown in Figure 7.4. The battery life increases by more than 80%. Based on these test simulation results, I assume the correctness of the simulation model.

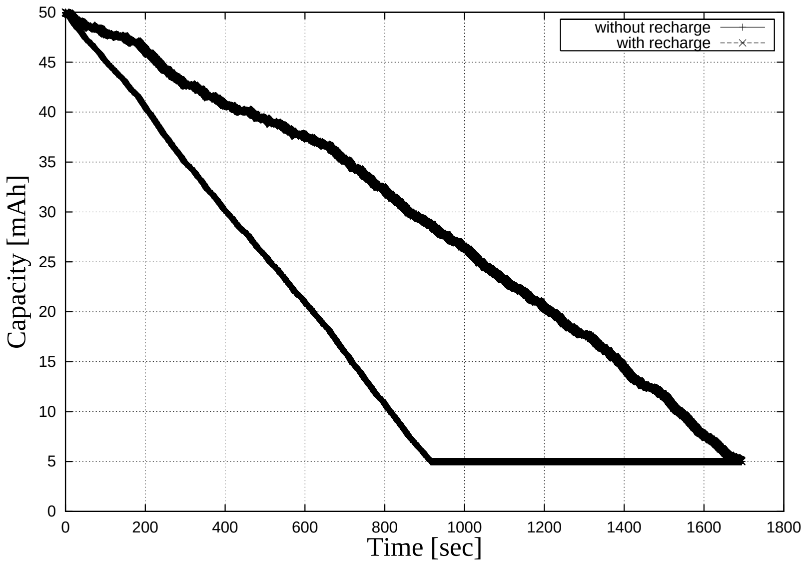


Figure 7.4: Battery life for voice transmission with SD: Capacity vs. time

The horizontal run of the lower curve after the cut-off voltage is reached is the result of an ongoing simulation run until the simulation with recharge stops.

### 7.2.2 Voice transmission

I simulated the battery life for voice transmission with and without self-recharge for all beacon times and ATIM windows with and without silence detection, which is shown for node A in Figure 7.5 and 7.6, respectively. For node B results are identical, since a phone call is assumed to use bidirectional communication.

Without silence detection the beacon time and ATIM window size have a smaller influence on the battery life. The gain is around 22%. In other words self-recharge only sporadically occurs. This is owed to the power saving algorithm in conjunction with the used beacon window size as well as the characteristics of the voice source. A 160 Bytes voice packet is generated every 20 ms leading to the conclusion that there hardly is a chance for a wireless node to go asleep, if the beacon window is larger than 20 ms. A wireless node will stay awake, if there is a packet to send or to receive within a beacon. If the beacon window is larger than 20 ms as it was assumed for these simulations, the probability is very high that a wireless node stays awake most of the time. This results in reduced self-recharge and therefore in little extension of the battery life. An option to increase battery life is to decrease the beacon window. But as already shown in [81], too small beacon window values

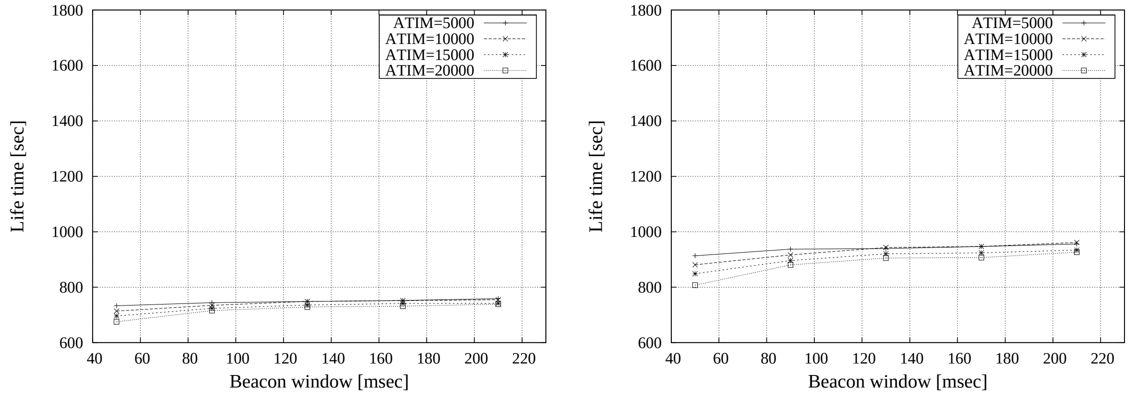


(a) w/o self-recharge (b) with self-recharge

Figure 7.5: Battery life for voice transmission w/o SD vs. beacon time and ATIM window

cause the throughput to drop significantly, which is not desirable having applications other than phone calls in mind.

If silence detection is used, the situation will change. The battery life extends without self-recharge because data packets are only generated during speech periods leading to a reduction in the amount of transmitted data. There is a considerable increase of battery life if the battery can self-recharge. The silence periods leave plenty of relaxation time for the battery.

The beacon time and the ATIM window only marginally effect the battery life. This is owed to the constant low load offered by the voice sources. There is a higher impact if silence detection in conjunction with battery recharge is considered. A small ATIM window and small beacon times result in the longest battery life. For ATIM window sizes larger than 5 ms, a beacon time of about 100 ms delivers the longest battery life. As already explained in [81] there is an optimal load dependent ATIM window beacon time ratio which delivers the best power saving values. An interesting conclusion is that a bursty source increases the self-recharge potential of the battery, which of course depends on the beacon window. Contrary a steady or even low traffic load as it is the case for voice transmissions without silence detection does impede self-recharge.

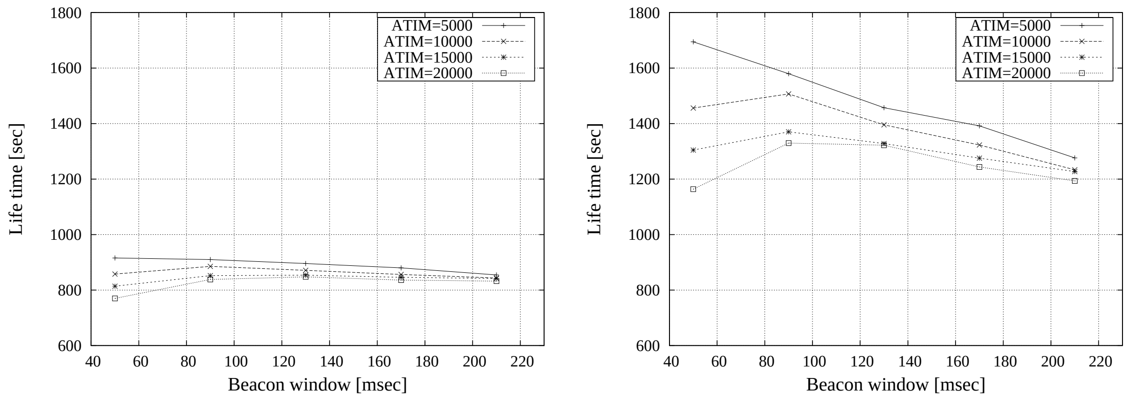


(a) w/o self-recharge (b) with self-recharge

Figure 7.6: Battery life for voice transmission with SD vs. beacon time and ATIM window

### 7.2.3 Video transmission

Similar to the audio results, the battery life is extended when transmitting video sequences and allowing for self- recharge. Please compare Figure 7.7 in this section and Figures D.14 on page 203 to D.18 on page 207 (Appendix D) for that purpose.

The battery life of node A generally is slightly lower than for node B, since node B is the receiving node and reception consumes less energy than transmission. The difference is small, though. Even if B is the receiver of video frames it will has to send a considerable amount of control traffic, which is required by the IEEE 802.11b MAC and the power save protocol.

Self-recharge significantly extendss the battery life. While the type of video sequence only has a marginal impact, the applied video codecs have a strong influence. A comparison of all figures leads to the conclusion that the H.263 coding with 256 kbit/s achieves the longest battery life assuming small beacon windows. This is caused by the (small) target bandwidth of 256 kbit/s and the relatively small average frame size (see Table 4.1 in Chapter 4) . In all cases but one, that is the office cam and H.263 with VBR, the MPEG-4 and the H.263 with VBR video codecs yield a higher source bit rate, which (would) explain the longer battery life for H.263 coding with 256 kbit/s.

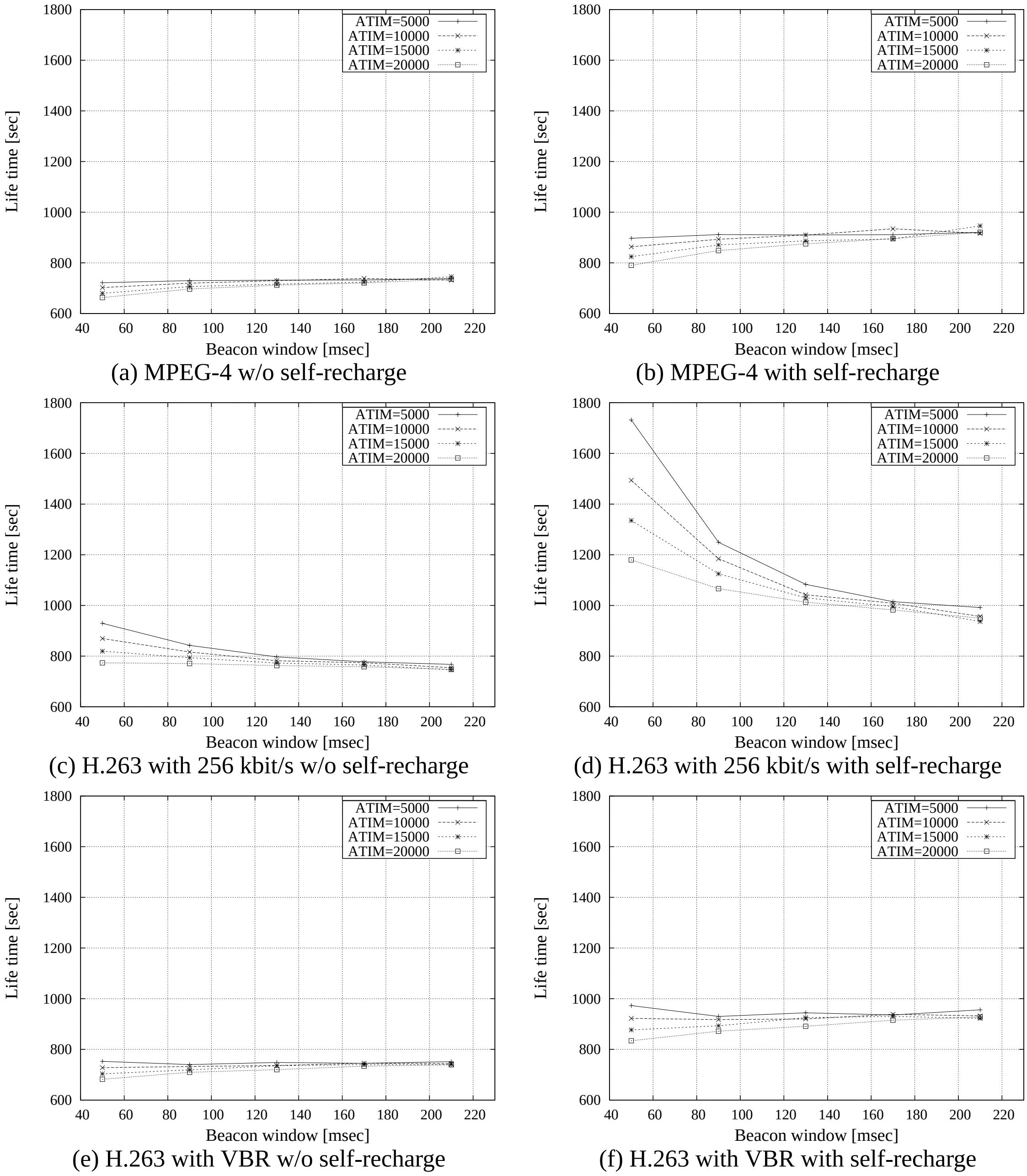


(a) MPEG-4 w/o self-recharge

(b) MPEG-4 with self-recharge

(c) H.263 with 256 kbit/s w/o self-recharge

(d) H.263 with 256 kbit/s with self-recharge

(e) H.263 with VBR w/o self-recharge

(f) H.263 with VBR with self-recharge

Figure 7.7: Battery life of node A vs. beacon time and ATIM window for the transmission of a movie

Because of this exception I reconsidered this issue and found that neither the load nor the (average) frame size are the dominant factors for the durability extension of the battery. Instead an analysis of the frame interarrival times revealed that high quality MPEG-4 generates frames at a rate of 25 frames/sec, H.263 with VBR at a rate of 12.5 frames/sec and H.263 with 256 kbit/s at an even lower rate which depending on the video type. A lower frame rate results in more relaxation time. The impact of the frame size is only marginal (see Figure 4.4). Even for large and fragmented frames, all frame fragments are very likely announced with a single ATIM frame and are sent in the same beacon window. Therefore, no relaxation time is lost. In conjunction with a lower transmission rate, the resulting (larger) spacing between two consecutive frames leaves more time for battery relaxation and therefore for self-recharge. A conclusion is that frames should be large enough to reduce the frame rate.

The beacon time and the ATIM window have a marginal influence on the battery life except for the H.263 codec with 256 kbit/s. The highest gain is achieved if both beacon time and ATIM window are small. Large beacon times like 200 ms result in a shorter battery life compared to other codecs. Note that large beacon windows result in a better throughput but not battery life, and vice versa. Thus the choice which codec should be used to extend the battery life depends on both required throughput and battery life. The following Table 7.2 summarizes the video transmission simulation results for the respective longest battery life.

The results impressively show the merit of the IEEE 802.11 Power Saving function if arrangements are made to permit for self-recharge. It can yield more than 300%; in other words, the life of the battery is trebled. Further on, a small beacon time (50 ms) delivers the best battery life performance for the H.263 Codecs. The MPEG codec requires a larger beacon time (210 ms) and small ATIM windows (5 .. 15 ms). The latter is also valid for the H.263 codecs. H.263 with 256 kbit/s yields the longest battery life due to its bandwidth limitation and the favorable source characteristics.

## 7.3 Practicability consideration

Now the question to discuss is: Can pulsed battery discharge work in reality to prolong battery life? The question can be positively answered. Pulsed battery discharge is already

Table 7.2: Battery life gain of self-recharge and selected parameter for node A

| **Parameter / Model** | **Beacon window** [ms] | **ATIM window** [ms] | **Sleep time** [sec] | **Load** [kbit/s] | **Battery life** [sec] | **Gain** [%] |
|---|---|---|---|---|---|---|
| Voice | 210 | 10 | 230.95 | 128 | 961.83 | 27.73 |
| Voice with SD | 50 | 5 | 652.27 | 55 | 1694.55 | 85.04 |
| Movie MPEG4 | 210 | 15 | 227.07 | 626 | 946.05 | 26.93 |
| Movie 256 | 50 | 5 | 672.39 | 256 | 1732.10 | 86.35 |
| Movie VBR | 50 | 5 | 234.19 | 359 | 972.85 | 29.24 |
| News MPEG4 | 210 | 5 | 234.31 | 741 | 917.28 | 25.23 |
| News 256 | 50 | 5 | 888.39 | 256 | 2100.30 | 115.65 |
| News VBR | 50 | 5 | 233.84 | 397 | 955.60 | 27.99 |
| Cam MPEG4 | 210 | 5 | 229.22 | 390 | 952.77 | 26.55 |
| Cam 256 | 50 | 5 | 1647.45 | 256 | 3178.00 | 205.53 |
| Cam VBR | 50 | 5 | 246.27 | 91 | 1000.30 | 31.11 |

unconsciously applied in various mobile battery driven systems. For instance wireless sensors or actuators often consist of simple wireless hardware, which sends send or receives data from time to time. In the inactivity phases the battery can relax and therefore self-recharge. A deep understanding of both battery recharge and discharge behavior and the interaction with the system design and control will even help to further extend the battery life.

An option to enable pulsed battery discharge is to assign dedicated batteries for the wireless network interface card and for any other node component. This option is not practicable because of the anticipated high implementation costs, size and system complexity. Moreover, there would be uncertainties how to dimension the single batteries for the entire system to work satisfactorily.

But if we further develop the concept of exclusive batteries for every node component, we end up with a single battery consisting of several cells and a cell usage control. Multiple cells are standard, e.g., for lead acid batteries and other battery types as well. However, an additional battery cell control hardware needed to assign cells for certain hardware components of a mobile node or even better switch on/off cells to provide a constant provision of energy parallely allowing certain battery cells to relax, is the crucial point. Examples of batteries with cell control hardware are readily available. For example Maxim Integrated Products offers a multi-cell battery (see [72]) with cell control hardware, although it is used to provide different output voltages. In [13] a simple battery cell scheduling algorithm is presented, which properly shapes the discharge of each cell to optimize the charge recovery of cells. In extension to that, a traffic management scheme is introduced, which exploits the knowledge of the cell charge state.

Last but not least, the benefit of pulsed battery discharge is still present if there is a relatively low background current superimposed with an intermittent high discharge current [14, 72]. This often is the case in mobile communications like TDMA based cellular phones, which draw a high currents during packet transmission and reception only (active mode). In the sleep mode the value of the current is much smaller. In other words, if the mobile node designer succeeds to concert most of wireless node activities at dedicated points in time, the remaining time with low currents serves as battery recovery phase.

## 7.4 Conclusion

In this chapter I discussed the potential of pulsed battery discharge when exploited in an IEEE 802.11 WLAN. Furthermore, I investigated the dependence on three common codecs when transmitting video data. Additionally, the influence of silence detection for voice transmission was analyzed.

I found that pulsed battery discharge driven by the IEEE 802.11 MAC protocol and its power saving function will significantly increase the battery life. The benefit can be as high as 300%. Regarding the different traffic types I can state that the larger the interframe spaces are the longer the battery life is. I conclude that the data source should be either bursty or packet sizes should be increased (at the same load) resulting in interframe spaces large enough to allow for the battery recovery. This can be achieved either by traffic shaping or by source adaptation. Regarding the setting of the beacon time and ATIM window the statement of small values for a good power save performance and a long battery life is confirmed although an application specific setting can further improve the results.

An open questions for further investigations is: How should batteries be discharged to deliver the maximum amount of energy and how should the wireless node system be adapted so that a sufficient discharge behavior is achieved. This definitely comprises traffic shaping, source adaptation, and concerted actions of wireless node components.

# Chapter 8

# Packet size dependent energy-efficient power control

In this chapter I address the problem of reducing energy consumption during the transmission phase of an IEEE 802.11 WLAN. In Chapter 6 I showed that the consumed energy depends on the packet size. Based on this observation I will show for a given network configuration, channel characteristics and packet length that there is an optimum RF transmission power, which assures a minimum energy expenditure for the actual transmitted bit of information. Based on this observation, a packet length dependent power control mechanism is developed, which offers a significant energy saving potential. Furthermore, an approach for adjusting the RF transmission power level based on the perceived packet error rate will show the feasibility of the implementation of a packet length dependent, energy-efficient power control scheme.

One of the most power demanding components of a WLAN NIC is the RF power amplifier. The RF power amplifier can consume more than 50% of the overall power consumption of the network interface (see table 2.2 in Chapter 5). The power consumption caused by the amplifier is relatively high, but controllable within a reasonable range as shown in Figure 5.3 in Chapter 5.

Two basic energy saving strategies follow from the facts above. First, the RF power amplifier should be turned off when not in use. This feature is realized in any implementation of a WLAN card (see Table 2.2 of Section 2.3). The entire transmit circuitry including the RF power amplifier, the RF/Intermediate Frequency (IF) converter, and the IF modem is turned off while the WLAN NIC is not sending. Additionally almost all parts except the WLAN NIC are put into sleep mode or are turned off if power saving is supported and no data is to be transmitted or to be received. Second, the RF transmission power might be reduced to decrease the power consumption of the RF power amplifier, although this may indirectly increase the overall power consumption. I believe that there is a large potential for energy-saving if the RF transmission power level is properly controlled according to the packet size. The metric to be optimized again is the consumed energy to successfully transmit one payload bit $E_{\mathrm{bit\_good}}$ (compare Equation (6.1), which depends on the packet size $\mathrm{ps}$, the transmission power $p_{\mathrm{tx}}$ and of course some other parameters $*$, which are not considered here:

$$E_{\mathrm{bit\_good}}\ [J/Bit] = f(\mathrm{ps}, p_{\mathrm{tx}}, *). \tag{8.1}$$

The basic idea is as follows: The reduction of the RF output power results in a reduction of the instantaneous power consumption of the WLAN NIC and the RF power amplifier in particular. This is certainly traded off to a certain extent by bit errors. An increase of the BER unavoidably leads to a higher probability of retransmissions either on the MAC, data link or transport layer, which in turn increases the energy consumption. On the other hand, an irreflective high RF power level setting could also lead to a needless power consumption, since the BER does not improve significantly after a certain point. Therefore the RF output power adjustment should be balanced with the number of retransmissions to achieve the lowest energy consumption. This requires a power control mechanism. It is shown for a dedicated network scenario that energy savings during the transmission process can be achieved using a simple power control algorithm. The algorithm employs a selection of the appropriate transmission power level according to the size of the next MAC frame to be transmitted.

This is investigated via simulation. In Section 8.1 I present the used simulation setup and the modeling assumptions. In Section 8.2 I derive a weighted performance metric according to the one presented in Section 6.1. Next in Section 8.3 I elaborate the relation of the transmission power and packet size, and in Section 8.4 and 8.5 I show the energy-saving potential when power control is applied. In Section 8.6 I present a practical power

Table 8.1: Simulation parameters

| Parameter | Value |
|---|---|
| Number of nodes | 2, 4, 8, 16 |
| Frame sizes | 64 … 2312 Bytes |
| TX power | 13 … 18 dBm |
| Traffic load | $> 100\%$ |
| Data rate | 2 Mbit/s |

control approach to save energy during the transmission process. Afterwards I draw the conclusions.

## 8.1 Simulation setup and assumptions

During these investigations I considered an IEEE 802.11 ad hoc network (no access point) with a different number of nodes. Implications of other radio cells (e.g., interference) were not assumed. Each mobile node is within transmission range of all other nodes, i.e., there are no hidden terminals. The node model is described in Section 4.2. The distance between a sending and a receiving node is approximately 30 meters. Mobility (around a center point for each node) is covered by the Gilbert-Elliot bit error model as described in Section 4.4.1, which allows for changes in bit error rate (good $\Leftrightarrow$ bad state) over time. It is further assumed that for each sender/receiver pair an independent radio channel exists, i.e., while one station receives a frame correctly other stations might receive the same frame incorrectly. Every node has a frame ready to send at every point in time. Therefore all nodes are involved in every channel access cycle. A mobile node always sends a frame of a fixed size to its successor, which is determined by the identifier of the node. A frame is sent with a constant RF transmission power to another node. Frame size and/or RF transmission power are changed in every simulation run. A summary of the simulation assumptions is given in Table 8.1. For the investigations I used a data rate of 2 Mbit/s. I would await qualitatively similar results for other data rates.

Table 8.2: Assumed parameters in Figure 8.1

| **Parameter** | **Value** |
|---|---|
| Frequency | 2.4 GHz |
| Channel noise | -111 dBm |
| Fade margin | 30 dB |
| Receiver noise figure | 7 dB |
| Antenna gain | $G_{tx} = G_{rx}$ =0 dB |
| Range | 30 meter → Path loss indoor= 80 dB |
| Modulation | DQPSK |
| Data rate | 2 Mbit/s |
| Bandwidth (despread) | 2 MHz |

**Channel modeling**

The RF transmission power has a direct influence on the BER of the radio channel and hence on the energy consumption of a wireless node. The assumed parameters are shown in Table 8.2. Throughout the investigations the Gilbert-Elliot channel model (see Section 4.4.1) is assumed. I determined the parameters in two steps. First I derived the mean BER. Since the mean BER does not reflect the characteristics of bit errors appropriately, the widely accepted Gilbert-Elliot channel model is used to take dynamic BER changes into account. Thus there are time phases with either higher bit error probabilities or lower bit error probabilities, which represents the bursty nature of the bit errors sufficiently for indoor radio channels. Therefore in a second step the Gilbert-Elliot model is parameterized to provide the previously computed mean BER.

The mean BER can be computed using Equation 2.9 which is solved for $\frac{E_\mathrm{b}}{N_0}$. The result has to be used with Equation 2.6 under the assumption of an AWGN channel to finally get the mean BER. Thus the mean BER for a transmission rate of 2 Mbit/s is

$$\mathrm{BER} = \frac{1}{2} \cdot e^{-10^{\frac{P_\mathrm{tx}+G_\mathrm{tx}+G_\mathrm{rx}-L-L_\mathrm{fade}-N-N_\mathrm{rx}}{10}} \cdot \frac{B_\mathrm{T}}{R}}. \tag{8.2}$$

The dependency of the BER on the transmission power is shown in Figure 8.1. Next the parameters (transition and bit error probabilities) of the two-state Gilbert-Elliot error

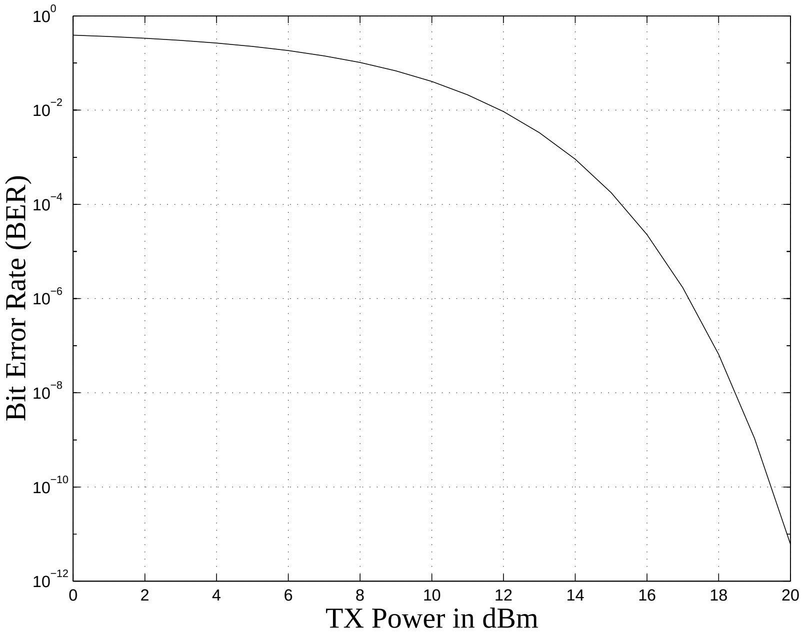


Figure 8.1: Bit Error Rate vs. RF transmission power

model have to be determined (see Appendix C.1). For that purpose the partition threshold $A_{\mathrm{thres}}$ and the mean R-SNR $\rho$ is adjusted in a way that the resulting mean BER (Equation C.15) matches the previously computed value (Equation 8.2). The resulting values for the transition and bit error probabilities are used to parameterize the two-state Gilbert-Elliot bit error model for the assumed RF transmission power. In Table C.2 of Appendix C the Gilbert-Elliot bit error model parameters for various mean BERs can be found.

## 8.2 Performance measures

Several metrics, for example RF transmission power, throughput, overall energy consumption, or mean consumed power can be used to express the energy efficiency improvement of a frame size dependent power control. Unfortunately, they only provide an unweighted estimate. For example, if a WLAN network interface is in sleep mode all the time, the mean power consumption would result in an excellent energy efficiency characteristic. On the other hand, no data is transmitted. Therefore I used the metric developed in Section 6.1,

$E_{\mathrm{bit\_good}}$, the energy expenditure to successfully transmit one bit of payload data. In other words, we take any energy such as for transmission of header information, acknowledgements, payload, retransmission, etc. required to transmit one bit of payload data into account. In turn, the less energy, necessary for all transmission tasks to successfully transmit one bit of payload data, is consumed the higher the energy efficiency.

The basic idea of my work is that a MAC frame should be transfered with a transmission power, which realizes a minimum energy expenditure for the transmission process. In an ideal case without bit errors, collisions, and protocol overhead, the energy $E_{\mathrm{ideal}}$ [Ws] required to transmit data equals the duration of the data transmission, $T$, multiplied with the mean transmitted power $P_{\mathrm{tx}}$. Note, that we only consider $P_{\mathrm{tx}}$ to show the effect of an appropriate adjustment of transmission power. Of course additional power is required to keep the whole or parts of the NIC active for transmission or reception, but this it is not taken into account here.

$$E_{\mathrm{ideal}} = P_{\mathrm{tx}} \cdot T \tag{8.3}$$

The transmission time for the ideal case can be computed from the bit time ($T_{\mathrm{bit}}$) and the number of transmitted data bits ($B_{\mathrm{succ}}$). Hence, from equation( 8.3) we get

$$E_{\mathrm{ideal}} = P_{\mathrm{tx}} \cdot T_{bit} \cdot B_{\mathrm{succ}} \tag{8.4}$$

for the required ideal energy, where

$$E_{\mathrm{bit\_ideal}} = P_{\mathrm{tx}} \cdot T_{\mathrm{bit}} \tag{8.5}$$

is the energy required to transmit one bit in the ideal case. In reality the energy to transmit data will be higher due to protocol overhead and retransmissions accounting for bit errors and collisions. Therefore I introduced the coefficient $\eta_{\mathrm{pr}}$, which is referred to as *protocol efficiency*:

$$\eta_{\mathrm{pr}} = B_{\mathrm{succ}}/B_{\mathrm{all}}, \tag{8.6}$$

where $B_{\text{succ}}$ is the number of successfully transmitted data bits and $B_{\text{all}}$ is the overall number of transmitted bits. The latter includes MAC control frames, transmitted data bits including retransmissions, MAC and PHY frame header, and trailer. $\eta_{\text{pr}}$ indicates how efficiently the protocol works during the transmission phase. In other words, $\eta_{\text{pr}}$ reveals in a long run how much payload is contained in every transmitted bit. $\eta_{\text{pr}}$ ranges from $0$ and $1$, whereas the value 1 will never be achieved because of physical and MAC layer overheads. By rewriting Equation 8.4 taking Equation 8.6 into account we get

$$\begin{aligned} E_{\text{res}} &= \frac{E_{\text{ideal}}}{\eta_{\text{pr}}} \\ &= \frac{P_{\text{tx}} \cdot T_{\text{bit}}}{\eta_{\text{pr}}} \cdot B_{succ} \\ &= P_{\text{tx}} \cdot T_{\text{bit}} \cdot B_{\text{all}}, \end{aligned} \tag{8.7}$$

the resulting energy, which now considers the total number of transmitted bits ($B_{\text{all}}$) to calculate the data bits ($B_{\text{succ}}$) over the radio link. The following equation

$$E_{\text{bit\_good}} = \frac{P_{\text{tx}} \cdot T_{\text{bit}}}{\eta_{\text{pr}}}, \tag{8.8}$$

represents the resulting energy per bit, which is eventually needed to successfully transmit one bit of payload information . This absolutely complies with the Equation 6.1 of Section 6.1. It accounts for the fact that several overhead bits have to be sent before successfully getting one payload bit over the radio link. By maximizing $\eta_{\text{pr}}$ we get the lowest $E_{\text{bit\_good}}$. As we will see in the next section, $\eta_{\text{pr}}$ can be controlled by $P_{\text{tx}}$. The motivation for doing so can be found in the length of the MAC frames. Small frames are less likely corrupted by bit errors than large frames. The key assumption to minimize $E_{\text{bit\_good}}$, which is verified in the next sections, is to achieve the same packet error rate for all frames independently of the packet size. To achieve the same (optimum) packet error rate, and in turn the same optimal level of retransmissions, small packets should be transmitted with less RF transmission power than large packets. Hence, RF transmission power should always be harmonized with the packet size to achieve the lowest energy needs.

Equation 8.8 is suitable to be used in the simulations since $P_{\text{tx}}$ and $T_{\text{bit}}$ are simulation parameters. The latter is indirectly determined by the transmission rate parameter R: $T_{\text{bit}} = 1/R$. The only parameter to be determined within the simulations runs is $\eta_{\text{pr}}$. This can be achieved by summarizing over all payload bits of successfully transmitted MAC frames and putting them into relation with all transmitted bits.

From the simulation results I determined the protocol efficiency. I computed the energy required to transmit one data bit using Equation 8.8.

## 8.3 Frame size dependent optimum RF transmission power

In the following I present the energy efficiency results. The presented results have a confidence level of $90\%$ and an accuracy of $0.1$. Figure 8.2 exemplarily shows the energy required to transmit one data bit successfully for frame sizes of 64 and 2312 Bytes (see Figure D.8 on page 197 for further results for other frame sizes). The curves confirm my assumption: There is an RF transmission power where the energy per bit is minimal. The curves also indicate that this optimal RF transmission power varies with the frame size. Smaller frames have a lower optimal RF transmission power than large frames. This is because the frame error probability at a given RF transmission power level is smaller for small frames than for larger frames. Therefore, a lower radio signal quality is necessary for small frames to achieve the same frame error rate as for large frames. Furthermore it can be seen that the required energy per successfully transmitted bit at the optimum transmission power is smaller for large frames than it is for small frames. The reason for this is the amount of the protocol overhead to be transmitted with each frame, which is smaller for large frames. Thus it is cheaper to transmit large frames at the optimum RF transmission power. Another fact is that the optimum RF transmission power is nearly independent of the number of stations. The increased number of stations means an increased energy consumption per bit while the optimum RF transmission power stays the same. In Figure 8.3 I plotted the optimum RF transmission powers for various frame sizes.

I have to admit that the results were obtained for a certain channel characteristic and distance, but I assume that there always is an optimum RF transmission power. The problem

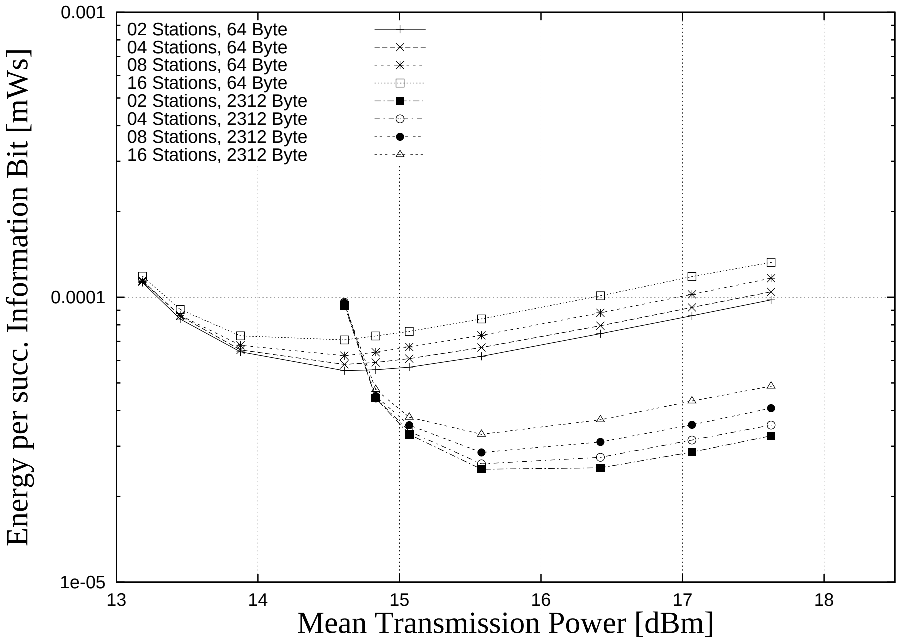


Figure 8.2: Energy per successfully transmitted information bit ($E_{\mathrm{bit\_good}}$) vs. RF transmission power $P_{\mathrm{tx}}$ for frame sizes of 64 Bytes and 2312 Bytes and different number of mobile nodes

is to find the packet size dependent optimal RF transmission powers. I elaborate this topic in a later section.

## 8.4 Frame size dependent power control

In this section I present a power control mechanism, which takes advantage of the observations described previously. From the Figures. 8.2 and 8.3 we can conclude that the RF output power level should be chosen based on the frame size to save energy. That is to say, before a MAC frame is transmitted, its size has to be determined. Based on the packet size the appropriate RF power level is selected. This particularly makes sense having various WLAN application scenarios in mind. For instance, WLANs often serve as the access link to the Internet or interconnection sub-network. Figure 4.3 on page 62 exemplarily shows the frame size distribution of TCP traffic for a 10 Mbit/s Ethernet segment connecting the main

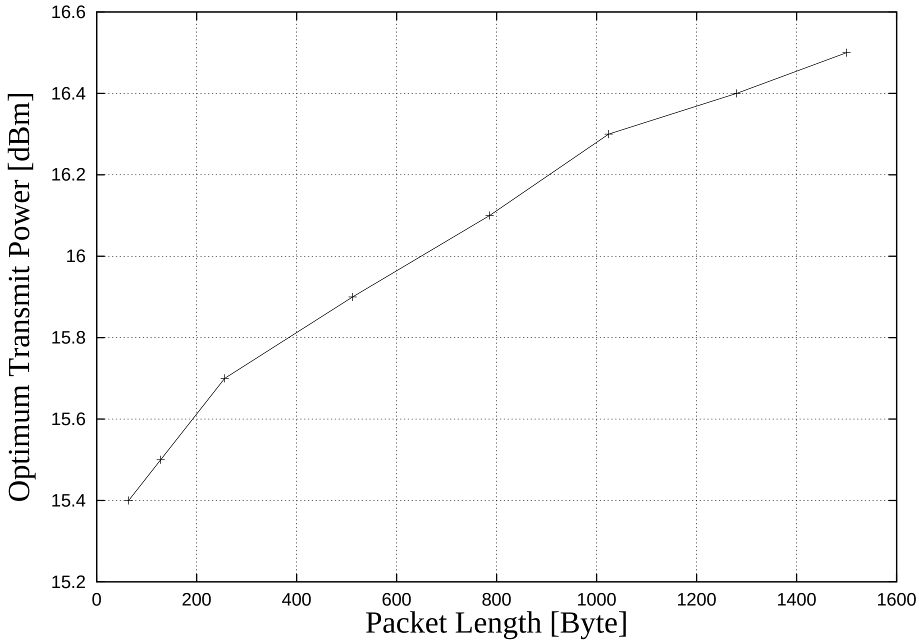


Figure 8.3: Optimum RF transmission power for various MAC frame sizes

campus of the Harvard University(USA) with the Internet in the year 1997 (see [95])[1]. This link carries various frame sizes, a property that can be exploited by the proposed power control mechanism.

I determined the usefulness of the proposed power control mechanism by simulation. For that purpose I developed a delay insensitive source model, which relies on the frame size distribution of the aforementioned Harvard trace (see Section 4.3.1). I did not sample the inter-arrival times from this trace, since it is difficult to scale from 10 Mbit/s to 2 Mbit/s, which is the assumed transmission speed of the wireless link in the simulation. Network traffic, especially Internet and LAN traffic, generally is very bursty (see e.g. [89] and [52]). I achieved the burst characteristics of the traffic by using the Pareto distribution as descibed in Section 4.3.1, which has a heavyly tailed distribution. The $\alpha$ parameter of the Pareto distribution is 1.5. The $k$ parameter is used to control the traffic intensity. The

[1] As stated in [89], the TCP traffic makes up a large share (up to 90%) of the overall network traffic. Traffic shares of protocols are currently changing, mainly due to the availability of multimedia software and services, which rely on UDP (User Datagram Protocol).

simulation setup is similar to the assumptions made in section 8.1 except for the previously mentioned load model. The simulation runs are stopped after the overall protocol efficiency, $\eta_{\mathrm{pr}}$, and the MAC transmission delay reach a confidence level of 90% at an accuracy of $0.1$. The MAC transmission delay is defined as the time which passes between the points in time when the MAC layer accesses the transmit queue and a successful frame transmission starts. IEEE 802.11 specificies up to 8 power levels for the Direct Sequence Spread Spectrum (DSSS) physical layer. According to Figure 8.3, these 8 power levels were set to the optimum RF transmission power of 64, 128, 256, 512, 768, 1024, 1280 and 1514 Bytes frames, respectively. A 400 Bytes MAC frame is hence transmitted with the optimum power of a 512 Bytes frame, a 1200 Bytes frame is transmitted with the optimum power of a 1280 Bytes frame and so on. For every transmitted frame (including control frames) I recorded the number of information bits, the number of control bits, and the corresponding transmission power. Using this information I calculated the energy $E_{\mathrm{bit\_good}}$, the energy used to transmit one payload bit in a long run (compare with Equation 8.8)

$$E_{\mathrm{bit}} = \frac{\sum_{i=1}^{N} P_{\mathrm{tx,i}} \cdot B_{\mathrm{all,i}}}{B_{\mathrm{succ}}} \cdot T_{\mathrm{bit}}, \tag{8.9}$$

where $N$ is the number of power levels (e.g. $N = 8$), $P_{\mathrm{tx,i}}$ is the RF transmission power of level $i$, $B_{\mathrm{all,i}}$ is the number of all bits (including overhead) sent at RF transmission power level $i$, $B_{\mathrm{succ}}$ is the number of the overall successfully received payload bits and $T_{\mathrm{bit}}$ is the transmission time of one bit. Figure 8.4(a) shows the energy saving advantages of our power control mechanism vs. the cases where only one transmission power level (15.3, 15.85 or 16.3 dBm) is used regardless of the frame size. These results are achieved assuming 4 mobile nodes in the radio cell. The curves reveal that the consumed energy when using the power control mechanism is lowest for all load levels. The gain is approximately 10%, 15% and 65% compared to the fixed RF power variants at 16.3 dBm, 15.85 dBm and 15.3 dBm, respectively. A fixed transmission power always leads to higher energy consumption since the transmission power is only optimal for one frame size. For instance 15.3 dBm is optimal for 64 Bytes frames, 15.85 dBm is optimal for 330 Bytes frames and 16.3 dBm is optimal for 1024 Bytes frames. For frames larger than the respective optimal frame size value the RF transmission power is too low resulting in retransmissions. On the other hand

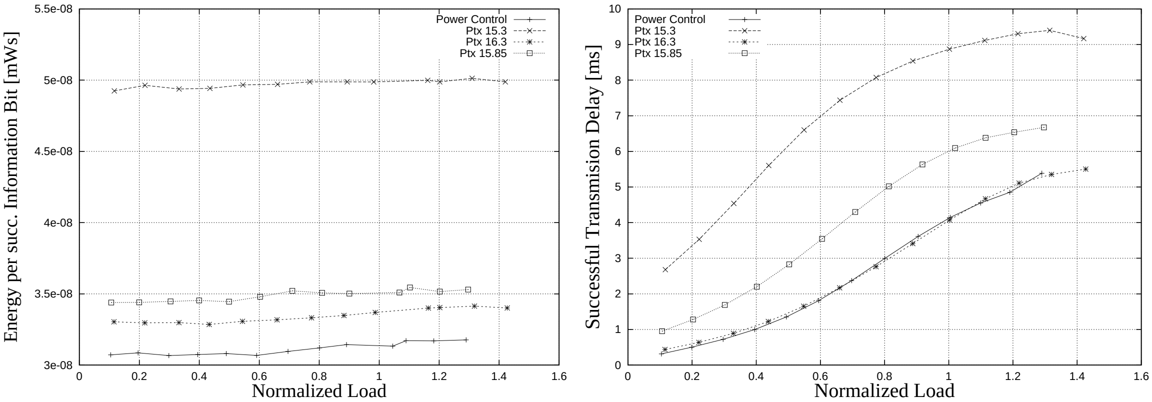


(a) $E_{\text{bit\_good}}$ (b) Latency

Figure 8.4: $E_{\text{bit\_good}}$ and Latency vs. load assuming 4 mobile nodes

for frames smaller than the optimum frame size the RF transmission power is unnecessarily high. In both cases energy is wasted. Similar graphs are achieved for simulations with different numbers of mobile nodes. The slight increase in energy consumption when increasing the load is a result of the higher collision probability, which is not influenced by the power control mechanism in this network setup, but which will play an important role when multi-hop or multi-cell scenarios are considered. Further simulations have shown that the achieved results for a fixed RF transmission power of 16.3 dBm deliver the best achievable energy per successfully transmitted bit. This curve is of course relatively close to the curve containing the power control results. But we have to keep in mind that these simulations are done assuming a certain traffic pattern. Fixed RF transmission power can not cope with changing traffic patterns while power control takes this into consideration by default. The fixed RF power level of 15.85 dBm is optimized for frame sizes of 330 Bytes, which is the mean frame size of the frame distribution used in our model.

Figure 8.4(b) shows the MAC transmission delay for simulations with fixed RF transmission power and power control, respectively. The power control curve is nearly identical to the curve for a fixed RF transmission power at 16.3 dBm. In the latter curve a large share of the frames are transmitted at a good signal quality, which leads to a waste of energy, but ensures a low frame error rate. This in turn results in a low MAC transmission delay. Obviously the power control does not add any delay despite the fact that frames are sent at their optimum (in many cases lower) RF transmission power. The use of a fixed RF transmission power of 15.3 dBm causes a considerable increase in the MAC transmission delay since many frames ($> 64\ \mathrm{Byte}$) are sent with too little transmission power. This leads to a higher frame error rate causing retransmissions, which result in larger delays.

## 8.5 Power control and frame fragmentation

The IEEE 802.11 specification also defines a frame fragmentation mechanism. The original motivation of this mechanism was the reduction of the packet error rate if the radio channel has a poor quality[2]. This can be due to environmental circumstances or a low RF transmission power limit. The proposed power control mechanism makes the motivation superfluous because it is now possible to actively influence the channel quality. If the channel is bad (e.g. the sender does not receive an acknowledgment) a higher RF power level can be used for the frame retransmission. But frame fragmentation still has its purpose. As shown in Section 8.3, smaller frames have a smaller optimal RF transmission value. Therefore frame fragmentation allows on the one hand for keeping legal RF power limits and still ensuring the desired channel quality as well as energy efficiency. On the other hand it reduces the interference level in neighboring radio cells assuming a multi-cell radio scenario because frames are only sent with the RF transmission power necessary for the frame size. This in turn improves the protocol efficiency as well as the available capacity and energy consumption in the neighboring radio cells. The price to pay is the increased overhead and a slightly increased energy consumption. A header and a trailer are added to every frame fragment. Despite this additional overhead, the energy efficiency may be improved considering the overall multi-cell radio network. Furthermore frame fragmentation is helpful if the RF transmission power level cannot be increased due to regulatory limits.

Simulations were used to show the difference in energy consumption using power control with and without fragmentation. The simulation setup is the same as described in the previous section except for the fact that frames larger than 512 Bytes are fragmented into 512 Bytes chunks, and the eight RF transmission power levels are set to the optimum values for frame sizes of 64, 128, 192, 256, 320, 384, 448 and 512 Bytes. Figure 8.5(a) shows the difference in energy consumption using power control with and without fragmentation. As

[2]Note, that smaller frames have a lower frame error probability.

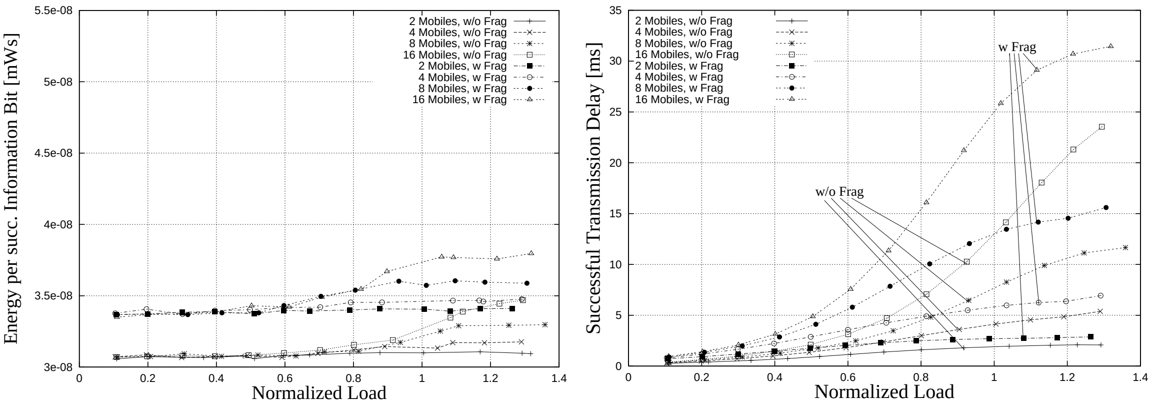


(a) $E_{\mathrm{bit\_good}}$ (b) Latency

Figure 8.5: $E_{\mathrm{bit\_good}}$ and latency vs. load using power control or fragmentation for various number of mobile nodes

assumed in my former considerations, the use of frame fragmentation slightly worsens the energy efficiency because transmission of smaller frames with RF power control is not as efficient as that of larger frames (compare Figure 8.2). This increase in energy consumption regarding a single radio cell can be a decrease considering the overall energy consumption of a multi radio cell network. The quantification of this improvement is left for further studies. The curve also reveals that the energy consumption increases for heavy load levels and an increased the number of mobile nodes. This is due to an increased collision probability leading to a lower protocol efficiency and in turn to an increased energy consumption[3]. In Figure 8.5(b) the MAC transmission delay is drawn. Frame fragmentation adds a slight delay. The reason for this are the necessary inter-frame spaces, in this case the SIFSs, and the acknowledgements that have to be received for every fragment of a frame.

## 8.6 A practical power control approach

IEEE 802.11 specification allows the implementation of power control, although the algorithm is left open to be defined by the manufacturers. The specification defines up to 8 power levels for DSSS systems. The simulation approach can be used to define appropriate

[3]Note, that power control can influence the channel quality but not the collision probability.

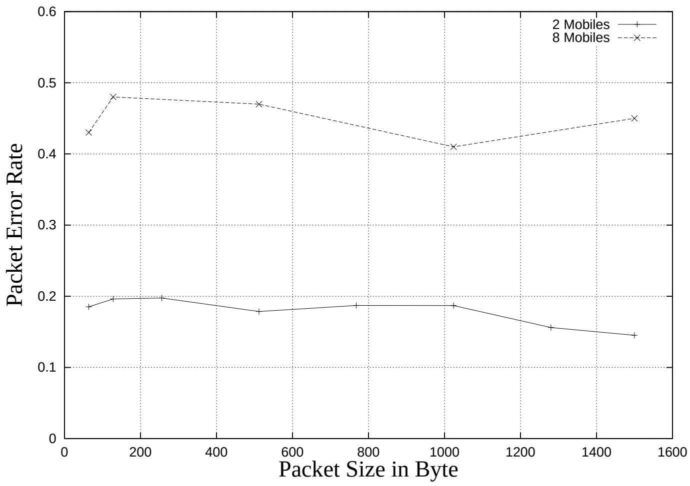


Figure 8.6: PER vs. packet size at the respective optimum RF transmission power for 2 and 8 mobile nodes

values for these power levels. For instance each power level can contain the average optimum RF transmission power value for a cluster of packet lengths. However, the optimum RF transmission power values depend on the actual network scenario and environment, which can have very different RF characteristics. It is unhandy, time consuming and probably inaccurate to compute the optimal RF transmission power levels for several possible application environments. Therefore I tried to find another metric, which selects the optimum RF transmission power for a certain packet size more dynamically and relatively independent of the network scenario. This leads us to the *optimal Packet Error Rate*.

In Section 8.3 I find that an optimal RF transmission power level exists for every packet length. Additionally, this optimal RF transmission power level is lower for small packets than for large packets. Furthermore, certain RF transmission power levels result in certain PERs depending on the packet size. Now let us compare the PERs at the optimum transmission power for the respective packet sizes. We can observe that the PERs almost have the same value. The PERs for different packet sizes and numbers of mobile nodes assuming the respective optimum RF transmission power are shown in Figure 8.6. We refer to the mean value of these PERs as optimal Packet Error Rate in the sense of energy consumption.

As the graph shows, this is almost independent of the packet size. Furthermore the optimal PER (about 0.19 for 2 nodes and 0.45 for 8 nodes) is influenced by the number of mobile nodes. The latter can be explained by the fact that the PER is the result of two independent processes. One process contains the packet errors caused by bit errors while the other one contains packet errors caused by collisions. The number of packet errors caused by bit errors is nearly equal for different numbers of nodes while the PER caused by collisions varies with the number of nodes. However, under normal operating conditions, where the local area network is overdimensioned (average load less than 20% and peak load around 30%), the packet errors caused by collisions are negligible.

Therefore a practical scheme to control the RF transmission power energy-efficiently should be PER based. A practical energy efficient power control approach has to perform two major tasks: It has to adapt to the optimum PER. Since the optimum PER may change, an update of the optimal PER has to be performed from time to time. Second, after the optimum PER is known, the optimum RF transmission power values for given ranges of packet sizes have to be determined.

**RF power adaption** Assuming that the optimum PER is known, every mobile node has to record the perceived PER for various ranges of packet sizes while sending packets at a given initial RF transmission power level. The PER can be easily obtained from the NIC. If the recorded PER for a certain packet size range is smaller than the optimal PER, the transmission power for this cluster of packet sizes is reduced and vice versa. The procedure is repeated until the optimal packet error rate is determined for every cluster of packet sizes. The advantage of this modified scheme is that a mobile node only has to hold one single optimum PER value, which should automatically be adjusted from time to time. using this value, packet size dependent optimal RF transmission power values will be found during operation.

**Optimum PER search** The optimum PER can be determined dynamically by changing the power level from time to time to a random value for a certain packet size range. the consumed power during transmission and the goodput are recorded. By using Equation (6.1) shown in Section 6.1 $E_{bit\_good}$ can be computed. If this test $E_{bit\_good}$ is better than the present $E_{bit\_good}$, a new (optimum) PER was found and all RF power levels for all packet sizes ranges are adjusted accordingly to achieve the requested new optimum PER and hence the most energy-efficient transmission adjustment. Figure 8.6 additionally contains a curve for eight mobile nodes. The optimal PER is higher because of additional errors caused by collisions, but the RF transmission power values will be the same as for four mobile nodes after the power adaption phase. The analysis such as adaptation speed, accuracy and quantification of the energy saving gain are out of scope here and to be investigated later.

## 8.7 Summary

The obtained results show that a significant amount of energy can be saved during the transmission phase if an energy-aware power control is used. Furthermore I found that there is an optimal packet error rate, which can be exploited by the power control mechanism to achieve the optimum transmission power for every packet size. The optimal packet error rate of course dependents on the assumed channel model. The determination of the optimal packet error rate for other channels can be accomplished by an integrated power measurement module allowing the NIC to determine the energy consumption, to acquire the most energy efficient PER and to adjust the RF transmission power accordingly. The analysis and the tuning of such a mechanism are out of scope here and to be investigated in further studies. Although I used the particular example of IEEE 802.11, the proposed approach is generally applicable to other WLAN networks, which use some kind of link level error control. A side effect of power control is the possible reduction of electro-magnetic radiation.

# Chapter 9

# Energy-efficient power control in multi-hop ad hoc environments

As previously shown, controlling the transmission power can offer many performance benefits. These benefits include both capacity improvements and energy savings. In this chapter I investigate the energy savings, capacity improvements and tradeoffs of power control in a multi-hop wireless packet network with a distributed media access control. Several general ad hoc network topologies are explored. It is shown that power control increases the network capacity and saves energy in all investigated scenarios and that utilizing a larger number of intermediate hops between source and destination nodes improves the energy efficiency. However depending on the network topology, increasing the number of nodes may reduce the capacity.

There has been a lot of research on power control in cellular networks [77, 5] in the past years and many techniques such as those employed in CDMA (code division multiple access) networks are currently being used in practice. More recently researchers have demonstrated that integrating power control into ad hoc type wireless packet networks can provide considerable benefits in capacity and energy consumption using both theory [35] and simulations [59]. These networks, unlike cellular networks, operate without support of a fixed infrastructure. A set of wireless nodes that are distributed over a locally limited area constitute a multi-hop ad hoc network forwarding each others traffic as needed to provide a transmission path between source and destination. That is, two nodes that are out of transmission range discover a path via intermediate forwarding nodes so that packets can reach their intended destination[1]. A large amount of related work has focused on tuning the MAC protocols for maximum channel utilization. However, more recently new protocols have been proposed that integrate power control into the MAC layer for further capacity enhancement and their benefits have been demonstrated using simulation tools [97, 60].

Power control has been shown to provide significant performance benefits for single hop wireless ad hoc networks with distributed medium access control although here the benefits in a multi-hop scenario are of interest. By utilizing intermediate hops between a given source-destination pair and applying power control to each hop, further performance gains are possible. The goal here is to evaluate the tradeoffs and benefits of using multiple hops between source and destination. For comparison a generic (ideal) power controlled MAC protocol is evaluated against the non-power controlled IEEE 802.11 protocol for various ad hoc network topologies.

This chapter is organized as follows. First, the use of power control in multi-hop wireless networks is discussed and motivated in Section 9.1. In Section 9.2 the Generalized Power Controlled protocol is presented. The following Section 9.3 shows the network scenarios, in which the Generalized Power Controlled (GPC) and non-power controlled IEEE 802.11 MAC protocol are compared. In the next Sections 9.4 and 9.5 the used simulation environment and the achieved results are shown. The chapter is finished with a summary of the results and further research options.

## 9.1 Motivation

Transmission power control is motivated by two possible benefits: energy savings and capacity increase. The energy savings are achieved by minimizing the average transmission power. It is shown below that the transmission power level is directly related to the power consumption of the wireless network interface. The second benefit is accomplished by using the network resources more efficiently. That is, by allowing a larger number of simultaneous transmissions, power control increases the overall network capacity. These issues are further discussed in the following two sections.

[1] The mechanism for discovering the appropriate forwarding node between source and destination is beyond the scope of this thesis.

### 9.1.1 Energy consumption

One of the basic components of any wireless device is a power amplifier. This component boosts the power of the data signal so it has enough power to reach other nodes in the network. The power amplifier, as compared to other wireless network interface components, consumes a considerable portion of the network interface power (see Section 5). The power consumed by the power amplifier increases or decreases with the strength (power) of the transmitted signal. Considerable energy savings can be anticipated by controlling the RF transmission power.

The instantaneous power consumption for Intersil's WLAN PRISM I 11 Mbit/s chipset is shown in section 5.2.1. Notice that the power amplifier may take more than three times of the power of any other individual component and consumes almost half of the total energy consumed by the network interface card, assuming that all components are in operation. This ratio is expected to continue to increase for future WLAN interface cards, as the processing components become more power efficient and power saving techniques are implemented. In fact an increase in the RF output power level leads to an over-proportional increase in the total power consumed by the WLAN interface. The results show that the increase from 1 to 50 mW in RF output power leads to an increase of about 500 mW in the overall power consumption of the Aironet PC4800B WLAN NIC.

To obtain a better idea of the degree of transmission power reduction (and therefore energy savings) that power control can provide, we must look at the basic path loss model since this dictates the relationship between the transmission range and the required transmission power. The path loss typically causes the signal to attenuate with distance in the order of $1/d^{\alpha}$ [76], where $d$ represents the distance between transmitter and receiver and $\alpha$, the path loss coefficient typically ranging from 2 to 6. As a result, modest differences in transmission ranges will result in considerable differences in required transmission power to maintain the same signal quality at the receiver. This is shown in Figure 9.1, where the signal strength is plotted for different distances between source and destination and also different bit error rates (BER). It can be concluded that either minimizing the power that is necessary to reach the destination and/or utilizing multiple intermediate hops produce

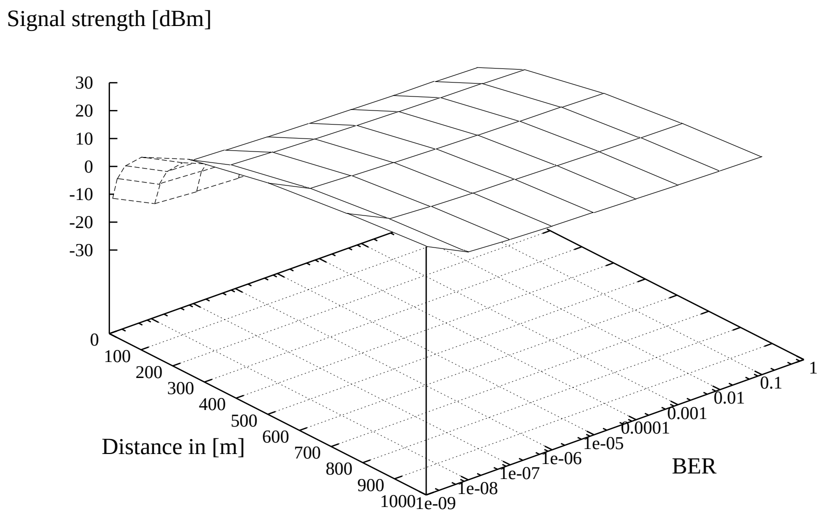


Figure 9.1: Signal strength needed for various distances and required QoS levels. The graph was computed for an IEEE 802.11 type network interface. A DQPSK modulation (2 Mbit/s), an AWGN channel, $1/d^4$ path loss, no antenna gains, 7 dB receiver noise, 20 dB fade margin and a channel noise power of -111 dBm is assumed. Particularly in the lower BER and in the lower distance regions a strong change in signal strength can be noted.

significant power savings as a result of reduced power consumption of the power amplifier. Particularly a steep incline of the signal strength for smaller distances between mobile nodes can be noted.

The selection of the proper power level to save as much energy as possible is a challenging task, which depends on numerous factors. A few of these factors include: the mobile node density (number of nodes per area unit), network traffic load, the topology and distribution of mobile nodes, and available mobile node resources (battery life and link bandwidth). These and other factors are further explored in Section 9.3.

### 9.1.2 Capacity

As outlined at the beginning of the chapter, in this thesis I focus on a network model where mobile nodes communicate on a single shared channel without the assistance of

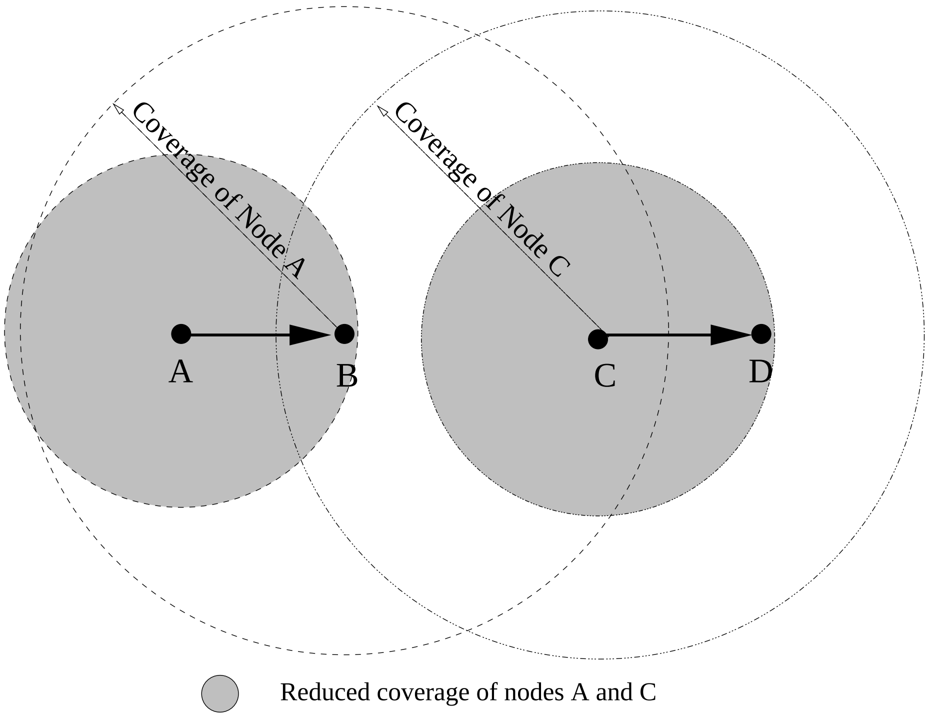


Figure 9.2: Capacity enhancements observed with transmission power control

a fixed supporting infrastructure. Previous MAC protocols have been presented for such networks [46, 6, 22, 31] that used fixed transmission power levels. While these protocols allow transmission that avoid collisions in the sender and receiver neighborhoods, they also limit the amount of spectral reuse since they are designed to work with fixed transmission power levels. Therefore, if we consider a case like the one demonstrated in Figure 9.2, we can see that with current MAC protocols the transmission from A to B would prevent C from sending to D since C is in range of B[2]. However, if A reduces its transmission power level to be just enough to reach B, and likewise C only sends with enough power to reach D, both transmissions could happen simultaneously[3]. Such a power controlled MAC could therefore provide significant capacity increases.

[2]Many protocols additionally use the RTS/CTS mechanism as defined in [46] to avoid the effects of hidden terminal scenarios. In the Figure 9.2, B would respond with a CTS to an RTS of A preventing the transmission from C to D even if C cannot hear A.

[3]If the RTS/CTS mechanisms and/or an immediate acknowledgment are used then also B would have to respond using a reduced transmission power to allow for an simultaneous transmission.

These benefits have been demonstrated with both theoretical studies [35] and simulations [59] that integrate power control into ad hoc type wireless networks with distributed medium access control. In [60] and [97], MAC protocols are presented showing considerable throughput gains.

### 9.1.3 Performance measures

The potential of power control in wireless ad hoc networks is evaluated by comparing the non-power controlled IEEE 802.11 and an ideal Generalized Power Controlled MAC protocol (GPC) in three different network topology scenarios; the latter is described later.

Both protocols are compared in terms of the achieved network capacity $C$ (Goodput) and required energy to successfully transmit one bit of payload (goodput bit) from the sender to the receiver $E_{bit\_good}$ (see Equation (6.1) for more details). $C$[4](see Equation 9.1) is the overall goodput within the network normalized by the corresponding transmission rate of 2 Mbit/s ($\mathrm{TX\_Rate}$).

$$C = \frac{\mathrm{Thr}}{\mathrm{TX\_Rate}} \tag{9.1}$$

Signal energy refers to the transmission power level of each packet multiplied by the duration of the packet summed over the total number of sent packets (successfully and unsuccessfully) multiplied by the total time transmitting for all nodes. Then the signal energy per goodput bit (compare Equation (8.8)) can be expressed as

$$E_{\mathrm{bit\_succ}} = \frac{\sum_{i=1}^{K} \mathrm{Pt_i} T_{\mathrm{i}}}{\sum_{j=1}^{S} L_{\mathrm{j}}}, \tag{9.2}$$

where $K$ represents the total number of packets sent (including control packets) for the duration of a simulation run (from all nodes including intermediate hops), $S$ is the total number of successfully transmitted packets between source and destination, $\mathrm{Pt}_i$ is the RF transmission power of packet $i$, $T_i$ the time to transmit packet i and $L_j$ is the number of payload bits of the j*th* successfully sent packet. Note that $\mathrm{Pt}_i T_i$ is the energy used to send a

[4]C is also referred to as network capacity since it denotes the maximum achievable goodput for a certain network topology scenario.

given packet (packet energy). The total number of successfully transmitted packets, $S$, are calculated from source to destination and not between intermediate hops, while the packet energy is summed over all packet transmissions. Therefore it accounts for the aggregate energy used by all hops to send a bit to the final destination so that the single hop and differing number of multi-hop cases can then be compared objectively.

Here the RF signal energy expenditure is used instead of the total energy used by the network interface because I wanted to show the particular advantage of power control with respect to capacity and energy saving. I only wanted to measure just the energy of the transmitted signal, which is related to the average transmission power level and the radiation absorbed by nearby humans, so these results are relevant for any current or future wireless network interface cards. The signal energy is divided by the number of successfully sent bits so that the overhead incurred by retransmissions is taken into account.

## 9.2 Generalized power controlled MAC protocol

A MAC protocol arbitrates the shared medium access among several end systems. IEEE 802.11 (see Chapter 2.2) is chosen as non-power controlled MAC. A generalized power controlled MAC (GPC) which is defined below serves as the power controlled counterpart. The latter exploits the perfect knowledge of the network and demonstrates the potential benefits of integrating power control into the MAC protocol. It is derived from the MAC protocol presented in[60].

Instead of defining the mechanisms for a specific power controlled MAC protocol, GPC outlines a power controlled MAC protocol framework which can be applied to most power control implementations for shared channel infrastructureless (ad hoc) networks. GPC is a hypothetical protocol, which assumes perfect (global) knowledge of the link gain between any two nodes, the noise at any potential destination and the upper bound of a transmitter's signal power necessary to protect other receivers. The upper transmission power limit is the maximum transmission power that all nodes currently in the process of receiving packets can tolerate before packets are corrupted. The protocol, like IEEE 802.11, follows the RTS-CTS-DATA-ACK message exchange. However, all messages are only sent with enough power to reach the destination with the desired signal power (link quality). GPC will back off if the destination requires more power than other nodes can tolerate (interference). It initially starts with over-compensated transmission power instead of making power adjustments during the transmission. That is, the sender transmits with slightly more power than actually needed to reach the destination. In a multiple access environment, adjusting the transmission power in the middle of a packet transmission is not practical because of the behavior of the wireless ad hoc environment. Some of these behavior factors include: non-deterministic (stochastic) contention delays, the bursty nature of a random access channel and the continuously varying channel attenuation between any two nodes.

A true power controlled MAC would obtain the information that GPC is provided with (with absolute accuracy) through measurements, which would provide imperfect information. Therefore the performance of GPC demonstrates the upper bound of any other power controlled MAC protocol that is based on a collision avoidance framework.

## 9.3 Network topology scenarios

This section outlines several network topologies, which are evaluated later in terms of energy consumption of the transmission process and network capacity using the non-power controlled IEEE 802.11 protocol[5] and the aforementioned GPC protocol respectively. The network topology dictates how nodes communicate (their communication hierarchy) and the placement of certain nodes. Two main types of ad hoc networks are considered. One is referred to as a non-clustered ad hoc network, where all nodes within the network take part in every type of network function such as relaying of packets. The second is referred to as a clustered ad hoc network. In a clustered ad hoc network nodes are grouped into clusters with designated forwarding agents relaying packets between clusters.

The motivation for implementing forwarding agents is to reduce the complexity of the routing algorithm and take advantage of nodes with larger capacity and energy resources. Using specific nodes in a cluster for forwarding packets can significantly reduce the amount of routing overhead (number of packets required to establish and maintain routes) since in this case the routing discovery would only require packets to be sent to the forwarders (as opposed to every node in the network). This would reduce the complexity of the routing

[5] It is assumed that the IEEE 802.11 protocol operates in the Distributed Coordination Function (DCF) mode.

algorithm to the order of the number of clusters, instead of the order of the number of nodes in the network. In addition a network consisting of heterogeneous mobile nodes (with differing available resources) such as cell phones, PDAs, laptops, vehicles, and fixed access points can benefit from nodes with more resources to send over longer distances.

Another factor to consider for forwarding agents is whether their position can be controlled. If the network can control the position of the forwarding agents, they will be placed such away that any distance from a node to the forwarding node is upper bounded or they will be placed according to the mobile node density in certain areas.

The different types of networks considered here are evaluated in Section 9.5 in terms of their energy savings and capacity improvement or tradeoff. Each of the evaluated network scenarios is defined and an example is given to show how they apply to real networks.

- *Scenario I – Non-clustered ad hoc networks*: This type of network assumes that all nodes have equal resources and routing is computed in a totally distributed fashion. That is any node can be a forwarder. Therefore the routing requires some sort of control packets to be sent between every reachable node to find an appropriate route. An example of this would be a sensor network where every node has equal (computation and energy) resources. An advantage of such an algorithm is that every possible route is considered to provide every source-destination pair with the shortest route. However, as stated above, such an algorithm will imply significant overhead if there is even a modest amount of mobility in the network since routes will often become interrupted so that new ones must be found.
- *Scenario II – Clustered ad hoc networks with forwarding agents whose positions can be controlled*: Here nodes are grouped into clusters that form around designated forwarding agents (based on locality). The placement of these forwarders can be controlled to provide coverage and reachability. Nodes within a cluster can communicate directly while nodes in different clusters have to use forwarding agents. In Section 9.5.2 this scenario is tested with uniform placement, where the distance between forwarders is chosen to maintain full connectivity. An example of such a paradigm is one where dedicated wireless nodes are actively placed to support a set of users with PDAs (Personal Digital Assistants). Furthermore, in this scenario two cases are investigated. In the first case, the energy resources of the forwarding agents

are unlimited such as a vehicle or a node with a fixed power supply, and in the second case, the energy resources of the forwarding agents are limited such as for battery powered mobiles nodes.

- *Scenario III – Clustered ad hoc networks with forwarding agents whose positions are not controllable*: This scenario is similar to the last except that the locations of the forwarding agents cannot be controlled and are random. Such a configuration might result if we consider vehicles or other nodes with more resources that have other purposes than to purely serve as supporting infrastructure for mobile nodes with limited resources. An example of this paradigm may be where a public safety officer's handheld radio communicates through the closest public safety vehicle, which would then relay the corresponding packets to other vehicles, and then to the intended receiver. One problem with this scenario is that outages may have to be tolerated since the placement of forwarding agents is random and may be out of range of the mobile nodes or other forwarding agents. Like in the previous scenario, forwarding agents are also considered that may or may not have limited power resources.

The performance of these scenarios is evaluated in Section 9.5 in terms of energy consumption and network capacity for a non-power controlled MAC, IEEE 802.11 and a generalized power controlled MAC, GPC.

## 9.4 Simulation environment

To evaluate the performance of these MAC protocols in the different network topologies, the *ns2* simulator is used with the CMU wireless extensions [16]. The data rate for this configuration was set to 2 Mbit/s, the packet size was fixed to 2 kBytes, the RF transmission power overcompensation was set to be 2 dB, the transmission power range for GPC ranged from -5 dBm to 22 dBm, and the maximum fixed transmission power level of IEEE 802.11 was 20 dBm at maximum. Note that the maximum power level of GPC is set to be 2 dB above the fixed power level of IEEE 802.11 by the overcompensation. The maximum fixed range for IEEE 802.11 and the maximum transmission range for GPC are such that source-destination pairs could be a maximum of 500 meters apart to receive a valid data packet.

The RF transmission power required to send a valid signal to its destination depends on the gain between source and destination. A simple path loss model as given in [76] is applied. As long as the sender-receiver distance is within the Freznel zone, the signal is attenuated proportionally to $\frac{1}{d^2}$. For distances outside the Freznel zone the path loss is proportional to $\frac{1}{d^4}$. Some thermal noise (-104 dBm), a receiver sensitivity of -64 dBm and a receive threshold of -60 dBm are also assumed. A signal is assumed to be valid, if the signal-to-interference-ratio (SIR) is at least 10 dB. The nodes of these scenarios (100) are uniformly distributed in an area of 350 by 350 meters for these experiments.

For the traffic model several source-destination pairs are picked randomly (according to a uniform distribution) off-line. When the simulation starts, the sources generate packets according to independent Poisson processes. The results show 100 source-destination pairs averagely generating 16 (2 kByte) packets per second. This packet generation rate keeps the sources busy to ensure that the nodes in areas with possible spectral reuse have packets to send.

A simple off-line routing algorithm, which chooses the route requiring the fewest number of intermediate hops, i.e., shortest path for the given range settings, is implemented. Note that this may be suboptimal regarding intermediate hops for a power controlled protocol since ideally we would also want to take spectral reuse into account. However, this simple method ensures that the same routes are used for both 802.11 and GPC so that the effects of the routing algorithm can be neglected and results are comparable.

For different numbers of intermediate hops (hence transmission ranges between source and destination) energy efficiency and goodput performance are investigated and non-power controlled and power controlled MAC protocols are compared. Simulation results are gathered for nodes with maximum transmission ranges of 500, 250, 166, 125, 82, and 62.5 meters. That is to say, the RF transmission power for IEEE 802.11 simulations is fixed (not power controlled) for the given range, while for the GPC simulations the power level is only based on the power needed to reach the particular destination. For Scenario I, these ranges correspond to a maximum number of hops of 1, 2, 3, 4, 6, and 8 respectively, based on the network size (350 by 350 meters) the nodes are distributed in.

For Scenario II, the corresponding maximum hops are 1, 4, 6, 8, 10, and 12, since the packets are only relayed through the forwarding agents if source and destination do not belong to the same cluster. For Scenario III the forwarding agents are placed randomly. This means that connectivity cannot be guaranteed unless the transmission range covers the entire network area (500 m or the diagonal of the 350 by 350 m network). Therefore for this case the maximum transmission range is fixed to 500 meters and the number of forwarding agents is set to be the number needed to ensure full coverage in Scenario II using a uniform node placement (see Section 9.5). For Scenario I and II the results are shown in dependency on the increasing maximum number of hops between source and destination (decreasing transmission ranges). Note that these are the respective maximum hops. The averages will be less since the source-destination pairs are chosen randomly. The corresponding averages for the different topologies are shown in Figure 9.3. Note that in Scenario III the maximum number of hops between forwarding agents is almost one since the transmission range covers the entire network area, as discussed above. The forwarding agents themselves can also inject traffic. Therefore the number of average hops decreases slightly when the number of forwarding agents reaches a significant portion of the total nodes. This trend is an artifact of the network topology and the communication pattern and is also shown in Figure 9.3, where the average number of hops for the Scenario III curve slightly drops for the largest number of forwarding agents (corresponding to the 62.5 meters range shown on the x-axis). This situation is not visible in Scenario I and II since there the forwarding agents still have to make use of other forwarding agents (limited transmit power) to send data to their respective destination.

## 9.5 Capacity and energy results

Following the structure introduced in Section 9.3, the energy saving potential and the network capacity of 802.11 and GPC for a non-clustered ad hoc network (Scenario I) are given first.

### 9.5.1 Non-clustered ad hoc network

The performance results are shown as a function of a decreasing transmission range which in turn requires a larger number of average hops (see Figure 9.3). Figure 9.4 shows the

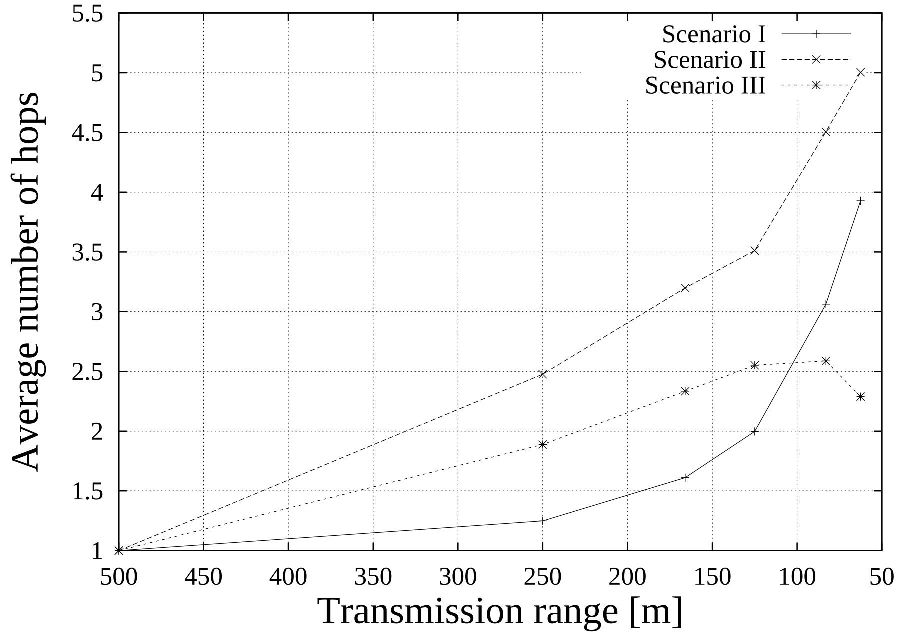


Figure 9.3: Average number of hops between source-destination pairs with different transmission ranges for both GPC and IEEE 802.11 simulations

signal energy as the transmission range is decreased. As anticipated in Section 9.1.1, the signal energy significantly decreases as the transmission range decreases. GPC, the power controlled MAC protocol, shows an additional improvement over the non-power controlled IEEE 802.11 MAC protocol. However, the advantage also decreases as the transmission range is decreased. This is because as the maximum transmission range decreases, the difference between the optimal RF power setting of the GPC protocol and the fixed RF power setting of the IEEE 802.11 protocol also decreases, limiting the benefit of power control.

Figure 9.5 shows the network goodput for 802.11 and GPC for the same ranges as used in the presented energy saving figure. The goodput of IEEE 802.11 at 500 meter starts below 100%[6], while the goodput for GPC is slightly higher. This is because every node is within transmission range of any other node in the IEEE 802.11 case only permitting a single transmission at any point in time. Otherwise a collision would result. However, GPC can

[6] 100% is equivalent to 2 Mbit/s, the used transmission rate in the simulations.

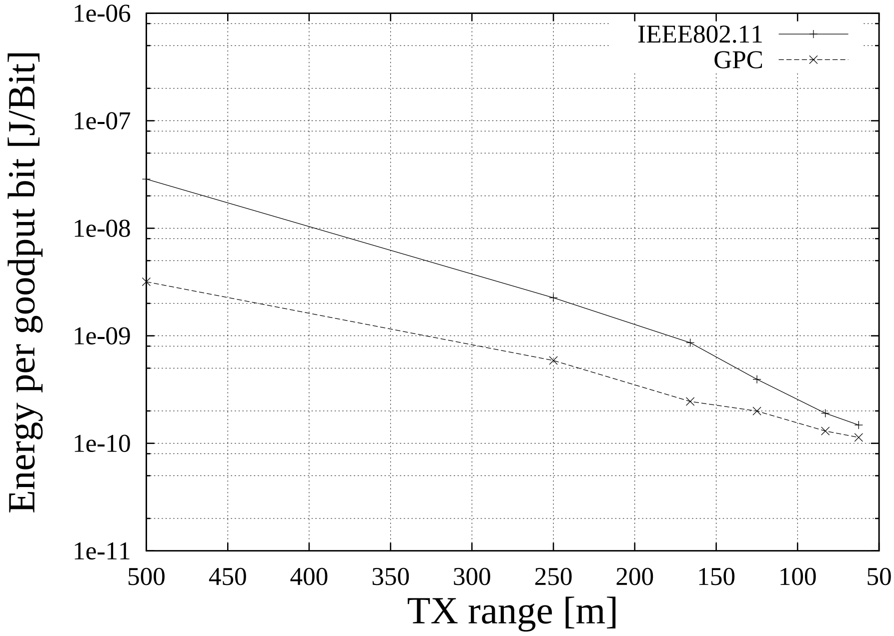


Figure 9.4: Signal energy per goodput bit for an infrastructureless network with different transmission ranges

take advantage of spectral reuse since it adapts its transmission power to the level needed to reach the intended receiver. This behavior can also be observed in the goodput results for other scenarios presented below. The goodput actually drops as the number of hops is increased (transmission range is decreased). This might be counter-intuitive considering the theoretical analysis presented in [35] since as the range is halved, the maximum number of hops is doubled while the area of the transmission decreases by a factor of four. This should allow for more simultaneous transmissions despite the cost of requiring additional time slots to send the packet to the destination. However, this analysis does not account for the fact that packet flows with multiple hops can only be sent at the rate of the slowest (highest contention) link. The analysis of this theoretical study assumes that each link is able to send packets independent of the last hop, i.e., each hop has a sufficient number of buffered packets to be sent when transmission capacity become available. This is obviously not the case for a real scenario, where only the slowest link can take full the advantage of the additional spectral reuse offered by the decreased transmission ranges.

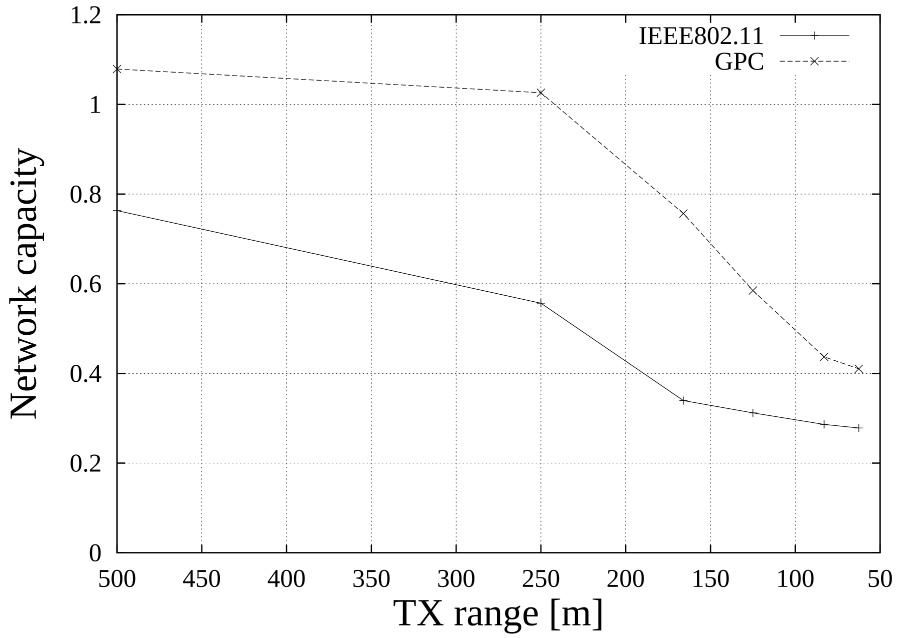


Figure 9.5: Normalized goodput for an infrastructureless network with different transmission ranges

Another characteristic to consider is that the goodput curves do not decline smoothly with decreasing transmission range. Particularly, the decline from 500 meters to 250 meters is more gradual than for the following sections. This is because even at 250 meters most nodes are still within one hop of each other. Only nodes at opposite corners are actually 500 meters apart. Furthermore nodes near the center are in range of all other nodes. Therefore the goodput drops more gradually in the first than in the remaining sections, where a larger number of nodes require multiple hops to reach their destination. The goodput benefits (number of successfully delivered packets) of power-controlled over non-power controlled MAC protocols decrease slightly with the range. For the same reason the energy benefits of power controlled over non-power controlled MAC protocols decrease with the range.

Another issue to take into consideration is the routing protocol used to achieve these results (refer to Section 9.4). It selects the routes based on the minimum number of hops between source and destination, so the optimum is also employed for IEEE 802.11 in the power controlled case (for unbiased comparison at the MAC level). A better choice for power controlled networks would be the use of metrics that take the number of hops, the aggregate path power consumption (summed over the power required at each intermediate link), and spectral reuse gains into account for node densities in various environments to make the best path decisions. This however is beyond the scope of this dissertation, but mentioned here to highlight the fact that additional benefits are still possible – particularly for the energy expenditure – when utilizing transmission power controlled protocols.

Let us distinguish between two spectral reuse cases specified in the preceding two paragraphs. The first spectral reuse case that applies to both IEEE 802.11 and GPC is due to the decreased maximum transmission range and the utilization of intermediate hops. This range dictates the number of intermediate hops that must be used between a given source-destination pair. The second additional spectral reuse case is from reducing (or controlling) the transmission power to the level needed to reach the intended receiver (next intermediate) that must be chosen from the nodes within the fixed maximum range, which is varied between 500 meters and 62.5 meters. The first case will only be realized for IEEE 802.11 if the output power is manually adjusted (restricted), while GPC dynamically adjusts the power to the intended receiver. In accordance with the limitations of current non-power controlled MAC protocols like IEEE 802.11, it can be concluded that even if the particular transmission power level of IEEE 802.11sending node is adjusted to satisfy the intended destination (e.g., IEEE 802.11h), it will still not be sufficient since this would violate the collision avoidance framework set forth by the communal structure of shared channel ad hoc networks.

### 9.5.2 Ad hoc networks with controlled placed forwarding agents

The next investigated network topologies (Scenario II from Section 9.3) are the ones which designate a subset of nodes as forwarding agents for a cluster of nodes chosen either for strategic reasons (see [40]) or because they have more available resources. Nodes directly send to nodes in the same cluster, but they use the forwarding agent to send to nodes of other clusters.

A simple method would be to uniformly place some number of forwarding agents in the

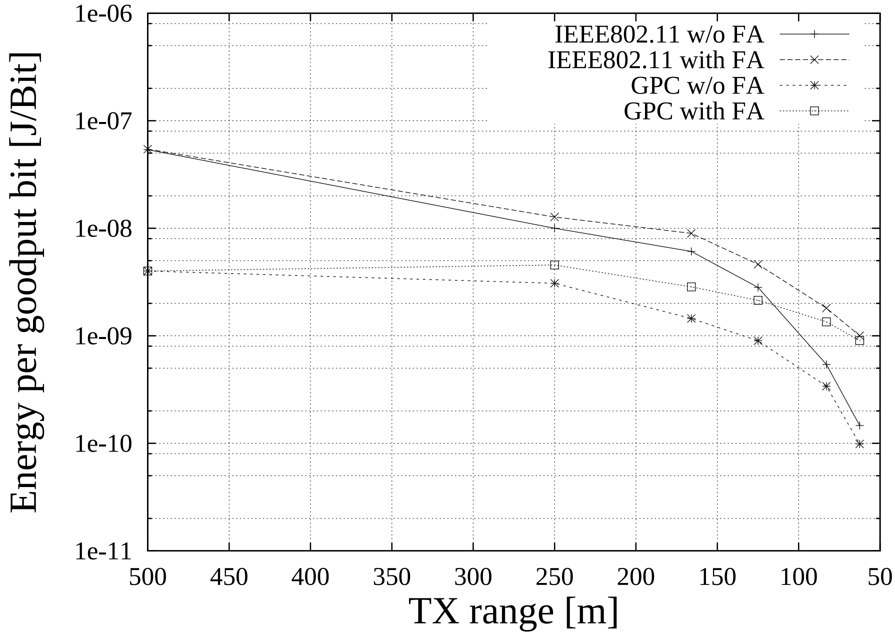


Figure 9.6: Signal energy per goodput bit for uniform forwarding agent placement with different transmission ranges

network area. However, instead of placing a specified number of forwarding agents in the network area, the maximum transmission range is specified and then a minimum number of forwarding agents is then placed in a way that any location in the network is within range of a forwarding agent and every forwarding agent is within range of its adjacent forwarding agent. The number of forwarding agents required to cover the network area for the previously stated transmission ranges (500, 250, 166, 125, 82, and 62.5 meters) in this case are 1, 4, 9, 16, 25, and 36, respectively.

In Figure 9.6 the energy per goodput bit is shown for both 802.11 and GPC for two different cases. The first case does not account for the energy consumed by the nodes designated as forwarding agents assuming they have infinite resources such as a vehicle or node with a fixed power supply (referred to as w/o FA in the graph). In the second case the signal energy consumption of the forwarding agents is taken into account (they may have more resources available such as a laptop as compared to a sensor, but their power must still be considered; referred to as with FA in the graph). The results shown in the figure

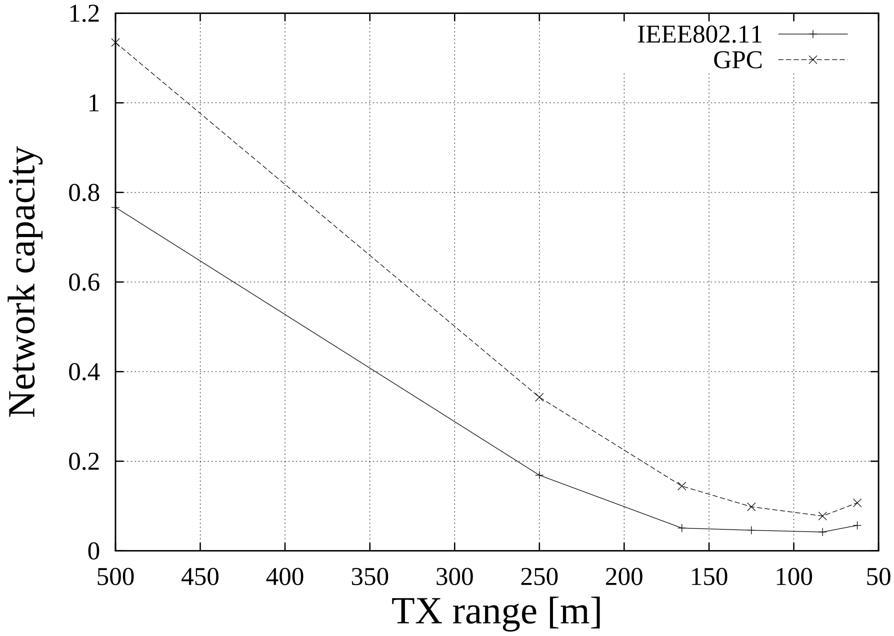


Figure 9.7: Normalized goodput for uniform forwarding agent placement with different transmission ranges

again demonstrate considerable energy savings as the transmission range is decreased and additional intermediate hops are utilized. As expected, the power controlled protocol also saves energy over the non-power controlled protocols, although the benefit again decreases as the maximum transmission range decreases. The difference in energy expenditure between the cases that account for the forwarding agent power consumption and those that do not are small for large transmission ranges. However, this difference increases as the transmission range decreases, since the number of forwarding nodes between source and destination increases as the range decreases.

The network goodput for this scenario is shown in Figure 9.7. It drops more than in the previous scenario shown in Figure 9.5. This is because all packets are forced to communicate to nodes in other clusters via a single forwarding agent and the number of nodes in other clusters increases as the range decreases, because the cluster size decreases while the number of clusters increases. If we consider the point of the figure corresponding to the 250 meters transmission range, we see that considerably less packets are delivered than for the infrastructureless case. This is because the forwarding agent employs the 802.11 distributed MAC algorithm which provides equal access rights to all nodes, including those designated as forwarding agent. Therefore if N-1 sources are all trying to send through a single forwarding agent, which must relay the packets to N-1 destinations, the one forwarding agent will have to compete with the N-1 sources to send to the N-1 destinations, but only receive $1/N$ share of the network resources. This will severely limit the number of packets that are allowed to reach their destinations, which is why the goodput is severely reduced when using the distributed 802.11 MAC with forwarding agents. As the number of forwarding agents is increased and the transmission range is reduced, the rate initially declines because it takes more hops. However is then starts to increase because the number of nodes the forwarding agent has to compete with decreases.

The power controlled protocol has a considerable advantage over the non-power controlled protocol for long transmission ranges, but the advantage fades as the range is decreased, since similar to Scenario I, there is less control range of the transmission power to exploit.

### 9.5.3 Ad hoc networks with randomly placed forwarding agents

The next figures again show results for a scenario with predesignated forwarding agents. However, this time the placement of these forwarding agents is random as described in Scenario III of Section 9.3. The motivation behind using forwarding agents in this scenario is that I want to take advantage of nodes with more resources as forwarders if they are within range. For each range the number of forwarding agents is equal to the number of uniformly placed forwarding agents in Scenario II to cover the graph for the corresponding range. Since the placement of the forwarding agents is not controlled and therefore random, there is no guarantee that all nodes are reachable from all other nodes. So as mentioned when discussing the simulation setup, the maximum transmission range for this topology scenario was set a constant value of 500 meters, but the number of forwarding agents was set to 1, 4, 9, 16, 25, and 36. Note that the transmission range shown in Figure 9.3 corresponds to these numbers of forwarding agents for the random forwarding agent placement curve in this figure.

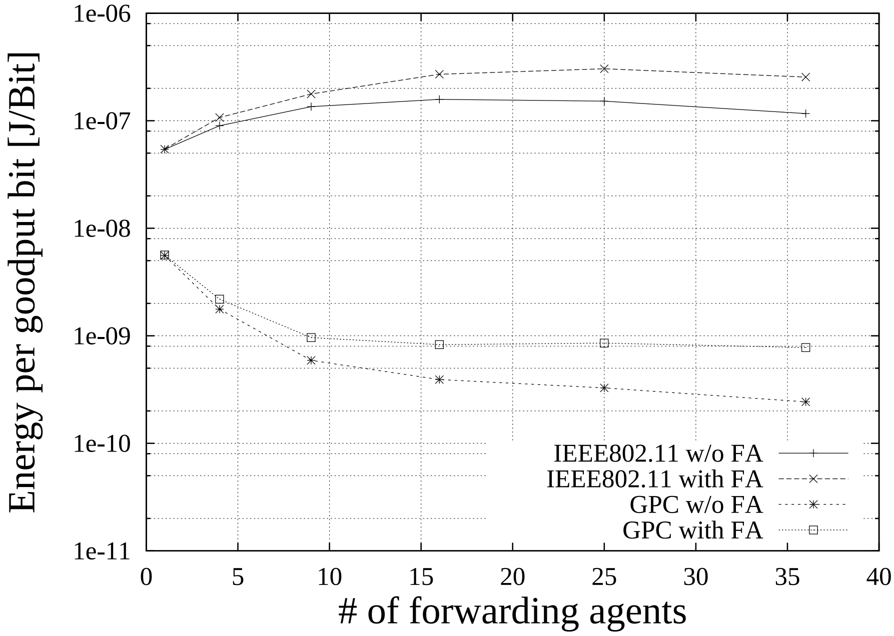


Figure 9.8: Signal energy per goodput bit for random forwarding agent placement with different transmission ranges (# of forwarding agents)

The signal energy used per goodput bit for this scenario is shown in Figure 9.8. The signal energy for IEEE 802.11 actually increases with the number of forwarding agents. This is because the cluster size on average decreases with the number of forwarding agents, but the non-power controlled 802.11 protocol is unable to reduce its transmission power to the size of the cluster distance to the forwarder. The GPC signal energy decreases because the power is reduced as the average distance to the forwarding agent is reduced. Note the energy consumed by both protocols changes dramatically at first because the average distance to the nearest forwarding agent significantly decreases as the first few are added, but the average distance to the forwarder decreases less significantly as the number of forwarders is further increased. For the last points the energy consumption decreases for both protocols particularly for those curves which neglect the forwarding agent power consumption. This is due to the number of forwarding agents becoming a considerable fraction of the overall sources. Thereby the average number of hops decreases (see Figure 9.3) without changing the distance between forwarding agents or forwarding agents and regular nodes. Therefore

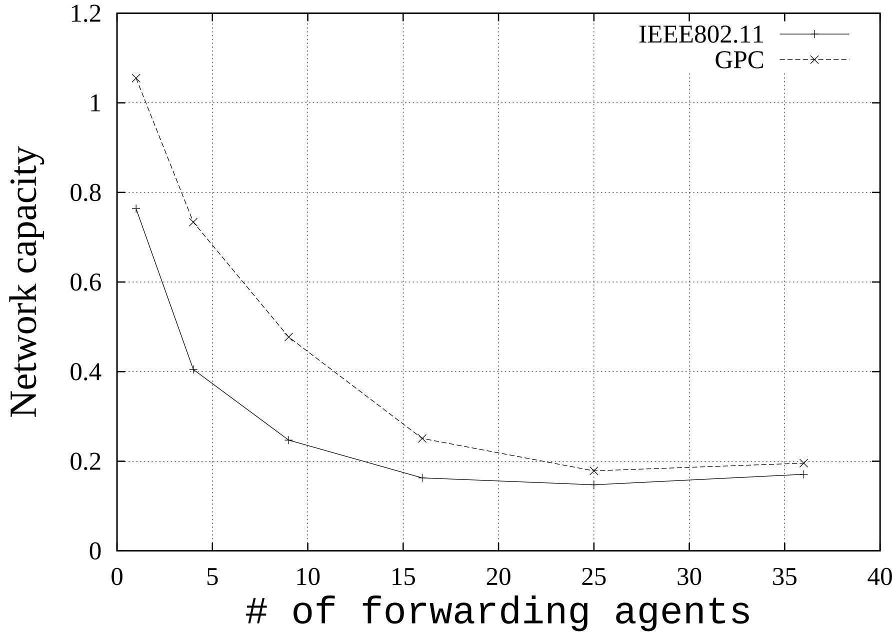


Figure 9.9: Normalized goodput for random forwarding agent placement with different transmissions ranges (# of forwarding agents)

the number of successfully transmitted packets is increased without changing the average transmission power. In turn, the energy per goodput bit drops. More energy is consumed for the case of random forwarding agents placement than for the uniform case, even though the average distance between a node and its forwarding agent should be the same when many forwarders are used. However in the random case the penalty is higher for forwarders farther away than the average than the gain for forwarders closer than average since the gain is superlinear.

The goodput for the network with random placement of forwarding agents is shown in Figure 9.9. The goodput for this scenario drops as the number of forwarding agents is increased. There are several factors contributing to this. First, as the number of forwarding agents is increased, the cluster size decreases and therefore the number of nodes in the same cluster decreases while the number of clusters increases. Therefore on average, a larger number of hops is required. In addition the number of access points available for sending to other clusters is limited by the number of forwarding agents within range. Furthermore as discussed in the uniform placement case, all nodes in the cluster are contending with the forwarding agent. In turn, the number of packets that can be sent to other clusters is limited by the nodes contending in the the same cluster. This effect becomes less significant as the number of nodes in the cluster decreases, but the dependence on the forwarding agent increases as the cluster size shrinks. These factors cause the goodput to continue to decline with an increasing number of forwarders until the forwarders become a considerable fraction of the total nodes, suddenly reducing the average hop count (refer to Figure 9.3).

The goodput for the random placement case is better than for the uniform placement case because the average number of hops is considerably smaller as shown in Figure 9.3. Power controlled protocols provide the greatest benefits over non-power controlled protocols when the distance between source and destination is rather large and the average number of hops is rather small.

## 9.6 Summary

In this section the advantages of power controlled MAC protocols in multi-hop wireless ad hoc type packet networks regarding both energy savings when transmitting and goodput were evaluated. A Generalized Power Controlled MAC protocol was compared with a non-power controlled protocol (IEEE 802.11) in three different common network setups. It was shown that there are significant benefits in energy savings by utilizing both intermediate nodes and a power controlled protocol when sending between those nodes. The capacity was shown to increase when implementing power control. From this study it can be concluded that using power control is always beneficial. For the sake of comparability, a simple shortest path routing algorithm was used. I want to add that the energy expenditure can be further decreased if a more sophisticate routing algorithm is applied.

Using infrastructure with designated forwarding agents sending packets between clusters on single shared wireless data channel will gradually limit the capacity as the number of clusters is increased, but improve the energy consumption performance. In addition when forwarding agents can be utilized that do not have limited energy resources, the additional energy savings may additionally justify their use. It was also found that the controlled placement of forwarding agents for the cluster approach is the optimum for the non-power controlled case. Using shorter transmissions ranges with more hops provides considerable improvements in energy savings although it reduces goodput. The overall energy savings for an increased number of hops outweigh the reduced goodput. Finally, the results indicate that power control is very beneficial in wireless environments because the distances between source and destination or forwarders change.

A meaningful extension of this work would be an evaluation of the benefit of multi-hop networks regarding radio exposure. A decreased distance causes an overproportional decrease of the required RF power to achieve a desired radio link quality. Therefore the received/absorbed power at a certain location decreases. Of course there are tradeoffs, which need to be considered. First, a reduced transmission range makes it necessary to transmit the packet multiple times, which increases exposure . Second, as shown before, the goodput degrades considerably. This may require to increase the transmission rate to compensate the reduced network goodput. However, an increased transmission rate requires more RF power to ensure the same link quality as for lower data rates. Furthermore the energy to store, process, and relay the packet in forwarding agents was not taken into account. Although the costs for these activities were reduced considerably in recent years and will be further reduced, they can use a large fraction of the overall energy if there is a large number of intermediate nodes between source and destination. The evaluation how the number of intermediate nodes influences the energy consumption is an worthwhile issue for further research.

**Acknowledgement**

I owe thanks to Dr. Jeffrey Monks, who jointly worked with me on this topic. He was a Ph.D. student of the University of Illinois Urbana-Champaign, USA at the time this investigations were performed. He provided the base of the simulation model, the foundations of the GPC protocol and fruitful discussions.

# Chapter 10

# Exposure reduction by using the multi-hop approach

Wide-spread concerns on potential health hazards by electro-magnetic exposure[1] were raised in many countries. Although there is no ultimate consensus on radiation power limits and their respective health impacts, methods to reduce the received/absorbed power are necessary because of the rapid deployment of wireless communication technologies and the concerns they introduce. The previous chapter showed that multi-hop communication and the essential power control reduce the energy needed for the radio signal and improve the capacity. I tried to investigate how multi-hop communication and power control influences exposure. For this purpose I used a well known IEEE 802.11 network and the simple chain network topology scenario.

The intuition that multi-hop has the potential to reduce exposure is actually justified by the super-linear path-loss coefficient. If the received signal should have a certain strength, the sender has to overproportionally increase the RF power for long distances compared to short distances; in other words $P_{\text{recv}} = P_{\text{send}}/d^{\alpha}$, where $P$ is the RF transmission and reception power, respectively, $d$ is the distance and $\alpha$ is the path loss coefficient[2]. Consequently dividing the distance, e.g., in half, and sending the frame twice in order to cover the whole distance, the radiated power is reduced yielding $P_{\text{send}}(d^{\alpha}) > 2 \cdot P_{\text{send}}((\frac{d}{2})^{\alpha})$. Therefore it appears obvious that the multi-hop approach is able to reduce electro-magnetic radiation

[1] Exposure or received power are synonymously used in this chapter.
[2] See Appendix B.2 for typical path loss coefficients.

exposure. But the solution is not that trivial. Sending a frame twice or more means a longer transmission time and therefore a lower individual goodput. From the previous chapter we know that multi-hop increases the network capacity but not the individual goodput of a certain node. This effect might be counteracted by switching to a higher transmission rate; IEEE 802.11b provides four transmission rates. Additionally having a contention based MAC protocol in mind, the collision rate caused by simultaneous transmission and therefore the power expenditure to transmit a frame successfully increases. Accumulation effects caused by simultaneous transmission could also compensate the exposure reduction gain.

In this chapter I want to take a critical view on how exposure can be reduced reasonably by applying multi-hop in conjunction with power control. In the next section I introduce the metrics to quantify the reduction of received power. I used discrete event simulation for the investigations. The model and the assumptions are described in Section 10.2. In Section 10.3 I show and discuss the results and I conclude the chapter in Section 10.5.

## 10.1 Measurement metrics

The effects of electromagnetic radiation can be roughly classified into thermal and non-thermal effects. Thermal effects are heating of human tissue or body parts. These effects are well known and legal radiation power limits prevent impairment and damage of the human body. Thermal effects under normal physiological conditions cover non-thermal effects as formation of pearl chains, chains of orientation, deformation, fusion, rotation and vesicle ejection. There are many studies about non-thermal effects, but many of the results either have profound deficiencies, cannot be verified, or work with a unrealistically high radiation power. Particularly, the interaction between electromagnetic fields and atoms for small field strengths is not known. Because of these uncertainties I use various metrics to express the level of exposure – health aspects are out of the scope of this dissertation. The used metrics are:

**Time-weighted average of received power –** Time-weighted average of the sum of the power received at a given measuring point. This is equivalent to the integral of the total power profile divided by the total simulated time.

**Distribution of received power values –** The distribution of power values lets us draw conclusions on what fraction of time a certain received power level occurs.

**Peak power –** The power that is referred to as the highest received power value.

**Goodput –** Another interesting metric is the goodput, since it represents the benefit or penalty of the multi-hop approach.

**Energy per goodput bit –** The average power and the goodput can be combined to build the metric of energy that arrives at a measuring point per successfully transmitted bit (compare with Equation 6.1, Section 6.1).

These metrics represent the respective average over all freely placeable measure points, except for the peak power. Additionally aggregated metrics could be the 90% percentile or standard variation of received power, but all of these metrics are contained in the distribution function. Exposure or received power should be not confused with emission. Exposure describes the signal strength or energy that is received at a given point whereas emission describes the signal strength or energy radiated at the source of signal.

## 10.2 Model and assumptions

The basis of the investigation is an IEEE 802.11b network as described in Section 2.2 and modeled in Sections 4.1 and 4.2. As far as the MAC protocol is concerned, no MAC supplements like frame fragmentation, RTS/CTS, or power saving are used. Frames are sent at one of the four possible transmission rates (1, 2, 5.5, or 11 Mbit/s) and are retransmitted up to eight times in the case of errors. Furthermore, before a transmission takes place, a node has to assess the transmission channel for its occupancy, which is often referred to as Clear Channel Assessment (CCA). I assumed an occupation of the channel by another node for a received signal strength above -76 dBm.

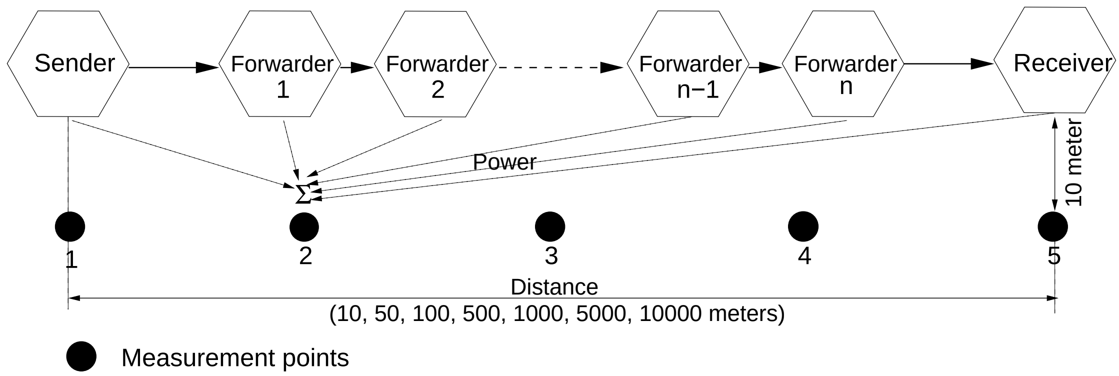


Figure 10.1: Simple node chain model

### 10.2.1 Network topology

For the sake of simplicity I used a simple wireless node chain model. A sender and a receiver are placed at the opposite ends of the chain. A certain number of forwarders can be placed between the sender and receiver. If there are forwarders, all hops have the same length. Each node within the chain behaves according to the IEEE 802.11b specification. The distance between sender and receiver is freely configurable as well as the number of forwarders. The RF transmission power is computed so that each node reaches its successor with the power needed to ensure a certain link quality (see Section 2.1.2). I assumed bit error rates of $10^{-6}$ and $10^{-8}$, respectively. Figure 10.1 sketches the simple node chain model and in Figure 10.2 exemplarily shows the RF transmission power, which is significantly reduced with a higher number of forwarding nodes.

### 10.2.2 Channel model

The simple node chain network topology is a special case of a multi-hop network. In a multi-hop network several nodes can transmit frames simultaneously; here – due to power control – a pipeline effect can be possible. Simultaneous transmissions of frames can result in interference and in turn in packet errors. Therefore I used the interference-based channel model presented in Section 4.4.2. For simplicity an AWGN channel is assumed. Simultaneous transmissions result in a lower SINR (see Equation 4.2) at the respective receivers, which in turn determine whether the respective receivers are able to decode the packet

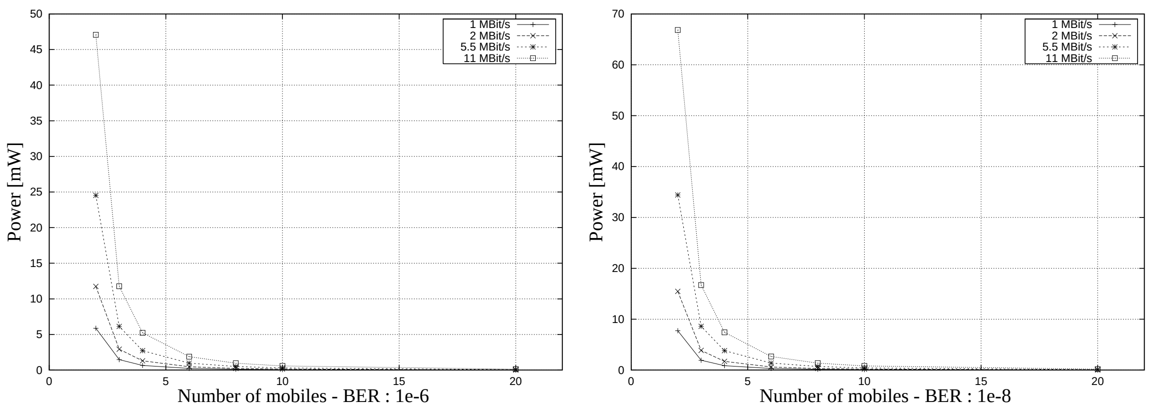


Figure 10.2: Emission power for a distance of 100 meters and a varying # of forwarders

according to the used transmission rate.

### 10.2.3 Traffic model

The sending node transmits packets towards the intended receiver via the forwarding nodes. Frames are generated at a rate, which keeps the blocking transmit queue with a capacity of 1000 frames constantly filled. Forwarding nodes and the receiver do not inject packets into the transmit chain on their own. Packet sizes are drawn from the Harvard trace as described in Section 4.3.1.

### 10.2.4 Measurements

Several simulations are performed using the aforementioned traffic model with various fixed transmission rates, number of forwarders, and distances between sender and receiver. The resulting radiation is accumulated by a line of five measuring points, which are 10 meters apart from the network node chain. Measuring point one is at the sender location and measuring point is at the receiver location. The other three measuring points are equidistantly placed between them. Note that a measuring point may receive RF power from more than one wireless node of the transmit chain because of simultaneous transmissions (collisions or pipelining). A measuring point records the individual transmission power of any node of the transmission chain according to the equation below and the time instances

Table 10.1: Simulation parameters

| **Parameter** | **Value** |
|---|---|
| Distance sender-receiver in meter | 10, 50, 100, 500, 1000, 5000, 10000 |
| Number of forwarders | 0 . . . 18 |
| Data rate in Mbit/s | 1, 2. 5.5, 11 |
| Traffic type | Harvard Internet access link, variable packet size |
| Traffic load | $> 100\%$ |
| Power control | yes (BER $10^{-6}$ and $10^{-8}$) |
| Fade margin in dBm | 30 |
| Antenna gain (TX/RX) in dB | 0 |
| Path loss exponent | 2 |
| CCA threshold in dBm | -76 |

where the received signal starts and stops, respectively.

$$P_{\mathrm{ex\_i,j}} = \frac{P_{\mathrm{tx\_j}}}{\mathrm{Pathloss_{i,j}}}, \tag{10.1}$$

where $P_{\mathrm{ex\_i,j}}$ is the received power at measuring point $i$, $P_{\mathrm{tx\_j}}$ is the radiated power of node $j$, and $\mathrm{Pathloss_{i,j}}$ is the path loss between chain node $j$ and measuring point $i$. The simulations are stopped when a total of 30.000 packets were correctly received by the receiver.

A summary of the simulation parameters is given in Table 10.1:

## 10.3 Results

Using the metrics introduced above I examined the power data collected at the measuring points. The goodput was obtained from the receiver node, which recorded all successfully received frames for that purpose. Although I generally assume that a reduction of received power will result in a decreased health risk, I want to stress the fact that I cannot estimate how the health risk is effected. Furthermore, I exemplarily show results of the investigations for two reasons: First, the range of the variable parameters is relatively wide resulting in

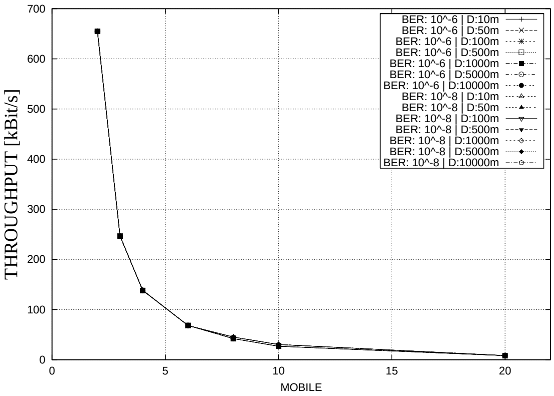


(a) Data rate of 1 Mbit/s

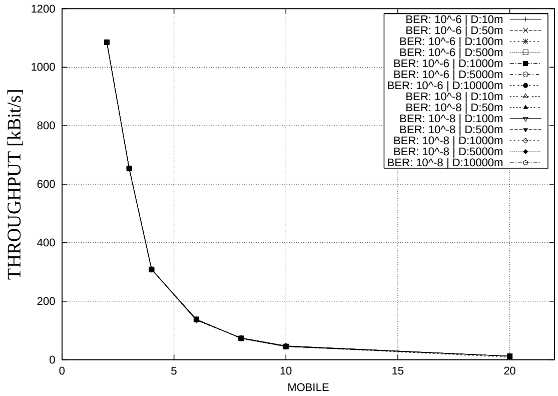


(b) Data rate of 2 Mbit/s

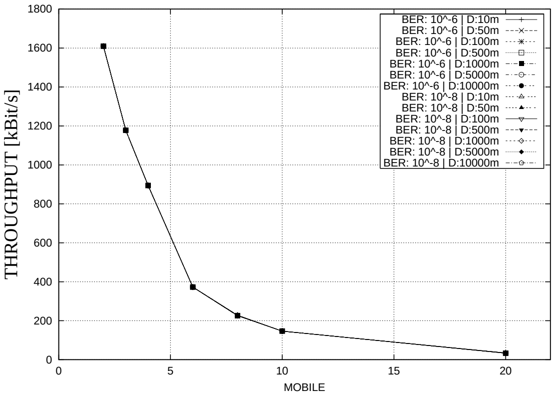


(c) Data rate of 5.5 Mbit/s

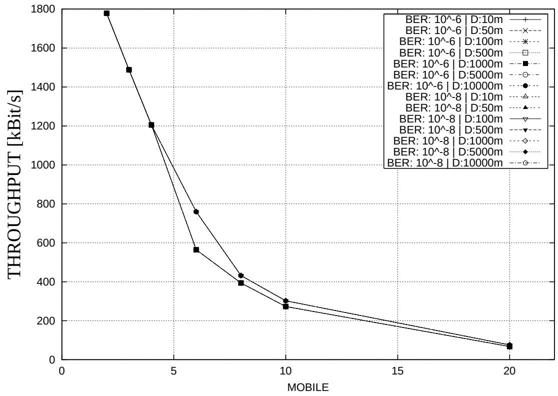


(d) Data rate of 11 Mbit/s

Figure 10.3: Goodput of the multi-hop network

numerous tables and graphs. Second, many graphs offer different quantities but similar characteristics. Therefore I would like to refer the reader to the TKN technical research report [56] for all results.

### 10.3.1 Goodput

In Figure 10.3 we see the end-to-end throughput (goodput) for various transmission rates, number of forwarders, distances and bit error rates. It is evident that the goodput decreases dramatically as the number of forwarders is increased: The more hops in the transmission path the more often a frame is received and sent[3]. Moreover neighboring nodes contend

[3] One the other hand the capacity of the (chain) network will likely increase (see Chapter 9) because of spectral reuse.

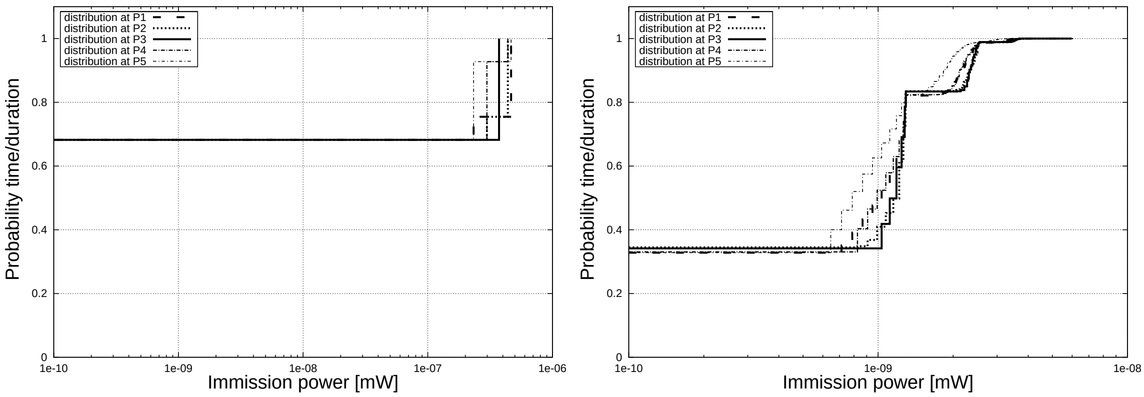


(a) Direct (b) 18 Forwarder

Figure 10.4: Probability distribution function of received power

BER = $10^{-6}$, distance = 100 meters, transmission rate = 11 Mbit/s

for the channel so that a node spends a considerable amount of time in the backlog state instead of transmitting or receiving. The goodput increases notably as the transmission rate increases. The bit error rate almost has no noticable effect since both values are very low. In Figure 10.3(d) a small difference can be identified. Here the goodput is slightly higher for the (lower) bit error rate of $10^{-8}$. The distance influences the goodput because power control ensures a stable link quality.

The goodput results raise the question whether the goodput decrease caused by the use of forwarders can be compensated to a certain extent by switching to a higher data rate. The decision to do so depends on the optimization factor. Considering exposure, a possible benefit due to more forwarders can be traded off by a higher radiation power, which is necessary to provide the same link quality with a higher, more fragile transmission rate. Therefore we look at received power values next.

### 10.3.2 Received power

Figure 10.4 exemplifies the probability distribution function of the received power for no (direct) and 18 forwarders (multi-hop) and a sender-receiver distance of 100 meters. It turns out that the received power for the multi-hop case is much smaller than for the direct case. The received power values are also more gradual for the multi-hop case. In other words, the maximum received power value is seldomly reached. In the direct case, the received power

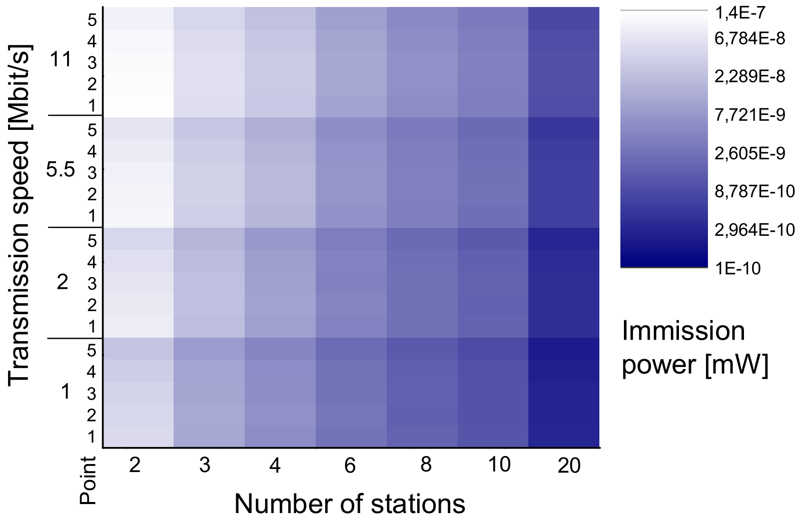


Figure 10.5: Average received power vs. total number of stations and transmission rate
BER = $10^{-6}$, distance = 10 meters

alternates between the maximum and zero.

Further measures can be derived from the power probability distribution function. The average received power is shown in Figure 10.5 for a varying number of intermediate hops, all transmission rates and every measuring point. A lighter color means a higher power value. We can see that a larger number of forwarders leads to a lower received power. The figure attests our assumption: Multi-hop in conjunction with power control reduces exposure because of shorter transmission distances and an overproportional (exponential) decrease in the necessary RF transmission power. Even possible accumulation effects due to simultaneous transmissions do not compensate the benefits of multi-hop. The measuring points show some differences in the amount of received RF power. Measuring point one is strongly exposed while measuring point five receives the lowest level of received power. The reason lies in the transmission node chain: While the sender injects frames until 30.000 frames are successfully received, only a fraction the sent packets arrives at the receiver due to frame losses inbetween resulting in a decreased radiation at the end of the transmission node chain. Further on, the transmission rate significantly effects the received power. For higher transmission rates more power is required to achieve the same level of the link

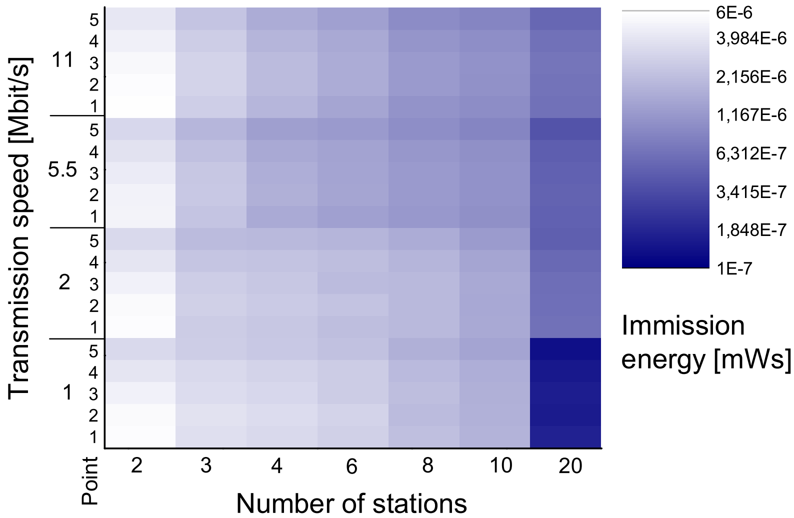


Figure 10.6: Average exposure energy vs. total number of stations and transmission rate
BER = $10^{-6}$, distance = 10 meters

quality, which leads to a higher average received power.

### 10.3.3 Received energy

Now let us examine the received energy in Figure 10.6. In particular I want to know how multi-hopping impacts the amount of received energy, which is weighted with the number of successfully received bits. For an increasing number of forwarders the received energy figure is quite similar to the obtained received power figure. The received energy per goodput bit decreases. Here the lower transmission power proportionally impacts the received energy when using more forwarders. There is a difference regarding the transmission rate. A higher transmission rate not necessarily results in a higher received energy because of a higher RF transmission power to yield the required link quality. For example, at 11 Mbit/s with two to eight forwarders (four or ten nodes), the received energy is lower than for 1 or 2 Mbit/s. This is a result of the higher protocol overhead for higher transmission rates, for example various interframe gaps where no transmission takes place. The fraction of transmission time is smaller for higher data rates than for lower data rates compared to the overall time to succesfully transmit 30.000 frames. If the number of forwarders is very high, e.g., 18 (20 nodes), the effect will be inverted. The lowest data rate (1 Mbit/s) shows the best received power values for 18 forwarders because the lower RF transmission power for the shorter hop distances and a low transmission rate prevails the aforementioned protocol overhead effect.

The bottom line is that a larger number of forwarders always results in lower received power and energy values. Furthermore, higher transmission rates lead to a higher received power, but not necessarily to a higher energy consumption. For two or more mobiles a higher data rate results in less received energy. If the number of forwarders is very high, e.g. 18, higher data rates result a slightly increased received energy. The conclusion to draw is that it makes sense to develop an algorithm to control the data rate depending on the number of hops.

## 10.4 Comparing results

I follow the question whether the goodput degradation when using more forwarders can be compensated to a certain degree by switching to a higher transmission rate without sacrificing the reduction of received power. The results as shown above are hardly conclusive in this respect because of the multitude of results and the lack of an evaluation criterion. I solved the problem by selecting examples of simulation results where the goodput is on a comparable level.

Figure 10.7(a) shows the average received power, Figure 10.7(b) shows the average received energy, and Figure 10.7(c) and 10.7(d) show the respective peak values. The goodput is assumed to be approximately 600 kBytes but varies around this value depending on the transmission rate and the number of hops.

Figure 10.7 reveals that more hops (forwarders), even in conjunction with a higher transmission rate to counteract the goodput degradation, still result in an exposure reduction. The goodput stays on a similar level (around 600 kBytes) for up to six forwarders. Above six forwarders, i.e., eight nodes, in the transmit chain, the highest transmission rate of 11 Mbit/s cannot compensate the goodput degradation introduced by more forwarders anymore. The goodput suddenly decreases to a very low level. With another radio technology,

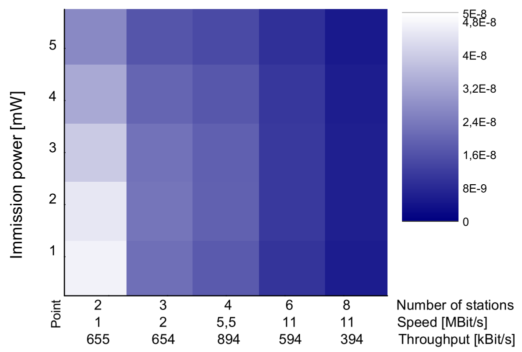


(a) Power

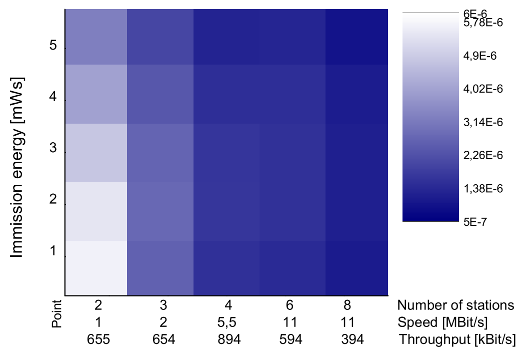


(b) Energy

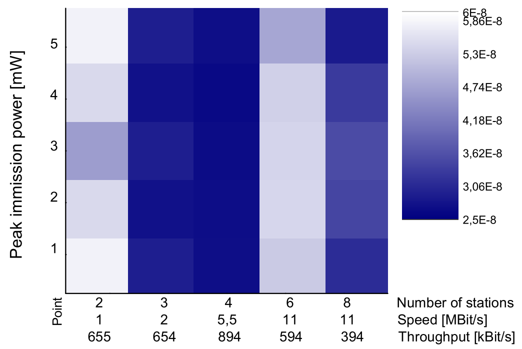


(c) Peak power

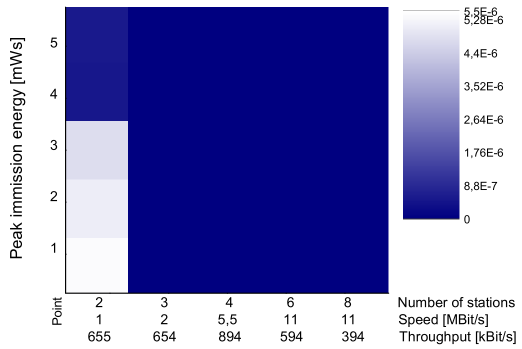


(d) Peak Energy

Figure 10.7: Comparable exposure results (power, energy and peak values)

BER = $10^{-6}$, distance = 10 meters

such as HIPERLAN/2, the exposure reduction could certainly be further reduced because of higher transmission rates, which go up to 54 Mbit/s, and by using more forwarders.

Taking a closer look at the Figures we can see that two forwarders (four nodes in chain) offer the best goodput. Any additional forwarder decreases the goodput. The received peak power as well as the received energy decrease with the number of forwarders in any case as a result of the reduced RF transmission power. The received peak power may increase with more forwarders by accumulation effects as shown in Figure 10.7(c), but the general trend, that is to say a decrease of exposure when using more forwarders, is still observable. This is also backed up by the energy received at the peak power, which decreases with more forwarders although, for example, for four forwarders, the received peak power is higher than for two or six forwarders. The received power is location dependent as a typical power pattern shows. The exposure at measuring point one is always the highest one and at measuring point five it is the lowest one because of traffic injection near measuring point one. Only a fraction of it arrives near measuring point five point five or at the receiver, respectively. There can be exceptions particularly considering the received peak power. For instance in Figure 10.7(c) for the no forwarder case, measuring point three receives the highest received power of all measuring points, which is a result of accumulation effects by simultaneous transmissions. But the general trend, that the measurement point closest to the injection of data into the transmit chain receives the highest received power, still holds. More results, which additionally cover a bit error rate of $10^{-8}$ and distances of 50 and 100 meters are shown in Figure D.9 on page 198 until Figure D.13 on page 202. All results can be found in [56].

## 10.5 Conclusion

In this chapter I proved that the multi-hop approach reduces electromagnetic exposure, which is assumed to reduce the health risk. Here, the necessary RF transmission power shrinks superlineary with respect to the (hop) distance, since the multi-hop approach (the placement of several intermediate nodes between the sender and receiver) shortens the hop distance.

I showed that as more forwarding nodes are used, the received power and the received energy are also reduced. I also found that the lowest transmission rate (1 Mbit/s) emits the least power and least energy per successfully transmitted bit. Furthermore there is a general rule: The higher the transmission rate, the higher the received power. This could lead to the wrong conclusion that either the number of forwarding nodes has to be increased or the transmission rate has to be reduced in order to reduce exposure. This is not the case since both measures, in particular an increased number of forwarding nodes, can lead to a significant goodput degradation.

In order to take advantage of the multi-hop approach to reduce exposure while keeping the network goodput on a comparable level, I analyzed the adaption of the transmission rate. It turned out that transmission rate adaption is an appropriate measure to counteract goodput degradation by using more forwarding nodes. The received power is still lower for more forwarders, but a higher transmission rate is necessary, which requires more RF power to achieve the same radio link quality.

I want to mention that power control is an indispensable instrument in conjunction with multi-hop for exposure reduction. With power control the RF transmission power is tuned according to the distance of intermediate nodes so that the link quality is kept on a stable level. Otherwise exposure could be significantly increased because of either retransmissions as a result of frame transmission errors or unnecessary high RF transmission power.

Drawing a final conclusion I want to add that if no forwarding nodes are used, the transmission rate should be as low as possible in order to provide the required quality of service (goodput) while keeping the exposure level low. When using forwarding nodes, a rule of thumb is to use the highest transmission rate and adjust the number of forwarders accordingly. A general rule is that a higher transmission rate requires a higher number of forwarders for exposure reduction.

There are still several issues to be investigated, because only the exposure reduction using multi-hop in combination with power control for the singular case of the node chain model was shown. First, more complex and realistic network topologies should be analyzed. Second, an exposure sensitive routing strategy as well as network layout have to be developed. Additionally I believe that exposure can be substantially reduced if the MAC protocol itself supports the multi-hop communication better. It is shown that a limiting factor is the goodput. With a higher goodput the energy expenditure per successfully transmitted bit is further decreased.

# Chapter 11

# Conclusions

This dissertation is a summary of my work during the past few years. Most of this work has already been published. When I started working on energy consumption aspects of WLANs, the improvement of energy efficiency mainly had a hardware perspective. Therefore this dissertation was one of the first attempts to tackle the problem from a communication protocol perspective. This dissertation shows that the IEEE 802.11 MAC protocol has a considerable energy saving potential.

In the following I recapitulate the challenge of the dissertation and the general strategy I used to tackle the problem. Afterwards I revisit the contributions laid out in Section 1.2 on page 6 and evaluate to what extent I have met them. Finally, I address shortcomings of the dissertation and motivate further research.

## 11.1 Challenge and solution path

The challenge of this dissertation was the efficient use of constrained energy resources in wireless communication. The dissertation pursued the particular question how the operation time of a wireless node can be increased from a MAC protocol perspective.

The particular wireless technology considered in this dissertation is IEEE 802.11. IEEE 802.11 networks are very popular and commonly used as wireless Internet access technology. Although IEEE 802.11 is based on various physical layers, the common element is the MAC protocol. Therefore I chose the IEEE 802.11 MAC protocol as starting point for the work on different aspects of the efficient use of energy. In many cases the results of the dissertation can be also applied to other wireless technologies.

## 11.2 Contributions

The contributions of this dissertation are a set of methods and detailed investigations with the purpose of a better understanding of energy consumption, and with the goal to improve the energy efficiency in wireless communication. These contributions are summarized and discussed next.

**Measurement of the power consumption of a WLAN network interface** The first step in the dissertation was to perform power consumption measurements of an IEEE 802.11 WLAN network interface. Albeit vendors provide a general figure of the WLAN NIC (and IC) power consumption in the respective data sheets, they had not been determined in detail before. My measurements resulted in particular power consumption values. These were used later in this dissertation to parameterize models and to give insights into the instantaneous power consumption characteristics of a WLAN network interface. The fact that the used RF transmission power level has a strong impact on the instantaneous power consumption in the TX mode is very important for energy efficient power control schemes. Moreover it could be shown that the used transmission rate has a negligible effect. Next I investigated how the average power consumption of a certain task, e.g., reception or transmission of a packet, is influenced by the packet size, the transmission rate and the RF transmission power. The results show that the RF transmission power influences the averagely consumed power, although not as much as it is the case for the instantaneous power consumption results. The transmission rate again only has a small influence, while the packet size has a large influence. Large packets lead to a higher average power consumption for the transmitting node which is the opposite for the receiving node.

**Determination of the WLAN network interface energy consumption** Power consumption obviously is not a sufficient metric to describe energy efficiency of a wireless system using constrained energy resources like a battery. Therefore I used the metric consumed energy. Because energy consumption has to be set into relation with the considered result I weighted it with the number of successfully transmitted information bits ($E_{\text{bit\_good}}$). $E_{\text{bit\_good}}$ was determined for different packet sizes, distances, transmission rates, and RF transmission powers. I showed that the packets should be as large as possible to maximize energy efficiency. If distances become too long regarding the transmission power, e.g., the link quality cannot be ensured, an optimal transmission packet size has to be used. The results revealed another interesting insight: Transmission rate adaption only makes sense within a relatively narrow zone of $15$ to $20$ meters where the position (distance) of this zone depends on the actual RF transmission power. If the distance to the intended receiver is smaller, the transmission rate should always be as high as possible to communicate energy-efficiently. If the receiver is further away, that is to say outside the aforementioned zone, the lowest transmission rate should be used to enable a successful wireless communication. In fact, if the distance is substantially longer than the zone distance, no communication will be possible at all, which corresponds to our practical experiences with IEEE 802.11 WLAN network interfaces.

**Battery self-recharge** Based on the measurement results I focused on the exploitation of the self-recharge phenomenon of batteries. More precisely, I pursued the question whether the load pattern generated during the transmission of differently coded multimedia streams is sufficient to allow for a battery recovery using the self-recharge phenomenon. The results show an impressive extension of battery life of up to 300% using the power-saving function of the IEEE 802.11 network interface. Moreover, it became clear that the more bursty the traffic, the better the utilization of the battery. Henceforward, the encoding technique of multimedia sources should be chosen accordingly. H.263 with a 256 kbit/s bandwidth limitation offers the best battery utilization performance of the three investigated encoding techniques because it generates a traffic pattern with relatively large inter-frame spaces.

**Energy-efficient power control** Both power and energy consumption results revealed a strong relation to the packet size. In order to exploit this relation for the purpose of energy saving, the influence of the packet size was investigated in more detail. The analysis reveals an ideal transmission packet size for every RF transmission power value (and vice versa). For the radio channel and a the network scenario used in this case study the optimum packet sizes and in turn the gain in energy consumption were determined. Since the radio channel parameters (distance, modulation, quality) differ in practice, an auto-adapted, energy-efficient, and packet size dependent power control approach is proposed.

**Power control in multi-hop networks** One of the questions that arises when considering multi-hop networks is how power control contributes to both the reduction of energy consumption and the improvement of network throughput. Since this strongly depends on the type of the multi-hop network topology, three basic multi-hop network topology types were defined and analyzed. For the sake of comparison a network technology without power control (IEEE 802.11b) and with power control (GPC) were analyzed. The latter was defined as an idealized MAC protocol using an optimal power control scheme. It was shown that there are extensive benefits in energy saving by utilizing power control in conjunction with an increasing number of intermediate (forwarding) nodes. In general, the use of power control in any case results in a lower energy consumption and an increased network capacity. The use of static, although in a sense optimal transmission power settings, results in a worse performance. The results also reveal that the use of a logical infrastructure (clustering) with designated forwarding agents will gradually limit the capacity as the number of clusters increase, but furtherly reduces energy consumption. It also was shown that a controlled clustering, i.e., uniform placement of forwarding agents, is most beneficial for IEEE 802.11 (without power control). The study of power control in multi-hop networks demonstrates that the introduction of intermediate nodes always leads to energy savings, however inducing a throughput penalty.

**Exposure reduction by using multi-hop** Electromagnetic exposure is a potential health risk. Therefore I attempted to answer the question whether multi-hop in conjunction with power control leads to a reduction of received power. Again, the investigated object was an IEEE 802.11 network consisting of a certain number of nodes located in a row. The results confirmed the idea: The more intermediate nodes (forwarder) are introduced, the less power is received. Moreover I found that a lower the transmission rate will lead to a lower received power. Another interesting insight of the study is the location dependency of received power. The received power is highest at the point of injection of data and lowest at the point of reception for the considered network setup. In turn an exposure reduction could be achieved by using low transmission powers for nodes that are in an exposure critical area; all other nodes may use higher transmission powers. The study also disclosed the drawback of an (unconditioned) insertion of intermediate nodes – a vast end-to-end throughput drop. Data rate adaption can compensate the throughput drop. The results reveal that this approach is successful up to a certain extent without sacrificing the reduction of received power.

## 11.3 Discussion of results

The results of this thesis reveal that there is energy saving or operation time extention potential in WLAN communication from the MAC protocol perspective. However the question arises how much the investigated mechanisms contribute to energy saving. Also some conclusion need to be drawn what methods have high potential to save energy in wireless communication. Although I can not argue by hard numbers, a high level comparison of energy saving options and their effects is still possible.

Without doubt the energy consumption of a WLAN interface heavily depends on the electronic design and the particular elements used. For instance, the RF power amplifier has a considerable impact. The design of an efficient low-cost RF power amplifier, which is tunable over a wide range, is very challenging. Likewise the efficient implementation of baseband processing makes a difference. Although the dissertation does not contribute in this regard, the energy saving gain of power control and transmission rate control (by reduced power consumption) depends on the power amplifier and baseband processor efficiency. Because these efficiency are relatively low in todays WLAN implementation for the sake of low costs, power and transmission rate control play a minor role for energy saving directly induced by the power consumption of the circuitry (compare Chapter 5 and 6). However this should not be confused with energy saving by adaptation of RF power and transmission rate to achieve a given link quality. As shown in Chapter 8 it is important to set the transmission power into relation with the packet size assuming certain radio channel characteristics. Using a higher or lower RF transmit power level leads to an unnecessary increased overall energy consumption because of retransmissions or oversized RF transmission power. As a matter of fact the reduction (up to a certain degree) of RF transmission power is generally beneficial in terms of energy consumption in multi-cell or multi-hop networks because of reduced power consumption, and more important, because of spatial reuse. This effect is revealed in Chapter 9 where quite considerable energy savings are visible.

The WLAN network interface operat3ion control, which is performed by the MAC protocol, is besides the type of electronic circuitry the other main factor influencing the energy consumption figure. In Chapter 7 it is shown that energy consumption will be considerably reduced if the WLAN interface can go asleep during idle times. This of course directly depends on the traffic pattern. Thereby a proper traffic shaping in conjunction with the power saving mechanism can save further energy as experiments with differently encoded video data indicate. Moreover, the sleep mode provides better utilization of the very limited chemical energy contained in batteries of the mobile nodes.

In summary, the type and design of the electronic circuitry, RF power control and MAC power saving control of the WLAN interface are the key issues for reducing energy consumption and extending the operation time of a wireless node, respectively. The latter offers the highest impact on energy consumption. It makes particular sense to point research in this direction. Although not investigated in this dissertation it is also a matter of fact that the operation time of a wireless node can be considerably further enhanced from the network perspective if sophisticated routing strategies are used, and if the protocols of the various protocol stack levels are harmonized.

## 11.4 Issues for further research

Many other researchers have seized the topic of energy-efficient communication in wireless networks by exploring similar and of course quite different issues such as energy efficient routing, transport protocols or applications. Nonetheless some issues, which arise from this dissertation, have only been considered marginally or have not been tackled at all.

Despite my own measurements more detailed measurements of wireless node power consumption would be desirable. Indeed there are several publications on power consumption measurements for various WLAN interfaces. But wireless communication is a composition of applications, the particular operating system, communication protocols, (peripheral) hardware, and other components interacting with each other. A power consumption profile of all components involved in the wireless communication process could provide more insight on what consumes the energy, how the components interact, and how the operation could be optimized or concerted to consume less energy or to exploit batteries better.

A major problem inherent to multi-hop communications, is the vast throughput reduction as more intermediate nodes (forwarders) are used. As shown in the dissertation, the throughput proportionally influences the energy consumption. The development of MAC protocols or techniques particularly tailored to improve the throughput in multi-hop communication, see for instance [74], will lead to further energy savings.

The exposure problem is also of particular interest because of the public concern. It was shown in this thesis that multi-hop is a method to reduce exposure. A general problem, that is not only interesting in the case of exposure reduction but also for energy efficiency and network capacity improvement, is how the number of intermediate nodes can be determined in practice. It is certainly possible to calculate optimal parameter settings off-line, but it is still unclear how this should automatically be accomplished with limited and frequently changing information on the mobile environment. Another interesting, probably unusual approach to reduce exposure could be a location-oriented power control scheme. For example, consider a pair of nodes in a multi-hop network exchanging information via a certain number of intermediate nodes. The nodes in urban areas, which probably are the sender and the receiver, could use lower RF transmission power, and nodes in distant areas (forwarder) where exposure does not matter could use higher RF transmission power. The goal of such a procedure is a reduction of necessary intermediate nodes, which will result in both higher throughput and lower exposure (in areas where it matters).

# Appendix A

# List of Acronyms

**ACK** Acknowledgment

**AID** Association Identifier

**AP** Access Point

**ARQ** Automatic Repeat Request

**ATIM** Asynchronous Traffic Indication Map

**AWGN** Additive White Gaussian Noise

**BER** Bit Error Rate

**BPSK** Binary Phase Shift Keying

**BSS** Basic Service Set

**BW** Backoff Window

**CCITT** Comite Consultatif International Telegraphique et Telephonique

**CA** Collision Avoidance

**CAM** Constant Awake Mode

**CBR** Constant Bit Rate

**CCA** Clear Channel Assessment

**CCK** Complementary Code Keying

**CEPT** European Conference of Post and Telecommunication

**CF** Contention Free

**CFP** Contention Free Period

**CP** Contention Period

**CPU** Central Processing Unit

**CRC** Cyclic Redundancy Check

**CS** Carrier Sense

**CSMA/CA** Carrier Sense Multiple Access / Collision Avoidance

**CTS** Clear-to-Send

**CW** Contention Window

**DBPSK** Differential Binary Phase Shift Keying

**DCF** Distributed Coordination Function

**DCLA** DC Level Adjustment

**DES** Discrete Event Simulation

**DIFS** Distributed Inter-Frame Space

**DQPSK** Differential Quadrature Phase Shift Keying

**DR** Data Rate

**DS** Distribution System

**DSSS** Direct Sequence Spread Spectrum

**DTIM** Delivery Traffic Indication Map

**DTMC** Discrete Time Markov Chain

**EIFS** Extended Inter-Frame Space

**ETSI** European Telecommunications Standards Institute

**ESS** Extended Basic Service Set

**FCC** Federal Communications Commission

**FCS** Frame Check Sequence

**FEC** Forward Error Correction

**FIFO** First-In-First-Out

**FFT** Fast Fourier Transformation

**FHSS** Frequency Hopping Spread Spectrum

**GFSK** Gaussian Frequency Shift Keying

**GMSK** Gaussian Minimum Shift Keying

**GPC** Generalized Power Controlled

**GUI** Graphical User Interface

**HIPERLAN** HIgh PErformance Radio Local Area Network

**IC** Integrated Circuits

**IEEE** Institute of Electrical and Electronics Engineers

**IF** Intermediate Frequency

**IFFT** Inverse Fast Fourier Transformation

**IBSS** Independent Basic Service Set

**IR** Infrared

**ISI** Inter-Symbol-Interference

**LAN** Local Area Network

**LBT** Listen Before Talk

**LOS** Line-Of-Sight

**MA** Multiple Access

**MAC** Medium Access Control

**MPDU** MAC Protocol Data Unit

**MTU** Maximum Transfer Unit

**NAV** Network Allocation Vector

**NIC** Network Interface Card

**NiCd** Nickel-Cadmium

**NiMH** Nickel-Metal-Hydride

**OFDM** Orthogonal Frequency Division Multiplexing

**OS** Operating System

**OSI** Open System Interconnection

**PBCC** Packet Binary Convolutional Coding

**PC** Point Coordinator

**PCMCIA** Personal Computer Memory Card International Association

**PCF** Point Coordination Function

**PCM** Pulse Code Modulation

**PDA** Personal Digital Assistants

**PER** Packet Error Rate

**PHY** Physical Layer

**PIFS** Priority Interframe Space

**PLCP** Physical Layer Convergence Protocol

**PLW** PSDU Length Word

**PMD** Physical Medium Dependent

**PPDU** Physical Layer Protocol Data Unit

**PPM** Pulse Position Modulation

**PS** Power Saving

**PSDU** Protocol Service Data Unit

**PSF** PLCP Signaling Field

**OSI** Operating System Interconnection

**QAM** Quadrature Amplitude Modulation

**QoS** Quality of Service

**QPSK** Quadrature Phase Shift Keying

**RF** Radio Frequency

**R-SNR** Received Signal-to-Noise Ratio

**RTS** Ready-to-Send

**RX** Receive

**SD** Silence Detection

**SFD** Start Frame Delimiter

**SIFS** Short Inter-Frame Space

**SNR** Signal-to-Noise-Ratio

**SINR** Signal-to-Interference-Noise-Ratio

**SS** Spread Spectrum

**SSID** Service Set Identifier

**ST** Slot Time

**TCP** Transmission Control Protocol

**TIM** Traffic Indication Map

**TSF** Timing Synchronization Function

**TX** Transmit

**VBR** Variable Bit Rate

**WLAN** Wireless Local Area Network

**WPAN** Wireless Personal Area Network

**WWW** World Wide WEB

# Appendix B

# Selected PHY and channel parameters

## B.1 PHY layer dependent parameters

This table contains a selection of parameters that are influenced by the physical layer type, and impact the IEEE 802.11 MAC operation and performance.

Table B.1: PHY influenced parameters

| **Parameter** | **IR** | **FHSS** | **DSSS** | **OFDM** |
|---|---|---|---|---|
| Slot time [$\mu s$] | 8 | 50 | 20 | 6 |
| CCA time [$\mu s$] | 5 | 27 | $\leq 15$ | $\leq 4$ |
| Rx/Tx turnaround time [$\mu s$] | 0 | 20 | $\leq 5$ | 8.8 |
| SIFS [$\mu s$] | 7 | 28 | 10 | 13 |
| Preamble length [$\mu s$] | 41/25$^{\dagger}$ | 96 | 144/72$^{\ddagger}$ | 19 |
| MAC header length [$\mu s$] | 16/20$^{\dagger}$ | 32 | 48 Bit | rate dependent |
| $\mathrm{CW}_{\mathrm{min}}$ | 63 | 15 | 31/7$^{\ddagger}$ | 15 |
| $\mathrm{CW}_{\mathrm{max}}$ | 1023 | 1023 | 1023/127$^{\ddagger}$ | 1023 |

† – 1/2 Mbit/s
‡ – long/short PPDU

## B.2 Typical path loss exponents

Table B.2: Typical path loss exponents

| Environment | Path loss exponent |
|---|---|
| Free space | 2 |
| Urban area cellular radio | 2.7 to 3.5 |
| Shadowed urban area cellular radio | 3 to 5 |
| In building line-of-sight | 1.6 to 1.8 |
| Obstructed in building | 4 to 6 |
| Obstructed in factory sites | 2 to 3 |

# Appendix C

# Computation of the channel error parameters

This appendix covers the mathematical basis to compute the Gilbert-Elliot bit error model parameter used in the simulations.

## C.1 Gilbert-Elliot bit error model

This is the mathematical description of the Gilbert-Elliot error model as already described in [18] and derived from [94]. A Rayleigh-fading channel, BPSK or QPSK modulation, and some movement are assumed.

- $K$ isthe number of states, $S$ = $\{s_0, .., s_{\mathrm{K}-1}\}$ the set of states.
- **T** := $((t_{\mathrm{i,j}}))_{\mathrm{i,j}\in\{0,..,\mathrm{K}\}}$ the time-homogeneous state transition matrix of the underlying Markov chain. **T** is a stochastic matrix.
- $\vec{p}$ := $(p_0, .., p_{\mathrm{K}-1})^{\mathrm{t}}$ is the steady state vector of **T**.
- $\vec{e}$ := $(e_0, .., e_{\mathrm{K}-1})^{\mathrm{t}}$is a vector of bit error probabilities $e_{\mathrm{k}}$ for the state $s_{\mathrm{k}}$.
- The mean bit error rate $e$ is thus given by $e$ = $\mathbf{p}^{\mathbf{t}}\mathbf{e}$.
- A suitable model is defined by **T**, **e** and **p**.
- $A$ isthe Received Signal-to-Noise Ratio (R-SNR) with the probability distribution function $\mathrm{pdf}\ p_{\mathrm{A}}(a) = \frac{1}{\rho} \cdot \exp(-\frac{a}{\rho})$, and $0 = A_0 < A_1 < \ldots < A_0 = \infty$ is a partition

of the range R-SNR. The Discrete Time Markov Chain (DTMC) is defined to be the in state $s_\mathrm{k}$ at the time $t$ if R-SNR$(t) \in [A_\mathrm{K}, A_\mathrm{K-1})$.

- $f_\mathrm{m} := \frac{v}{\lambda}$ is the maximum Doppler frequency, where $v$ is the receiver speed and $\lambda$ is the wavelength.
- Then the numbert $N_\mathrm{a}$ is the expected number of times per second where R-SNR drops below a given level $a$:

$$N_\mathrm{a} = \sqrt{\frac{2\pi a}{\rho}} \cdot f_\mathrm{m} \cdot \exp\left(-\frac{a}{\rho}\right) \tag{C.1}$$

- define

$$F(\alpha) = \int_{-\infty}^{\alpha} \frac{1}{\sqrt{2\pi}} \cdot \exp\left(-\frac{x^2}{2}\right). \tag{C.2}$$

- The following steps are needed:
  - chosse $K$, $\lambda$, and $v$ ($v > 0$), and the symbol rate $R_\mathrm{t}$, and
  - determine the range of the R-SNR and define a partition $A_0, .., A_\mathrm{K}$ of the range, such that $A_0 = 0$ and $A_\mathrm{K} = \infty$,
  - choose $\rho$.
  - Then for $k \in \{0, .., K-1\}$

$$e_\mathrm{k} = \frac{\int_{A_\mathrm{k}}^{A_\mathrm{k+1}} \frac{1}{\rho} \cdot \exp(-\frac{1}{\rho}) \cdot (1 - F(\sqrt{2a}))da}{\int_{A_\mathrm{k}}^{A_\mathrm{k+1}} \frac{1}{\rho} \cdot \exp(-\frac{a}{\rho})da}, \tag{C.3}$$

  - for $k \in \{0, .., K-1\}$

$$p_\mathrm{k} = \exp\left(-\frac{A_\mathrm{k}}{\rho}\right) - \exp\left(-\frac{A_\mathrm{k+1}}{\rho}\right), \tag{C.4}$$

  - define $R_\mathrm{t}^{(\mathrm{k})} := R_\mathrm{t} \cdot p_\mathrm{k}$.

- Proceed with:
  - set
$$N_{\mathrm{k}} := N_{\mathrm{a}}(A_{\mathrm{k}}) = \sqrt{\frac{2\pi A_{\mathrm{k}}}{\rho}} \cdot f_{\mathrm{m}} \cdot \exp\left(-\frac{A_{\mathrm{k}}}{\rho}\right), \tag{C.5}$$
  - set $t_{\mathrm{i,j}} = 0$ for $|i-j| > 1$,
  - for $k \in \{0, .., K-2\}$ set
$$t_{\mathrm{k,k+1}} = \frac{N_{\mathrm{k+1}}}{R_{\mathrm{t}}^{(\mathrm{k})}}, \tag{C.6}$$
  - for $k \in \{0, .., K-1\}$ set
$$t_{\mathrm{k,k-1}} = \frac{N_{\mathrm{k}}}{R_{\mathrm{t}}^{(\mathrm{k})}}. \tag{C.7}$$
- And finally:
  - $t_{0,0} = 1 - t_{0,1}$,
  - $t_{\mathrm{K-1,K-1}} = 1 - t_{\mathrm{K-1,K-2}}$, and
  - for $k \in \{1, .., K-2\}$:
$$t_{\mathrm{k,k}} = 1 - t_{\mathrm{k,k-1}} - t_{\mathrm{k,k+1}}. \tag{C.8}$$
- Note, that the following formula for the $e_{\mathrm{k}}$ computation behaves better from a computational point of view:

$$e_{\mathrm{k}} = \frac{\gamma_{\mathrm{k}} - \gamma_{\mathrm{k+1}}}{p_{\mathrm{k}}} \tag{C.9}$$
$$\gamma_{\mathrm{k}} = \exp\left(-\frac{A_{\mathrm{k}}}{\rho}\right)\left(1 - F(\sqrt{2A_{\mathrm{k}}})\right) + \sqrt{\frac{\rho}{\rho+1}} F\left(\sqrt{\frac{2A_{\mathrm{k}}(\rho-1)}{\rho}}\right) \tag{C.10}$$

## C.2 Practical derivation of the model parameters

The equations presented previously were used to compute parameters for a two-state Gilbert-Elliot model. The following table contains the used assumptions.

Table C.1: Assumptions for channel parameters computation

| **P**arameter | **D**escription | **P**arameter |
|---|---|---|
| $v$ | velocity of mobile node[m/s] | $1.4$ |
| $\lambda = \frac{c}{f_{\text{radio}}}$ | wavelength of emitted radio signal [m] | 0.125 |
| $f_{\text{m}} = \frac{v}{\lambda}$ | Doppler frequency [Hz] | $\approx$ 11.2 |
| $R_{\text{t}}$ | transmission rate [Mbit/s] | 1, 2, 5.5, 11 |
| $K$ | number of channel states | 2 |
| $A_{\text{Thres}}$ | R-SNR partition threshold [dB] | variable |
| $\rho$ | mean R-SNR [dB] | variable |

The channel parameters are computed as shown below:

- With the number of channel states $K = 2$, the steady state vector of **T** is given by

$$\vec{p} := \begin{pmatrix} p_0 \\ p_1 \end{pmatrix} = \begin{bmatrix} \exp\left(-\frac{A_0}{\rho}\right) - \exp\left(-\frac{A_1}{\rho}\right) \\ \exp\left(-\frac{A_1}{\rho}\right) - \exp\left(-\frac{A_2}{\rho}\right) \end{bmatrix} \tag{C.11}$$

  yielding $R_{\text{t}}^{(\text{k})}$ as well by multiplying $R_{\text{t}} \cdot p_{\text{k}}$.

- Furthermore, the error probability vector is given by

$$\vec{e} := \begin{pmatrix} e_0 \\ e_1 \end{pmatrix} = \begin{bmatrix} \gamma(A_0, \rho) - \gamma(A_1, \rho) \\ \gamma(A_1, \rho) - \gamma(A_2, \rho) \end{bmatrix}. \tag{C.12}$$

- $N_{\text{k}}$ reduces to

$$\vec{N} := \begin{pmatrix} n_0 \\ n_1 \end{pmatrix} = \begin{bmatrix} \sqrt{\frac{2\pi A_0}{\rho}} \cdot f_{\text{m}} \cdot \exp\left(-\frac{A_0}{\rho}\right) \\ \sqrt{\frac{2\pi A_1}{\rho}} \cdot f_{\text{m}} \cdot \exp\left(-\frac{A_1}{\rho}\right) \end{bmatrix} \tag{C.13}$$

- and the transition matrix **T** is

$$\mathbf{T} := \begin{pmatrix} n_{00} & n_{01} \\ n_{10} & n_{11} \end{pmatrix} = \begin{bmatrix} 1 - \frac{N_1}{R_{t0}} & \frac{N_1}{R_{t1}} \\ \frac{N_1}{R_{t0}} & 1 - \frac{N_1}{R_{t1}} \end{bmatrix}. \tag{C.14}$$

- The mean BER is

$$\overline{\mathrm{BER}} = p_0 \cdot e_0 + p_1 \cdot e_1. \tag{C.15}$$

- Further on, the mean bad phase and good phase duration are

$$\overline{\mathrm{BadPhase}} = \frac{1}{R_\mathrm{t}} \cdot \frac{T_{0,0}}{T_{0,1}}, \tag{C.16}$$

$$\overline{\mathrm{GoodPhase}} = \frac{1}{R_\mathrm{t}} \cdot \frac{T_{1,1}}{T_{1,0}}. \tag{C.17}$$

## C.3 Gilbert-Elliot model parameters

This table contains the parameters for a two-state Gilbert-Elliot bit error model as used in Section 8.1. For various mean BERs the bit error probability, the transition probability and the corresponding sojourn times are shown for the good and bad state, respectively.

Table C.2: Gilbert-Elliot channel parameters for various mean BERs

| **Mean BER** | **BER** | | **Transition probabilites** | | **Sojourn times [ms]** | |
|---|---|---|---|---|---|---|
| | Good state | Bad state | G→B | B→G | Good state | Bad state |
| 1e-02 | 3.368e-03 | 2.734e-02 | 9.937e-07 | 1.527e-05 | 79 | 17 |
| 1e-03 | 7.480e-04 | 3.209e-03 | 5.398e-06 | 3.386e-05 | 92 | 14 |
| 7e-04 | 5.397e-04 | 2.239e-03 | 4.923e-06 | 3.760e-05 | 101 | 13 |
| 4e-04 | 3.001e-04 | 1.189e-03 | 4.190e-06 | 4.495e-05 | 119 | 11 |
| 1e-04 | 8.897e-05 | 3.323e-04 | 3.035e-06 | 6.339e-05 | 164 | 7 |
| 6e-05 | 4.614e-05 | 3.386e-04 | 3.525e-06 | 5.413e-05 | 141 | 9 |
| 4e-05 | 2.970e-05 | 2.145e-04 | 3.142e-06 | 6.114e-05 | 159 | 8 |
| 1e-05 | 1.016e-05 | 7.150e-05 | 2.383e-06 | 8.147e-05 | 209 | 6 |
| 6e-06 | 2.624e-06 | 7.904e-05 | 3.142e-06 | 6.114e-05 | 159 | 8 |
| 4e-06 | 1.920e-06 | 5.736e-05 | 2.899e-06 | 6.652e-05 | 172 | 7 |
| 1e-06 | 7.130e-07 | 2.090e-05 | 2.250e-06 | 8.643e-05 | 222 | 5 |
| 1e-07 | 5.635e-10 | 3.950e-06 | 2.800e-06 | 6.896e-05 | 178 | 7 |
| 1e-08 | 1.446e-11 | 9.937e-06 | 1.982e-06 | 9.838e-05 | 252 | 5 |

# Appendix D

# Additional performance figures

For readability reasons, not all performance graphs were included in the text. The graphs, which were left out, are shown below.

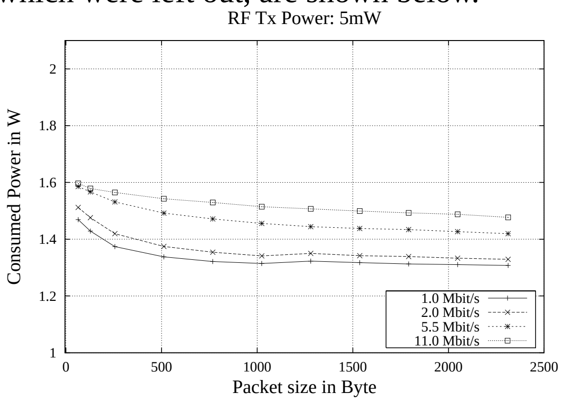


(a) RX mode at 5 mW RF power

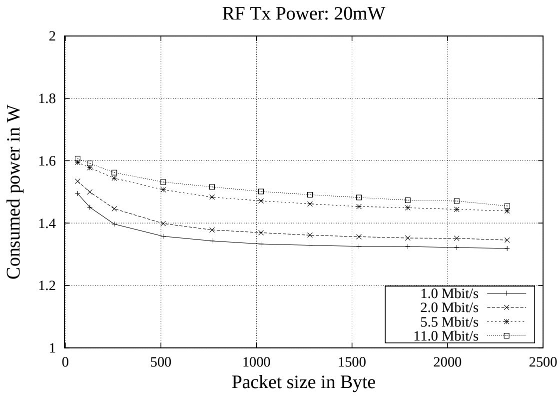


(b) RX mode at 20 mW RF power

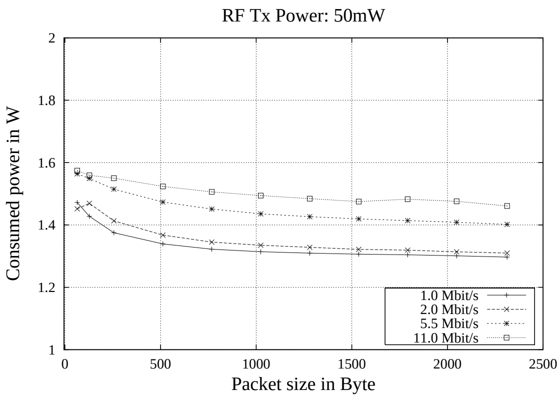


(c) RX mode at 50 mW RF power

Figure D.1: Average power consumption for different packet sizes during reception

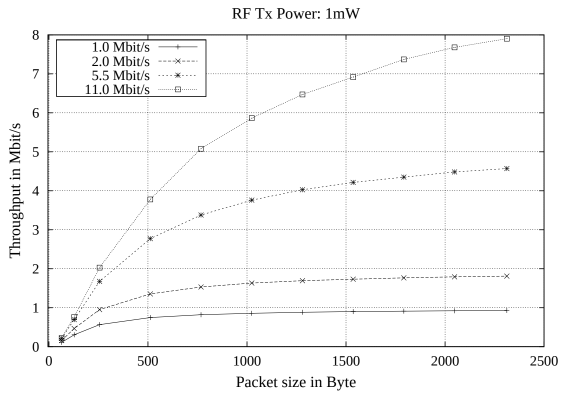


Figure D.2: Measured throughput for different packet sizes for a distance of 5 meters

The throughput at a transmission power of 5, 20, or 50 mW is identical since the distance is small and the transmission rate (modulation) has no influence on the packet error ratein this case.

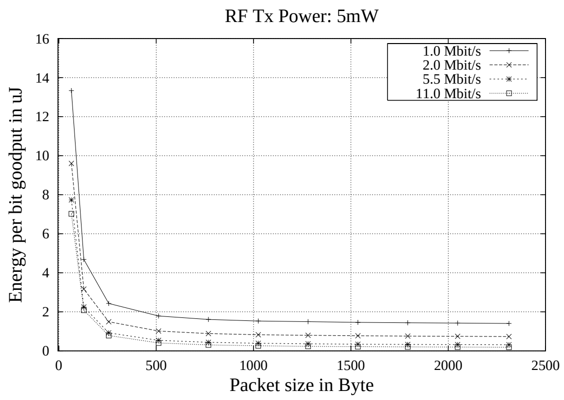


(a) RX mode at 5 mW RF power

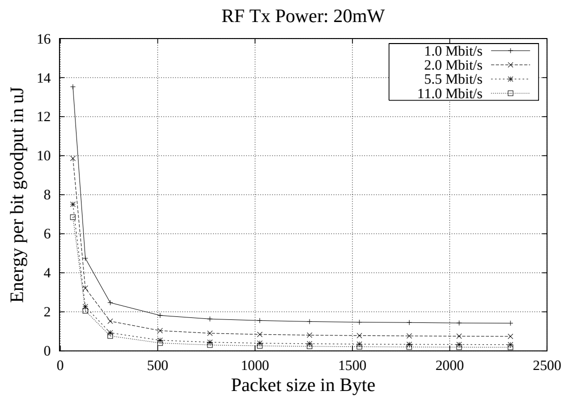


(b) RX mode at 20 mW RF power

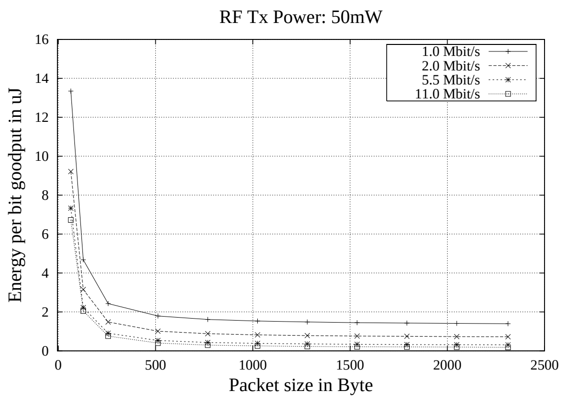


(c) RX mode at 50 mW RF power

Figure D.3: Measured RX energy per goodput bit for different packet sizes for 5 meters

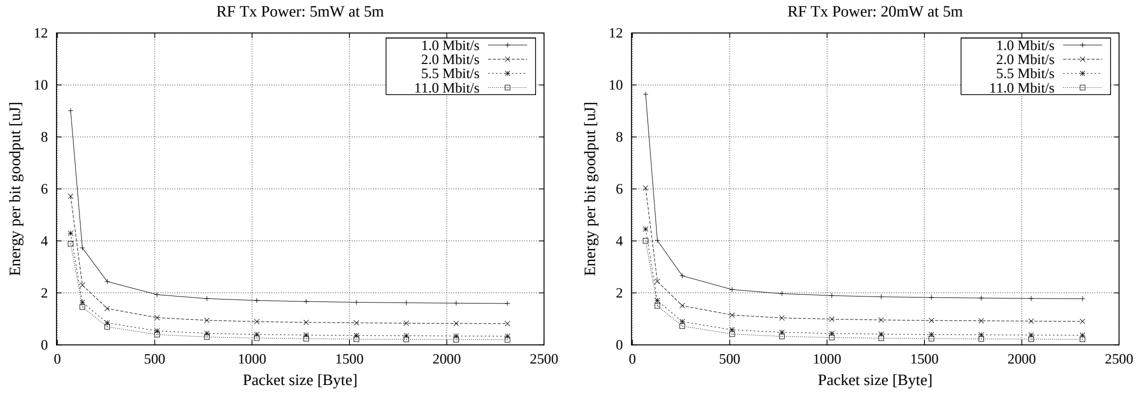


(a) Tx: 5 mW, 5 meters

(b) Tx: 20 mW, 5 meters

Figure D.4: Simulated energy per goodput bit at 5 meters for during transmission

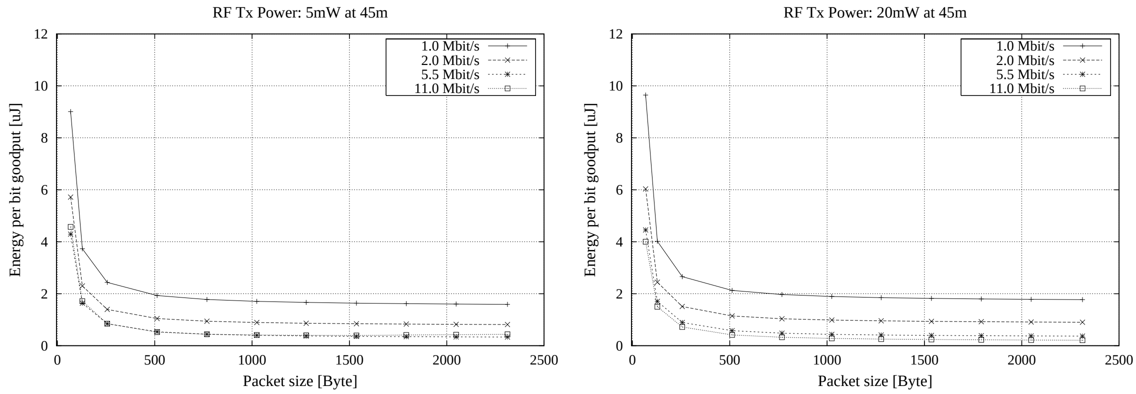


(a) Tx: 5 mW, 45 meters

(b) Tx: 20 mW, 45 meters

Figure D.5: Simulated transmission energy per goodput bit at 45 meters

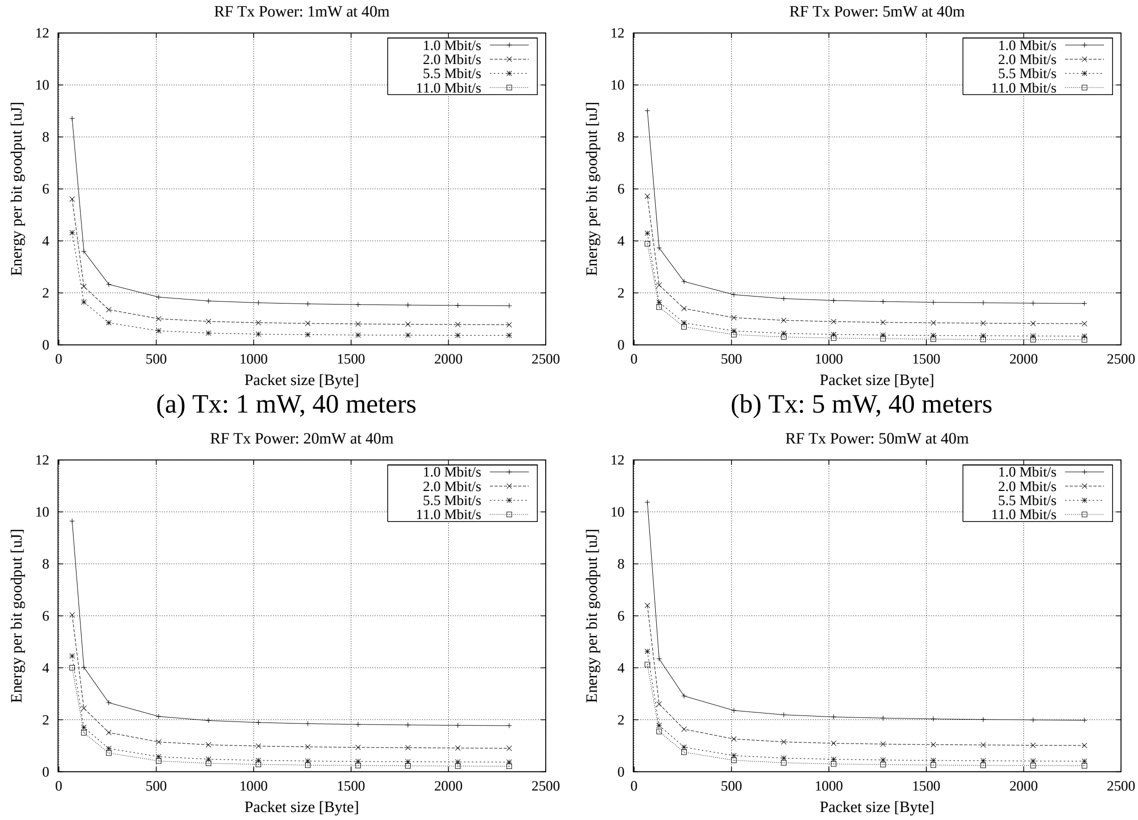


(a) Tx: 1 mW, 40 meters

(b) Tx: 5 mW, 40 meters

(c) Tx: 20 mW, 40 meters

(d) Tx: 50 mW, 40 meters

Figure D.6: Simulated transmission energy per goodput bit at 40 meters

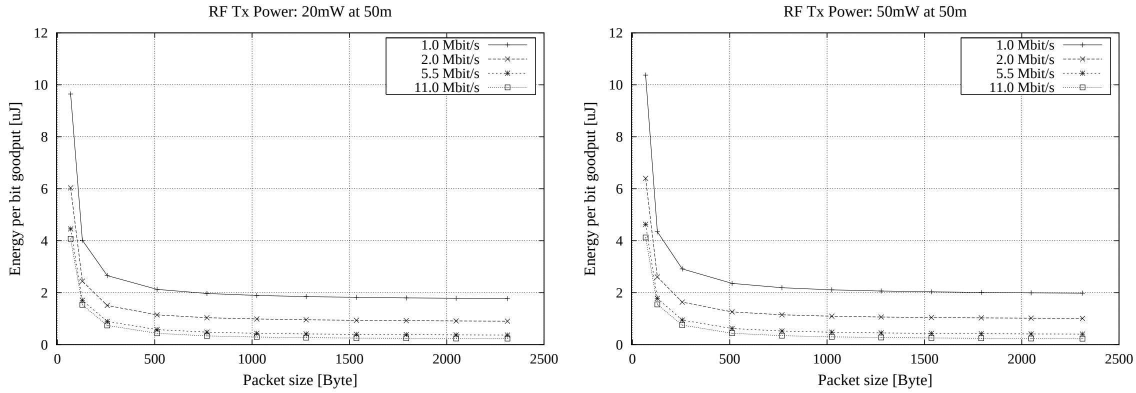


(a) Tx: 20 mW, 50 meters (b) Tx: 50 mW, 50 meters

Figure D.7: Simulated transmission energy per goodput bit at 50 meters

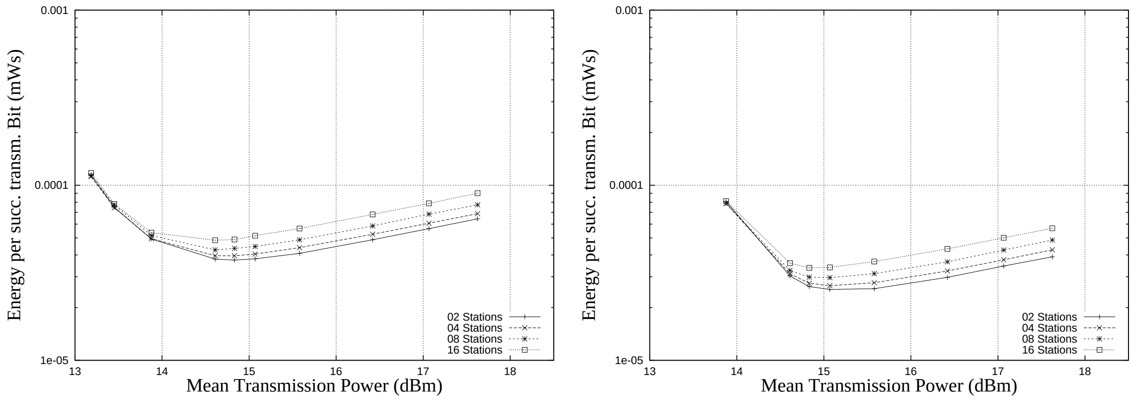


(a) Packet size 128 Bytes (b) Packet size 512 Bytes

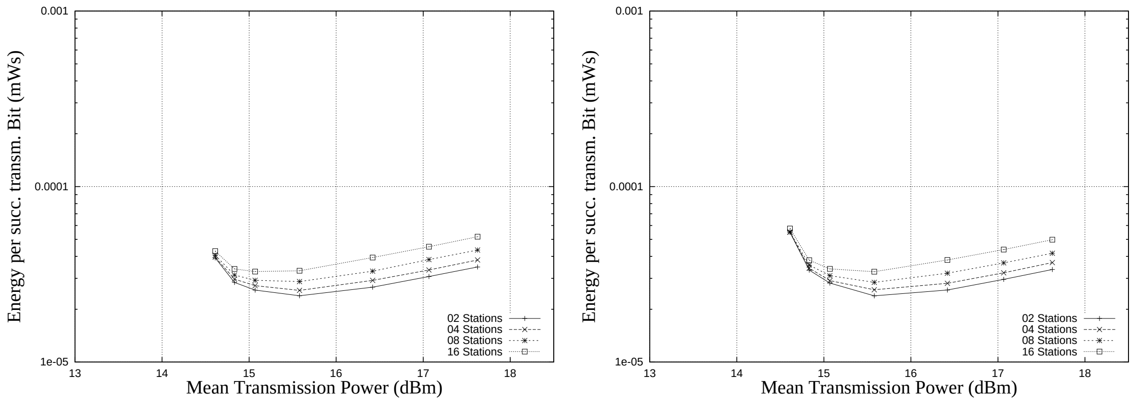


(c) Packet size 1024 Bytes (d) Packet size 1536 Bytes

Figure D.8: Energy per successfully transmitted information bit ($E_{bit\_res}$) vs. RF transmission power $P_{tx}$ for different frame sizes and number of mobile nodes

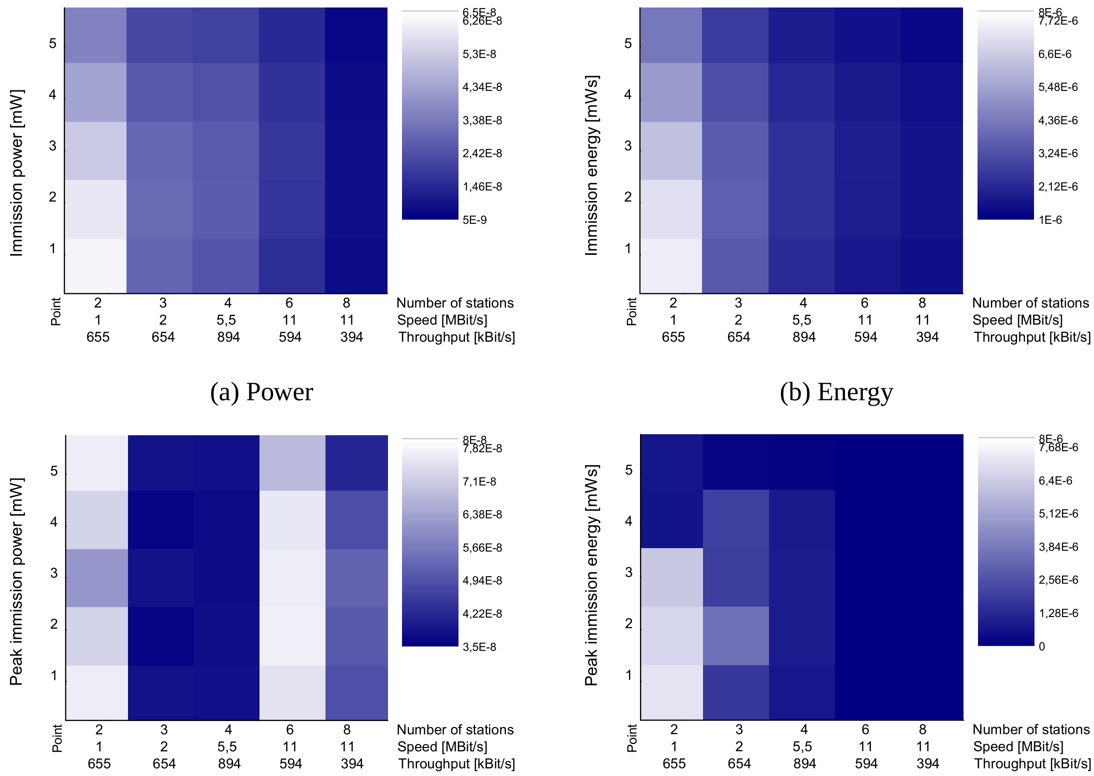


(a) Power

(b) Energy

(c) Peak power

(d) Peak Energy

Figure D.9: Comparison of exposure results (power, energy and peak values)

BER = $10^{-8}$, distance = 10 meters

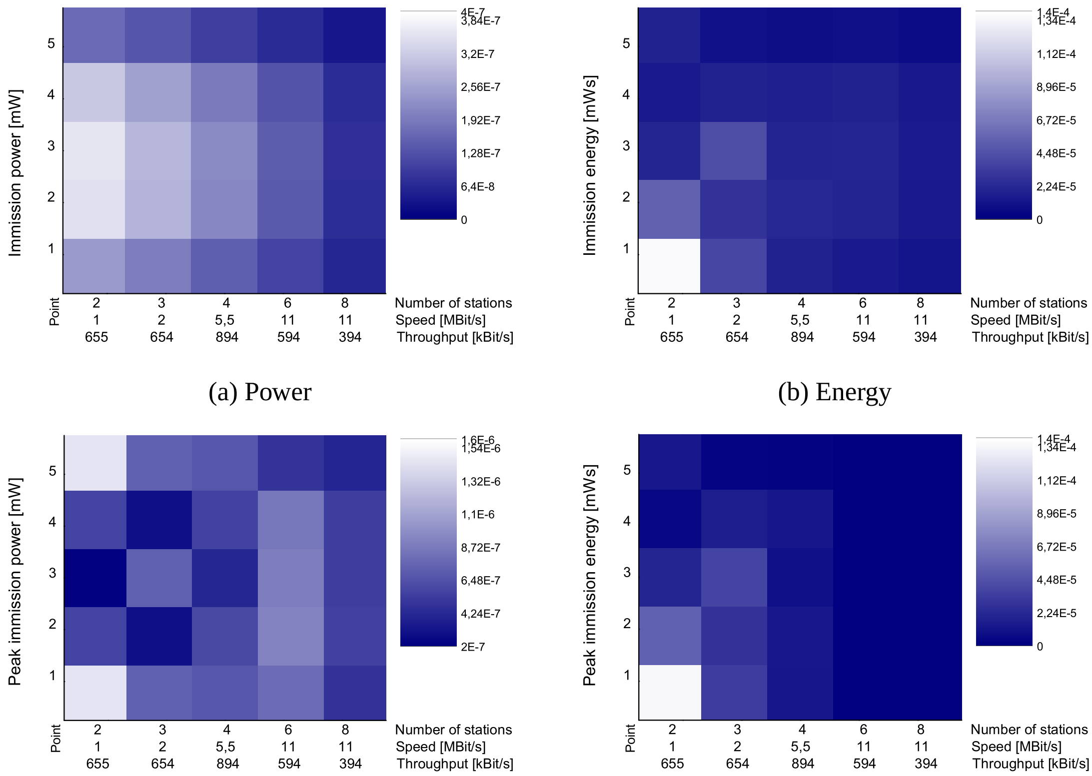


(a) Power

(b) Energy

(c) Peak power

(d) Peak Energy

Figure D.10: Comparison of exposure results (power, energy and peak values)

BER = $10^{-6}$, distance = 50 meters

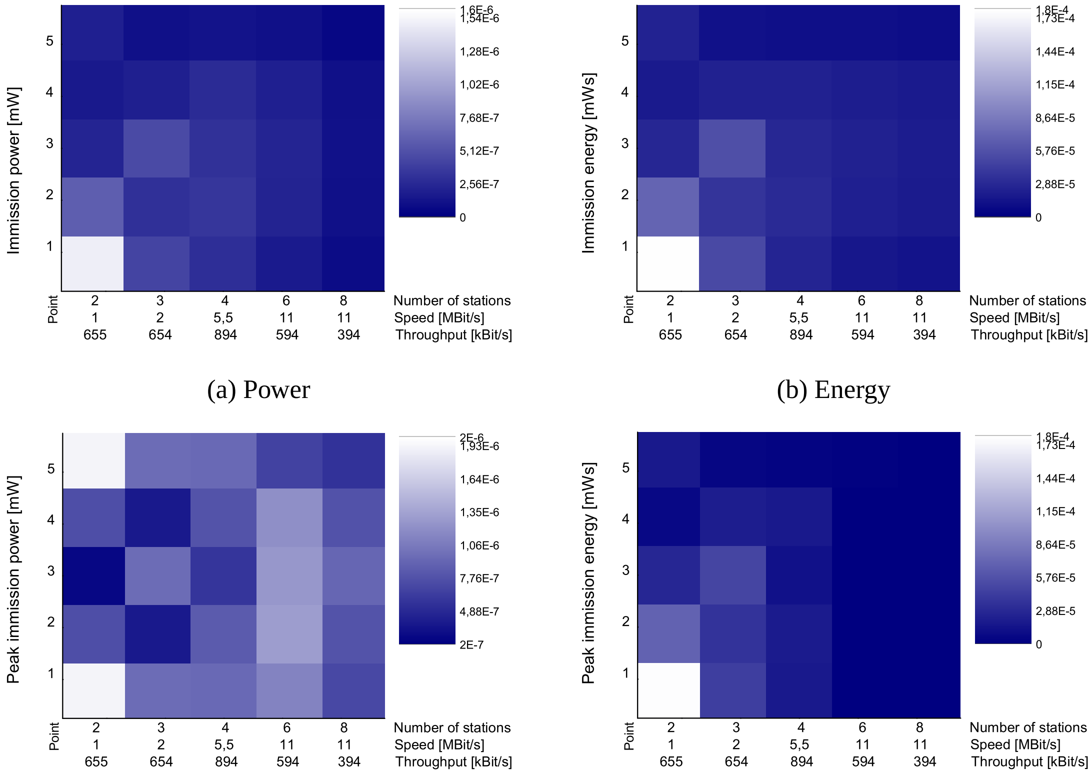


(a) Power

(b) Energy

(c) Peak power

(d) Peak Energy

Figure D.11: Comparison of exposure results (power, energy and peak values)

BER = $10^{-8}$, distance = 50 meters

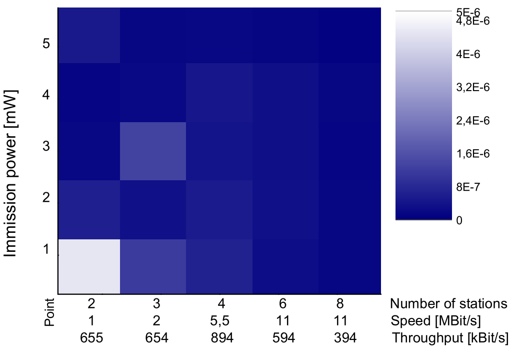


(a) Power

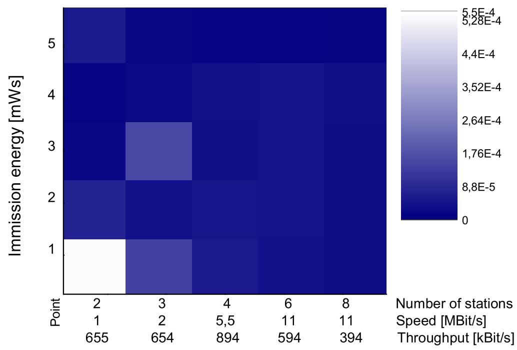


(b) Energy

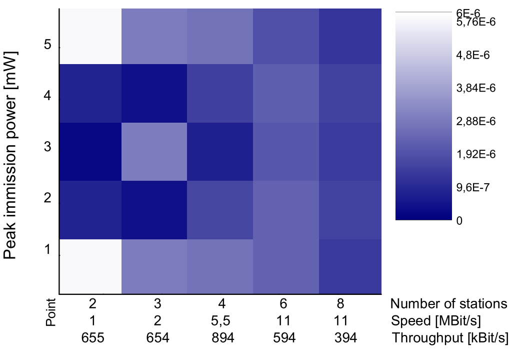


(c) Peak power

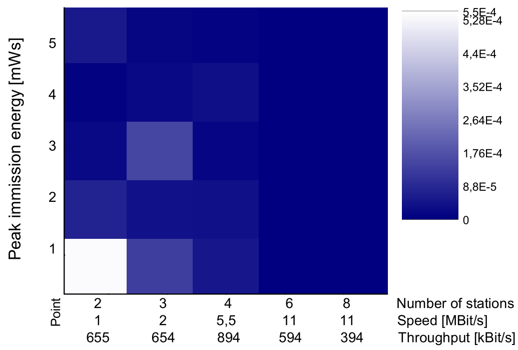


(d) Peak Energy

Figure D.12: Comparison of exposure results (power, energy and peak values)

BER = $10^{-6}$, distance = 100 meters

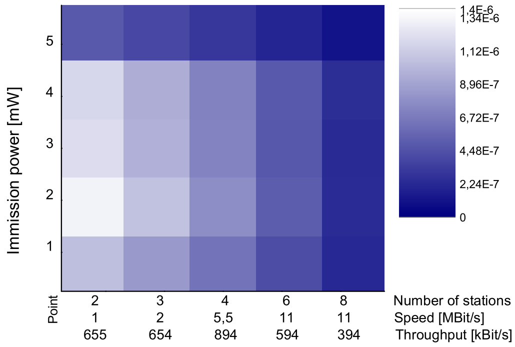


(a) Power

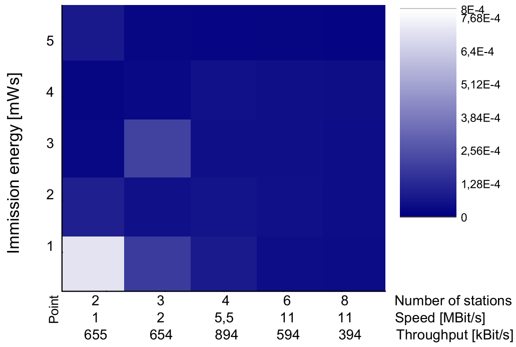


(b) Energy

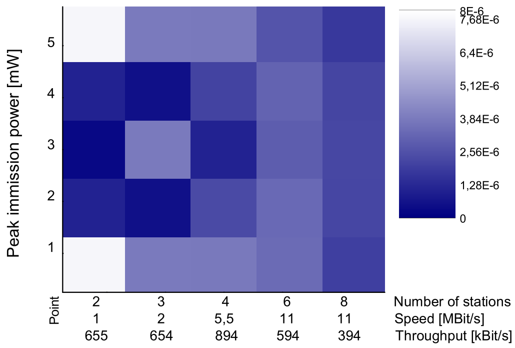


(c) Peak power

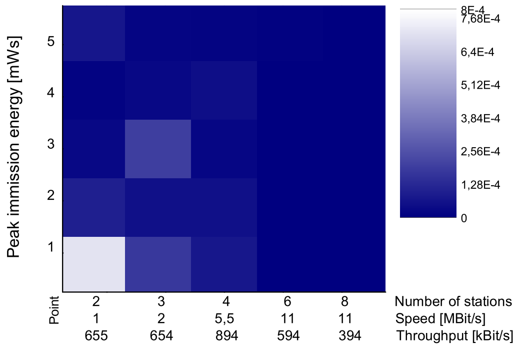


(d) Peak Energy

Figure D.13: Comparison of exposure results (power, energy and peak values)

BER = $10^{-8}$, distance = 100 meters

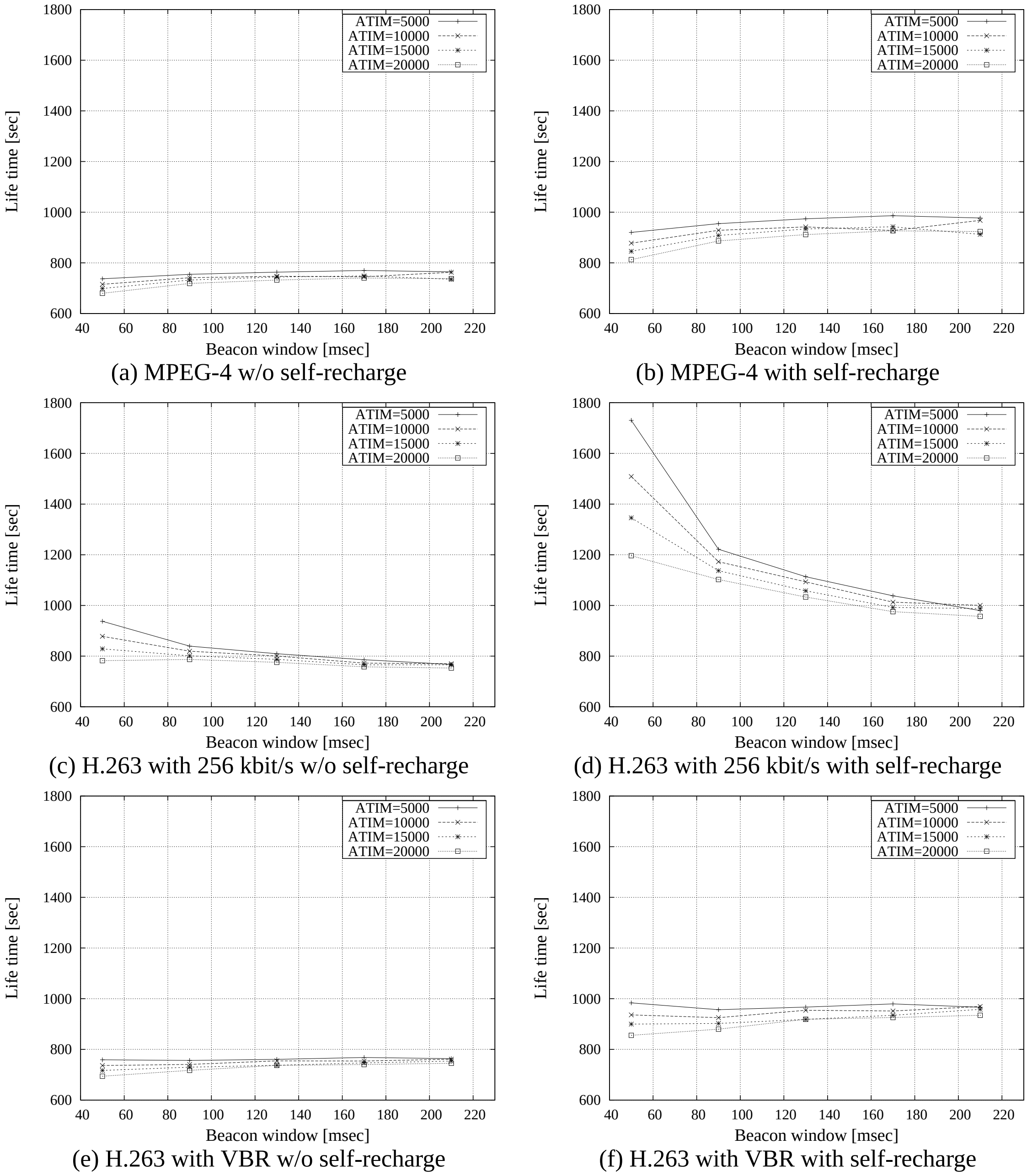


(a) MPEG-4 w/o self-recharge

(b) MPEG-4 with self-recharge

(c) H.263 with 256 kbit/s w/o self-recharge

(d) H.263 with 256 kbit/s with self-recharge

(e) H.263 with VBR w/o self-recharge

(f) H.263 with VBR with self-recharge

Figure D.14: Battery life of node B vs. beacon time and ATIM window for the transmission of a movie

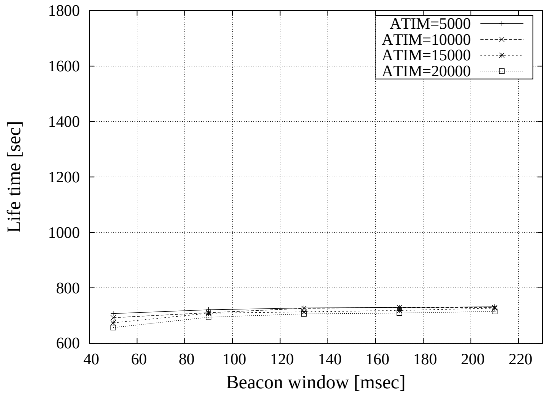


(a) MPEG-4 w/o self-recharge

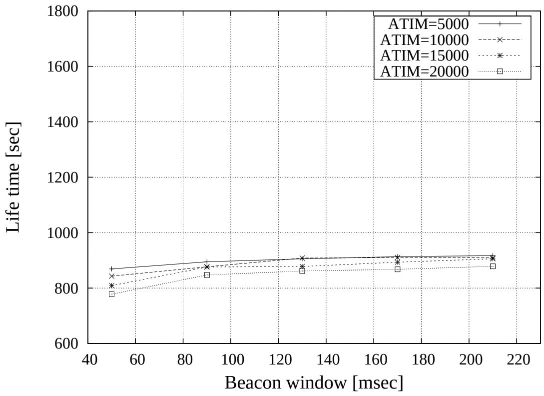


(b) MPEG-4 with self-recharge

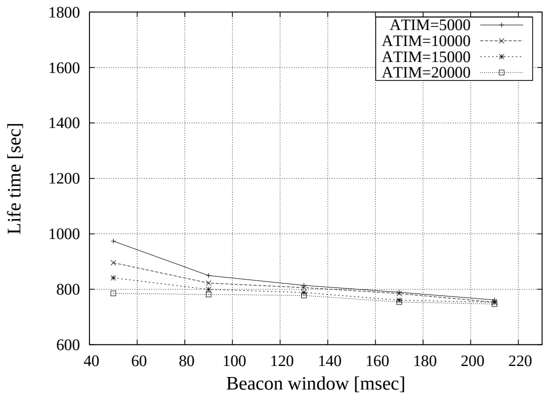


(c) H.263 with 256 kbit/s w/o self-recharge

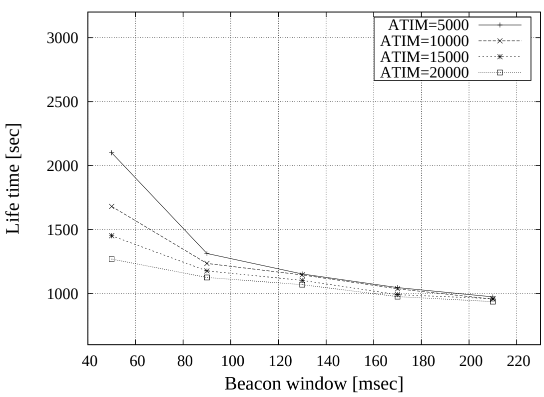


(d) H.263 with 256 kbit/s with self-recharge

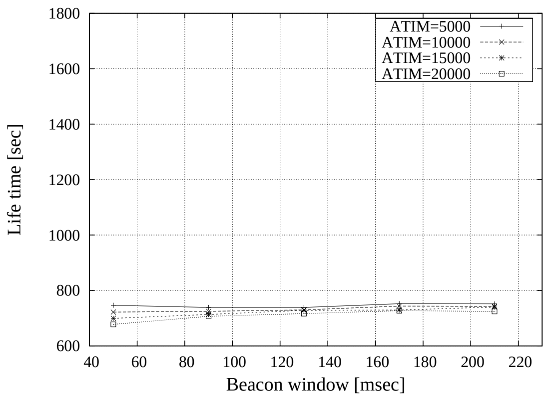


(e) H.263 with VBR w/o self-recharge

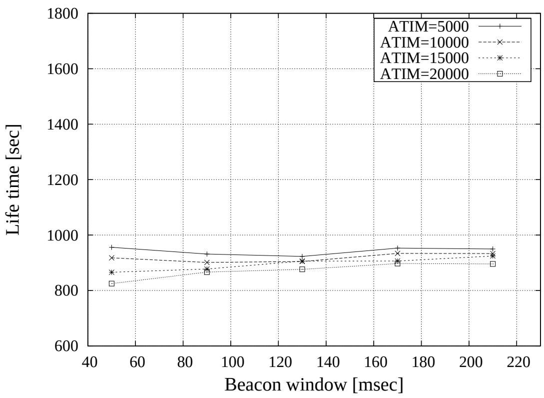


(f) H.263 with VBR with self-recharge

Figure D.15: Battery life of node A vs. beacon time and ATIM window for the transmission of a news video

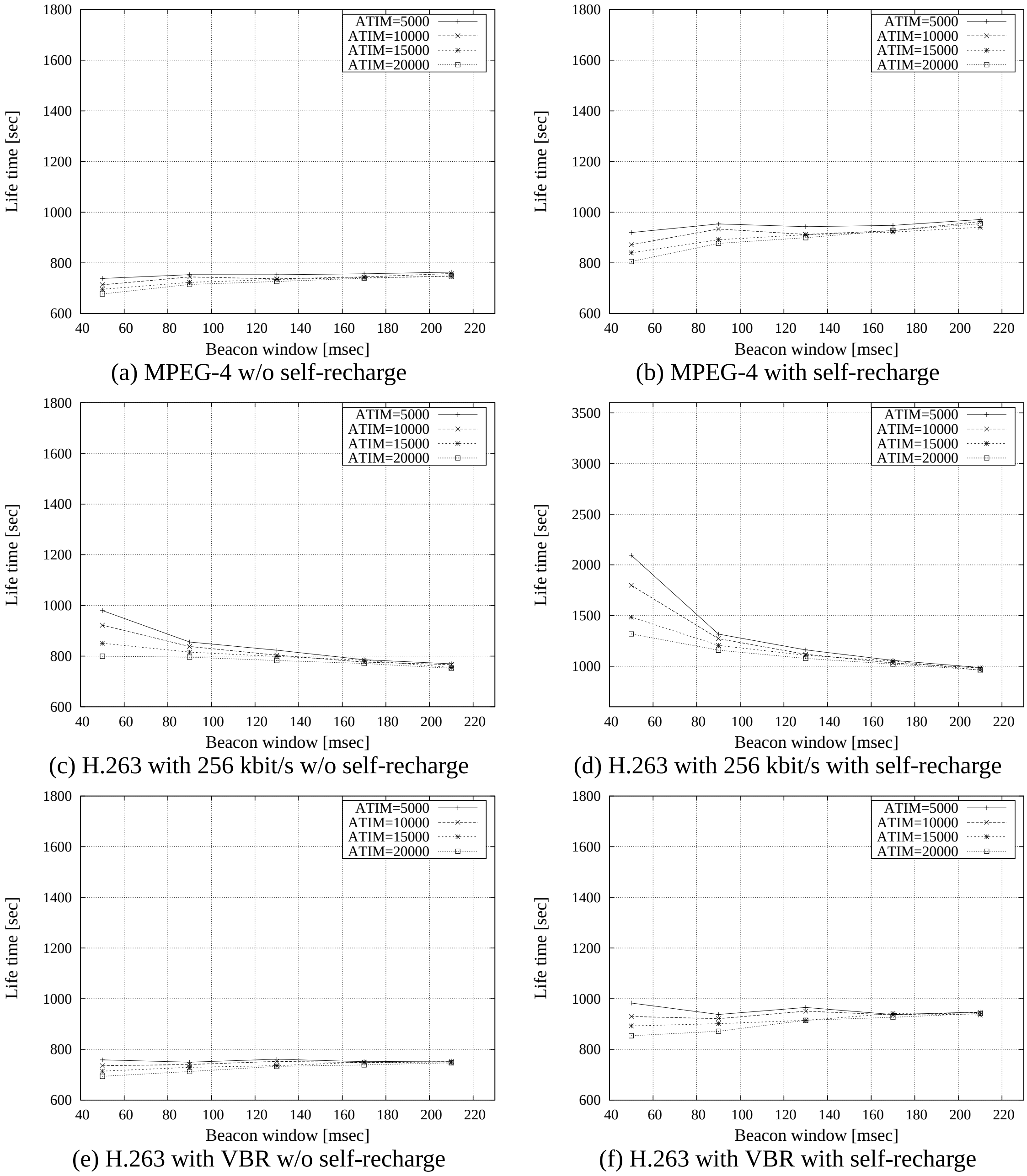


Figure D.16: Battery life of node B vs. beacon time and ATIM window for the transmission of a news video

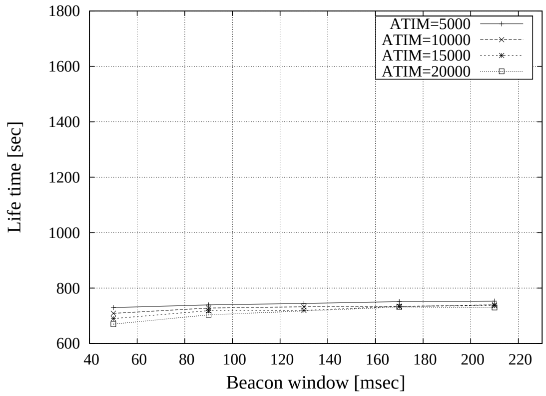

(a) MPEG-4 w/o self-recharge

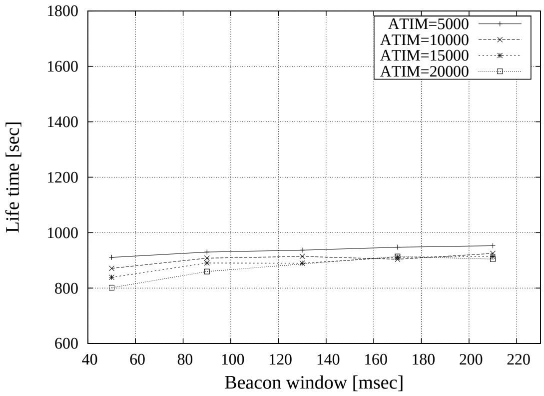

(b) MPEG-4 with self-recharge

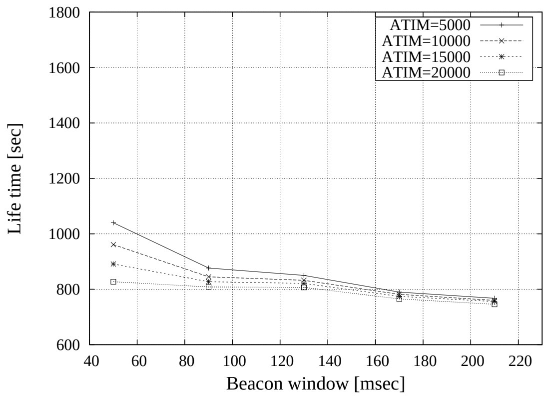

(c) H.263 with 256 kbit/s w/o self-recharge

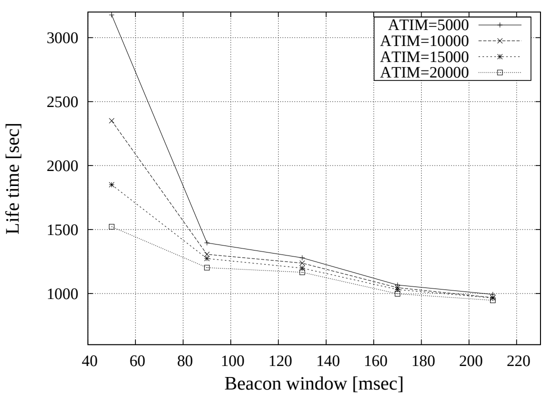

(d) H.263 with 256 kbit/s with self-recharge

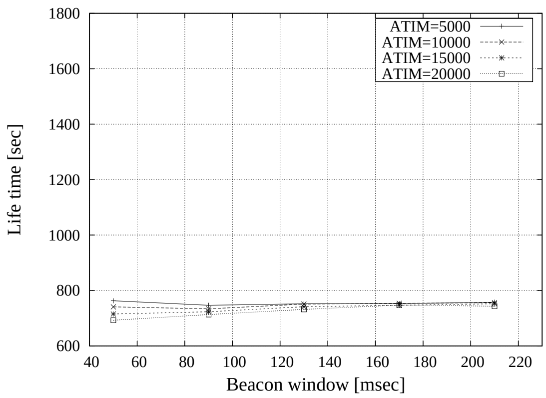

(e) H.263 with VBR w/o self-recharge

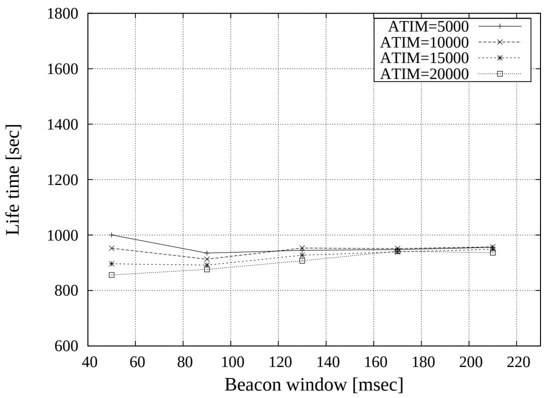

(f) H.263 with VBR with self-recharge

Figure D.17: Battery life for node A vs. beacon time and ATIM window for the transmission of an office cam video

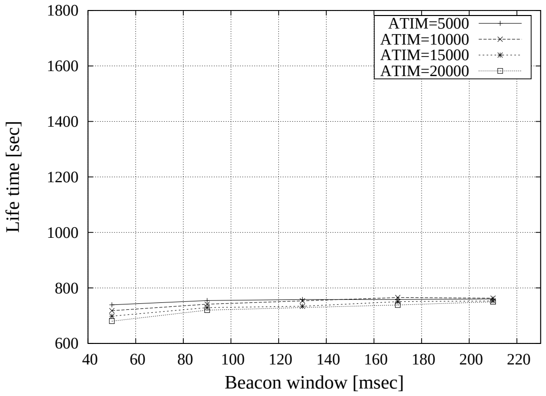


(a) MPEG-4 w/o self-recharge

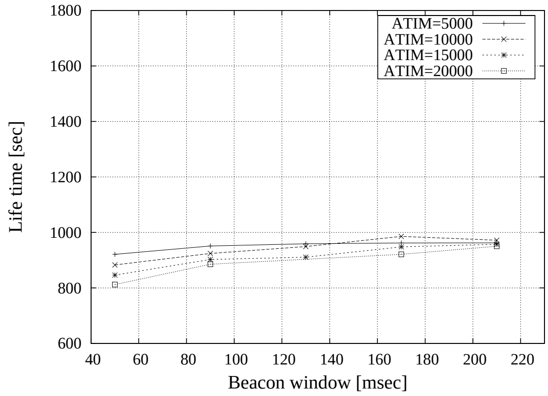


(b) MPEG-4 with self-recharge

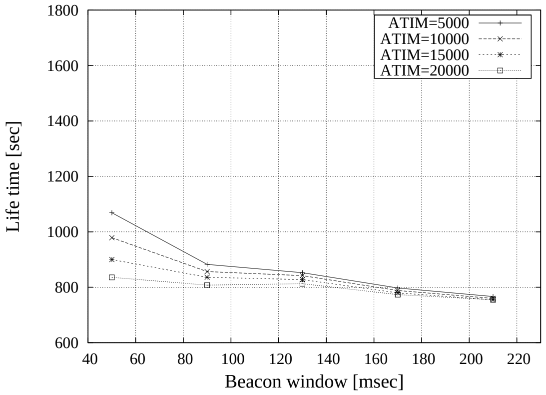


(c) H.263 with 256 kbit/s w/o self-recharge

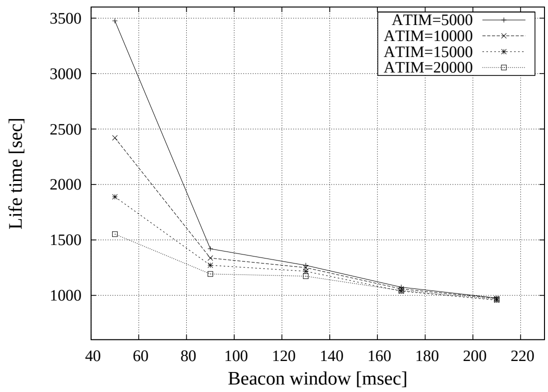


(d) H.263 with 256 kbit/s with self-recharge

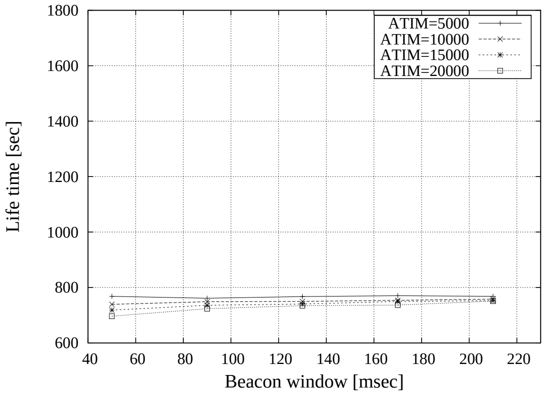


(e) H.263 with VBR w/o self-recharge

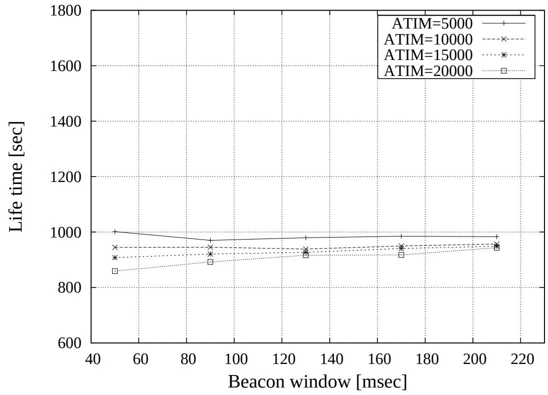


(f) H.263 with VBR with self-recharge

Figure D.18: Battery life of node B vs. beacon time and ATIM window for the transmission of an office cam video

# Appendix E

# Publications and talks

The following list contains research related publications and talks that arose from my research work at the Telecommunication Networks chair (Prof. Dr.-Ing. Adam Wolisz) of the Technical University Berlin. The entries marked with an asterisk (*) at the end are directly related to this dissertation. Almost all findings contained in this thesis were published at the time of their emergence.

## E.1 Journal articles

1. J.-P. Ebert, D. Hollos, H. Karl, and Marc Löbbers. Does Multi-Hop Communication Reduce Electromagnetic Exposure? submitted to the *Computer Journal*, The British Computer Society, Swindon, United Kingdom. (*)

2. J. P. Monks, J.-P. Ebert, A. Wolisz, and W. W. Hwu. Energy Saving and Capacity Improvement Potential of Power Control in Multi-hop Wireless Networks. *Computer Networks*, Elsevier Science B.V., 41:313–330, 2003. (*)

3. J.-P. Ebert and A. Wolisz. Combined tuning of RF power and medium access control for WLANs. *Mobile Networks & Applications*, 6(5):417–426, September 2001. (*)

4. J.-P. Ebert, B. Stremmel, E. Wiederhold, and A. Wolisz. An energy-efficient power control approach for WLANs. *Journal of Communications and Networks (JCN)*, 2(3):197–206, September 2000. (*)

5. H. Woesner, J.-P. Ebert, M. Schläger, and A. Wolisz. Power-saving mechanisms in emerging standards for wireless LANs: The MAC-level perspective. *IEEE Personal Communication Systems (Special Edition on Power Saving)*, 5(3):40–48, June 1998. (*)

6. J.-P. Ebert, R. Holtkamp, A. Wolisz, and L. Ramel. A distributed media access control for wireless ATM environments. In J. M. Holtzmann and M. Zorzi, editors, *Advances in Wireless Communications*, pp. 93–108. Kluwer, April 1998.

## E.2 Conference articles

7. J.-P. Ebert, B. Burns, and A. Wolisz. A trace-based approach for determining the energy consumption of a WLAN network interface. In *Proc. of European Wireless 2002*, pp. 230–236, Florence, Italy, February 2002. (*)

8. J. P. Monks, J.-P. Ebert, A. Wolisz, and W. W. Hwu. A study of the energy saving and capacity improvement potential of power control in multi-hop wireless networks. In *Proc. of Workshop on Wireless Local Networks*, Tampa, Florida, USA, November 2001. also in Proc. of Conf. of Local Computer Networks (LCN). (*)

9. A. Koepsel, J.-P. Ebert, and A. Wolisz. A performance comparison of point and distributed coordination function of an IEEE 802.11 WLAN in the presence of real-time requirements. In *Proc. of 7th Intl. Workshop on Mobile Multimedia Communications (MoMuC2000)*, Tokyo, October 2000.

10. J.-P. Ebert and A. Wolisz. Combined tuning of RF power and medium access control for WLANs. In *Proc. of IEEE Intl. Workshop on Mobile Multimedia Communications (MoMuC'99)*, pp. 74–82, San Diego, CA, USA, November 1999. (*)

11. J.-P. Ebert and A. Wolisz. Power saving in wireless LANs: Analyzing the RF transmission power and MAC retransmission trade-off. In *Proc. of European Wireless '99 and ITG Fachtagung Mobile Kommunikation*, pp. 187–192, Munich, Germany, October 1999. (*)

12. M. Bronzel, D. Hunold, G. Fettweis, T. Konschak, T. Doelle, V. Brankovic, H. Alikhani, J.-P. Ebert, A. Festag, F. Fitzek, and A. Wolisz. Integrated Broadband Mobile System (IBMS) featuring wireless ATM. In *Proc. of ACTS Mobile Communication Summit 97*, pp. 641–646, Aalborg, Danemark, October 1997.

13. J.-P. Ebert, R. Holtkamp, A. Wolisz, and L. Ramel. A distributed media access control for wireless ATM environments. In *Proc. of 6th WINLAB Workshop on Third Generation Wireless Systems*, S. 93–108, New Brunswick, NJ, USA, März 1997. also published in *Advances in Wireless Communications*, S. 93–108. Kluwer, April 1998.

14. R. Holtkamp, J.-P. Ebert, A. Wolisz, and L. Ramel. A distributed media access control (DMAC) for wireless ATM networks. In *Proc. of 5th Intl. Conf. on Telecommunication Systems - Modeling and Analysis*, pp. 501–508, Nashville, TN, USA, March 1997.

15. G.-P. Fettweis, K. Iversen, M. Bronzel, H. Schubert, V. Aue, D. Maempel, J. Voigt, A. Wolisz, G. Walf, and J.-P. Ebert. A closed solution for an Integrated Broadband Mobile System (IBMS). In *Proc. of Intl. Conf. on Universal Personal Communications (ICUPC'96)*, pp. 707–711, Cambridge, Massachusetts, October 1996.

16. J. Weinmiller, H. Woesner, J.-P. Ebert, and A. Wolisz. Modified backoff algorithms for DFWMAC‘s Distributed Coordination Function. In *Proc. of 2nd ITG Fachtagung Mobile Kommunikation '95*, pp. 363–370, Neu-Ulm, Germany, September 1995.

17. J. Weinmiller, H. Woesner, J.-P. Ebert, and A. Wolisz. Analyzing the RTS/CTS mechanism in the DFWMAC media access protocol for wireless LANs. In *Proc. of IFIP TC6 Workshop Personal Wireless Communications (Wireless Local Access)*, pp. 117–130, Prag, Czech Republik, April 1995. Verlag der Augustinus Buchhandlung.

18. J.-P. Ebert, B. Rathke, and A. Wolisz. A conceptual framework to integrate mobility into ISDN. In *Proc. of Intl. Conf. Wireless Computer Networks WCN'94*, pp. 986–993, September 1994.

## E.3 TKN technical reports

19. B. Matzen, J.-P. Ebert, and H. Karl. Electromagnetic immission reduction for radio communication networks by using a multi-hop as hoc approach. Technical Report TKN-03-004, Telecommunication Networks Group, Technical University Berlin, Germany, February 2003. (*)

20. B. Burns and J.-P. Ebert. Power Consumption, Throughput and Packet Error Measurements of an IEEE 802.11 WLAN Interface. Technical Report, TKN-01-007, Telecommunication Networks Group, Technical University Berlin, Germany, August 2001. (*)

21. J.-P. Ebert, Stephan Aier, Gunnar Kofahl, Alexander Becker, Brian Burns, and Adam Wolisz. Measurement and simulation of the energy consumption of a WLAN interface. Technical Report, TKN-02-010, Telecommunication Networks Group, Technical University Berlin, Germany, June 2002. (*)

22. J.-P. Ebert and A. Willig. A Gilbert-Elliot bit error model and the efficient use in packet level simulation. Technical Report TKN-99-002, Telecommunication Networks Group, Technical University Berlin, Germany, March 1999. (*)

## E.4 Other reports

23. M. Schläger, J.-P. Ebert, A. Wolisz, and W. Franz. Quittierung in lokalen Multihop-Funknetzen. Technical Report, Daimler-Benz Forschung Ulm, Germany, November 1995.

## E.5 Talks

1. J.-P. Ebert. Combined tuning of RF power and medium access control for WLANs. *Berkeley Wireless Research Laboratory (BWRC)*, Berkeley, CA, USA, November 1999. (*)

2. J.-P. Ebert. Media Access Control (MAC) protocols for Wireless Networks (WN). *ITG expert group meeting (FG 52.5, PON - Passive Optical Fibre Networks)*, Stuttgart, Germany, October 1997. (*)

3. J.-P. Ebert. Modeling and performance analysis of WMAC protocols. *TUBKOM Colloquium on Advanced Networking*, Berlin, Germany, December 1994.

# Bibliography


[1] E. Ayanoglu, S. Paul, T. F. LaPorta, K. K. Sabnani, and R. D. Gitlin. Airmail: A link-layer protocol for wireless networks. *ACM/Baltzer Wireless Networks*, 1(2):161–174, 1995.

[2] A. Bakre and B. R. Badrinath. I-TCP: Indirect TCP for mobile hosts. In *15th International Conference on Distributed Computing Systems*, May 1995.

[3] H. Balakrishnan, V. N. Padmanabhan, S. Seshan, and R. H. Katz. A comparison of mechanisms for improving TCP performance over wireless links. *IEEE/ACM Transactions on Networking*, 5(6):756–769, 1997.

[4] H. Balakrishnan, S. Seshan, E. Amir, and R. H. Katz. Improving tcp/ip performance over wireless networks. *Proc. MobiCom '95, Berkeley, CA*, pages 2–11, November 1995.

[5] N. Bambos. Toward Power-Sensitive Network Architectures in Wireless Communications: Concepts, Issues, and Design Aspects. *IEEE Personal Communications*, 5:50–59, June 1998.

[6] V. Bharghavan, A. Demers, S. Shenker, and L. Zhang. MACAW: A Media Access Protocol for Wireless LAN's. *Proceedings of ACM SIGCOMM*, 24:212–25, Oct. 1994.

[7] N. Borisov, I. Goldberg, and D. Wagner. Intercepting Mobile Communications: The Insecurity of 802.11. In *The Seventh Annual International Conference on Mobile Computing and Networking*, Rome, Italy, July 2001. ACM Sigmobile.

[8] K. Brown and S. Singh. M-TCP: TCP for mobile cellular networks. *ACM Computer Communication Review*, 27(5), 1997.

[9] B. Burns and J.-P. Ebert. Power Consumption, Throughput and Packet Error Measurements of an IEEE 802.11 WLAN Interface. Technical Report TKN-01-007, Telecommunication Networks Group, Technical University Berlin, August 2001.

[10] F. Cameron, M. Zukerman, and M. Gitlits. Adaptive transmission parameters optimisation in wireless multi-access communication. In *Proceedings of IEEE ICON '99*, pages 91–95, Brisbane, Australia, September 1999.

[11] A. Cerpa and D. Estrin. ASCENT: Adaptive Self-Configuring Sensor Networks Topologies. In *Proc. INFOCOM*, New York, NY, June 2002. http://lecs.cs.ucla.edu/Publications/papers/ASCENT-Infocom-2002.ps.

[12] C.-F. Chiasserini and R. R. Rao. Importance of a Battery Pulsed Discharge in Portable Radio Devices. In *Proc. of Int. Conf. on Mobile Computing and Networking (MobiCom '99)*, Seattle, USA, August 1999.

[13] C.-F. Chiasserini and R. R. Rao. Energy Efficient Battery Management. In *IEEE INFOCOM 2000*, Tel Aviv, Israel, March 2000.

[14] H. S. Choe and K. M. Abraham. Synthesis and characterization of $LiNiO_2$ as a cathode material for pulse power batteries. In *MRS Symposium Proceedings*, volume 496, pages 101–107, December 1997.

[15] T. L. Cignetti, K. Komarov, and C. Schlatter-Ellis. Energy Estimation Tools for the Palm. In *ACM MSWiM 2000: Modeling, Analysis and Simulation of Wireless and Mobile*, August 2000.

[16] CMU Monarch Project. http://www.monarch.cs.cmu.edu/, Dec. 1999.

[17] Energizer Battery Company. Discharge of batteries. http://www.data.energizer.com, 2001.

[18] J.-P. Ebert and A. Willig. A Gilbert-Elliot Bit Error Model and the Efficient Use in Packet Level Simulation. Technical Report TKN-99-002, Technical University Berlin, Telecommunication Networks Group, March 1999.

[19] The Editiors. Part11: Wireless LAN Medium Access Control (MAC) and Physical Layer Specifications: High Speed Physical Layer in the 5 GHz Band. IEEE Draft Standrard P802.11/D1.4, Institute of Electrical and Electronics Engineers, Inc., October 1998.

[20] The Editors. Part11: Wireless LAN Medium Access Control (MAC) and Physical Layer Specification. IEEE Standard 802.11, Institut of Electrical and Electronics Engineers, Inc., November 1997.

[21] The Editors. Broadband Radio Access Network (BRAN); HIgh PErformance Radio Local Area Network Type I; Functional specification. ETSI standard EN 300 652 V.1.2.1, European Telecommunications Standards Institute, July 1998.

[22] The Editors. Carrier Sense Multiple Access with Collision Detection Access Method and Physical Layer Specifications. IEEE Standard 802.3, Institut of Electrical and Electronics Engineers, Inc., September 1998.

[23] The Editors. Part 11: Wireless LAN Medium Access Control (MAC) and Physical Layer (PHY): Higher Speed Physical Layer (PHY) Extension in the 2.4 GHz band. IEEE Standard 802.11b, Institut of Electrical and Electronics Engineers, Inc., September 1999.

[24] The Editors. Broadband Radio Access Network (BRAN); HIPERLAN Type 2; Data Link Control (DLC) Layer; Part2: Radio Link Control (RLC) sublayer. ETSI standard ETSI TS 101 761-2 V1.2.1, European Telecommunications Standards Institute, April 2001.

[25] The Editors. Etsi hipeerlan/1 standard. Standard, European Telecommunications Standard Institute, April 2001.

[26] T. A. ElBatt, S. V. Krishnamurthy, D. Connors, and S. Dao. Power Management for Throughput Enhancement in Wireless Ad-Hoc Networks. In *ICC 2000*, New Orleans, LA, June 2000. IEEE.

[27] L. M. Feeney and M. Nilsson. Investigating the Energy Consumption of an Wireless Network Interface in an Ad hoc Networking Environment. In *IEEE Infocom 2001*, Anchorage, Alaska, April 2001.

[28] F. Fitzek. MPEG-4 and H.263 Video Traces for Network Performance Evaluation (Extended Version). Technical Report TKN-00-05, Telekommunikationsnetze, Technische Universität Berlin, July 2000.

[29] F. Fitzek and M. Reisslein. MPEG–4 and H.263 Video Traces for Network Performance Evaluation. *IEEE Network*, 15(6):40–54, November/December 2001.

[30] J. Flinn and M. Satyanarayanan. Energy-aware adaptation for mobile applications. In *Proc. of the 17th ACM Symposium on Operating Systems Principles*, Kiawah Island Resort, SC, USA, December 1999. ACM.

[31] C. Fullmer and J. Garcia-Luna-Aceves. Floor Acquisition Multiple Access (FAMA) for Packet-Radio Networks. *Proceedings of ACM SIGCOMM*, Sept. 1995.

[32] Bill Garon. *PRISM$^{TM}$PC Card Wireless LAN Evaluation Kit Users Guide*. Harris Semiconductor Wireless Products, Harris Corporation, USA, February 1998. Application Note AN9790.

[33] E. N. Gilbert. Capacity of a burst-noise channel. *Bell Systems Technical Journal*, 39:1253–1265, September 1960.

[34] J. Gomez, A. T. Campbell, M. Naghshineh, and C. Bisdikian. Conserving Transmission Power in Wireless Ad Hoc Networks. In *9th International Conference on Network Protocols*, Riverside, California, November 2001. IEEE.

[35] P. Gupta and P. Kumar. The Capacity of Wireless Networks. *IEEE Transactions on Information Theory*, IT-46:388–404, March 2000.

[36] J. C. Haartsen. The Bluetooth Radio System. *IEEE Personal Communications*, 7(1):28–36, February 2000.

[37] Z. Haas and P. Agrawal. Mobile-TCP: An asymmetric transport protocol design for mobile systems. *ICC'97, Montreal, Canada*, June 1997.

[38] http://www.handspring.com.

[39] G. P. Harmer, B. R. Davis, and D. Abbott. A Review of Stochastic Resonance: Circuit and Measurement. *IEEE Transactions on Instrumentation and Measurement*, 51(2):299–309, April 2002.

[40] W. R. Heinzelman, A Chandrakasan, and H. Balakrishnan. Energy-efficient Communication Protocol for Wireless Microsensor Networks. In *Proceedings of the 33rd International Conference on System Sciences (HICSS '00)*, Maui, Hawaii, January 2000.

[41] G. D. Holland, N. H. Vaidya, and P. Bahl. A rate-adaptive MAC protocol for multi-hop wireless networks. In *Proceedings of the Seventh Annual ACM/IEEE Conference on Mobile Computing and Networking (MOBICOM)*, July 2001.

[42] T. Imielinski, S. Vishwanathan, and B. R. Badrinath. Energy efficient indexing on air. In *Proc. of the Int. Conf. on Management of Data (ACM SIGMOD)*, pages 25–37, May 1994.

[43] http://sourceforge.net/projects/airo-linux/. WWW.

[44] D. B Johnson and D. A Maltz. Dynamic Source Routing in Ad Hoc Wireless Networks. In Imielinski and Korth, editors, *Mobile Computing*, volume 353. Kluwer Academic Publishers, 1996.

[45] A. Kamerman and L. Monteban. WaveLAN-II: A high performance wireless LAN for the unlicensed band. *Bell Labs Technical Journal*, pages 118–133, Summer 1997.

[46] P. Karn. MACA - A New Channel Access Method for Packet Radio. *ARRL/CRRL Amateur Radio 9th Computer Networking Conference*, pages 134–140, Sept. 1990.

[47] R. Kraemer and M. Methfessel. A Vertical Approach to Energy Management. In *Proc. of European Wireless ’99 & ITG Mobile Communications*, München, Deutschland, October 1999.

[48] R. Kravets and P. Krishnan. Power Management Techniques for Mobile Communications. In *MobiCom’98*, Dallas, Texas, October 1998.

[49] R. Kravets, K. Schwan, and K. Calvert. Power-aware communication for mobile computers. In *International Workshop on Mobile Multimedia Communications (MoMuC’99)*, San Diego, USA, Octopber 1999.

[50] B. Krishnamachari, R. Bejar, and S. B. Wicker. Distributed Constraint Satisfaction and the Bounds on Resource Allocation in Wireless Networks. In *Sixth International Symposium on Communications Theory and Application*, Ambleside, UK, July 2001. ISCTA.

[51] R. M. LaFollete. Design and performance of high specific power, pulsed discharged, bipolar lead acid batteries. In *10th Annual Battery Conference on Applications and Advances*, pages pp. 43–47, Long Beach, USA, January 1995.

[52] W. Leland, M. Taqqu, W. Willinger, and D. Wilson. On the Self-Similar Nature of Ethernet Traffic. *IEEE/ACM Transactions on Networking*, 2(1):1–15, February 1994.

[53] P. Lettieri and M. B. Srivastava. A QoS-aware Energy-Efficient Wireless Node Architecture. In *Proc. of the Sixth IEEE International Workshop on Mobil Multimedia Communications (MoMuC’99)*, pages 252–261, San Diego, CA, USA, November 1999.

[54] P. A. Lettieri. *Architectural Strategies for Energy Efficient Wireless Multimedia Systems*. Dissertation, University of California, Los Angelas, USA, 2000.

[55] J. R. Lorch and A. J. Smith. Software Strategies for Portable Computer Energy Management. *IEEE Personal Communications*, 5(3):60–72, June 1998.

[56] B. Matzen, J.-P. Ebert, and H. Karl. Electromagnetic immission reduction for radio communication networks by using a multi-hop ad hoc approach. Technical Report TKN-03-004, Telecommunication Networks Group, Technische Universität Berlin, February 2003.

[57] Mesquite. CSIM18. http://www.mesquite.com, WWW.

[58] E. Modiano. An adaptive algorithm for optimizing the packet size used in wireless arq protocols. *Wireless Networks*, 5(4):279–286, July 1999.

[59] J. Monks, V. Bharghavan, and W. Hwu. Transmission Power Control for Multiple Access Wireless Packet Networks. *IEEE Conference on Local Computer Networks LCN*, 25:12–21, Nov. 2000.

[60] J. Monks, V. Bharghavan, and W. Hwu. A Power Controlled Multiple Access Protocol for Wireless Packet Networks. *Infocom*, 20:1–11, Apr. 2001.

[61] K. J. Negus, A. P. Stephens, and J. Lansford. HomeRF: Wireless Networking for the Connected Home. *IEEE Personal Communications*, 7(1):20–27, February 2000.

[62] http://www.netperf.org. World Wide Web.

[63] D. Newman and K. Tolly. Wireless LAN: How far? How fast? *Data Communication Magazine*, March 1995.

[64] V. D. Park and M. S. Corson. A Highly Adaptive Distributed Routing Algorithm for Mobile Wireless Networks. In *INFOCOM 1997*, pages 1405–1413, Kobe, Japan, April 1997. IEEE.

[65] G. Pei, M. Gerla, and T.-W. Chen. Fisheye State Routing in Mobile Ad Hoc Networks. In Ten-Hwang Lai, editor, *ICDCS Workshop on Wireless Networks and Mobile Computing*, pages D71–D78, Taipei, Taiwan, ROC, April 2000.

[66] C. Perkins and P. Bhagwat. Highly Dynamic Destination-Sequenced Distance-Vector Routing (DSDV) for Mobile Computers. In *ACM SIGCOMM'94 Conference on Communications Architectures, Protocols and Applications*, pages 234–244, 1994.

[67] C. E. Perkins. Ad-hoc On-Demand Distance Vector Routing. In *MILCOM '97 panel on Ad Hoc Networks*, November 1997.

[68] Software radio. *Personal Communications*, 6(4), August 1999.

[69] Energy Management in Personal Communications and Mobile Systems. *IEEE Personal Communications*, 5(3), June 1998.

[70] J. Pouwelse, K. Langendoen, and H. Sips. Dynamic Voltage Scaling on a Low-Power Microprocessor. In *Proc. 7th ACM MOBICOM*, Rome, Italy, July 2001. IEEE.

[71] C. E. Price, K. M. Sivalingam, J. C. Chen, and P. Agrawal. Power-aware Scheduling Algrithms for Wireless Networks. In *Proc. of Intl. Conference on Intelligence Computing and VLSI*, Kalyani, India, 2001.

[72] Maxim Integrated Products. Energy management for small portable systems. http://www.maxim-ic.com.

[73] J. M. Rabaey and M. Pedram, editors. *Low Power Design Methodologies*. Kluwer Academic Publisher, Boston/Dordrecht/London, 1996.

[74] D. Raguin, M. Kubisch, H. Karl, and A. Wolisz. Queue-driven Cut-through Medium Access in Wireless Ad Hoc Networks. In *to appear in Wireless Communications and Networking Conference (WCNC)*, Atlanta, GA, March 2004. IEEE.

[75] R. Ramanathan and R. Rosales-Hain. Topology Control of Multihop Wireless Networks using Transmit Power Adjustment. In *Proc. IEEE Infocom*, Tel-Aviv, Israel, March 2000.

[76] T. S. Rappaport. *Wireless Communication: Principles and Practice*. Prentice Hall, 1998.

[77] F. Rashid-Farrokhi and et. al. Downlink Power Control and Base Station Assignment. *IEEE Communications Letters*, 1:102–104, July 1997.

[78] B. Rathke, T. Assimakopoulos, R. Morich, G.Schulte, and A. Wolisz. SNUFFLE: Integrated Measurement and Analysis Tool for Wireless Internet and its Use for in-House Environment. In *10th Intl. Conf. for Computer Performance Evaluation (TOOLS'98)*, Palma de Mallorca, Spain, September 1998.

[79] B. Rathke, M. Schläger, and A. Wolisz. Systematic Measurement of TCP Performance over Wireless LANs. Technical Report TKN-01BR98, Telekommunikationsnetze, Technische Universität Berlin, Telecommunication Networks Group, December 1998.

[80] V. Rodoplu and T. H.-Y. Meng. Minimum Energy Mobile Wireless Networks. *IEEE Journal on Selected Areas in Communications*, 17(8):1333–1344, August 1999.

[81] C. Roehl, H. Woesner, and A. Wolisz. A Short Look on Power Saving Mechanisms in the Wireless LAN Standard IEEE 802.11. In J. M. Holtzmann and M. Zorzi, editors, *Advances in Wireless Communications*, pages 219–226. Kluwer, April 1998.

[82] S. Roundry, D. Steingart, L. Frechette, P. Wright, and J. M. Rabaey. Power sources for wireless sensor networks. In *Proceedings of the 1st. European Workshop on Wireless Sensor Networks*, Berlin, Germany, January 2004.

[83] M. Schlaeger, B. Rathke, S. Bodenstein, and A. Wolisz. Advocating a remote socket architecture for internet access using wireless LANs. *Mobile Networks and Applications (Special Issue on Wireless Internet and Intranet Access)*, 6(1):23–42, January 2001.

[84] S. Singh and C. S. Raghavendra. PAMAS - Power Aware Multi-Access Protocol with Signalling for Ad Hoc Networks. *ACM SIGCOM Computer Communication Review*, 28(3), July 1998.

[85] P. Sinha and S. Krishnamurthy. Scalable Unidirectional Routing using ZRP (Zone Routing Protocol) extensions for Ad-hoc networks. Technical report, HRL Laboratories, Malibu, CA, August 1999.

[86] K. M. Sivalingam, J.-C. Chen, P. Agrawal, and M. Srivastava. Design and analysis of low-power access protocols for wireless and mobile ATM networks. *ACM/Baltzer Wireless Network Networks*, 6(1):73–87, 2000.

[87] B. Sklar. *Digital Communications - Fundamentals and Applications*. Prentice Hall, International edition, 1988.

[88] M. Stemm and R. H. Katz. Measuring and Reducing Energy Consumption of Network Interfaces in Hand-Held devices. *IEICE Transactions on Communications*, E80-B(8):1125–1131, 1997.

[89] K. Thompson, G. J. Miller, and R. Wilder. Wide Area Internet Traffic Patterns and Characteristics. *IEEE Network*, 11(6):10–23, November/December 1997.

[90] http://www.transmeta.com.

[91] V. Tsaoussidis, H. Badr, X. Ge, and K. Pentikousis. Energy Throughput Tradeoffs in TCP Error Control Strategies. In *Proc. of 5th Symposium on Computers and Communication*, France, 2000.

[92] M. Venis. Testing NiCd and NiMH Batteries. WWW, June 1997. Vencon Technologies Inc.

[93] Your 802.11 network has No Clothes. http://www.cs.umd.edu/ waa/wireless.pdf, March 2001. WWW.

[94] H. S. Wang and N. Moayeri. Finite state Markov channel - a useful model for radio communication channels. *IEEE Trans. on Vehicular Technology*, 44(1):163–171, 1995.

[95] S. Wang, R. Morris, and A. Hwan. Harvard Network Traces and Analysis. WWW, March 1997. http://www.eecs.harvard.edu/net-traces/harvard-mar-13-1997-12:39.tar.gz.

[96] R. Wattenhofer, L. Li, P. Bahl, and Y.-M. Wang. Distributed Topology Control for Power Efficient Operation in Multihop Wireless Ad Hoc Networks. In *Infocom*, volume 3, Anchorage, April 2001. IEEE.

[97] S. Wu, et. al. Intelligent Medium Access for Mobile Ad Hoc Netowrks with Busy Tones and Power Control. *IEEE Journal on select areas in communications*, 18:1647–57, Sept. 2000.

[98] Y. Xu, J. Heidemann, and D. Estrin. Geography-informed energy conservation for ad hoc routing. In *Seventh Annual ACM/IEEE International Conference on Mobile Computing and Networking*. ACM, July 2001.

[99] M. Zorzi and R. R. Rao. Energy constrained error control for wireless channels. *IEEE Personal Communication Magazine*, 4:27–33, December 1997.

[100] M. Zorzi and R. R. Rao. Energy efficiency of TCP in a local wireless environment. *ACM Mobile Networks and Applications*, 6(3):265–278, June 2001.

[101] J. Zyren and A. Petrick. Tutorial on Basic Link Budget Analysis. Application Note AN9804, Harris Semiconductor, Apr. 1998.